THE KINETICS AND MECHANISM OF THE POLYMERIZATION OF METHYL METHACRYLATE INITIATED BY ORGANOMAGNESIUM COMPOUNDS.

A Thesis presented by

BRETT OLIVER BATEUP B.Sc. (Hons.)

for the degree of Doctor of Philosophy in the Department of Physical and Inorganic Chemistry at the University of Adelaide.

May 1974.

"It is no mere taste for paradox which leads one to doubt whether progress in a subject is reflected only in the increasing size of the books written about it."

(Hinshelwood, *Kinetics of Chemical Change.* 1940.)

CONTENTS

CONTENTS (continued) *Page number*

CONTENTS (continued) Page number

CONTENTS (continued) Page number

CONTENTS (continued) *Page number*

SUMMARY

The polymerization of methyl methacrylate (MMA) initiated by organomagnesium compounds in toluene/THF solution has been investigated in detail.

Detailed kinetic experiments were performed using n-BuMgBr, sec-BuMgBr and $(n\text{-Bu})_2Mg$. These studies included the dependence of polymerization rate on the initiator, monomer and tetrahydrofuran (THF) concentration, as well as the effect of temperature. Polymerizations have been done using tert-BuMgBr, tert-BuMgCl, n-BuMgI, iso-BuMgBr, $(sec\text{-Bu})_2Mg$ and $(tert\text{-Bu})_2Mg$.

Polymer microstructure has been studied using a high resolution 60MHz n.m.r. spectrometer and the effect of alkyl group, halide group, excess magnesium bromide and mixtures of Grignard reagents was investigated. Temperature was also shown to affect the polymer chain configuration.

Molecular weights and molecular weight distributions of polymers were determined using gel permeation chromatography (g.p.c.) to supplement the tacticity data. An estimate of the initiator efficiency and rate constant was made.

Ultra-violet spectra of the polymerizing solution were measured and information concerning the unusual temperature effect on polymerization was obtained.

An adiabatic reaction calorimeter was designed to operate at low temperature whilst under high vacuum and the heats of

polymerization were determined.

Vapour phase chromatography (v.p.c) was used to determine the number of active carbon-magnesium bonds present in the system during polymerization. The presence or absence of various side products which lead to very low initiator efficiency in these systems was detected using v.p.c and mass spectrometry.

A critical evaluation of the results obtained during this work and those reported by other researchers in this field has been made in an attempt to elucidate the extremely complicated mechanisms operating during the polymerization. Some of the complexities have been resolved.

This thesis is a record of research carried out in the Department of Physical and Inorganic Chemistry at the University of Adelaide between July 1971 and April 1974 and to the best of my knowledge and belief is completely original work, except where due reference is made.

(Brett O. Bateup)

ACKNOWLEDGEMENT

I am indebted to my supervisor, Dr. P.E.M. Allen, for his continuous support and guidance throughout the duration of this project.

My thanks go to Mrs. Gwen Haines for typing this thesis; to the glass-blowers Gavin Duthie and Tony Trivett; to Tony Bastin and Arthur Bowers in the General Workshop and to the electronics experts, Keith Shepherdson and John Beard for their assistance in designing and constructing much of the equipment used for this research.

I am also grateful to the Australian Government for granting me a Commonwealth Post-graduate Award and to the Australian Research Grants Committee for supporting this work.

Finally, I would like to thank my parents for their never ceasing help and encouragement.

CHAPTER 1

ORGANOMAGNESIUM CHEMISTRY

1.1 *Introduction.*

There is little doubt that Grignard reagents are the most important synthetic tool in Organic Chemistry. This is because they are very reactive compounds and can be easily prepared under normal laboratory conditions. It is not surprising therefore, that a great amount of research has been devoted to determining the structure and composition of these compounds and to the exact mechanisms by which they react. What is surprising, is that these problems are only starting to be solved after almost three quarters of a century. However, it is not until one starts searching through the hundreds of papers that have been written about these compounds possessing the simple empirical formula RMgX, that one becomes aware of how complex the above problems really are. The number of conflicting reports arising from seemingly identical conditions are many, and only after careful scrutiny can the least reliable ones be neglected.

Much of the controversy concerning the composition of Grignard reagents has now been resolved and some excellent reviews have recently appeared in the literature.[1-3] The reactions of Grignard reagents with various organic functional groups have been catalogued[4] and annual reviews of the most recent advances in organomagnesium chemistry are also available.[5-7]

However, by comparison, studies of organomagnesium compounds as polymerization initiators are still in their infancy and the mechanism or mechanisms by which these reagents react with unsaturated monomers under polymerization conditions are far from clear. To elucidate these mechanisms, knowledge of the composition of the initiating species is essential and a detailed review of the most significant experimental findings concerning this problem follows, (section 1.2). It is also useful to know the way in which organomagnesium compounds react with the functional groups that the monomer may contain (e.g. carbonyl, nitrile) as well as the reactions with monomers under non-polymerization conditions, (section 1.3.2).

1.2 *The composition of organomagnesium compounds.*

1.2.1 *The Grignard Reagent.*

In 1900 at the University of Lyon in France, Victor Grignard prepared the first alkyl magnesium halide from an alkyl halide and magnesium metal in diethyl ether. He represented the product as RMgX[8] and in 1912, was awarded the Nobel Prize for his work with these compounds which now bear his name.

In 1912, Jolibois[9] suggested that Grignard reagents were better represented by the unsymmetrical dimer formulation $R_2Mg.MgX_2$ and in 1929, Schlenk and Schlenk[10] proposed the following equilibria to explain the composition of Grignard reagents in ethereal solution.

$$R_2Mg + MgX_2 \rightleftarrows 2RMgX \qquad (1.1)$$

or

$$R_2Mg + MgX_2 \rightleftarrows R_2Mg.MgX_2 \qquad (1.2)$$

Subsequently, many papers were published concerning the existence and the position of the Schlenk equilibrium 1.1, but most of these earlier conclusions were not valid either on the basis of information known at the time or more recently.

A clear picture concerning the structure and composition of Grignard reagents only began to emerge in the mid 1960's when Ashby showed that these compounds were monomeric in tetrahydrofuran (THF)[11-13] and were best represented by the equilibrium 1.3 in diethyl ether.

$$\text{Dimer} \rightleftarrows R_2Mg + MgX_2 \rightleftarrows 2RMgX \rightleftarrows \text{Dimer} \qquad (1.3)$$

In 1966 Smith and Becker [14,15] determined the equilibrium constant for the Schlenk equilibrium for a number of Grignard reagents in dilute solution by measuring the heat of reaction on addition of a solution of MgX_2 to a solution of R_2Mg. Their results are shown in Table 1.1. In diethyl ether the predominant species is RMgX whereas in THF a nearly statistical distribution was observed.*

---

* The reader should note that the phrases, "the Schlenk equilibrium is nearly statistical in THF" or "in THF a nearly statistical distribution occurs" have been adopted from Ashby's work[3,31] and are synonymous with the statement, "in THF, the proportions of R_2Mg, MgX_2 and RMgX are such that $K_{1.1} \simeq 4$ at room temperature or slightly above."

Table 1.1

Equilibrium constants for the Schlenk equilibrium in diethyl ether and THF from ref. 14,15.

$$R_2Mg + MgX_2 \overset{K_{1.1}}{\rightleftarrows} 2RMgX$$

RMgX	$K_{1.1}$ (Et_2O)	$K_{1.1}$ (THF)
EtMgCl	-	5.5
EtMgBr	480	5.1
EtMgI	>630	-
PhMgCl	-	1.7
PhMgBr	55	3.8
PhMgI	> 15	-

The exact nature of the association of Grignard reagents in ether was investigated in 1969 by Ashby and co-workers[16,17] and their results are reproduced in figures 1.1 to 1.6. From fig.1.1 it appears that bromine or iodine is a much better bridging group than alkyl or aryl groups (with the exception of the methyl group at low concentrations) and the inference is that association is predominantly through the halogen atoms. The phenyl Grignard reagents associated past the dimer stage (fig. 1.2) and the best representation in these workers' opinion was a linear polymeric model of the form

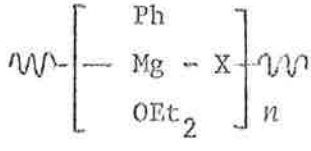

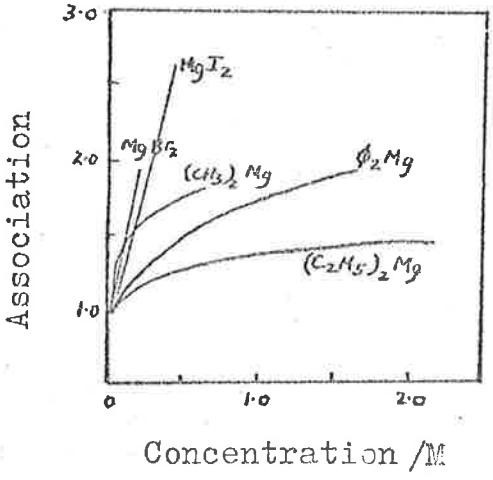

Figure 1.1. Association of magnesium halides, alkyls and aryls in diethyl ether.

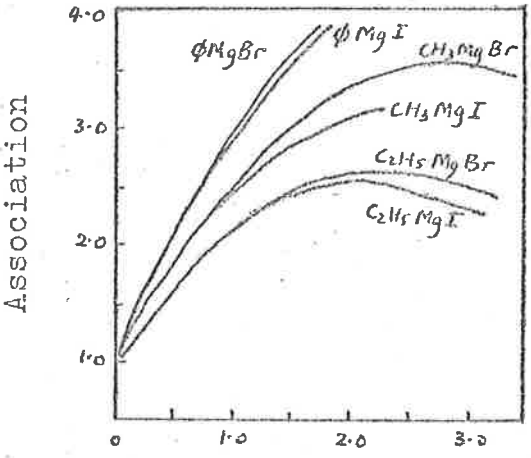

Figure 1.2. Association of alkyl- and aryl-magnesium bromides and iodides in diethyl ether.

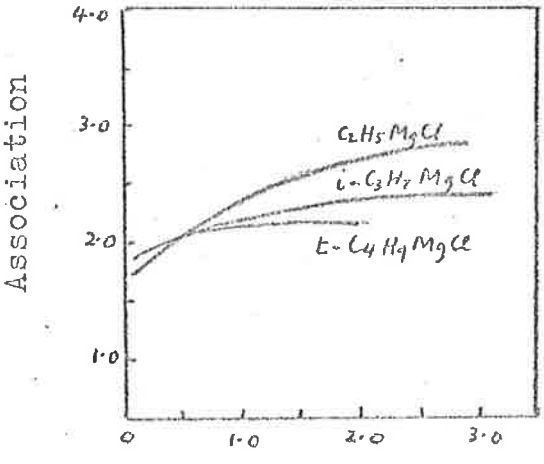

Figure 1.3. Association of alkylmagnesium chlorides in diethyl ether.

They rejected mixed bridge dimers and trimers of the type

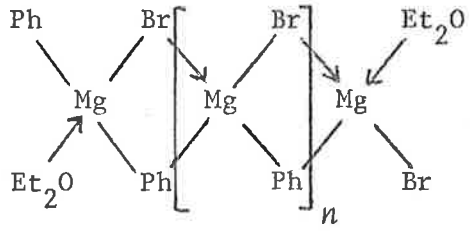

on the basis that magnesium halides and Grignard reagents hold only one molecule of ether tightly per magnesium atom even though the crystal structure of phenyl magnesium bromide shows two molecules of ether co-ordinated to the magnesium.[26]

The curvature of the plots for the methyl and ethyl-magnesium bromides and iodides in diethyl ether was attributed to non-ideality at high concentrations, and equilibrium calculations assuming a linear polymeric model appeared to be more consistent than any other representation.

The alkyl and aryl-magnesium chlorides and the recently discovered alkylmagnesium fluorides[18,19] were found to be dimeric in diethyl ether over the whole concentration range studied. (Fig.1.3 and 1.4), the curvature in figure 1.3 again assumed to be due to non-ideality at high concentrations.

The plots for association of Grignard compounds in THF are shown in figs. 1.5 and 1.6 and it appears that dialkyl magnesium compounds as well as alkylmagnesium chlorides, bromides and iodides are monomeric over a wide concentration range, whereas the fluorides are dimeric. Apparently fluorine is a strong enough bridging group

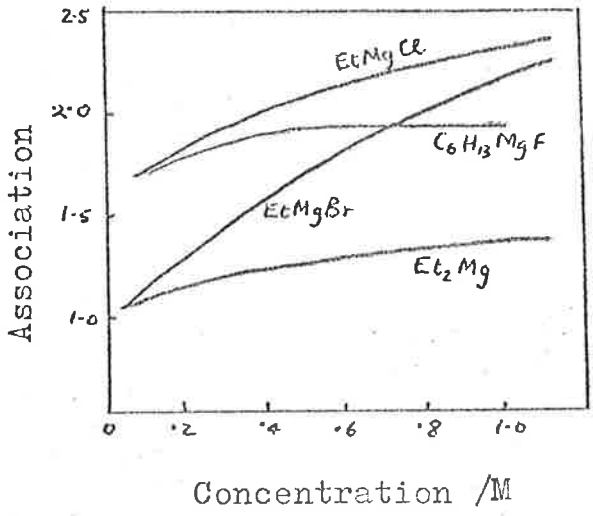

Figure 1.4. Association of n-amylmagnesium fluoride in diethyl ether.

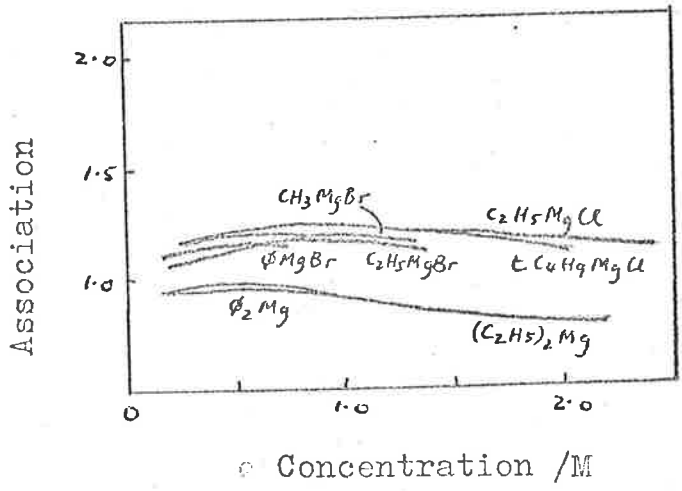

Figure 1.5. Association of several Grignard compounds in THF.

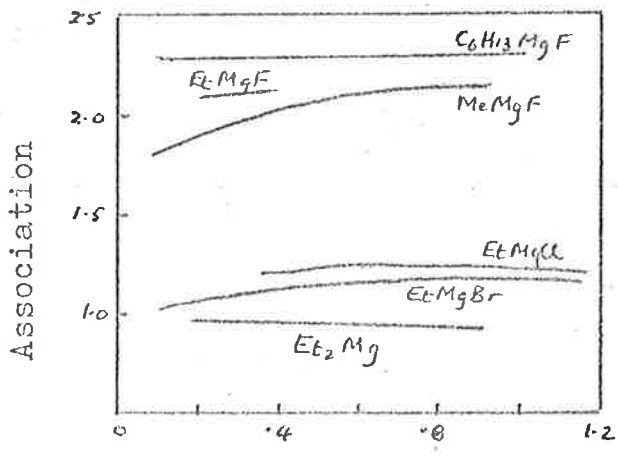

Figure 1.6. Association of alkylmagnesium fluorides in THF.

to prevent a strong base such as THF from cleaving the bridge bonds. Association in THF of organomagnesium compounds where the bridging group is -OR or $-NR_2$ is also known.[20]

Although the major species in ethereal solutions of Grignard reagents are essentially covalent compounds there are small amounts of ionic species present. The exact nature of these species is uncertain, however both cation and anion contain magnesium[21,22] and extensive association into ion-pairs and ion-triplets is likely[23] in a low dielectric constant solvent such as diethyl ether. The electrolysis of Grignard reagents produces results consistent with a cation of empirical formula RMg^+ and possible anion structures would be X^- or $RMgX_2^-$. All of these species would be solvated and some may be associated as well.[24] The organic products of electrolysis are consistent with the formation of radicals at the electrode with such reactions as: abstraction of hydrogen from the solvent to form RH, disproportionation of R into RH and olefin, and coupling to R_2.

Before finishing this section something should be said about the solvation of Grignard compounds. The magnesium atom in the compound RMgX, may increase its co-ordination number by either intra- or intermolecular interactions resulting in election-deficient bonds. In the first case, electrons may be available from the groups R or X within the same molecule; in the second, electron donating ligands co-ordinate with the metal atom. These ligands may be other RMgX molecules or other species such as solvent molecules or both.

Grignard compounds tenaciously retain ether[25,26] (or THF) and in most cases decomposition occurs before complete desolvation. The crystal structure of phenylmagnesium bromide crystallised from ether (in greater than two fold excess) shows magnesium tetrahedrally bonded to phenyl, bromine and two diethyl ether molecules.[26] Even though it is often unwise to extrapolate solid state structures to those in solution it seems likely that organomagnesium compounds exist in solution with the magnesium bound to four atoms in an essentially tetrahedral or slightly distorted tetrahedral configuration, (see e.g. ref. 27).

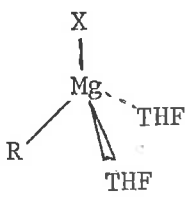

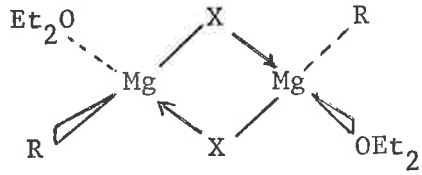

1.2.2 *Dialkyl and diaryl-magnesium compounds.*

Although the first reported preparation of these compounds was in 1866[28] they have received little attention compared with the Grignard reagents. They are more reactive than their Grignard counterparts (section 1.3) and appear to be monomeric in THF (fig. 1.6). In diethyl ether, dimethyl magnesium is dimeric even at quite low concentrations in accord with the strong bridging character of the methyl group. However, as the alkyl group becomes

larger and/or branched, association is less likely to occur.

The most striking difference between these compounds and Grignard reagents is their low affinity for ether. Whereas it is almost impossible to desolvate Grignard reagents, dimethyl magnesium is only sparingly soluble in diethyl ether and crystallises quite readily as an unsolvated polymer.[29] This ability to lose ether diminishes as the organic moiety becomes larger and diphenyl, di-isopropyl and di-tertiary butyl magnesium form stable 1:2 complexes with ether or THF.[30]

1.2.3 *Conclusions concerning the composition of organomagnesium compounds.*

The composition of Grignard reagents is a function of the solvent, the nature of the R group, the nature of the haolgen and the temperature.

In tetrahydrofuran, Grignard reagents are best represented by the Schlenk equilibrium with the equilibrium constant

$$K_{1.1} = [RMgX]^2 / [R_2Mg] [MgX_2] \simeq 4 \qquad (1.5)$$

Thermodynamic parameters for the system tert-butyl-magnesium chloride are $\Delta H^\circ_{1.1}$=37 kJ mol^{-1} and $\Delta S^\circ_{1.1}$=63 $JK^{-1}mol^{-1}$ at 315K. [31]

All Grignard compounds and R_2Mg compounds are monomeric in THF except the alkyl magnesium fluorides which are dimeric, probably

associated through a double fluorine bridge.

In diethyl ether the best representation of Grignard compounds is again the Schlenk equilibrium although in this solvent $K_{1.1}$ varies with the R group and the halogen. However in all cases the equilibrium favors the RMgX species. The fluorides and chlorides are dimeric (associating through double halogen bridges) while the bromides and iodides are monomeric below 0.1 mol dm^{-3}, associating in a linear polymeric form at higher concentrations.

In triethylamine, Grignard compounds are monomeric, the Schlenk equilibrium favouring RMgX when R is primary and X=Cl or Br. When R is branched and X=I a significant Schlenk equilibrium exists.

In all of the above structures the magnesium is solvated by one or more solvent molecules resulting in an essentially tetrahedral configuration.

Alkyl group exchange does take place in organomagnesium compounds and the rate and mechanism of exchange depend upon three factors: the structure of the alkyl group; the presence or absence of traces of oxygen, which reacts with organomagnesium compounds to form alkoxides which are extremely good bridging groups, and the nature of the solvent which has only a secondary effect on the exchange reaction. Exchange rates in general are rapid, being faster than, or comparable with, the n.m.r. time scale and in only a few instances has this technique been successful in distinguishing between the species R_2Mg

and RMgX in solutions of Grignard reagents.[31,32,33] The mechanism of the exchange reaction is still uncertain but studies on alkyl exchange between organomagnesium compounds and alkyl mercury halides,[34,35] suggests that the reaction proceeds via a bimolecular process with retention of configuration. The 'intermediate' proposed[31] to explain these observations was the mixed bridge structure (I)

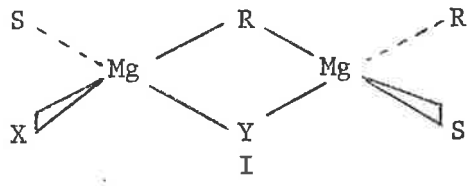

I

where S is the solvent, X is the halide and Y can be a halide or alkoxide group. The stability of I is paramount in determining the rate of exchange. As R becomes branched (especially at the α-carbon atom[36]) the exchange rate decreases, e.g. in tert-butyl-MgCl the rate is approximately 4 seconds at 315K in THF and two distinct n.m.r. signals corresponding to (tert-butyl)$_2$Mg and (tert-butyl)MgCl can be distinguished, whereas CH_3MgCl in the same solvent shows only one n.m.r. signal even at 173K.[31] The nature of the group Y, which may be an alkyl in the dialkylmagnesium case, or a halide or alkoxide, also has a great influence on the rates of exchange. When Y is an alkoxide group (-OR), exchange is rapid because of the enhanced bridging ability of this group.[20] It is therefore important to exclude all traces of oxygen from Grignard reagents

since traces of oxygen not only alter the kinetics of reactions involving these compounds but also their apparent molecular association values.[37]

Solvent-effects on the rates of alkyl exchange and inversion of configuration appear to follow the trend that the stronger the base (in the Lewis sense) the slower the exchange and inversion rate. House and co-workers[35] explain this solvent-effect in terms of a shift in a rapid pre-equilibrium between an unreactive disolvated organomagnesium compound and a reactive monosolvate. Although this mechanism was originally proposed to explain the dialkyl magnesium system it can be quite readily extended to explain similar observations made on the Grignard system.

1.3 *Reactions of organomagnesium compounds.*

1.3.1 *Reactions with ketones and nitriles.*

The controversy surrounding the composition of Grignard reagents over the decades led to an arithmetic progression of theories concerning the mechanisms by which these compounds react with certain organic functional groups, e.g. ketones and nitriles. Again it is difficult to separate the wheat from the chaff because of the drastic effect that minute amounts of impurities can have on the reactant and consequently the reaction, but many of the earlier theories can be rejected on the basis that assumptions made, concerning the nature of the Grignard reagent, have subsequently been proved incorrect.

Of the more recent theories, the overall third order kinetics[38] (first and second order with respect to ketone and Grignard respectively) was interpreted in terms of reaction of an extra molecule of RMgX with a ketone-Grignard complex by way of a six-centred transition state such as II.

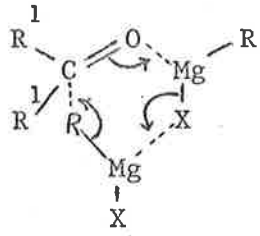

II

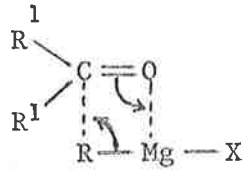

III

Second order kinetics have also been observed[39] and have been explained by a simple bimolecular reaction between the Grignard and ketone or a unimolecular decomposition of their complex via the four-centre transition state III.

This discrepancy between the observed orders of reaction may have resulted from impurities present in the magnesium used to prepare the Grignard reagent. Using single crystal magnesium (99.9995% pure) Ashby and his co-workers[39c-e] have shown that the reaction between methyl magnesium bromide and excess 2-methyl-benzophenone in diethyl ether was first order with respect to the reactive organomagnesium species. Their proposed mechanism was

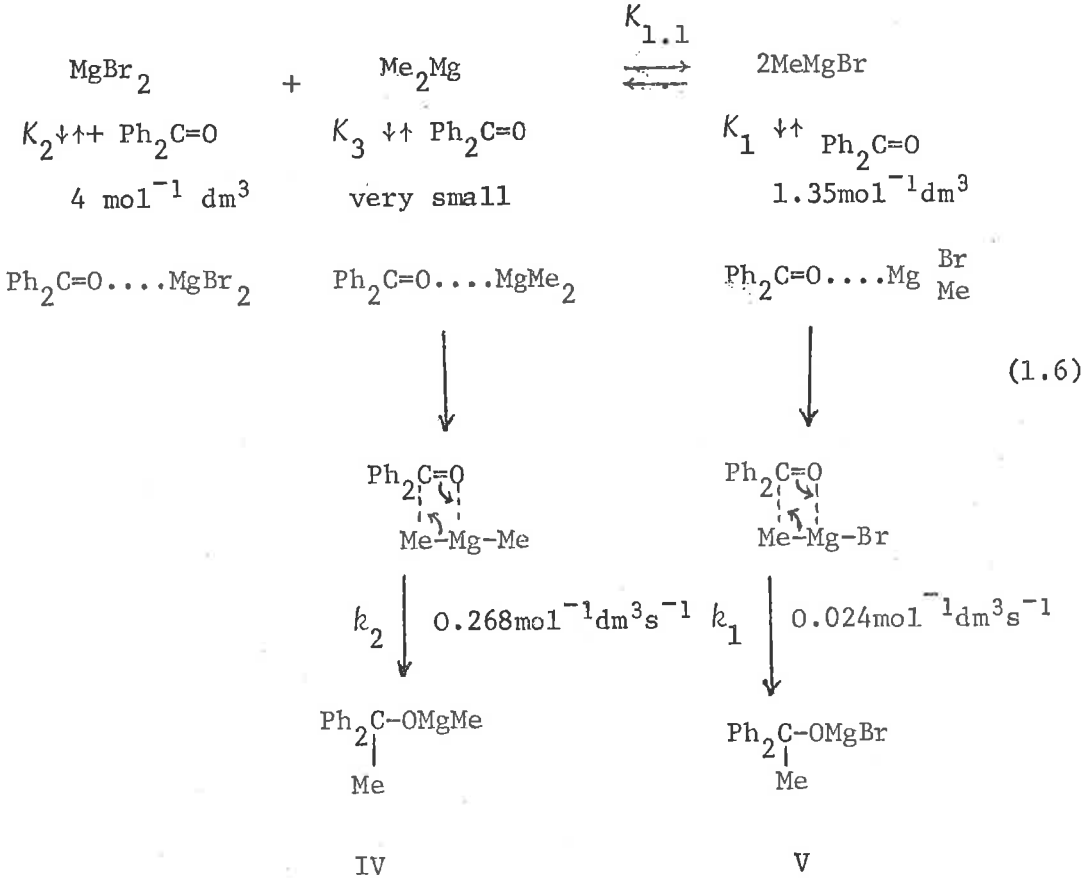

(1.6)

Complex formation between the ketone and the various species in the Schlenk equilibrium was observed using u.v. spectroscopy but they were uncertain whether the reaction proceeded via these complexes or by a direct bimolecular process.[39d] This uncertainty was also shared by Holm[27,40] who studied the reaction between normal-butyl magnesium bromide and acetone using infra-red spectroscopy. In diethyl ether, the ketone-Grignard complex was detected but not in tetrahydrofuran and he suggested that the reaction proceeded via the complex in some instances and by a bimolecular process in others.

Other important conclusions resulting from Ashby's work[39e]

are that Me_2Mg reacted ten times faster than MeMgBr, and the reaction path of Me_2Mg does not finish at structure IV. In the presence of $MgBr_2$, IV reacts according to (1.7)

$$ROMgMe + MgBr_2 \rightarrow ROMgBr + MeMgBr \qquad (1.7)$$

However, in the absence of $MgBr_2$, IV dimerises and successively reacts with two more ketone molecules in two pseudo first order processes, (1.8)

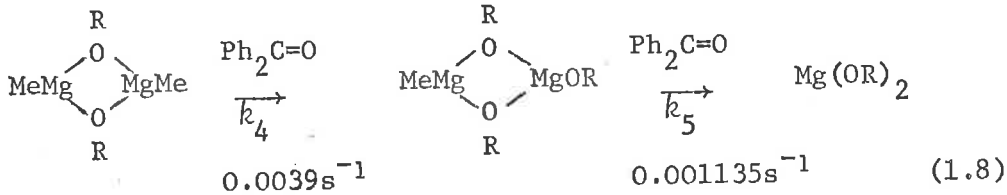

(1.8)

Recently, these workers have studied in detail the reaction between benzonitrile and both Me_2Mg[41a] and MeMgBr.[41b] The conclusions drawn concerning the mechanism were identical to those drawn from the addition of Grignard reagents to ketones.

1.3.2 *Reactions with α, β-unsaturated carbonyl compounds.*

According to Organic Chemists the two pathways by which organometallic compounds can react with α, β- unsaturated carbonyl substrates are those which ultimately lead to 1,2 or 1,4 addition products, (1.9).

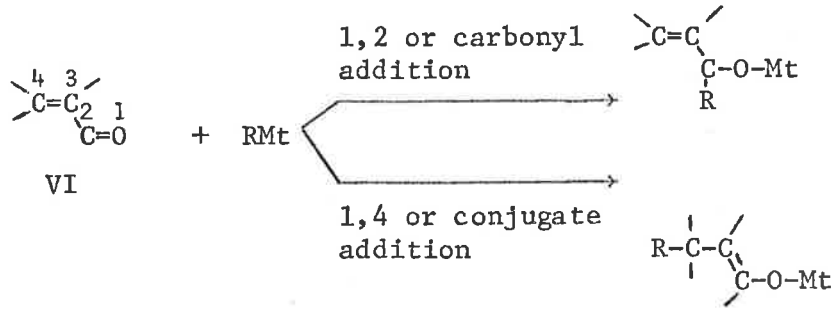

(1.9)

However, when monomers from this class polymerize by an anionic mechanism, the high molecular weight polymers formed arise from successive 3,4 addition steps.

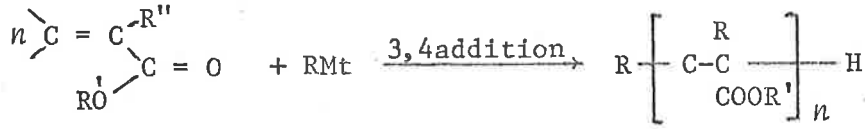

(1.10)

This apparent anomaly is easily explained because the anion formed during 1,4 addition has some carbanion (VII) and some alkoxide ion (VIII) character,

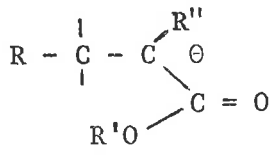

VII

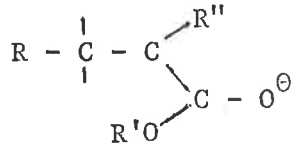

VIII

and the next reaction step leads to either 3,4 or conjugate addition products.[42]

The factors controlling the ratio of carbonyl to conjugate addition are not yet completely understood. Comparative studies

of phenyl compounds of Group II and IA metals with benzalacetophenone by Gilman and Kirby[43] and later by Hauser[44] showed that the ratio of 1,2 to 1,4 addition was strongly dependent on the nature of the organometallic species, especially the polarity of the carbon-metal bond. The more reactive (essentially ionic) organometallics of Group I (sodium and potassium) and II (calcium) gave predominantly 1,2 addition whereas 1,4 adducts were formed with the less reactive (essentially covalent) phenyl-lithium and PhMgBr. The carbonyl/conjugate addition ratio is also dependent on the nature of the substrate, the polarity of the solvent and the temperature, but a complete picture will not be obtained until these systems are studied under a wide set of rigidly comparable conditions to separate the influence of each of the above factors.

However, at the risk of unwarranted generality, a rough rule of thumb might be stated that; α, β-unsaturated aldehydes undergo 1,2 addition exclusively; the ratio of 1,2 to 1,4 addition to α, β-unsaturated ketones and esters falls as; the organometallic carbon-metal bond polarity decrease, as the electrophilicity of carbon atom C4 in VI decreases and as the steric accessibility of C4 increases.

Several mechanisms have been proposed for the conjugate addition of Grignard reagents to various α, β-unsaturated carbonyl

compounds. Lutz[45] suggested a cyclic transision state such as

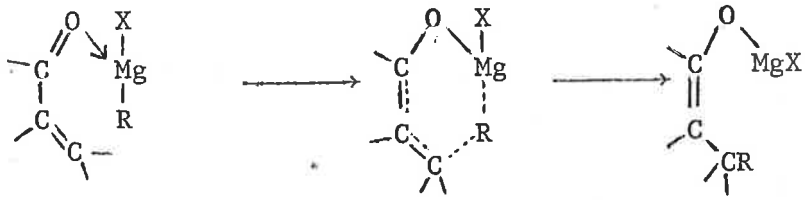

(1.11)

where initial formation of a 1:1 substrate: Grignard Wittig-'at' type complex was assumed. House[46] argued that because this mechanism did not accommodate various sterochemical requirements a better scheme would be the nucleophilic attack of the organomagnesium species from a direction perpendicular to the plane of the conjugated system.

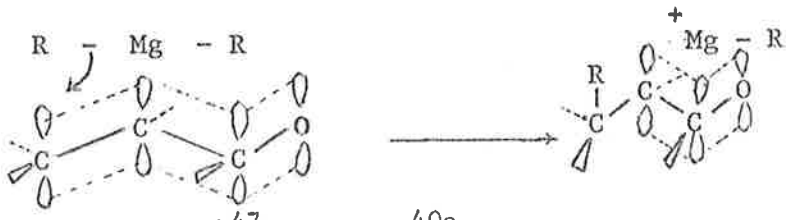

(1.12)

Munch-Petersen[47] and Holm[40a] have suggested that some systems follow reaction 1.11, while others, such as sec-butyl-crotonate, involve the attack of a second molecule of reagent on a Grignard-ester complex.

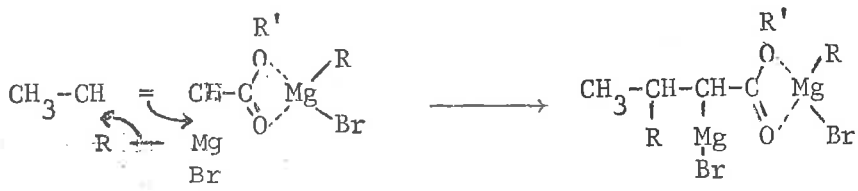

(1.13)

The addition reaction between α, β-unsaturated esters and

organomagnesium compounds is further complicated by the possibility of two-fold addition at the carbonyl carbon.

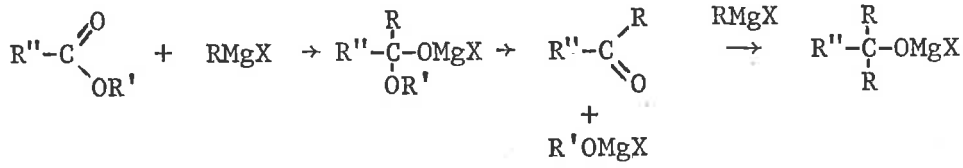

(1.14)

Hitherto, only the various addition reactions have been discussed but reactions such as reduction and enolization also occur in these systems. Both mechanisms are believed to involve an intra-molecular hydride ion transfer via a six-centred transition state[48]

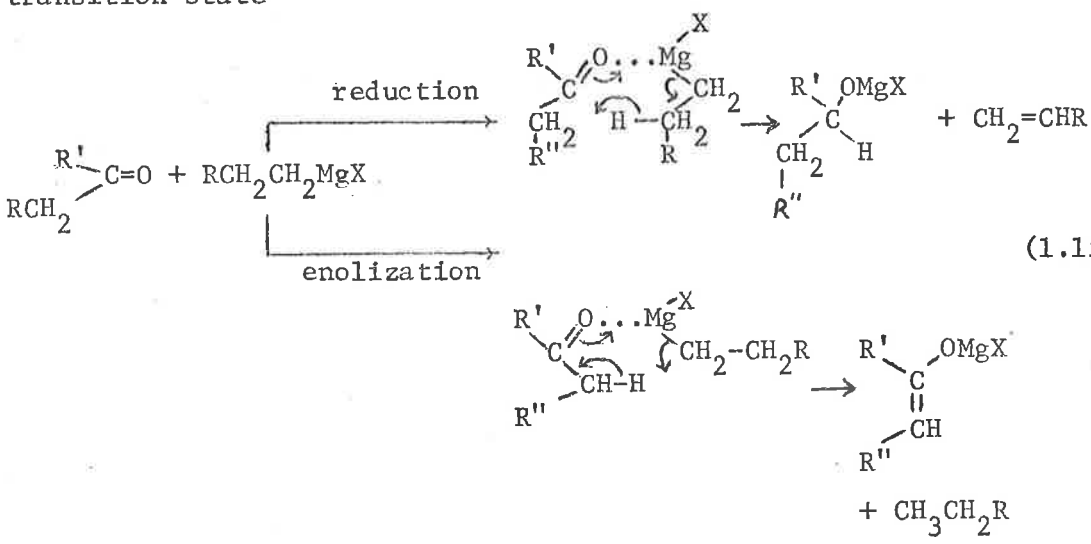

(1.15)

Increasing the size of the alkyl group of the Grignard reagent results in an increase of reduction and enolization and a decrease in addition. Evidence supporting the above mechanism

is that methyl magnesium halides only undergo addition and that reduction only occurs when the Grignard reagent possesses a β-hydrogen atom.

Finally, it should also be noted that the relative yields of the various products of the reactions of organomagnesium reagents with carbonyl compounds have been shown to be significantly influenced by trace impurities present in the magnesium used for the Grignard preparation.[49]

1.4 *Organomagnesium compounds as polymerization initiators.*

Although Grignard reagents have been used extensively for organic syntheses since 1900 it was not until around 1950 that their ability to initiate the polymerization of polar unsaturated monomers was discovered[50] and little interest was shown in these compounds as polymerization initiators until the late 1950's. Two factors that probably contributed to this lack of interest were; the lower reactivity of organomagnesium compounds towards unsaturated vinyl monomers compared with their organoalkali analogues and the confusion concerning the structure and composition of Grignard reagents prevailing at that time.

Since then, organomagnesium compounds have been reported to initiate the polymerization of a variety of vinyl monomers (for a detailed review, see ref. (51)) and the mechanism of the very

high stereospecific control exhibited by these initiators under certain conditions has been the subject of many papers.

1.4.1 *Acrylate and Methacrylate monomers.*

The most intensively studied monomer in this group is methyl methacrylate (MMA), $CH_2=C(CH_3)CO_2CH_3$. As discussed in section 1.3.2, α, β-unsaturated esters undergo a variety of reactions with Grignard reagents. High molecular weight polymers result from initial 1,4 (conjugate) addition (eqn. 1.9) and then successive 3,4 addition reactions (eqn. 1.10). Other reactions such as 1,2 addition, reduction, enolization, and metallation compete with polymerization, reducing initiation efficiency and making elucidation of the polymerization mechanism more difficult.

Owens *et al*[52] studied the reaction between MMA, MA and isopropyl acrylate and various organomagnesium compounds under polymerization conditions in toluene,[52a] ($[MMA]_o >> [G]_o$, T=273K) and under non-polymerization conditions in ether,[52b] ($[MMA]_o << [G]_o$, T =273K) where $[G]_o$ represents the initial concentration of active R-Mg bonds. In both cases the predominant products were polymer (structure XI with $n>3$), IX, X and XI, the only difference being in the relative proportions of products formed.

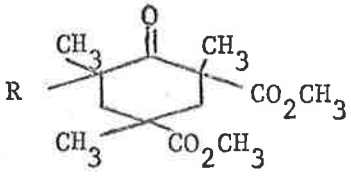

IX

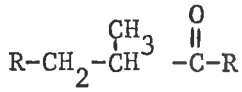

X

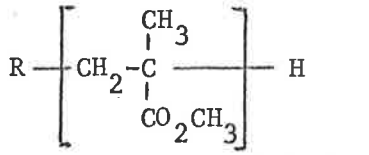

XI

Minor amounts of several other products were also dectected but no exclusive 1,2 adducts were observed. It was surprising that polymer, IX and XI were produced under conditions where $[MMA]_o < [G]_o$, however a possible explanation will be given later (see section 3.6 (c)). When $[MMA]_o >> [G]_o$ the polymer produced using PhMgBr had a broad molecular weight distribution ($\bar{M}_{viscosity}/\bar{M}_n > 20$) and infra-red spectroscopy indicated that many of the chains contained a cyclic ketone structure similar to IX as the terminal unit. Equation 1.16 was postulated.[52a]

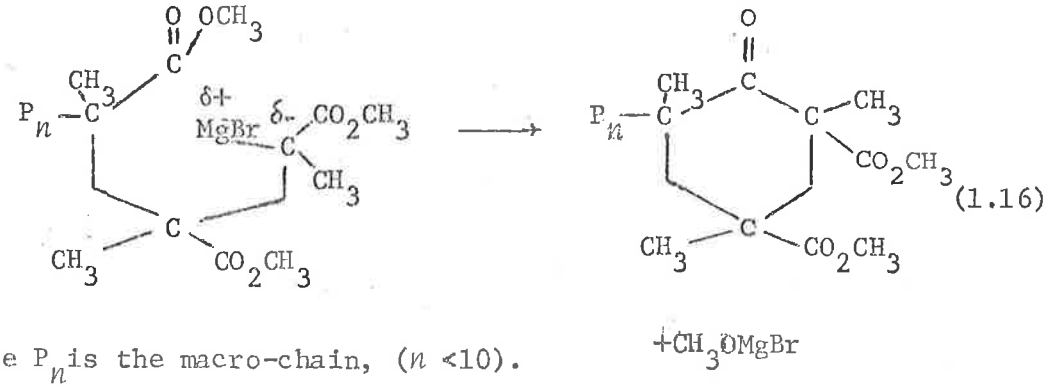

(1.16)

where P_n is the macro-chain, ($n < 10$).

Tsuruta *et al*[53] studied the reaction between n-BuMgBr in ether and hexane and various acrylate monomers at 293K and 243K. They did not observe any cyclic ketone IX but some carbonyl

addition occurred. The ratio of carbonyl to conjugate addition was a function of temperature and monomer structure. Bulky alkoxy groups reduced the amount of carbonyl addition whereas substitution of a methyl group at the β position reduced conjugate addition. In all cases, a significant amount of initiator was consumed in the formation of butane.

Two groups[54,55] have studied the kinetics of polymerization of MMA with n-BuMgBr in toluene and ether-toluene mixtures. At 223K, the orders of reaction were complex. In 1:9 diethyl ether:toluene[54a] solution the internal and external monomer dependence differ, presumably due to side product formation, whereas in toluene at 223K first order monomer ($[MMA]_o < 5$ mol dm^{-3}) and second order initiator dependence was observed.[55b] The rate versus temperature curve passed through a maximum (the inversion temperature T_i), the position being slightly dependent on the nature of R and X in the Grignard reagent. Above T_i, polymerization was very slow resulting from irreversible termination of the macro-chain as well as reduced initiation efficiency. One possible mechanism for termination of the macro-chain involving nucleophilic attack of a carbanionic chain end on the monomer carbonyl has been suggested in several systems.[56,57]

(1.17)

The high stereospecific control exhibited by Grignard reagents under certain conditions has been the subject of many papers and will be further discussed in sections 4.1 and 6.2. Suffice to say that no mechanism explaining all the observed facts has yet been proposed. Many early reports concerning the resulting polymer microstructure were limited because the use of high resolution n.m.r. spectroscopy for the determination of chain configuration (especially of PMMA) was unkown at that time, e.g. ref. 52c.

Watanabe *et al*[55b] found that isotactic poly-MMA could be obtained by the use of branched chain Grignard reagents (e.g. sec-BuMgBr) or n-octyl, n-hexyl and cyclo-hexyl-MgBr from 193K to 298K, or PhMgBr at room temperature. Straight chain Grignard reagents, such as n-BuMgBr, resulted in stereoblock polymer. Addition of diphenylamine or diethylamine to n-BuMgBr resulted in isotactic polymer as well as an increase in polymerization rate. The chlorides produced the least isotactic and the iodides the most isotactic polymer and Watanabe assumed a gegenion of the type $[RMg_2X_2]^+$ to explain the effects of R and X on the tacticity.[55c]

Using diphenyl-magnesium in toluene at 273K, Goode found that stereoblock PMMA was formed.[52c] The rate increased as $MgBr_2$ was added until the ratio was 1:1 and then the rate and molecular weight decreased. The polymer tacticity changed from

stereoblock to isotactic on the addition of $MgBr_2$ or MgI_2, but remained stereoblock when $MgCl_2$ was added.

Temperature also affects the polymer microstructure. A study of poly-acrylates formed using PhMgBr and Ph_2Mg in toluene and ether-toluene mixtures has shown that the mode of opening of the monomer double bond is determined at the very start of the reaction and changes in temperature after the first few minutes do not affect the polymer structure,[58,59] (see section 4.1.3).

Copolymerization studies of MMA and styrene using Grignard initiators have been attempted. With phenyl-magnesium bromide at 238K, Allen *et al*[54a] found that the copolymer contained 99.5% methylmethacrylate. Under these conditions, the propagating species is incapable of adding styrene.[60] It is thus either a poly MMA anion, or a species showing a very similar selectivity.

Using the same system, Dawans and Smets[61] concluded that the mechanism was complex, a marked increase in the styrene reactivity ratio above 253K being observed.

1.4.2 *Acrylonitrile and related monomers*

Mechanistic studies of the polymerization of acrylonitrile are hampered by the extremely low solubility of the polymer in its monomer and the common organic solvents. Extremely polar solvents such as hexamethyl-phosphoro-triamide (HMPA), dimethyl-suphoxide (DMSO) and dimethyl-formamide (DMF) are suitable, but

even the presence of catalytic quantities of these substances significantly alter the kinetics. At 198K, in DMF, polymerization initiated by BuMgCl is complete in a fraction of a minute compared with the initial rate of 1% /min in toluene.[62] The molecular weight and polymer yield increase in the presence of DMF or DMSO but only the yield increased when HMPA was added to the system.[63]

Kinetic studies of the acrylonitrile/butyl-magnesium chloride/ toluene system at 198K[64] show that less than 1% of the initiator forms high molecular weight polymer, the remainder being consumed in rapid side reactions. The molecular weight increased linearly with conversion and was independent of initial monomer concentration. The initial rate of polymerization was first order with respect to initiator and second order with respect to monomer.

The following mechanism was proposed

$$I + M \overset{K}{\rightleftarrows} (I.M) \overset{K_1}{\underset{+M}{\rightleftarrows}} (I.M_2) \qquad (1.17)$$

$$(I.M_2) \xrightarrow[k_3]{} \text{inactive compounds}$$

$$(I.M_2) + M \xrightarrow{k_1} M^* \qquad (1.18)$$

$$M_n^* + M \overset{K_2}{\underset{\text{rapid}}{\rightleftarrows}} (M_n^*.M) \xrightarrow[k_2]{\text{slow}} M_{n+1}^* \qquad (1.19)$$

where M_n^* = propagating species of degree of polymerization n, $n = 1, 2 \ldots n$

and the assumption, $K_2[M] >> 1$.

There are many similarities between these results and those obtained during the present investigation and the above mechanism, eqns. (1.17) to (1.19) will be referred to again later (section 3.6 (a)).

No extensive studies have been done on the microstructure of nitrile-containing polymers although isotactic polymethacrylonitrile has been prepared using organomagnesium initiators.[65]

1.4.3 *Miscellaneous vinyl and diene monomers.*

Organomagnesium compounds have been reported to initiate polymerization of a variety of monomers other than acrylates and nitriles. Most of the work has centred around the resulting polymer microstructure or more specifically the amount of crystallinity exhibited by the polymer.

Stereoregular polyvinyl pyridines have been produced using 2-vinyl pyridine monomer but not 4-vinyl pyridine.[66] In Natta's opinion, considerable remoteness of the nitrogen atom from the vinyl group eliminates the possibility that complexes of the growing chain can be formed by means of both donor positions in the monomer, and thereby excludes its rigid orientation in acts of growth. The role of complex formation as a factor influencing the microstructure of the polymer is exhibited in polymerization of 2-vinyl pyridine in the presence of catalytic quantities of Lewis bases, which either hinder or eliminate complex formation

between the growing chain and the monomer.

Other monomers that have been polymerized using organomagnesium catalysts include vinyl chlorides,[67] aldehydes[68] and ketones[53,69] which presumably propagate by some form of anionic coordination mechanism. The less reactive unsaturated hydrocarbon monomers (styrene, butadiene and isoprene) do not polymerize under ordinary conditions with organomagnesium initiators. High temperatures and pressures are required and the rates of polymerization are generally slow.[70]

Organomagnesium compounds also initiate the polymerization of vinyl ethers[71] and since these monomers are inert towards anionic initiators the mechanism in this case is probably cationic. A more detailed review of these reactions is given by Erusalimskii *et al.*[51]

1.5 *Aims of this investigation.*

As yet, no papers have appeared in the literature which contain detailed kinetic, molecular weight, molecular weight distribution and stereochemical control studies on the polymerization of MMA initiated by a series of Grignard reagents and dialkylmagnesium compounds.

Several papers have combined two or three of the above aspects but conclusions concerning the mechanism of the polymerization were hampered for several reasons. In some instances,

unavailability of high resolution n.m.r spectroscopy reduced the accuracy of microstructure determinations and molecular weights had to be determined by methods such as osmometry and viscometry which are subject to various inherent difficulties, either experimental and/or the values of semi-empirical constants needed for molecular weight calculations. The earlier papers were also hampered by the lack of knowledge of the exact composition of Grignard reagents in ethereal solvents and the effect that certain impurities have on the resulting reactions with unsaturated esters.

The aim of this investigation was to unravel the complexities and anomalies observed in the polymerization of MMA initiated by Grignard reagents. The initiator solutions were prepared in THF because they are monomeric in this solvent. Toluene was added to the reaction mixture to ensure a completely homogeneous system at the monomer concentrations and temperature used. By performing all reactions under high vacuum to eliminate oxygen and moisture it was hoped that a detailed mechanism could be proposed to explain the unusually high stereochemical control exhibited by certain Grignard reagents but not by others under identical conditions.

CHAPTER 2

GENERAL EXPERIMENTAL TECHNIQUE

Organomagnesium compounds react readily with water and oxygen to form alkanes and alkoxides respectively. Because the presence of alkoxides greatly enhances the rate of exchange in organomagnesium systems (section 1.2.3), and because water and oxygen terminate the polymerization of MMA initiated by Grignard reagents, conditions of maximum possible purity must be established. The purpose of this chapter is to describe the procedures developed to ensure that these conditions were met.

2.1 *High Vacuum System*

Except for the initial preparation of the initiator solutions (which were done under a stream of high purity nitrogen) all manipulations and reactions were performed under high vacuum.

The high vacuum system, fig. 2.1, consisted of two pyrex glass manifolds which could be used individually or concurrently. One manifold was used exclusively for solvent distillation and the other for evacuating reaction vessels. The manifolds were evacuated by two pyrex glass, three stage mercury diffusion pumps, backed by one single stage Dynavac rotary oil pump. The diffusion pumps were connected such that they could be operated independently or concurrently in series or parallel. Liquid nitrogen traps separated the manifolds from the diffusion pumps which were in

Figure 2.1. Schematic diagram of the high vacuum system.

B = ballast flasks

E = electrothermal heating tape

I = ionization gauge head

M_1 = solvent distillation manifold

M_2 = high vacuum manifold

P_1,P_2 = three stage mercury diffusion pumps

R = rotary backing pump

S = safety manometer

T = liquid nitrogen traps

V = pirani gauge head

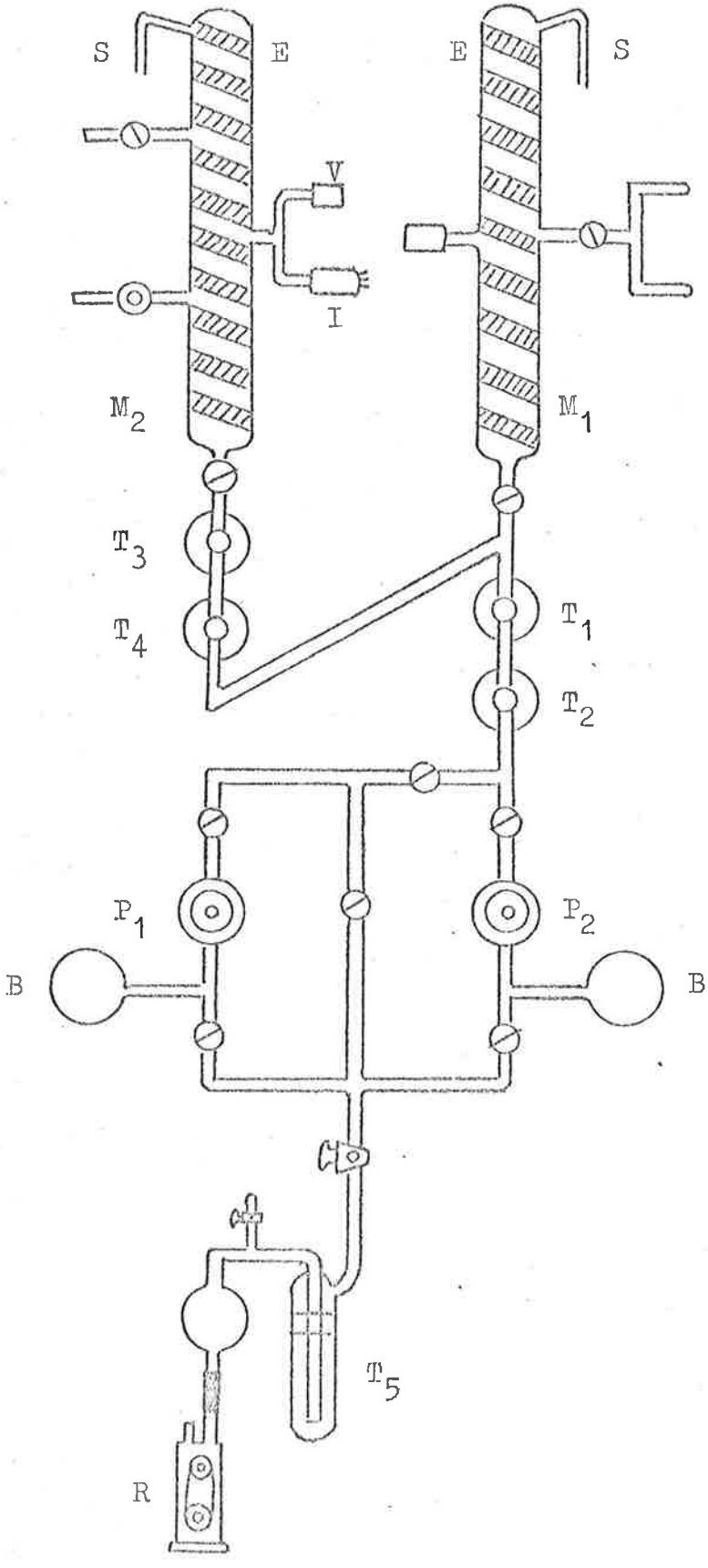
S
E
E
S
V
I
M2
M1
T3
T4
T1
T2
P1
P2
B
B
T5
R

turn separated from the rotary pump by another trap. Safety manometers were attached to each manifold and a pressure sensitive microswitch ensured that the diffusion pump heaters cut out whenever the water pressure dropped below a certain value. Each manifold was wrapped with Electrothermal heating tape (heated at a rate of 50 volts m^{-1}) to eliminate the monomolecular water layer that forms on the surface of glass.

Vacua were measured using an Edwards Pirani gauge to $10^{-3} Nm^{-2}$ and lower pressures were measured on a G.E.C. ionization gauge and appropriate head.

All glass assemblies for reaction studies were attached to the manifolds via Springham greaseless taps with Viton A diaphragms or high vacuum ground glass taps lubricated with Dow Corning high vacuum silicone grease.

2.2 *Purification of Reagents*

2.2.1 *Methyl methacrylate* (MMA)

MMA (I.C.I. Aust. Tensol cement No. 3 stabilized with 0.1% quinol) was washed five times with a 10% w/v caustic soda solution to remove the inhibitor and then washed with water until neutral to litmus. The MMA was then dried with anhydrous magnesium sulphate and allowed to stand on calcium hydride (CaH_2) overnight. This sample was outgassed four times and distilled under vacuum

onto fresh CaH_2. The MMA was then redistilled into a dispensing vessel with precalibrated break seals attached which had been previously flamed out to a pressure of 10^{-3} Nm^{-2}. These ampoules were kept frozen in a dry ice/ethanol bath in a darkened refrigerator to prevent any adventitious polymerization.

2.2.2 *Alkyl Halides*

The alkyl halides used for the preparation of the appropriate Grignard reagents were analytical reagent grade chemicals supplied by B.D.H., Ajax, or Pfaltz and Bauer, dependent upon availability and delivery time. The halides were refluxed over calcium hydride for 12 hours and distilled immediately before use, a generous fraction of the initial distillate being rejected.

1,2-dibromoethane (B.D.H. London, analytical reagent) was dried with calcium chloride, distilled, and a middle fraction collected.

2.2.3 *Toluene*

Toluene (BDH.,London, Eng., analytical reagent) was refluxed over CaH_2 for 24 hours and a middle fraction distilled onto fresh CaH_2. This was transferred to the vacuum line, outgassed four times and distilled onto fresh CaH_2 from which the toluene was distilled into a dispensing vessel with pre-calibrated breakseals attached.

2.2.4 *Tetrahydrofuran* (THF) (B.D.H. London, Eng. laboratory reagent stabilized with 0.1% quinol)

Since THF was the solvent used for preparing the initiator solutions its purity was critical. As discussed in section 2.3, the induction period before the Grignard reaction starts is dependent upon the amount of water in the solvent.

Two purification methods were adopted depending on the quantity of THF required. Large amounts of solvent for the Grignard preparation were treated with lithium aluminium hydride ($LiAlH_4$) which removed the inhibitor as well as drying the THF. After refluxing over $LiAlH_4$ for 12 hours, the THF was distilled, and a middle fraction collected. Freshly pressed sodium wire was added and the solution stored in the dark until needed.

Smaller amounts of tetrahydrofuran, suitable for diluting reaction mixtures, were prepared by refluxing over CaH_2, distilling onto fresh CaH_2 and transferring to the vacuum line. After outgassing thoroughly, the THF was distilled under high vacuum onto a sodium mirror to which one gram per 500 cm^3 of the THF of benzophenone was added. The blue colour of the Na-benzophenone radical anion developed rapidly, gradually giving way to the purple radical di-anion. The blue or purple colour was used as a guide to the THF purity over a period of time of storage in the refrigerator. Small quantities of the THF were distilled from this solution when required.

With some brands, e.g. Unilab, laboratory reagent grade THF, neither of the above purification methods was adequate. The Grignard reaction showed an unusually long induction period and polymerizations to which this "pure" THF was added were terminated spontaneously. Evidently, some commercial grades of THF contain an active impurity which cannot be removed by the methods employed here. This phenomenon has also been noted elsewhere.[72]

2.2.5 *Chloroform*

Chloroform (B.D.H. London, Eng. stabilized with 2% w/w ethanol) for polymer tacticity determinations was washed six times with water, dried over calcium chloride, distilled and a middle fraction collected. 60 MHz n.m.r spectroscopy showed no traces of impurity.

Chloroform for gel permeation chromotography (g.p.c.) was distilled without further purification.

2.2.6 *Dioxan*

1,4 Dioxan (Univar, Aust, analytical reagent) was dried over CaH_2, degassed and distilled under vacuum onto fresh CaH_2 and then distilled as required.

2.3 *Preparation of Initiator solutions.*

2.3.1 *Grignard reagents*

Solutions of Grignard reagents in THF were prepared using standard procedures.

Magnesium turnings (B.D.H., London, Eng. suitable for Grignard reactions) were washed with benzene, then ether, and dried at 373K for 12 hours.

Since Grignard reagents are sensitive to air and moisture it is essential that the apparatus is dry. The Grignard reagents were prepared in a 3 necked round bottomed flask fitted with a dropping funnel, reflux condenser and leak tube. Excess magnesium turnings and a portion of the THF required were added to the flask and the whole apparatus purged with high purity, nigrogen (99.9%). A solution of the freshly distilled alkyl halide in THF was placed in the dropping funnel and a small amount added to the reaction vessel to initiate the reaction. (The formation of Grignard reagents is a highly exothermic process, and though slow to begin with, accelerates very markedly when an appreciable amount of the reagent has been formed. It is therefore important not to add too much halide before the reaction is well started.) Gentle heating of the solution was generally enough to initiate the reaction in THF and thereafter the halide solution was added at such a rate to maintain steady boiling of the ether. The

maintenance of steady boiling has the advantage that the atmosphere of THF keeps air away from the reagent. When all the alkyl halide had been added, the solution was refluxed for half an hour to ensure that the Grignard reaction was complete. A high vacuum tap assembly, compatable with the vacuum line was quickly inserted in the reaction vessel and the whole vessel was transferred to the vacuum line. The solution was outgassed several times and a dispensing vessel was attached to the main reaction vessel which had been fitted with a side arm containing a sintered glass filter and a breakseal, as shown in figure 2.2.

After pumping and flaming out to a pressure of 10^{-3} Nm^{-2} the apparatus was sealed from the line at constriction A. The breakseal was ruptured and the Grignard solution filtered into the dispensing vessel. This was sealed at constriction B and the clear colourless solution poured into ampoules. This procedure eliminated cumbersome manipulations in a dry box and ensured that the initiator was in an oxygen and moisture free environment.

Several points should be noted concerning the Grignard preparation.

(1) The induction period at the beginning of the reaction is in part due to a thin layer of oxide that coats all magnesium that has been exposed to air. It is therefore preferable to use magnesium that has been freshly milled with a special carbide tool.

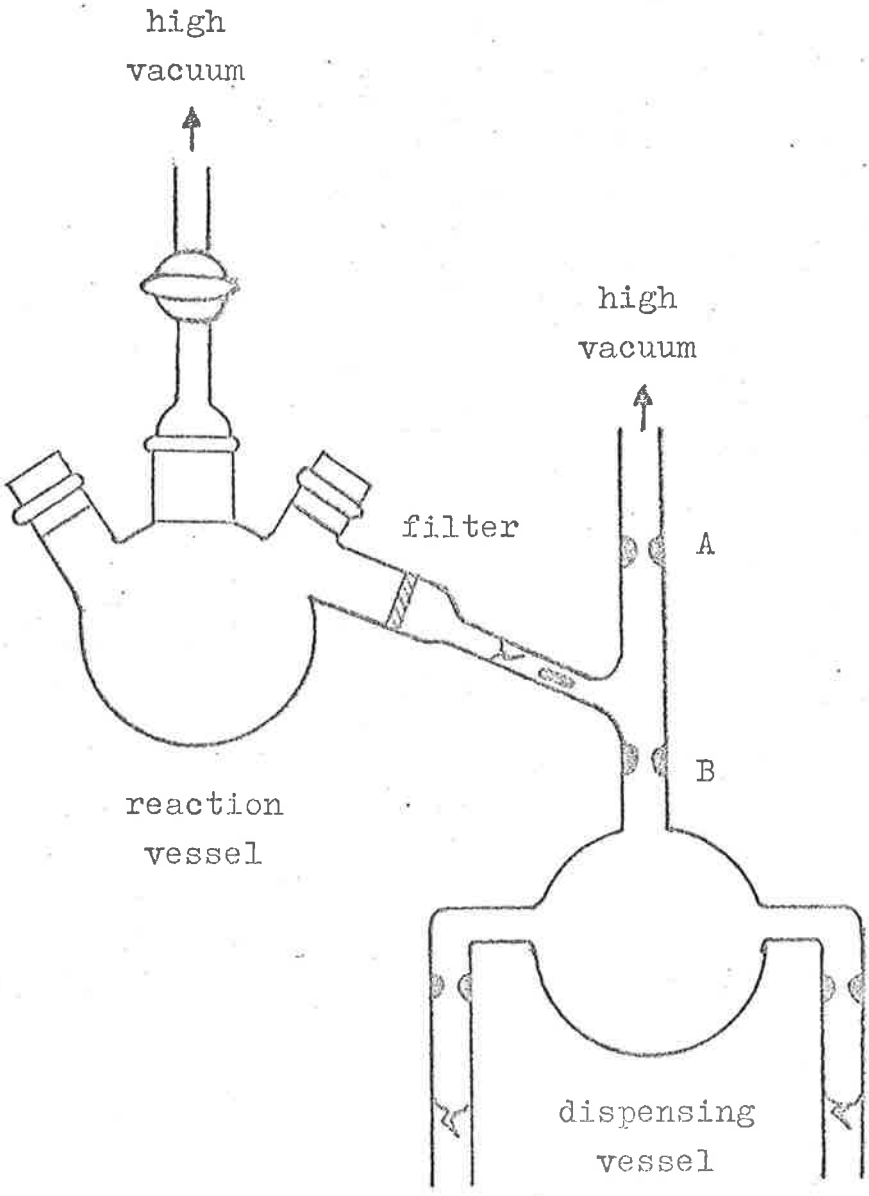

Figure 2.2. Apparatus used for transferring freshly prepared initiator solutions into precalibrated ampoules under vacuum.

However, the magnesium can be activated by the addition of crystal of iodine which attacks the magnesium to form ether soluble magnesium iodide and exposes a fresh metal surface. This method was *never* used and should not be used where the presence of magnesium iodide may affect the course and/or stereospecificity of the reaction. Another very good method which we employed for the less reactive halides was the addition of a few drops of ethylene dibromide. This compound attacks magnesium rapidly, forming ethylene and magnesium bromide and also dries the THF since the magnesium bromide forms THF insoluble hydrates. The presence of a *slight* excess of magnesium bromide has no effect on the resulting polymerization (section 4.2.1).

(2) The Grignard preparation does not proceed to completion. Good yields can be obtained when the least reactive bromides and chlorides are used and an adequate reaction rate maintained. One possible side reaction accompanying the preparation is coupling between RMgX and RX:

$$RMgX + RX \rightarrow MgX_2 + R_2$$

Vapor phase chromatography of a hydrolysed sample of n-BuMgBr failed to show any trace of n-octane in our system. One method that has been used (e.g. ref. 41) to remove volatile impurities from the Grignard reagent is to evaporate all of the ether under vacuum. The solid Grignard compound is then *gently* heated to

remove the last traces of volatiles and finally dissolved in freshly distilled ether. All of these operations must be done under high vacuum to ensure complete moisture and oxygen free conditions.

2.3.2 *Dialkyl magnesium compounds*

The most convenient laboratory method for preparing these compounds is to treat the corresponding Grignard reagent with a two fold excess of dioxan which precipitates the magnesium halide as the bis-dioxan complex, forcing the Schlenk equilibrium 1.1 to the left.[73,75] The dialkyl magnesium is left in solution.

$$R_2Mg + MgBr_2 \rightleftharpoons 2RMgX \qquad (1.1)$$

$$\downarrow \text{ 2 dioxan}$$

$$MgBr_2.2 \text{ dioxan}$$

The apparatus used is shown in figure 2.3. Dioxan was outgassed and the required amount distilled into the graduated cylinder attached to the reaction vessel which was then sealed from the line. The Grignard solution was broken in by rupturing the breakseal and the mixture thoroughly shaken. A white precipitate formed immediately. This solution was allowed to stand, with occasional shaking, for two days and the clear, colourless solution of dialkyl magnesium filtered into the dispensing vessel.

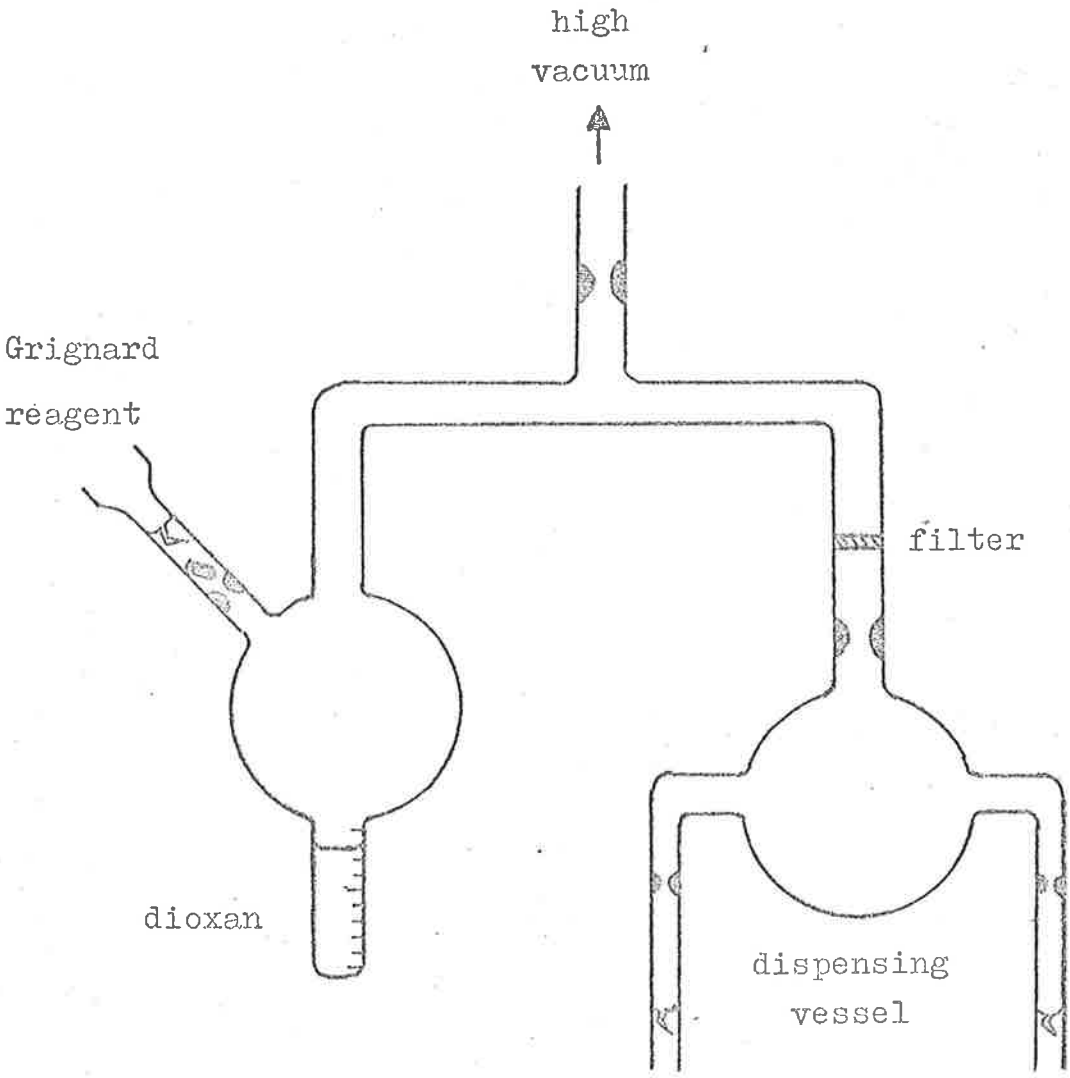

Figure 2.3. Apparatus used for preparing and dispensing a solution of dialkyl-magnesium from the corresponding Grignard reagent using the $MgBr_2$.bis-dioxan precipitation method.

The main disadvantage of this method is that the products are not always free from halogen and if this is a significant consideration the Mg - R_2Hg exchange procedure is to be preferred.[74,75]

Tests for the presence of bromide (Volhard's method[76]) in solutions of dialkymagnesium compounds prepared by the $MgBr_2$-bis-dioxan precipitation method were negative and it was therefore assumed that this method of preparation was adequate.

The other disadvantage of this method is the introduction of another potential solvating agent (1,4-dioxan) into the system. This disadvantage was neglected because although solvent polarity does affect the rates of exchange in organomagnesium systems (section 1.2.3) the effect is minor and the amount of excess dioxan remaining in the system after precipitation of the halide-dioxan complex would be negligible compared with the amount of THF in the solution.

2.3.3 *Magnesium bromide*

Commercial magnesium bromide consists of the hexahydrate $MgBr_2 \cdot 6H_2O$ and so is unsuitable to add to the polymerizing solution. Several methods are available for preparing small amounts of anhydrous bromide or the ether solvated magnesium bromide.[75] These consist of,

(1) direct combination of the elements,

(2) halide exchange between Mg and $HgCl_2$, and

(3) Reaction between magnesium and 1,2 - dibromoethane in ether.

The method used in this work was the latter where THF was the solvent.

$$Mg + BrCh_2CH_2Br \xrightarrow{THF} MgBr_2 + CH_2 = CH_2 \qquad (2.1)$$

The apparatus and method was identical to that used for the preparation of Grignard reagents (section 2.3.1). Because reaction 2.1 is very exothermic, the reaction vessel was frequently cooled with ice to prevent excessive frothing. The concentration of magnesium bromide was determined by Volhard's titration method which consists of acidifying the bromide solution with dilute nitric acid, reacting with excess of standard silver nitrate and the residual silver nitrate determined with standard ammonium or potassium thiocyanate, using ferric alum as indicator.[76]

2.3.4 *Standardization of Initiator solutions*

Many techniques have been used to determine the concentration of organomagnesium compounds. These include proton magnetic resonance,[77] ultra-violet spectroscopy[78] and various titration methods for determining the halide content (Volhard's method) or the concentration of active alkyl magnesium bonds.[4]

The method employed was the latter, and consisted of hydrolysing the active alkyl-magnesium bonds with standard acid and then titrating the remaining acid with standard alkali using phenolphthalein as indicator.

The Grignard reagent (5 cm^3) was pipetted into a flask containing distilled water (ca. 10cm^3). Standard hydrochloric acid (0.100 mol dm^{-3}) was pipetted into the flask and several drops of phenolphthalein indicator added. The solution was heated gently to complete the hydrolysis and then titrated with standard sodium hydroxide (0.100 mol dm^{-3}). The reactions are summarized as follows.

$$x\text{RMgX} + x\text{H}_2\text{O} \rightarrow x\text{RH} + x\text{MgX(OH)} \quad (2.2)$$

$$x\text{MgX(OH)} + x\text{HCl} \rightarrow x\text{MgX(Cl)} + x\text{H}_2\text{O} \quad (2.3)$$

and

$$y\text{R}_2\text{Mg} + 2y\text{H}_2\text{O} \rightarrow 2y\text{RH} + y\text{Mg(OH)}_2 \quad (2.4)$$

$$y\text{Mg(OH)}_2 + 2y\text{HCl} \rightarrow y\text{MgCl}_2 + 2y\text{H}_2\text{O} \quad (2.5)$$

where x, y are the proportions of RMgX and R_2Mg present in solution respectively.

A typical calculation is as follows:-

Volume of organomagnesium compound = 5.0 cm^3

Volume of 0.100 mol dm^{-3} HCl added = 40.0 cm^3

Volume of 0.100 mol dm^{-3} NaOH needed to titrate remaining HCl = 17.15 cm^3

$\therefore$ amount of acid that reacted with the organomagnesium compounds = 2.285×10^{-3} mol.

Total number of active R-Mg bonds = $(x + 2y)$ mol

Total amount of acid required to

hydrolyse the active R-Mg bonds = $(x + 2y)$ mol

$\therefore$ Amount of active R-Mg bonds present = 2.285×10^{-3} mol

Hence [active R-Mg bonds] = 0.45_7 mol dm^{-3}

Notice that the total initial concentration of active alkyl-magnesium bonds $[G]_o$ has been calculated, and not the individual concentrations of RMgX and R_2Mg.

In fact

$$[G]_o = [RMgX]_o + 2[R_2Mg]_o \qquad (2.6)$$

and the individual concentrations on the right hand side of eqn. (2.6) will be governed by the position of the Schlenk equilibrium. The factors affecting the position of this equilibrium were given in section 1.2.3 and the consequences will be discussed in section 3.6 (c).

2.4 *Polymerization technique*

2.4.1 *Dilatometry*

Dilatometry was used to follow the kinetics of the polymerization of MMA. The other well-used techniques of gravimetric analysis and spectrophotometric analysis were not used due to the inaccuracy of the former and the inapplicability of the latter. Gravimetric analysis suffers from several

disadvantages, viz., it is impossible to detect irregularities in the polymerization conversion curves during the course of any kinetic run and the presence of low molecular weight polymer as well as side products makes determination of the exact weight of polymer formed very difficult.

Spectrophotometric analysis of the decreasing monomer concentration has been applied successfully to styrene polymerizations[79] but here again, under certain condition, the presence of side products which absorb in the same region as the monomer complicate matters.[79c] In our system, the MMA ultra violet absorption is obscured by the strong toluene absorption and so spectrophotometry can not be used.

The dilatometers (volume ca. 9 cm^3) were constructed of pyrex glass with precision bore capillary tubing of internal radius 0.1 cm. Each dilatometer was calibrated by obtaining the weight of water required to fill them to a predetermined reference mark.

Figure 2.4 shows the dilatometer filling apparatus used throughout this work. Precalibrated ampoules of monomer, initiator and solvent (consisting of toluene and THF) were sealed to a reaction vessel, which was transferred to the vacuum line. After evacuating and flaming out to a pressure of 10^{-3} Nm^{-2} the apparatus was sealed from the line. The breakseals of initiator and solvent were ruptured, thoroughly mixed and then placed in a dry ice/ethanol bath at the required temperature, (223K for the

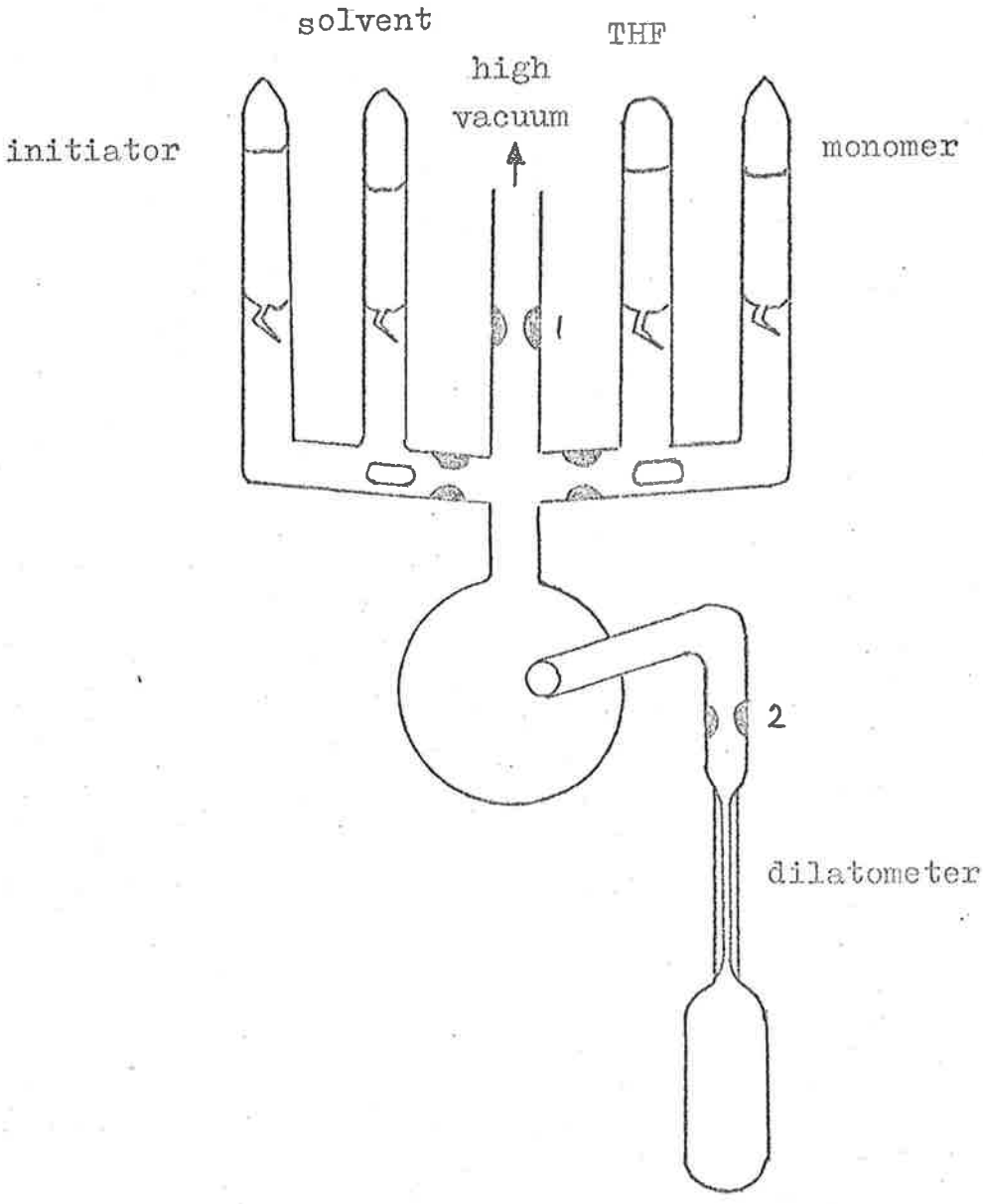

Figure 2.4. Dilatometer filling apparatus.

kinetic runs). The monomer ampoule was cooled to the required temperature by surrounding it with a vacuum jacket filled with dry ice. When both monomer and initiator were at the reaction temperature the monomer breakseal was ruptured and the mixture thoroughly shaken. The dilatometer, which had been precooled to prevent back distillation, was filled, sealed off at constriction 2 and placed in a Townsend and Mercer Minus Seventy Thermostat controlling to ± 0.1 degree. Rates were measured by following the decrease in height of the meniscus in the capillary using a vertically mounted cathetometer.

A slight modification of this kinetic procedure was made when determining Arrhenius parameters, section 3.3.4. One dilatometer was often used for multiple kinetic measurements. This was achieved by first measuring the rate at the lowest temperature of the set and after sufficient points had been recorded to determine the initial rate, the thermostat was rapidly heated to the next temperature, using two 1200 watt immersion heaters. This procedure rarely took more than three minutes and rate measurements were resumed as soon as the initial expansion in the capillary had ceased. The weight of monomer present initially at each temperature was determined from percentage conversion calculated from the previousv run. Zero height and times were determined by extra-polating the recorded height values back to the time at which the heaters were turned

on. This procedure minimized any effects of monomer consumption while the temperature was changing. Successive measurements on new dilatometers were begun at an overlapping temperature with the preceding rate runs to ensure reproducibility of the rates of polymerization.

During polymerization, the free monomer concentration falls as it is incorporated in the macromolecule and the change in monomer concentration is monitored by observing the volume change with time. If the meniscus level falls Δh cm in t minutes, the weight of monomer polymerized, m, is given by (2.7)

$$m = \frac{\pi r^2 \Delta h}{V_T} \quad \text{grams} \tag{2.7}$$

where r = radius of the capillary (0.1 cm) and

V_T = volume change in the polymerization of one gram of monomer at TK.

Now

$$V_T = \frac{1}{\rho_{mT}} - \frac{1}{\rho_{pT}} \tag{2.8}$$

where ρ_{mT} = density of monomer at T K and

ρ_{pT} = density of polymer at T K.

In systems (such as anionic polymerization) where the average molecular weight ($\bar{M}$) of the polymer increases with time, the density of the products (ρ_{pT}) will also be time dependent.

However, East *et al*,[80] have shown that in calculating the percentage conversion from the observed volume contraction, allowance need not be made for the change in polymer density that occurs.

Considering all factors of an addition polymerization, including the presence of initiator units, they derived the following expression for the decrease in volume observed (ΔV).

$$\Delta V = \left(\frac{1}{\rho_m} - \frac{1}{\rho_p}\right) \Delta w_n \qquad (2.9)$$

where Δw_n = the decrease in mass of monomer present in the reaction mixture.

Equations (2.8) and (2.9) are identical when $\Delta w_n = 1$.

From 2.7, the percentage polymerization, $P^{\%}$, is

$$P^{\%} = \frac{100.m}{w_o} = \frac{100.\pi.r^2\Delta h}{V_T \cdot w_o} \qquad (2.10)$$

$$= A\Delta h$$

where w_o = original weight of monomer at t = 0

and A = a constant.

The rate of percentage polymerization, $R_p^{\%}$, is

$$R_p^{\%} = A.\frac{d\Delta h}{dt}$$

which is simply the slope of the curve obtained by plotting the decrease in height of the meniscus versus the time. More will be said about this in section 3.2.

Continue at page 2-19.

It can also be shown[81] that,

$$\ln \frac{[M]_o}{[M]_t} = \ln (1 - A\Delta h) - \ln (1 - \frac{\Delta V}{V_o}) \qquad (2.13)$$

where $[M]_o$ = original monomer concentration at t = 0,

$[M]_t$ = monomer concentration at t = t,

V_o = volume of solution at t = 0

ΔV = volume change at t ⇒ t

Hence if a plot of $\ln \frac{[M]_o}{[M]_t}$ versus time is linear, the internal order with respect to monomer is unity. Care should be taken when studying these plots because at low conversions, i.e. < 10%, any minor deviation from linearity will not be detected especially if the conversion/time curve is linear. What may appear at low conversion, to be a linear ln(Mo/Mt)/time curve may not be linear when larger conversions are taken into account, e.g. figure 3.4 and 3.5.

2.4.2 *Ultra-violet spectroscopy*

Performing all reactions under high vacuum necessitated the use of specially designed high vacuum silica u.v. cells fitted with a graded pyrex seal to facilitate sealing onto the reaction vessel. Cell path lengths ranged from 0.1 cm up to 1 cm. depending on the concentrations used. The apparatus used for filling the cells was identical to that depicted in fig. 2.4

except that the dilatometer was replaced by a high vacuum u.v. cell.

Initial experiments were performed at ambient temperature after mixing at ca.223K and spectra were recorded on a Unicam S.P. 800 spectrophotometer using air as the reference.

Low temperature spectra were recorded on a Unicam S.P. 700 automatic recording spectrophotometer with a specially constructed sample compartment cover to accommodate the cells. This was necessary since their height, including the graded silica/pyrex seal, was 15cm. Originally, the cell carriage consisted of a hollow copper block fitted with an inlet and outlet tube. The coolant was dry nitrogen gas, cooled by passing it through two copper coils immersed in liquid nitrogen. By adjusting the nitrogen flow, the temperature, which was measured with 200 Ω thermistor, could be maintained to within ±5K. A more sophisticated cell holder was designed which could maintain the temperature to within ±0. 5K. Inside the cell block were placed two Solon, 25W, 240 volt strip heaters and a 100Ω STC, F22 thermistor which was connected to a solid state temperature controller designed in this Department. The coolant was again dry nitrogen gas passed through two heat exchangers immersed in liquid nitrogen. An extra gas inlet situated just below the cell face was incorporated to enable cold nitrogen gas to blow over the cell face and so prevent fogging.

All spectra were recorded using air as the reference and the first readings could generally be obtained approximately nine or ten minutes after mixing.

2.4.3 *Treatment of Polymers*

In most cases, the polymerizing mixture was terminated by opening to the atmosphere and then pouring into a ten fold excess of methanol. The methanol insoluble polymer precipitated immediately. This solution was acidified with hydrochloric acid to remove inorganic material and the solution stirred for several hours. The methanol insoluble polymer was filtered, dried and then dissolved in a minimum of benzene and freeze dried. The filtrate, which contained methanol soluble material such as low molecular weight polymer and side products, was evaporated to dryness. The residue was dissolved in benzene and the insoluble inorganic material filtered off. The benzene solution was then freeze dried and the weight of the methanol soluble material recorded.

The instances where the above procedure was not followed were in certain spectroscopic experiments where one drop of methanol was added to terminate the reaction. Also in experiments where the formation of methanol as a side product were investigated, the polymerizing solution was broken open under an atmosphere of nitrogen saturated with water and allowed to

stand for several hours (for details, see section 5.8).

In cases where the number of active alkyl magnesium bonds remaining during polymerization was determined, a solution of iodine in THF was used, (section 5.5).

2.4.4. *Determination of microstructure*

High resolution n.m.r. spectroscopy was used to determine the polymer chain configuration and the theory is discussed in Chapter 4.

Polymer samples were dissolved in ethanol free chloroform to give a final concentration of 3% w/w and spectra were run at 312K using a Varian T 60 n.m.r. spectrometer. Typical spectra are shown in figure 4.1. Proportions of isotactic, heterotactic and syndiotactic triads were obtained directly from the heights of the respective peaks. These values agreed to within ±1% of results obtained by integration.

At the end of this research a Bruker HX-90-E n.m.r. spectrometer was acquired and several samples were analysed using deuterochloroform as solvent and TMS as internal standard.

2.4.5 *Gel Permeation Chromatography.* (g.p.c.)

Molecular weights (MW) and molecular weight distributions (MWD) were determined using g.p.c. and a brief account of the

theory is given in section 4.3.

The instrument was a Waters Associates model 501 ALC/GPC instrument suitable for analytical liquid chromatography as well as g.p.c. The detector was an R-401 refractometer with a sensitivity greater than 6×10^{-6} RI full scale on the most sensitive range. Typically, a concentration change of 1 ppm corresponds to a 1% of full scale deflection on the most sensitive range.

The columns used were linear 4 foot Styragel columns of porosity 10^5 Angstroms. The advantages of the linear columns over the non-linear ones are obvious. Only one column need be used (instead of a bank of 4 or 5) which results in rapid results. Increased resolution is achieved by adding 2 or more columns of the same porosity.

The instrument was calibrated using narrow MWD samples of polystyrene and the curves are shown in figure 4.10.

Polymer samples were dissolved in chloroform to form a 0.2% w/v solution and the injection loop (volume = 5 cm^3) was filled. At a flow rate of 1.4 $cm^3\ min^{-1}$, the optimum injection time was 2 minutes. Using one column, the total time to obtain a chromatogram was 45 minutes.

Elution volumes, Ve, were measured by means of a siphon attached to the sample outlet. A photocell was attached to the siphon outlet and when the siphon emptied, a 'blip' was superimposed on the

recorder trace. The 'absolute' elution volume was thus replaced by what should probably be called the elution count.

CHAPTER 3

KINETIC EXPERIMENTS

3.1 *Introduction.*

The kinetics of the polymerization of MMA initiated by organometallic compounds are complex. Even when the observed rate law is first order in both monomer and initiator, the observed rate constant is generally complex, being a function of any solvating solvents, such as ethers, that may be present.[82] The kinetics are also complicated because of low initiator efficiency due to the susceptibility of the monomer carbonyl group to nucleophilic attack leading to unwanted side reactions such as carbonyl addition and/or chain termination.[83-85]

Polymerizations initiated by Grignard reagents suffer from all of these drawbacks and several others which are not encountered with organometallic initiators such as sodium naphthalene[86] or the dianion of the sodium salt of α-methyl styrene tetramer.[82] In these systems the initiating species is known, whereas with Grignard reagents, both R_2Mg and RMgX are known to react with α, β-unsaturated esters and so both should be capable of initiating polymerization. Also, the magnesium halide present in the Grignard solution, may play more than a passive role in the polymerization as is postulated in the reaction of Grignard reagents with ketones and nitriles (section 1.3).

This chapter describes the kinetic experiments performed using various Grignard reagents as well as the ultra-violet spectra of the

polymerizing solution. As mentioned in Section 1.5, the Grignard reagents were prepared in THF because they are known to be monomeric in this solvent (although at low temperatures some dimeric species may exist[31]) and toluene was added to keep the solution homogeneous at the temperatures and concentrations employed.

3.2 *Treatment of Results.*

Dilatometry was used to follow the kinetics of the reaction and the relevant experimental procedure is described in section 2.4.1. From the contraction in height of the meniscus, values of $\ln([M]_o/[M]_t)$ can be calculated (eqn. 2.13) and a plot of this value versus time determines whether or not the polymerization is internally first order in monomer. Values of $\ln([M]_o/[M]_t)$ were calculated using a C.D.C. 6400 computer programmed in Fortran. Plots of $\ln([M]_o/[M]_t)$ versus time and percentage conversion versus time were also obtained and the slopes and intercepts with their respective standard errors were computed using the one program. The initial meniscus height at zero time was calculated by extrapolating the contraction versus time curve to t = 0.

From eqn. (2.10), the percentage polymerization, $P^{\%}$, is given by

$$P^{\%} = \frac{100.\pi r^2 \Delta h}{V_T \cdot w_o} \qquad (2.10)$$

where r = the radius of the capillary,

w_o = the weight of monomer present in the dilatometer at t = 0, and

V_T = the change in density on going from monomer to polymer.

Now $V_T = \left(\frac{1}{\rho_{mt}} - \frac{1}{\rho_{pt}} \right)$

where ρ_{mT} and ρ_{pT} are the density of monomer and polymer at the reaction temperature. ρ_{mT} was calculated using the data of Matheson *et al*[87] and ρ_{pT} from studies obtained by Moody.[88]

Since only a fraction of the total volume of the polymerizing solution was poured into the dilatometer, w_o, the original weight of monomer in the dilatometer was calculated from the expression

$$w_o = \frac{v_o^{293} \times \text{volume monomer} \times 0.944}{\text{total volume of solution}} \qquad (3.1)$$

where v_o^{293} = the volume of the solution in the dilatometer at 293K and 0.944 is the density of MMA at that temperature.

Since the volume of the solution present in the dilatometer can only be measured at the temperature of the reaction, a correction factor must be used to account for the density changes of the solution with temperature and THF concentration. Using the relationship obtained by Chaplin,[89]

$$\rho_{ST} = 0.6411 + 0.0238\chi_{THF} - 0.00094T \qquad (3.2)$$

where T = the temperature of polymerization and

χ_{THF} = the mole fraction of THF.

Hence

$$v_o^{293} = \frac{v_T \times \rho_{ST}}{\rho_{ST = 293}} \qquad (3.3)$$

where V_T = volume of solution measured at T K

and $\rho_{ST=293}$ = density of solution calculated at 293K.

The percentage polymerization and the percentage rate of polymerization, $R_p^{\%}$, could therefore be determined conveniently using dilatometry. One point should be noted. The rate of polymerization, R_p, is conventionally defined as the rate of disappearance of monomer,

$$R_p = -\frac{d[M]}{dt} \tag{3.4}$$

and the rate of percentage polymerization, $R_p^{\%}$, is defined as

$$R_p^{\%} = \frac{d}{dt}\{100([M]_o - [M]_t)/[M]_o\} \tag{3.5}$$

which becomes

$$R_p^{\%} = -\frac{100}{[M]_o}\frac{d[M]}{dt} \tag{3.6}$$

Therefore the rate of percentage polymerization is related to the conventional rate of polymerization by

$$R_p^{\%} = \frac{100}{[M]_o} \cdot R_p \tag{3.7}$$

This relationship is very significant, especially when the external order of reaction with respect to monomer is determined by dilatometry. A straight line plot of $\log_{10}(R_p^{\%})$ versus $\log_{10}[M]_o$ with slope zero will in fact represent an external order with respect to monomer of unity by virtue of eqn. (3.7).

3.3 *n-BuMgBr / MMA / toluene / THF*

Initial kinetic experiments were performed to determine suitable concentrations and conditions for study by dilatometry. The most convenient rate is of the order of 10 percent per hour, although faster rates can be measured. The major disadvantage with dilatometry was that readings could not be obtained much before 10 minutes after mixing and so any unusual effects, such as rapid monomer consumption during the first few minutes, could not be observed. Any such rapid monomer consumption can be detected by comparing the amount of polymer recovered with the observed kinetics. In all of our systems, the gravimetric yield agreed well with the theoretical yield (±1%) and it was concluded that rapid initial monomer consumption does not occur.

3.3.1 *Order with respect to N-BuMgBr*

The dependence of polymerization rate on the initial Grignard reagent concentration, $[G_n]_o$, was determined at 223K by keeping the monomer concentration and concentration of THF constant while varying the Grignard reagent concentration. This was achieved by keeping the volume of monomer and toluene constant and evaporating THF from, or adding to, the initiator solution to maintain a constant THF: toluene volume fraction of 1:2. Figures 3.1 and 3.2 show plots of $\log_{10}(R_{p_o}/\text{mol dm}^{-3}\text{s}^{-1})$ versus $\log_{10}([G_n]_o/\text{mol dm}^{-3})$ and R_{p_o} versus

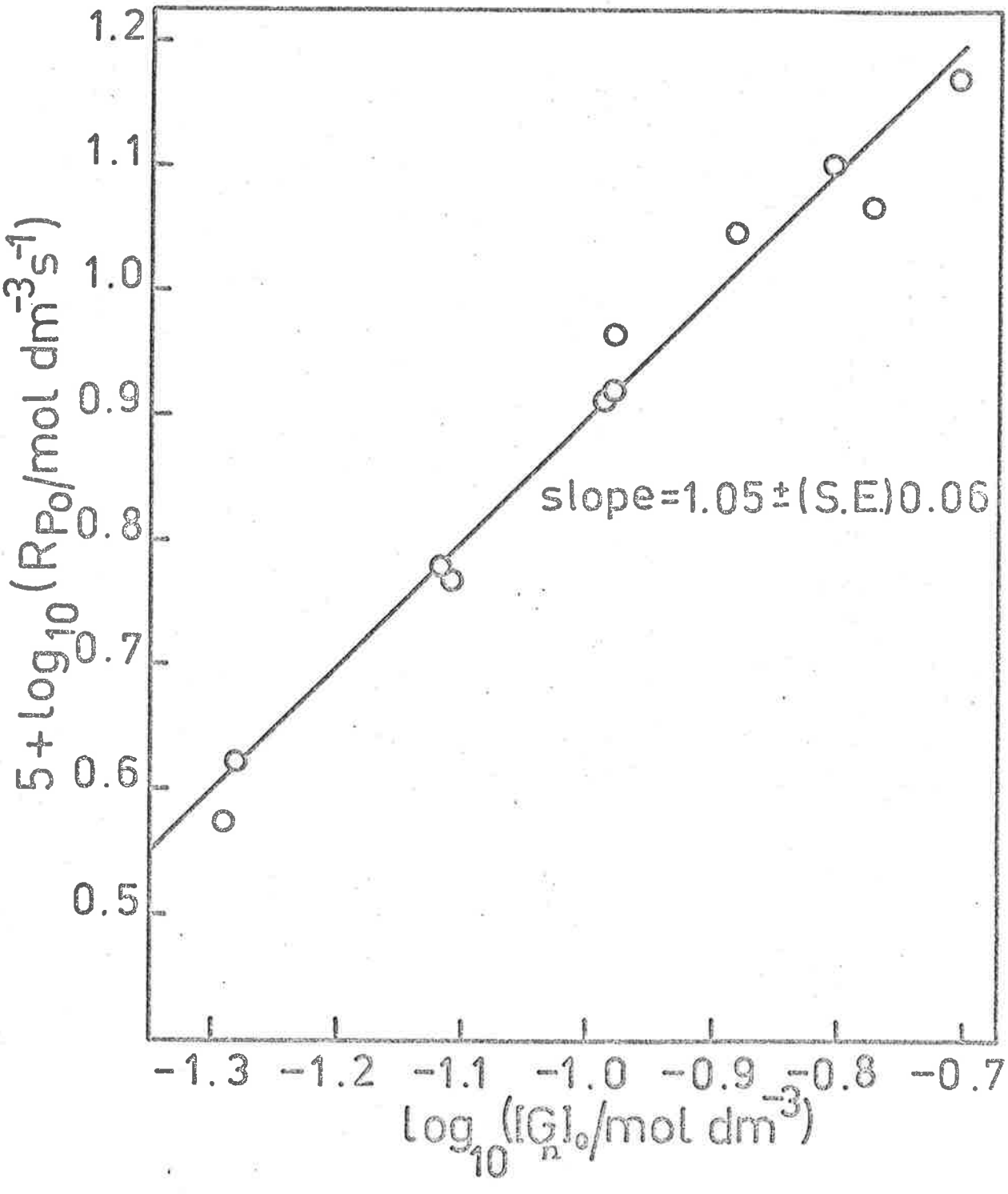

Figure 3.1. Dependence of initial rate of polymerization on initial concentration of active n-BuMg bonds where;

$$[G_n]_o = [\text{n-BuMgBr}]_o + 2[(\text{n-Bu})_2\text{Mg}]_o$$

T = 223K; $[\text{MMA}]_o$ = 2.76 mol dm^{-3}; [THF] = 2.87 mol dm^{-3}

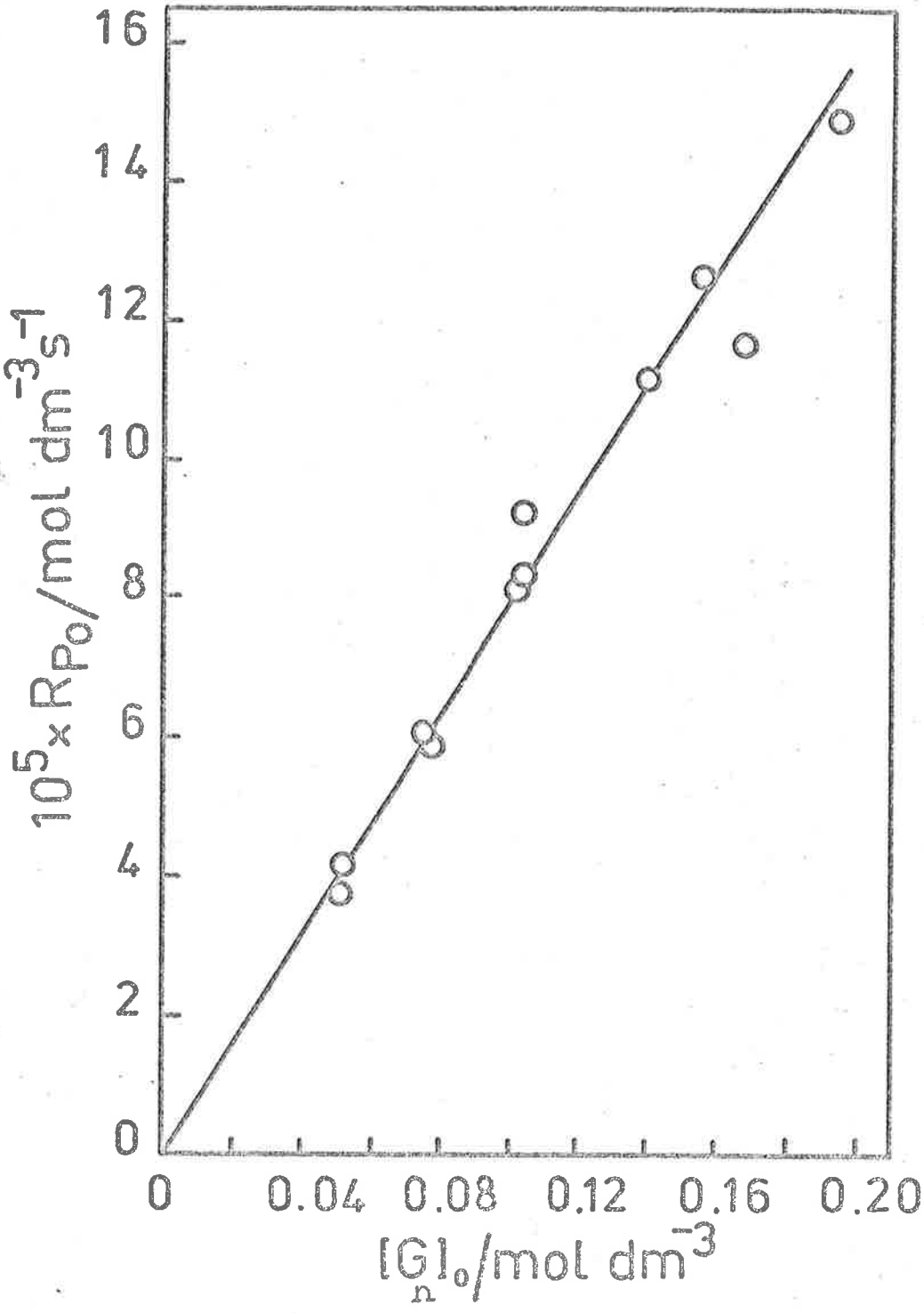

Figure 3.2. External first order dependence of initial rate of polymerization on the initial concentration of active n-BuMg bonds under the same conditions as stated in figure 3.1.

$[G_n]_o$ respectively. Here R_{p_o} /mol $dm^{-3}s^{-1}$ is the initial rate of polymerization obtained from the initial rate of percentage polymerization, $R^{\%}_{p_o}$, by means of equation (3.7) and $[G_n]_o$ is the initial concentration of active n-butyl-magnesium bonds as defined by equation (2.6),

$$[G_n]_o = [RMgX]_o + 2[R_2Mg]_o \qquad (2.6)$$

where the individual concentrations of $[RMgX]_o$ and $[R_2Mg]_o$ are determined by the Schlenk equilibrium at that particular temperature.

From figure 3.1 and 3.2 it can be concluded that the initial rate of polymerization is directly proportional to the initial alkyl-magnesium concentration $[G_n]_o$. When $[G_n]_o < 0.03$ mol dm^{-3}, the polymerization rate becomes very slow and irreproducible. The reason for this is uncertain, but it is most likely due to the presence of trace impurities in either the initiator, monomer or solvent. This idea is strengthened by the observation that although reproducibility is better than five percent for any one batch of initiator and monomer, correlation between different batches is less dependable.

Figure 3.3 shows plots of percentage conversion versus time over the concentration range studied. As can be seen, these plots are linear, even up to 40%, and the slopes give the rate of percentage polymerization. Linear conversion curves have also been reported by Watanabe *et al*[55b] (up to 40% conversion) and Allen *et al*[54a, b] (up to 5%) in diethyl ether: toluene (1:9) mixtures at 223K.

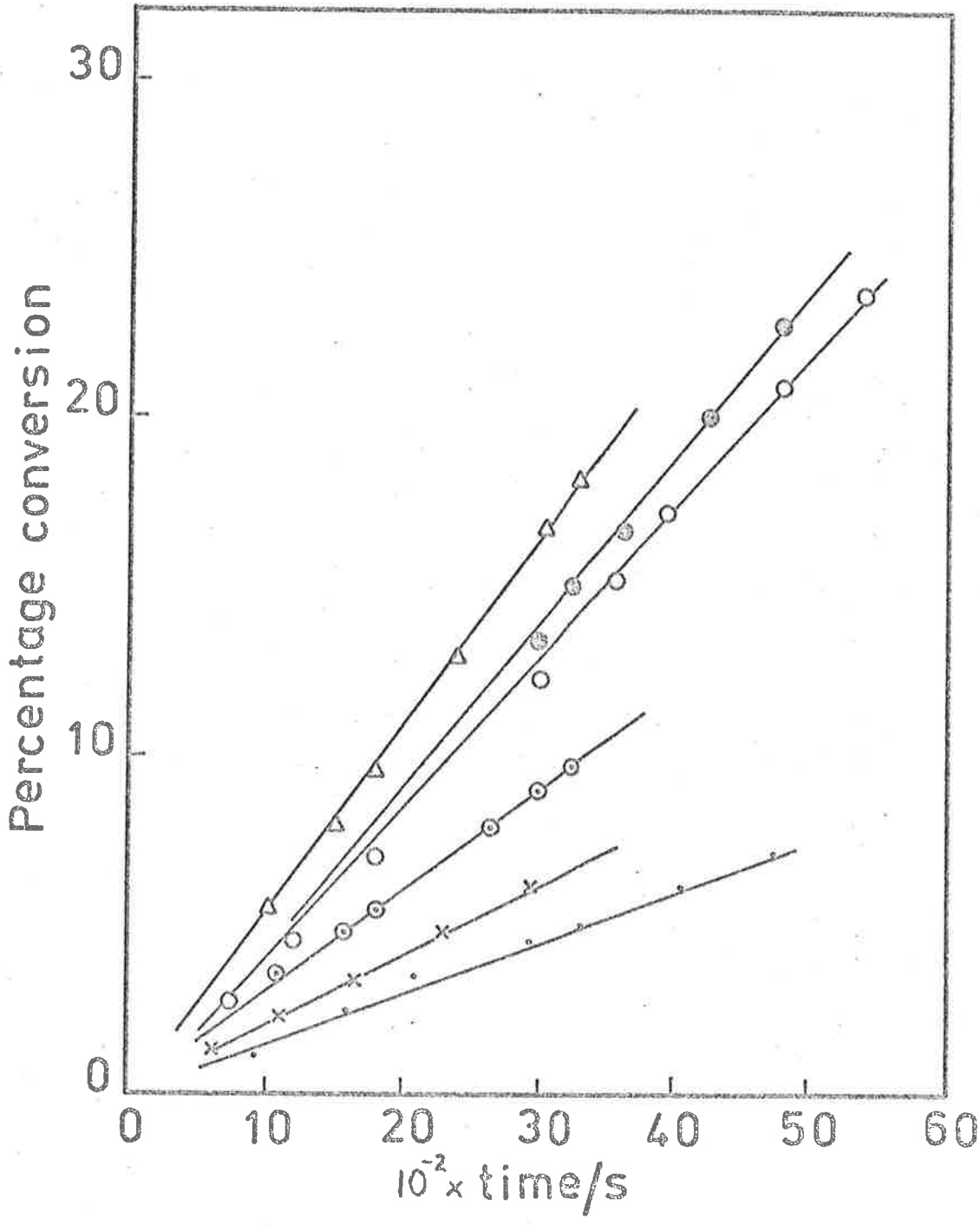

Figure 3.3. Percentage conversion versus time plots for various concentrations of active n-BuMg bonds. T = 223K; $[MMA]_o$ = 2.76 mol dm^{-3}; [THF] = 2.87 mol dm^{-3}; $[G_n]_o$/mol dm^{-3} = 0.195(Δ); 0.156(●); 0.13(○); 0.103(⊙); 0.077(x); 0.052(·).

TABLE 3.1

External order with respect to n-BuMgBr. (a)

$[MMA]_o = 2.7_6$ mol dm^{-3}

$x_{THF} = 0.28$; $[THF] = 2.8_7$ mol dm^{-3}

$T = 223K$

$[G_n]_o$/mol dm^{-3}	$\log_{10}[G_n]_o$	$10^5 R_{p_o}$/mol $dm^{-3}s^{-1}$	$\log_{10}(R_{p_o}$/mol$dm^{-3}s^{-1})+5$
0.051	-1.292	3.75	0.5740
0.052	-1.284	4.195	0.6227
0.076	-1.119	6.04	0.7810
0.078	-1.108	5.88	0.7694
0.10_3	-0.987	8.17	0.912
0.104	-0.983	9.30	0.9684
0.104	-0.983	8.33	0.9206
0.130	-0.886	11.11	1.045
0.156	-0.807	12.69	1.1035
0.168	-0.775	11.67	1.067
0.195	-0.7099	14.93	1.174

(a) Concentration of n-BuMgBr is defined according to eqn.(2.6)

The complete results of this series of experiments are recorded in Table 3.1.

3.3.2 *Monomer dependence*

As discussed in section 2.4.1, the concentration of monomer at any particular time t, can be calculated from the fractional volume contraction of liquid in the dilatometer between t = 0 and t.

Figures 3.4 (a) and (b) show plots of $\ln([M]_o/[M]_t)$ versus time for various values of $[G_n]_o$. It would appear from figure 3.4 (a) that the internal order with respect to monomer is unity. However, figure 3.4 (b) clearly shows the deviation from linearity of the first order plot when large conversions are considered. Monomer consumption appears to be first order up to 12 per cent conversion but at large conversions (figure 3.4 (b)) this assumption is incorrect. The ln/time curves are no longer linear, passing through the origin. This apparent discrepancy can be explained on the basis that it is very difficult to distinguish between linear and non-linear $\ln([M]_o/[M]_t)$/time plots over small conversions. Thus the internal order with respect to monomer appears to be *zero* which is consistent with the mechanism proposed by Erusalimskii for the acrylonitrile/Grignard system[64b], (section 1.4.2, eqn. 1.19).

The external monomer dependence was determined at different initial monomer concentrations and constant $[G_n]_o$ and χ_{THF} by varying the amount of toluene present to keep the total volume of

Figure 3.4(a). Integrated rate plots for the same runs as shown in figure 3.3.

When the time scales of figs. 3.4(a) and 3.3 are compared, it can be seen that none of the integrated rate plots above, have been calculated beyond 10 per cent conversion.

T = 223K; $[MMA]_o$ = 2.76 mol dm^{-3}; [THF] = 2.87 mol dm^{-3}; $[G_n]_o$/ moldm^{-3} = 0.195(Δ); 0.156(●); 0.13(○); 0.103(⊙); 0.077(×); 0.052(·).

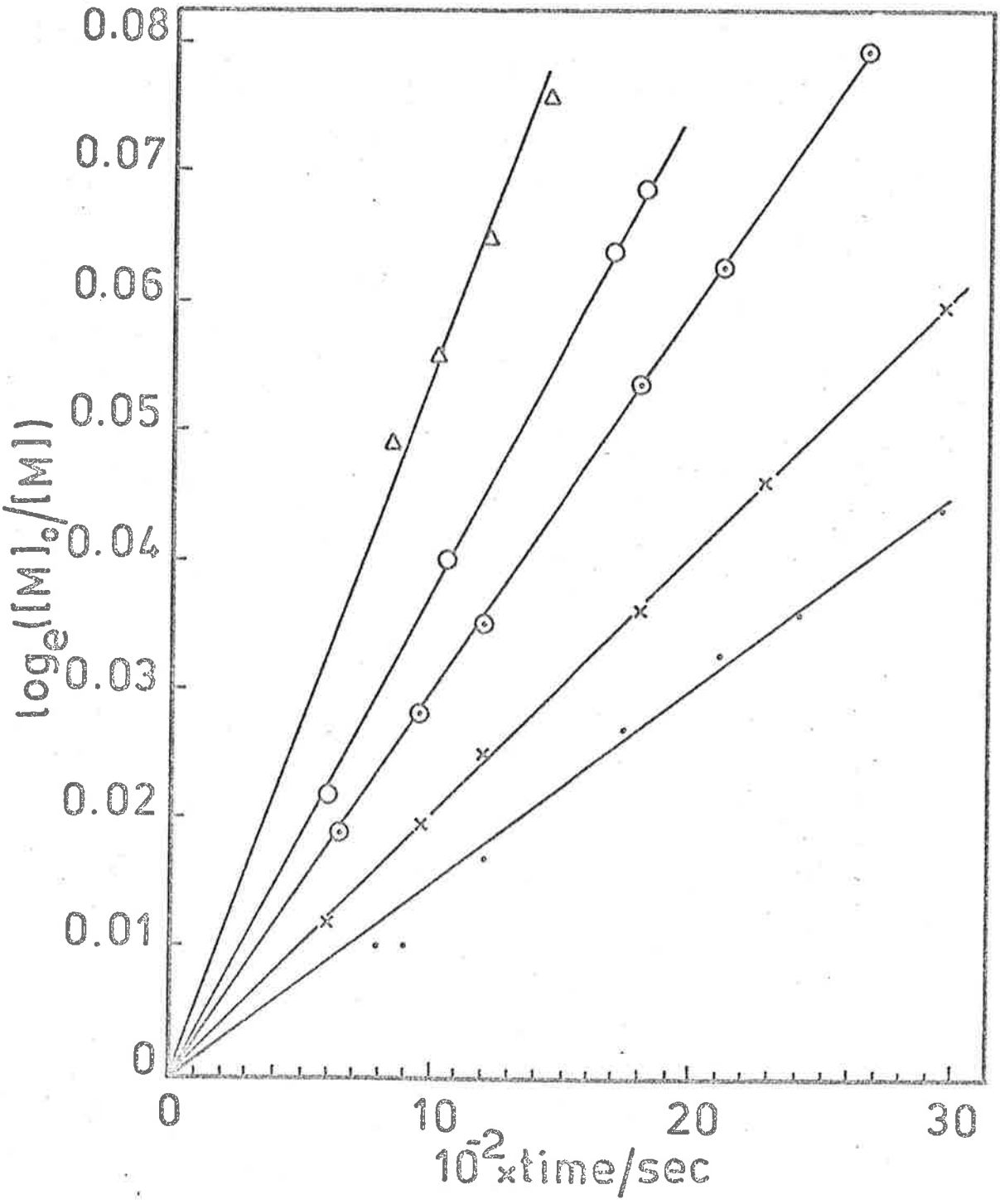
0.08
0.07
0.06
0.05
0.04
0.03
0.02
0.01
0
$\log_e([M]_o/[M])$
0
10
20
30
10^{-2} x time/sec

Figure 3.4(b). Integrated rate plots for two of the runs in fig. 3.4(a) taken over long conversions. The curves are no longer linear, and show a distinct upward deviation, indicating that the internal order with respect to monomer concentration is zero and not unity as would be predicted from fig. 3.4(a).

T = 223K; $[MMA]_o$ = 2.76 mol dm^{-3}; [THF] = 2.87 mol dm^{-3}; $[G_n]_o$/ mol dm^{-3} = 0.103 (⊙); 0.130 (○).

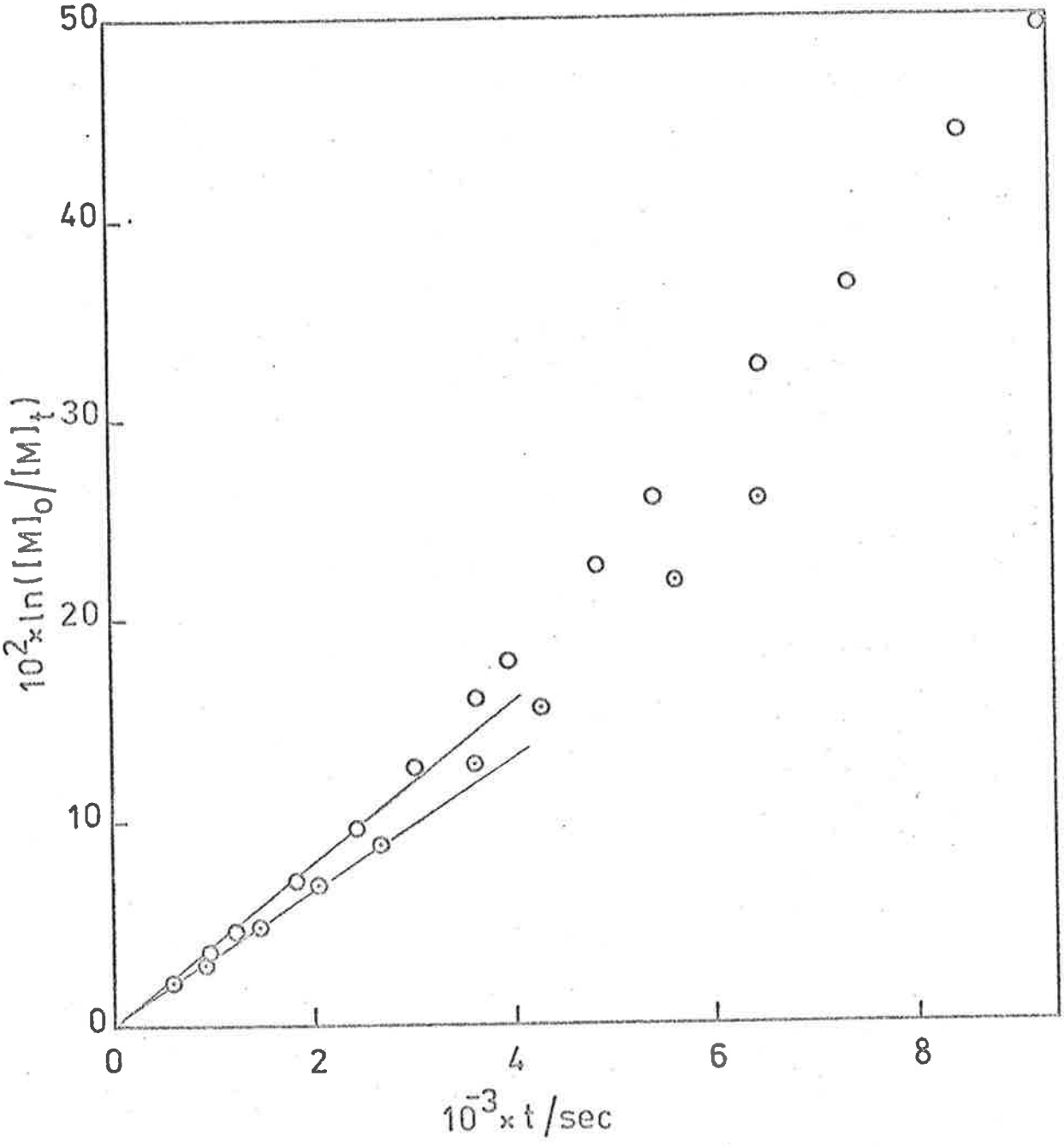
50
40
30
20
10
0
0
2
4
6
8
$10^2 \times \ln([M]_0/[M]_t)$
$10^{-3} \times t$ /sec

solution constant. The results are shown in figures 3.5 and 3.6.

Rate calculations were performed observing the precautions outlined in section 3.2 and it appears that the external order with respect to monomer is unity.

The lines and slopes of figures 3.5 and 3.6 are those determined by regression analysis. The standard error (S.E.) in the slope of the log- log plot is large because of the small number of points used for the determination. Analysis of the linear plot confirmed that the origin lay within the S.E. of the intercept. The 90% confidence limits were also determined and are shown in figure 3.6. The 100(1 - α) confidence limits were calculated using the expression[90]

$$y_{cl} = y_i \pm t_{\alpha/2}(\phi = n-2) \quad \sigma \left(\frac{1}{n} + \frac{(x_i - \bar{x})^2}{\Sigma(x_i - \bar{x})^2} \right)^{\frac{1}{2}} \qquad (3.8)$$

where y_{cl} = values of the confidence limits at x_i, y_i

$\bar{x}$ = mean x value

σ = standard error of y_i from the linear regression line

t = t test parameter

n = number of degree of freedom

α = probability parameter defining the 100 (1 -α) confidence limits.

In these experiments, $x_{THF} = 0.10$, [THF]= 1.0 mol dm^{-3} compared with $x_{THF} = 0.28$ [THF] = 2.8$_7$ mol dm^{-3} in section 3.3.1 above.

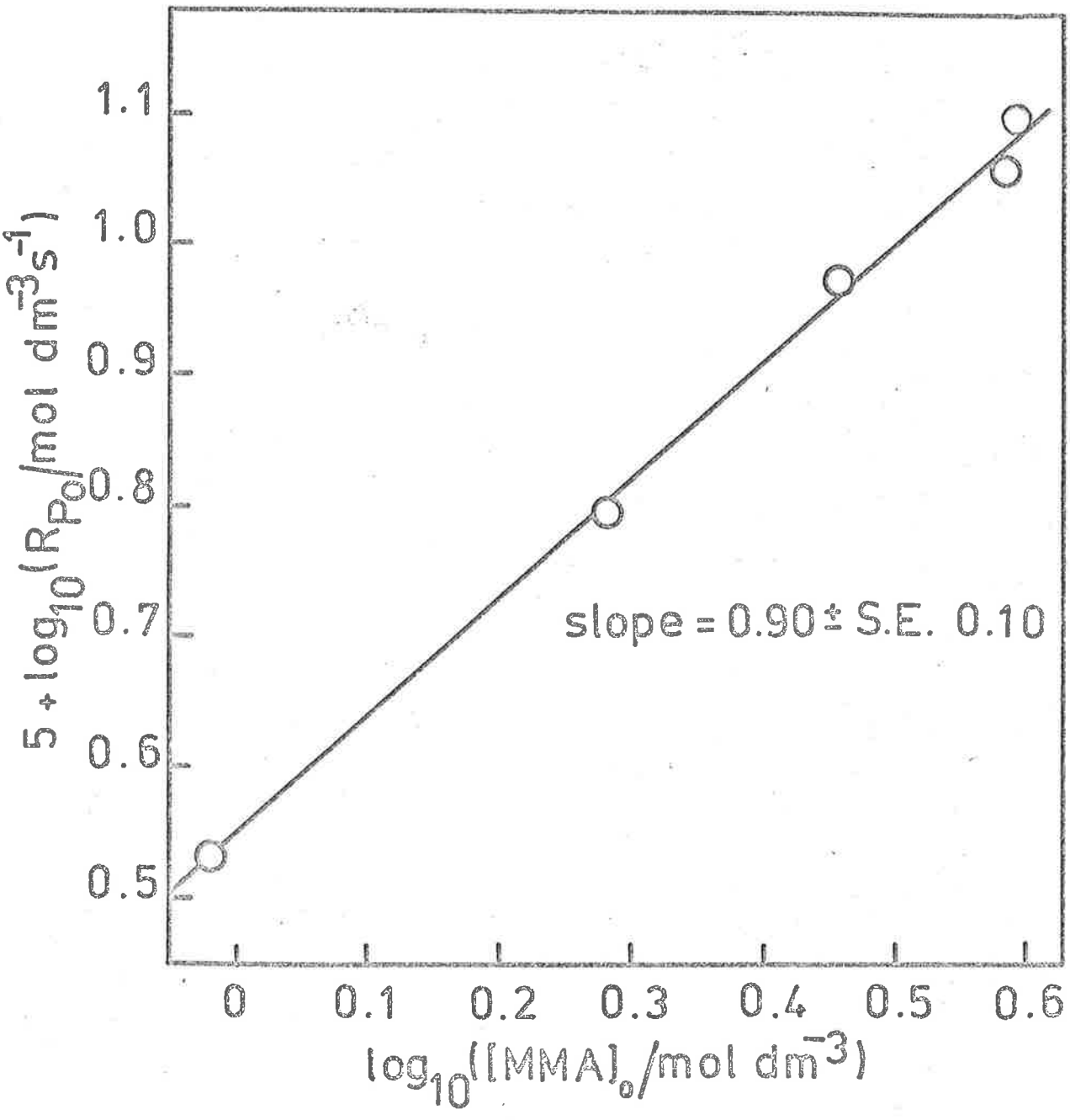

Figure 3.5. Dependence of initial rate of polymerization on initial monomer concentration.
T = 223K; $[G_n]_o$ = 0.036 mol dm^{-3}; [THF] = 1.0 mol dm^{-3}.

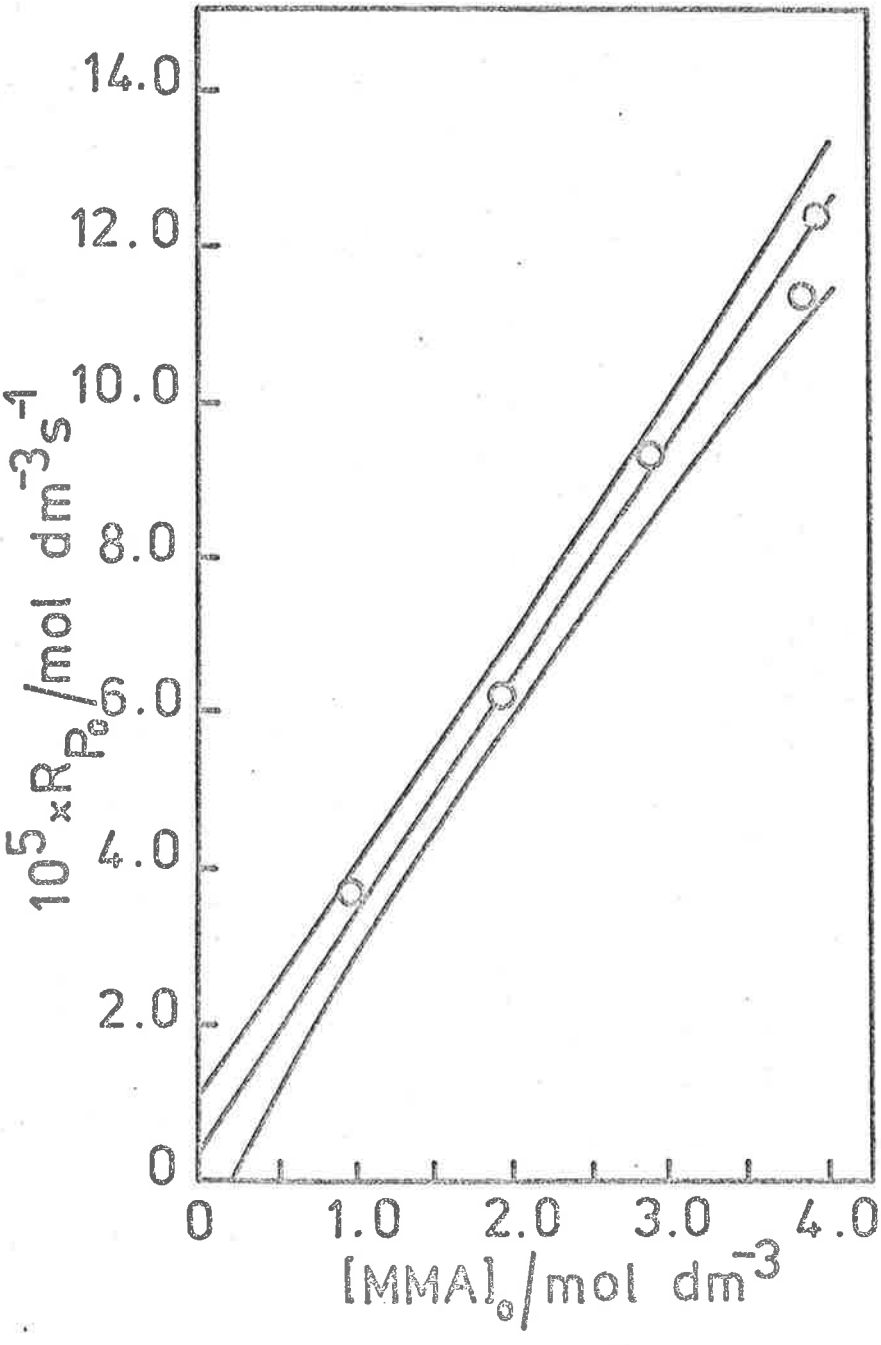

Figure 3.6. External first order dependence of initial rate of polymerization on the initial monomer concentration under the same conditions stated in figure 3.5. The 90% confidence limits are also shown.

However, we have found no evidence throughout the duration of this work to suggest that the order with respect to $[G_n]_o$ and/or $[M]_o$ should differ at different THF mole fractions even though the overall rate, R_{p_o}, is dependent on χ_{THF} (section 3.3.3).

3.3.3 *Effect of tetrahydrofuran*

Figure 3.7 shows the effect of THF mole fraction on the rate of polymerization. The error bars on the points are not the standard errors of the slopes calculated from the computer plots, but are an estimate of the maximum possible experimental error arising from errors in calibration of volumes, dispensing solutions and extrapolation of the conversion/time curves, etc. A maximum error in the rate of ±5% seemed realistic. No attempt was made to fit a linear relationship between R_{p_o} and χ_{THF} although such a relationship could be justified when $\chi_{THF} > 0.12$. At very low THF mole fractions, R_{p_o} appears to level off to a maximum, although in this region, errors in the calculation of χ_{THF} become significant. This may account for the deviation from linearity when $\chi_{THF} < 0.12$, but it is interesting to note that there is a marked change in polymer stereospecificity at this THF concentration, section 4.2.1, figure 4.4.

Nevertheless, it is obvious that the rate of polymerization decreases as the mole fraction of THF increases. This is consistent

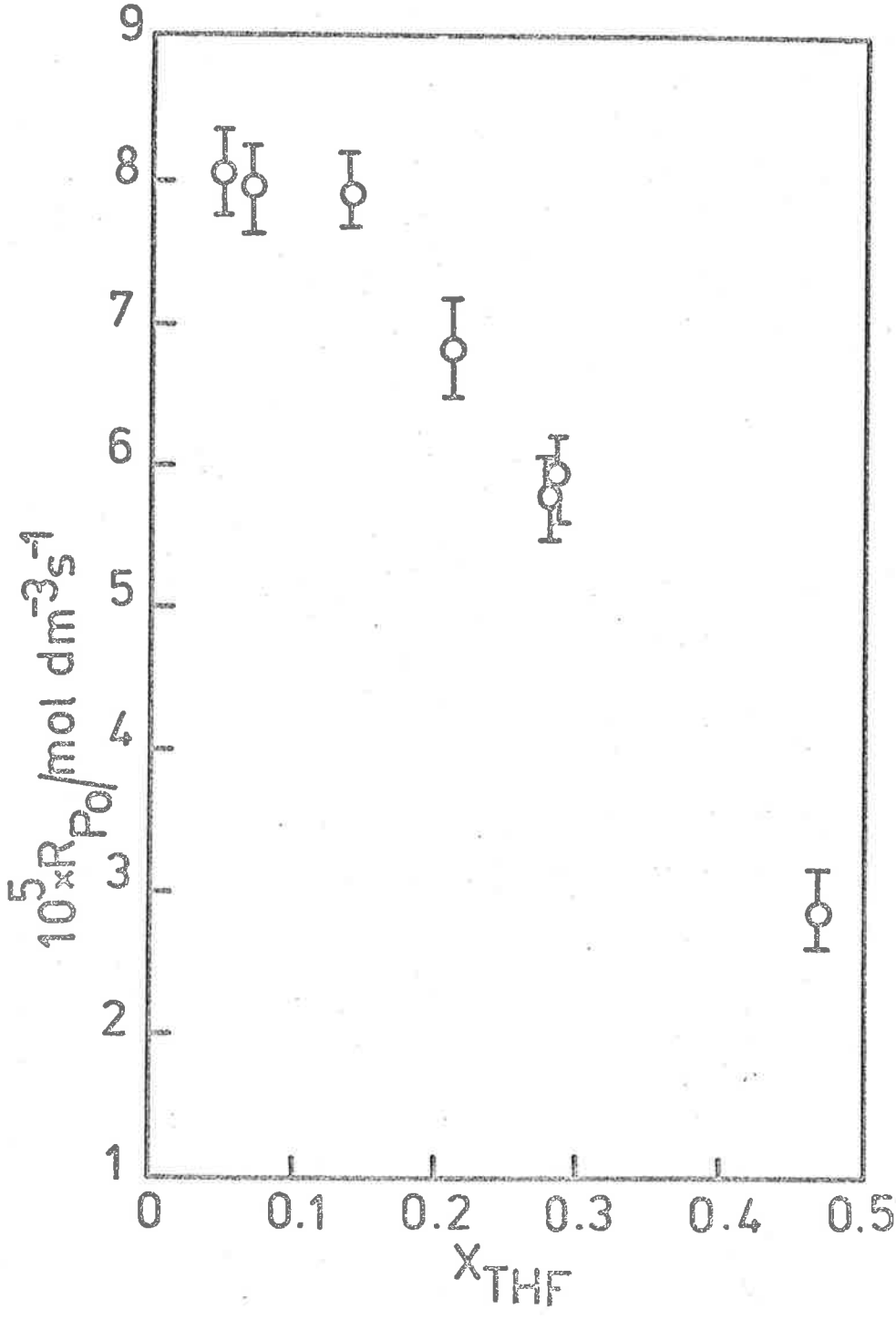

Figure 3.7. The effect of THF mole fraction (x_{THF}=0.1 THF) on the initial rate of polymerization using n-BuMgBr. T = 223K; $[G_n]_o$ = 0.10 mol dm^{-3}; $[MMA]_o$ = 2.76 mol dm^{-3}.

with the results obtained by Allen *et al* using n-BuMgBr in diethyl ether /toluene solutions at 223K.[54a]

3.3.4 *Temperature dependence*

The effect of temperature on the rate is shown in figures 3.8 and 3.9. The features are similar to those reported earlier for the diethyl ether/toluene system. In figure 3.8, $\chi_{THF} = 0.28$, ($[THF] = 2.8_7$ mol dm^{-3}) and curve I is the temperature dependence observed when initiation is performed at 223K and the dilatometer then placed in the thermostat at the required temperature. Curve II is the temperature dependence observed when initiation occurs at 263K for one minute and the rate then measured at the desired temperature. The arrows on the curves indicate the direction the temperature was varied when one dilatometer was used for more than one rate determination. The duplicated points on curve I are those where another dilatometer was freshly prepared (see section 2.4.1 for experimental details). From figure 3.8, the inversion temperature, T_i, occurs at ca. 251K and the activation energy below T_i is 17 ±S. E.1 kJ mol^{-1}.

Figure 3.9 shows the temperature dependence when $\chi_{THF} = 0.07$ $[THF] = 0.72$ mol dm^{-3}. In this case $T_i = 244K$ and the energy of activation when $T < T_i$ is 19 ± 2 k J mol^{-1}.

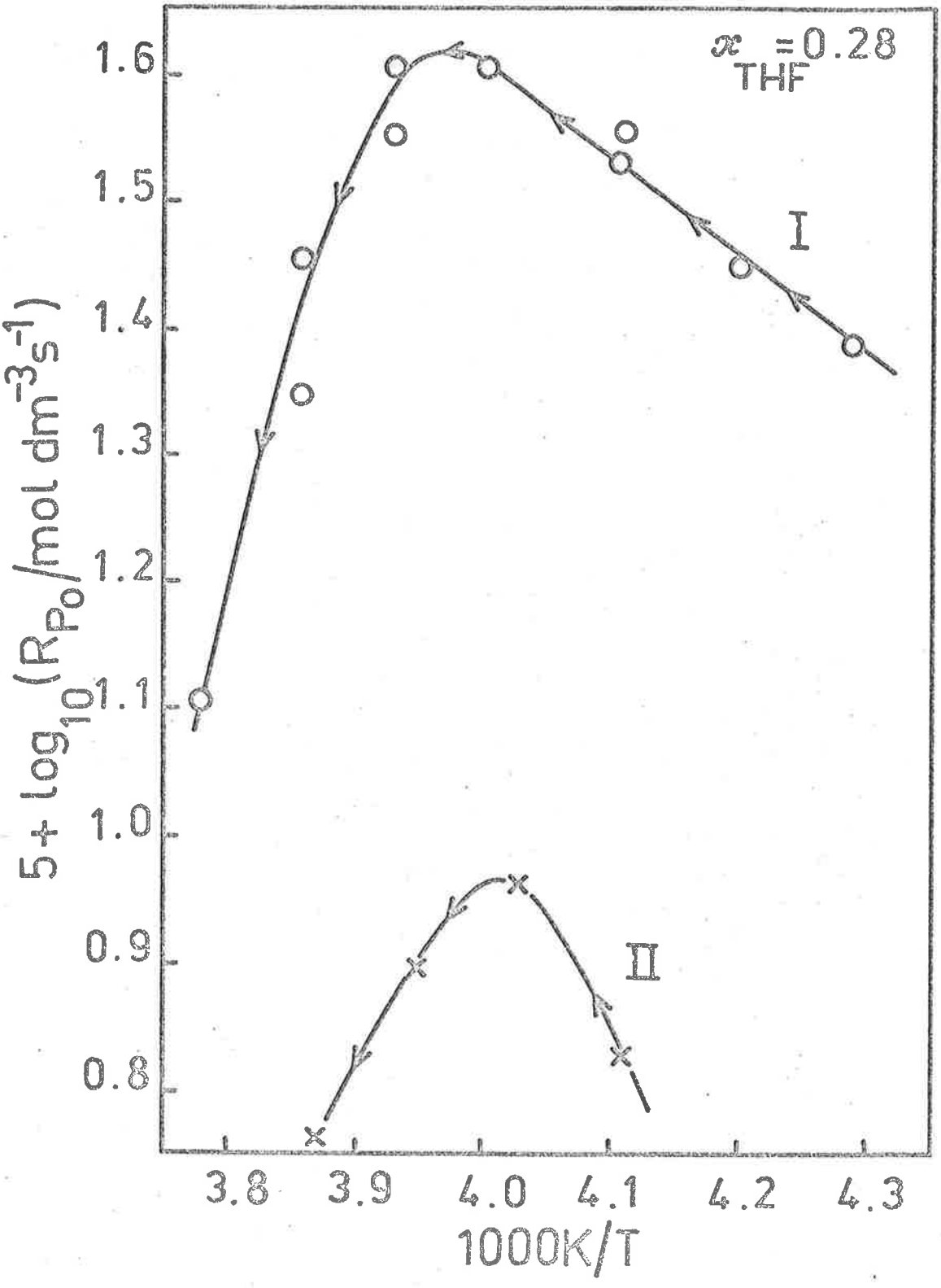

Figure 3.8. The effect of temperature on the initial rate of polymerization. Curve I = initiation below the inversion temperature; curve II = initiation at 263K for one minute. $[G_n]_o$ = 0.1M; $[MMA]_o$ = 2.76M; [THF] = 2.87M.

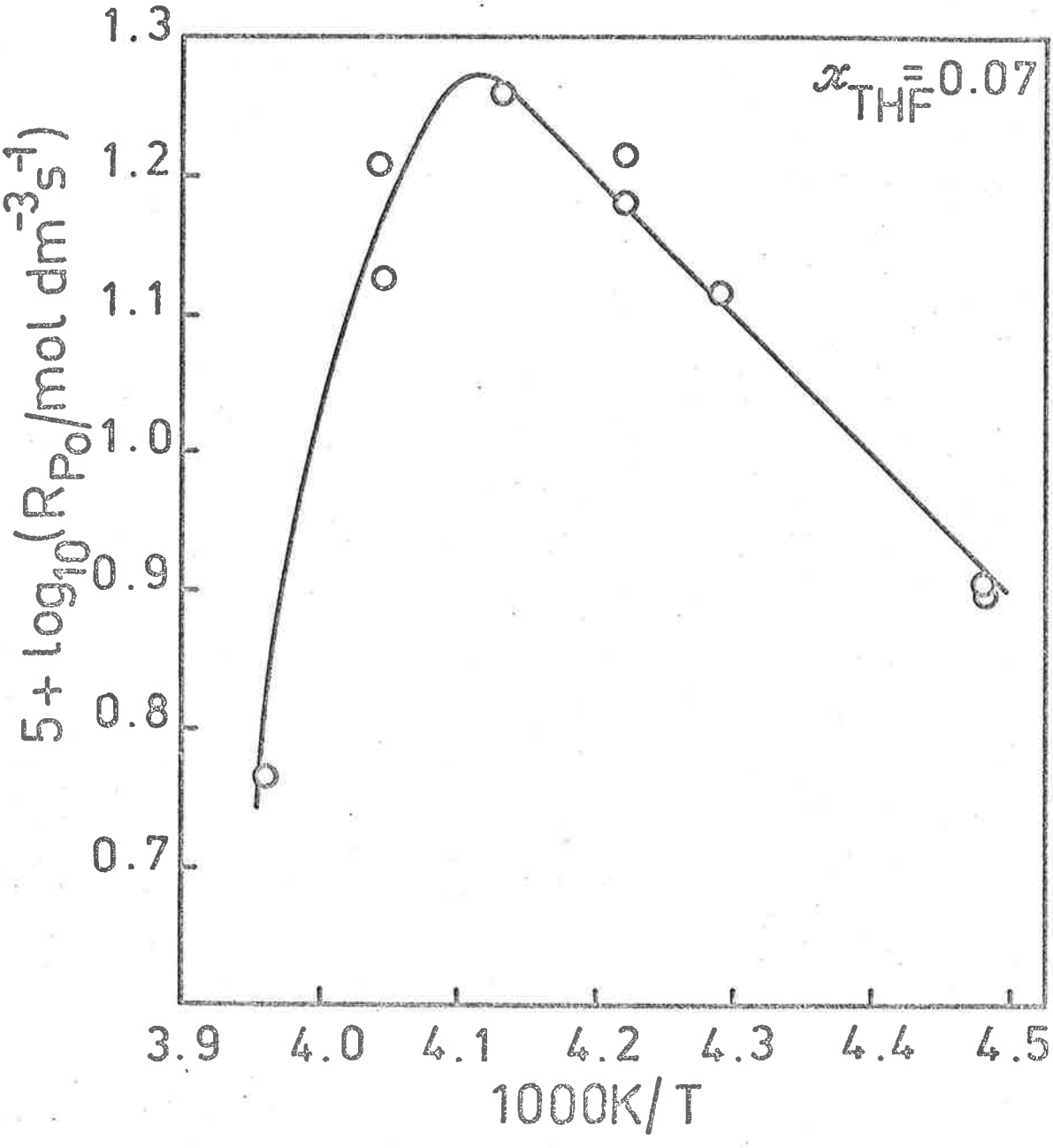

Figure 3.9. The effect of temperature on the initial rate of polymerization. Initiation temperature below the inversion temperature. $[G_n]_o$ = 0.10 mol dm^{-3}; $[MMA]_o$ = 2.76 mol dm^{-3}; [THF] = 0.72 mol dm^{-3}.

3.3.5 *Ultra-violet spectra of the polymerizing system*

The ultra-violet spectra of the MMA polymerization initiated by diphenylhexyl-lithium (DPHL) in dioxan[91] and the sodium salt of the α-Methyl styrene tetramer in THF/toluene[82] show an absorption maximum at ca.330nm which is relatively stable at low temperatures and is destroyed instantly by oxygen and/or methanol. This peak has been attributed to the propagating species of poly(methyl-methacrylate) although there is some controversy concerning the exact nature of the species causing this peak, e.g. ref. 92. Other absorption maxima have also been observed at very low and intermediate temperatures and these have been attributed to more reactive forms of the MMA anion and alkoxide side products respectively.[82]

In previous reports where Grignard reagents have been used, e.g. refs. 54,55, mixing MMA and the organomagnesium compound at low temperatures resulted in the instantaneous appearance of an intence yellow colour which has been observed in diethyl ether, THF and toluene solutions. This colour rapidly faded (within seconds) at temperatures above 258K and its lifetime was shorter in the presence of high MMA concentrations as well as with Grignard reagents which were the least efficient in initiating macro-chains.

In this investigation, a greenish-yellow colour appeared instantaneously on mixing the MMA and n-BuMgBr solutions at 223K and the initial aim of this series of experiments was to identify

this colour and to determine whether an absorption occurs at ca. 330nm as it does in the DPHL and $Na_2(\alpha\text{-MeSt})_4$ initiated systems.

Unfortunately, the lifetime of this colour was only 2 minutes at 223K and only slightly longer at lower temperatures and so it was impossible to obtain any information concerning the origin or fate of this colour.

Nevertheless, our spectroscopic studies did provide some interesting results which are shown in figures 3.10 and 3.11.

The spectra were run using air as the reference and as can be seen from figure 3.10, all absorptions below λ = 280nm are obscured by the strong toluene absorption. Also there was no evidence of any absorption at $\lambda >$ 320nm. Figure 3.10 shows the spectrum of the polymerizing mixture in a 1 mm cell taken at different temperatures from initiation, (215K) to ambient.

The spectra were run at increasing temperatures, the time interval between runs being no more than 5 minutes. At T < 253K, no significant absorption was evident at $\lambda \geq$ 280nm, however as the temperature rose above 253K, a peak appeared at λ = 300 nm and grew rapidly as T increased. The formation of this peak was irreversible i.e. the rate of growth could be controlled by lowering the temperature but the peak could not be eliminated, once formed. The peak position shifted slightly as the temperature was raised until at 298K, the absorption maximum was at λ = 296nm. In some cases, a shoulder was observed on the base of the toluene "cut off" even at

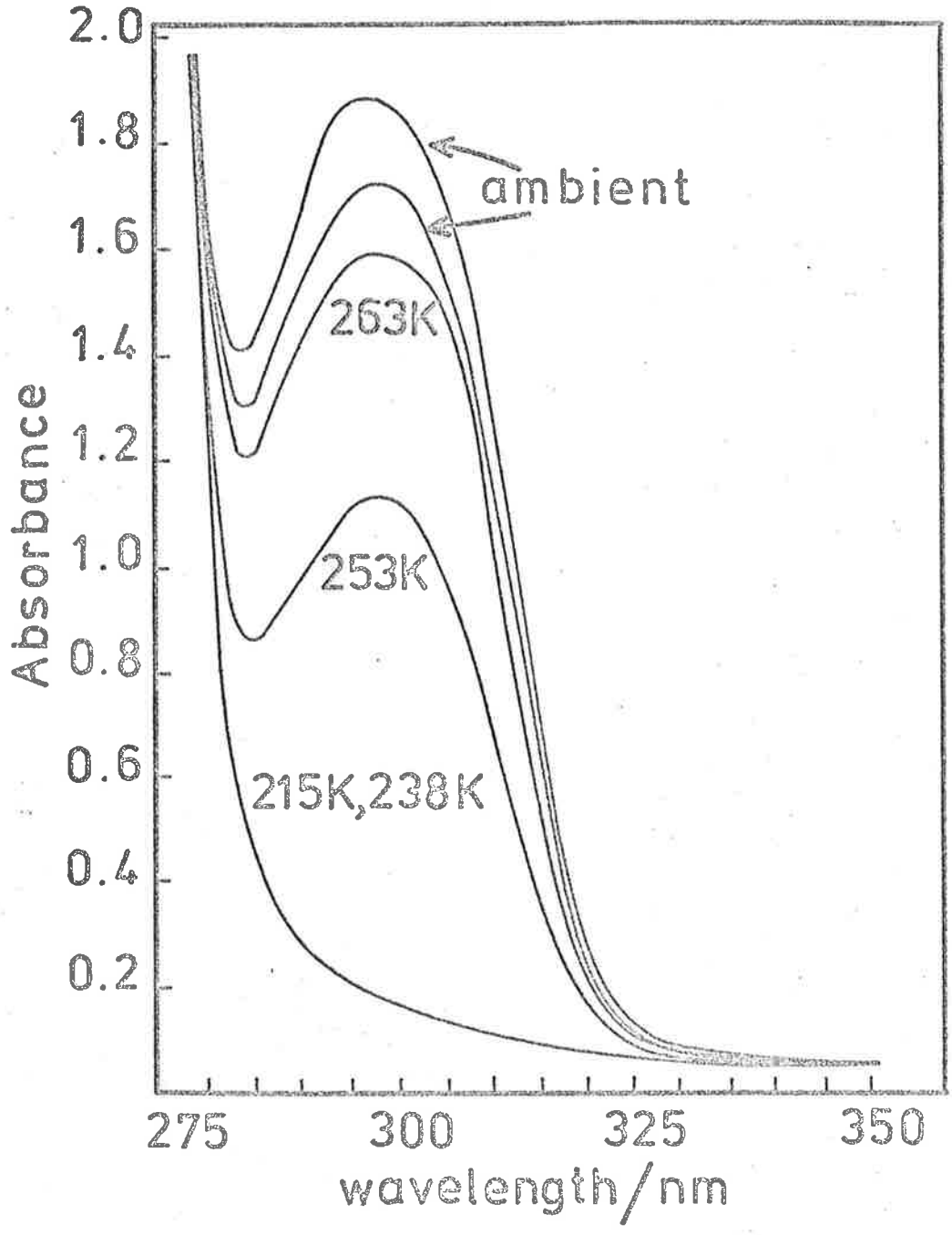

Figure 3.10. Ultra-violet absorption spectra of a polymerizing solution in a 1mm cell taken at various temperatures from initiation (215K) to ambient.

223K. On warming the solution, the shoulder intensity remained constant until T >253K, when the 296nm peak grew rapidly.

This shoulder, which was sometimes observed at low temperatures, was probably caused by the presence of a small amount of the same species which gives rise to the 296nm peak at higher temperatures. Small amounts of these high temperature products may be formed during filling and/or sealing off the cell if due care is not taken.

The spectrum of a solution with $[MMA]_o$ = 0.26 mol dm^{-3} and $[G_n]_o$ = 0.91 mol dm^{-3} was identical to that shown in figure 3.10. Under these conditions polymerization does not occur, however, when the solution was warmed from 205K to ambient, a peak again appeared at λ = 296nm and grew rapidly as the temperature was raised above 253K.

Figure 3.11 shows the termination properties of this peak under conditions when $[MMA]_o > [G_n]_o$ and when $[G_n]_o > [MMA]_o$. When these solutions were broken open at ambient temperature, and shaken in air, the 296nm peak did not diminish, but the addition of one drop of water or methanol almost completely destroyed it.

3.3.6 *The effect of additives*

In our attempts to identify the active propagating species in the Grignard system, small amounts of very strongly solvating solvents such as tetraglyme, CH_2-O-$(CH_2$-$CH_2O)_4$-CH_3, and hexamethyl-phosphoro-triamide, $((CH_3)_2N)_3$ P O, were added to the initiator solution. The

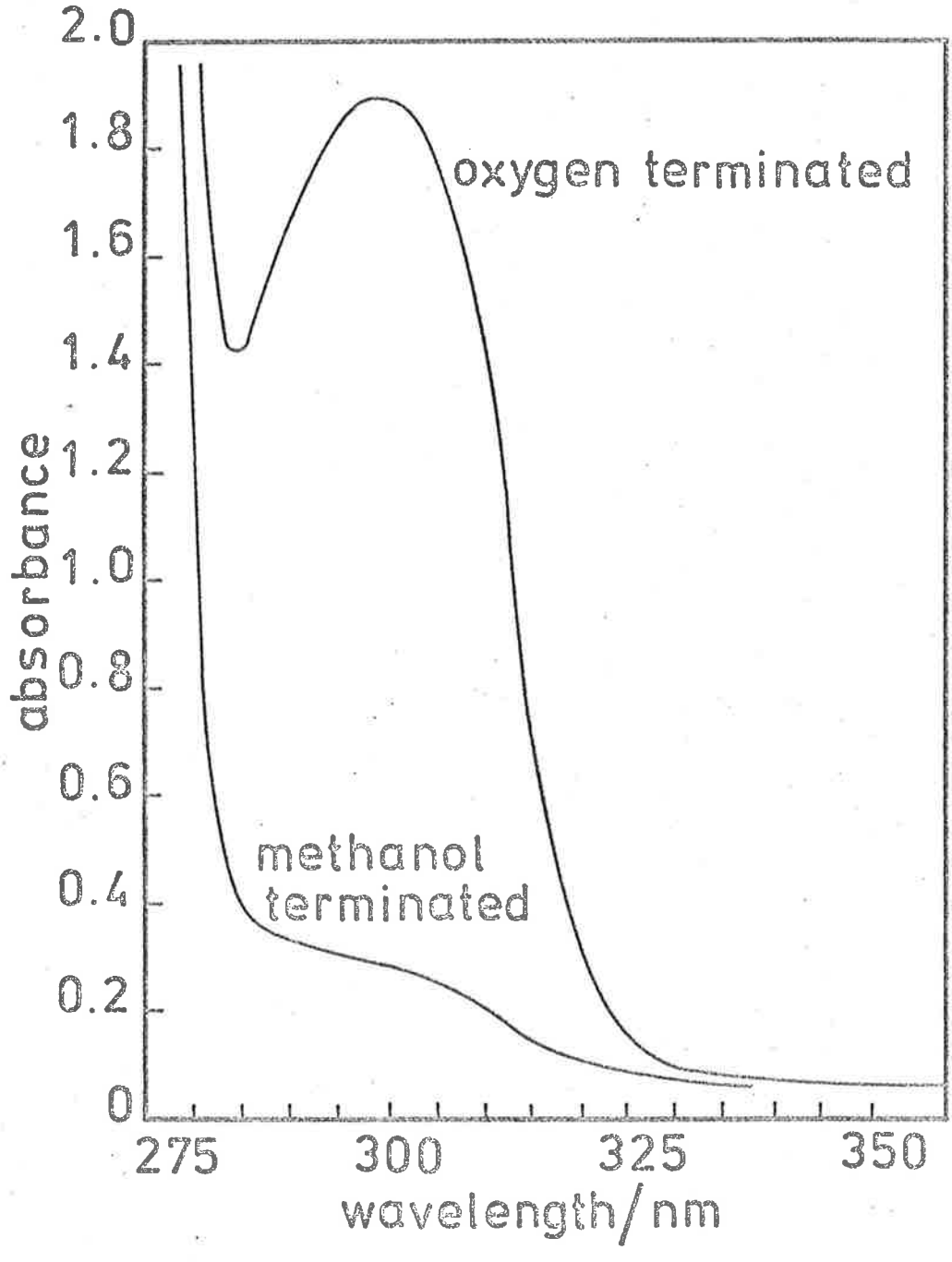

Figure 3.11. Termination properties of the u. v. absorption peak of figure 3.10. Spectra run in a 1mm cell at ambient.

effect of these solvents when added to such compounds as fluorenyl-Li or fluorenyl-Na is to solvate the cation, thereby increasing the concentration of free ions in the solution. Since free ions are much more reactive than ion pairs the rate of polymerization should be much faster in the presence of these solvating solvents.

It was hoped that in our system some of these effects might be observed since the co-polymerization studies of previous workers[54a] suggested some form of anionic propagating species in the MMA/Grignard system.

(a) *Tetraglyme*

The initial experiment consisted of adding sufficient tetraglyme to the initiator solution to ensure that the ratio of glyme: $[G_n]_o > 1$. Immediately the two reagents were mixed a white precipitate formed, the amount slowly increasing with time. A micro-analysis of this precipitate indicated the presence of magnesium and bromine in the ratio of 1:1.7. The supernatant liquid, obtained by decanting from the precipitate, was then tried as an initiator of polymerization. When MMA was added to a cooled solution of this liquid, the characteristic greenish-yellow colour observed in the Grignard system appeared instantaneously and the dilatometric conversion versus time curve was linear.

It is reasonable to assume that the addition of tetraglyme to the n-BuMgBr/THF solution resulted in the precipitation of $MgBr_2$,

forcing the Schlenk equilibrium in favour of $(n\text{-Bu})_2Mg$. The supernatant liquid therefore consisted of a solution of the dialkylmagnesium which initiated the polymerization. The similarities between the behaviour of the supernatant liquid (i.e. $(n\text{-Bu})_2Mg$) and the n-BuMgBr solution will be discussed in section 3.6 (c).

(b) *Hexamethyl-phospharotriamide.* (HMPA).

The same initial experiment as in part (a) was performed using HMPA instead of tetraglyme. On mixing the initiator and HMPA at room temperature no precipitate formed. However, on cooling to 223K the solution became heterogeneous. This process appeared reversible because the precipitate redissolved when the solution was warmed to room temperature. Breaking in the monomer at 223K produced no colour change and no polymerization.

When HMPA in toluene was added to the initiator at 223K and the monomer added without allowing the solution to warm, polymerization did occur although no colour change was evident.

This procedure was repeated at 211K and 197K and the rates of polymerization compared with the gravimetric yields. The results are shown in table 3.2. As can be seen, the rate increased with decreasing temperature and at 197K there was rapid monomer consumption in the initial stages of the polymerization.

TABLE 3.2

Rate of polymerization of MMA using n-BuMgBr in the presence of HMPA. [a] $x_{THF} = 0.09$ [THF] = 0.92 mol dm^{-3} [HMPA] = 0.28 mol dm^{-3}

Temp/K	$[MMA]_o$ /mol dm^{-3}	[I] /mol dm^{-3}	$10^5 R_{p_o}$ /mol $dm^{-3} s^{-1}$	Theoretical Yield/%	Actual Yield/%
223	2.77	0.10	4.0_1	5.9	6
211	2.77	0.10	6.4_2	11.3	10
197	2.77	0.10	2.5_7	2.23	13

(a) Rates measured 12 minutes after mixing.

These results can be interpreted in several ways. Firstly, it has been reported[93] that dimethyl sulphoxide (DMSO) and dimethyl formamide (DMF), react with Grignard reagents above 243K according to

$$H\text{-}\underset{\underset{O}{\|}}{C}\text{-}N(CH_3)_2 + RMgX \longrightarrow H\text{-}\underset{\underset{N(CH_3)_2}{|}}{\overset{\overset{OMgX}{|}}{C}}\text{-}R \qquad (3.9a)$$

An analogous reaction could be envisaged between HMPA and n-BuMgBr or $(n\text{-}Bu)_2Mg$ at high temperatures to form a product of the type $((Me)_2N)_3\,P(OMgX)R$. If this product is inactive towards MMA this would explain the results observed initially, i.e. that HMPA in some way deactivates the Grignard reagent towards monomer.

This particular phenomenon, that the addition of HMPA to an initiator deactivates the initiator has been noted in other systems,

e.g., the sodium and lithium salts of polystyrene are rapidly destroyed by HMPA even at low temperature. Polystyryl-K is stable at 203K in HMPA containing media, but above 233K, a spontaneous change readily takes place.[94]

At low temperature in the Grignard/DMF system, reaction (3.8) does not occur but complexing between DMF and RMgX does.

$$H\text{-}\overset{O}{\overset{\|}{C}}\text{-}N(Me)_2 + RMgX \longrightarrow H\overset{O}{\overset{\|}{C}}N(Me)_2 \cdot RMgX \qquad (3.9b)$$

A similar complexing probably occurs between RMgX and HMPA although when HMPA is in excess, 2:1 complexes will probably be formed. Such complexes have been observed.[29,95]

The increase in rate with decreasing reaction temperature could also be explained in several ways: complexing reactions such as eqn.(3.9b) are favoured at lower temperatures and so the increased rate could result from an increased concentration of active species. This assumes that the complexed form is more reactive than the uncomplexed form. If the rate determining step of initiation is displacement of a solvent molecule by MMA, then the stronger complexing agent such as HMPA would be expected to retard the rate of initiation. However, if the rate determining step is the breaking of the R-Mg bond then the strongest complexing agent should increase the polarity of the R-Mg bond and hence the reactivity.

In a comparative study of the factors influencing the rate of addition of dimethylmagnesium to benzophenone, House *et al*[96] found

that addition of solvating agents to the solution either accelerated or retarded the addition reaction depending on the additive. HMPA accelerated the reaction but their studies were hampered by the formation of insoluble materials when small amounts of HMPA were added to the organomagnesium compound in diethyl ether.

The greatly enhanced polymerization rate in the acrylonitrile/Grignard system at 198K when HMPA is added is probably explainable on the above hypothesis as are our results at 197K. The slower rates observed at 223K and 211K may arise from competing reactions of the type (3.9a) which may only become insignificant at the lowest temperatures.

Nevertheless, our results showed that presence of HMPA alters the rate, tacticity and molecular weight distribution which probably results from modification of the initiator as well as the propagating species.

It is rather surprising that HMPA did not complex with the $MgBr_2$ present in the Grignard reagent and precipitate the 2:1 bis HMPA:$MgBr_2$ compound as for dioxan and tetraglyme. As the above results confirm, this system is quite unlike the 'normal' organomagnesium polymerization of MMA and so although the results were interesting, no further investigations were done.

3.3.7 *Low temperature dilatometry*

In addition to the Arrhenius plots, (section 3.3.4) several dilatometric investigations were attempted at ca.200K, to see whether any similarities existed between the Grignard initiated polymerization and those initiated by various organo-alkali compounds. In these latter systems, rapid initial monomer consumption followed by a much slower rate has been observed at very low temperatures.[82]

At χ_{THF} = 0.34, [THF] = 3.38 mol dm^{-3}, $[MMA]_o$ = 2.5 mol dm^{-3} and $[G_n]_o$ = 0.10 mol dm^{-3}, the conversion versus time curve at 200K was linear and the rate of polymerization, calculated as outlined in section 3.2 was 5 x 10^{-5} mol $dm^{-3}s^{-1}$. The polymerization was terminated after 90 minutes and the gravimetric conversion of 10.2% agreed well with the theoretical dilatometric conversion 10.8%. Another run was performed with χ_{THF} = 0.07, [THF] = 0.76 mol dm^{-3} and $[MMA]_o$ = 2.95 mol dm^{-3}, $[G_n]_o$ = 0.11 mol dm^{-3} for 30 minutes and again there was no indication of rapid monomer consumption. It was noticeable at this temperature and low THF mole fraction, that the intense yellow colour, formed on mixing the monomer and initiator, persisted for almost 20 minutes.

3.4 *Secondary and tertiary-Butyl Magnesium bromides.*

3.4.1 *Sec-BuMgBr*

Many of the experiments detailed in section 3.3 were done using

sec-BuMgBr as initiator. In general, rates were found to be much faster than for the n-BuMgBr system, and so lower monomer and initiator concentrations were used. A yellowish colour with an average lifetime of 1 minute appeared when monomer and initiator were mixed and was less intense than that observed in the n-BuMgBr case.

Percentage conversion versus time curves were again initially linear, although at very high rates, the solutions became viscous and the rate decreased.

The initial rate of polymerization was externally first order with respect to the organomagnesium concentration, $[G_s]_o$, figure 3.12. Here $[G_s]_o$ represents the concentration of active sec-Butyl-magnesium bonds in the sec-BuMgBr solution. The external order with respect to monomer was not determined, but there is no evidence to suggest that the order is different from the n-BuMgBr system.

The effect of mole fraction of THF was not as marked as for the n-BuMgBr case, figure 3.13, but again a gradual decrease in R_{p_o} was observed as the mole fraction of the THF increased. As for the n-BuMgBr case, the tacticities and molecular weight distribution were markedly different at $\chi_{THF} < 0.1$ compared with $\chi_{THF} > 0.1$ (section 4.2.1 and 4.4.1).

At $\chi_{THF} = 0.14$, $[THF] = 1.4_4$ mol dm^{-3}, $[MMA]_o = 2.8$ mol dm^{-3} and $[G_s]_o = 0.04_4$ mol dm^{-3} comparison of the gravimetric and theoretical dilatometric yields obtained after 15 minutes polymeriza-

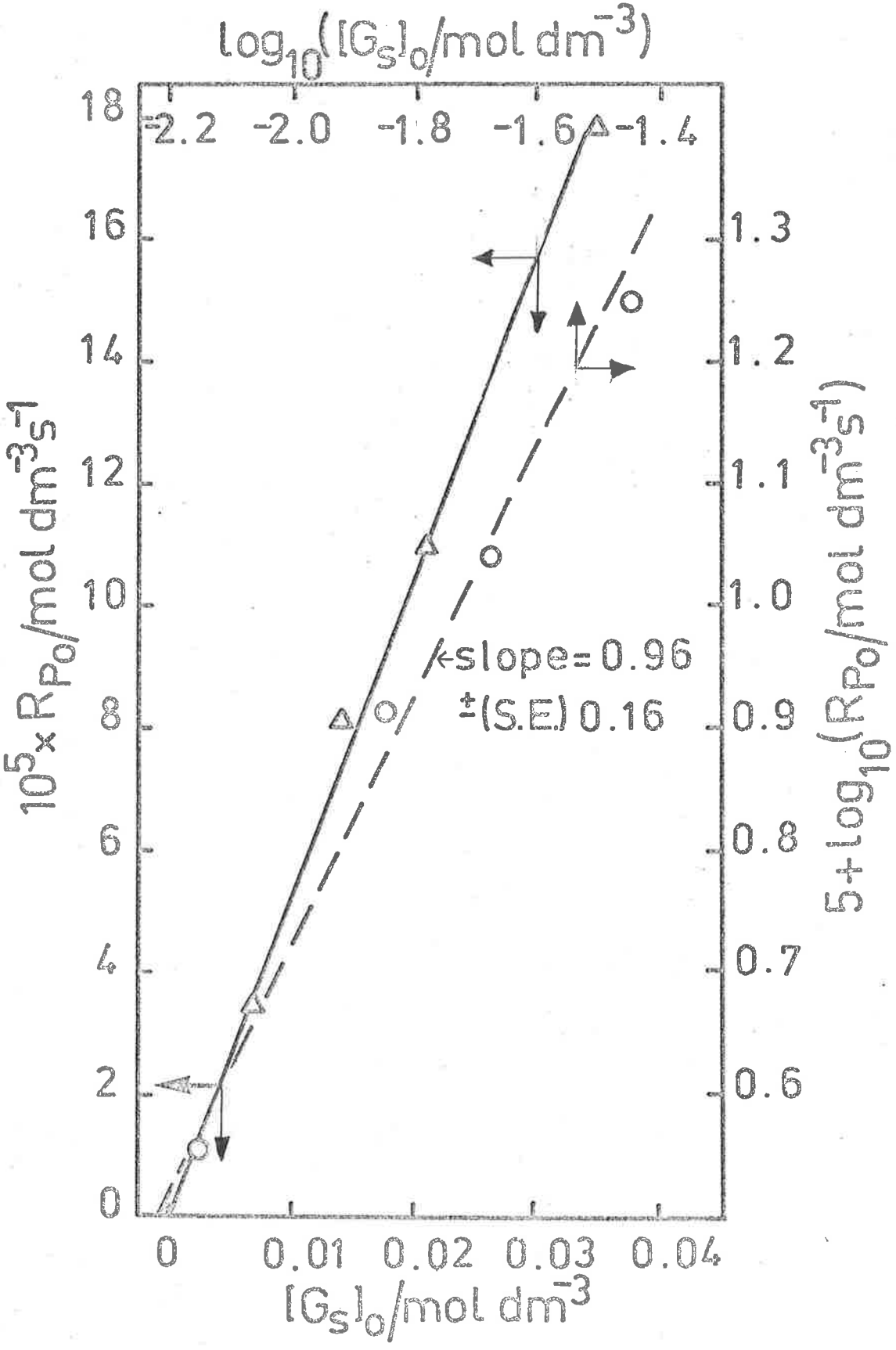

Figure 3.12. Dependence of initial rate of polymerization on the initial concentration of active sec-BuMg bonds. T = 223K; $[MMA]_o$ = 0.96 mol dm^{-3}; [THF] = 1.27 mol dm^{-3}.

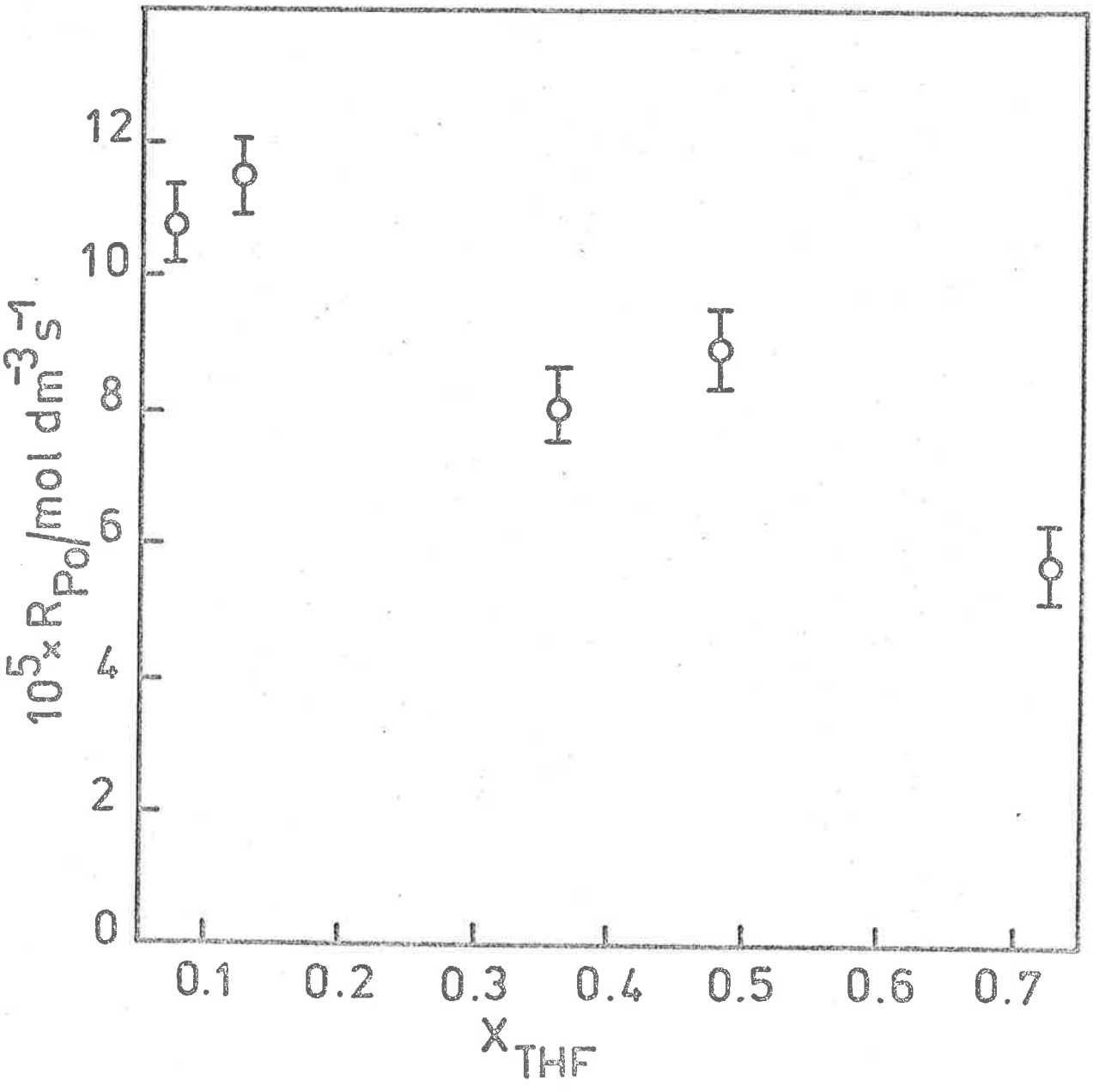

Figure 3.13. Effect of THF mole fraction on initial rate of polymerization using sec-BuMgBr. ($[THF] \approx 10.x_{THF}$) T = 223K; $[MMA]_o$ = 0.96 mol dm^{-3}; $[G_s]_o$ = 0.02 mol dm^{-3}.

tion at 200K showed that no abnormally rapid monomer consumption had occurred at this temperature.

3.4.2 *tert*-BuMgBr

Continuing the trend shown by the sec-BuMgBr initiator, rates of polymerization using tert-BuMgBr were the fastest of the series. When $[MMA]_o$ = 2.76 mol dm^{-3}, $[G_t]_o$ = 0.021 mol dm^{-3}, and χ_{THF} = 0.28, [THF] = 2.87 mol dm^{-3} the polymerizing solution turned solid within two minutes of mixing at 223K. The polymer recovered was "stringy" in appearance and as will be discussed later (section 4.2.1 and 4.4.1) was highly isotactic, of very high molecular weight and narrow molecular weight distribution.

In these systems there was no observable colour change on mixing and even when the concentration of monomer and initiator were reduced to 0.94 mol dm^{-3} and 0.0073 mol dm^{-3} respectively, the reaction solution was still too viscous to pour into a dilatometer after two minutes at 223K. Even rate determinations by gravimetric analysis were subject to large errors in this system because the very high molecular weight polymer formed was insoluble in quantities of benzone that were practical for freeze drying. This made accurate weight determinations difficult to obtain.

Many methods were tried in order to reduce the rate and/or the molecular weight of the polymer formed so that quantitative kinetic studies could be done, however all such attempts failed. By

decreasing the monomer concerntrations, gravimetric analysis indicated that very slow rates could be achieved, e.g. $[MMA]_o$ = 0.2 mol dm^{-3}, $[G_t]_o$ = 0.011mol dm^{-3}, χ_{THF} = 0.15, the percentage rate of polymerization $R_p^{\%}$, was ca. 0.2% per minute which is ideal for dilatometry. However the solution was still far too viscous to pour into the dilatometer. It appeared that the molecular weight was independent of the initial monomer concentration.

G.p.c. analysis confirmed this, although the molecular weight distribution did change with time, section 4.4.1.

Unfortunately, higher initiator concentrations could not be used in an attempt to reduce the molecular weight because of the low solubility of tert-BuMgBr in THF at 223K.

3.5 *Dialkyl magnesiums as polymerization initiators*

The only intensive dilatometric studies using the dialkylmagnesiums as polymerization initiators were done on the $(n\text{-Bu})_2Mg$ system. Preparation of these compounds has been described in section 2.3.2 and they were standardized as described for the Grignard reagents, section 2.3.4.

When MMA and $(n\text{-Bu})_2$ Mg in THF/toluene solution were mixed at 223K, a greenish-yellow colour, identical to that observed in the n-BuMgBr system, instantly developed and faded rapidly. Dilatometric studies were done to determine the external orders of reaction with respect to monomer and initiator concentrations, and from figures 3.14

Figure 3.14 (a) and (b). Dependence of initial rate of polymerization on the initial concentration of monomer.

T = 223K; $[G_n]_o$ = 0.10 mol dm^{-3}; [THF]= 2.6 mol dm^{-3}; where

$$[G_n]_o = 2[(n\text{-Bu})_2Mg]_o$$

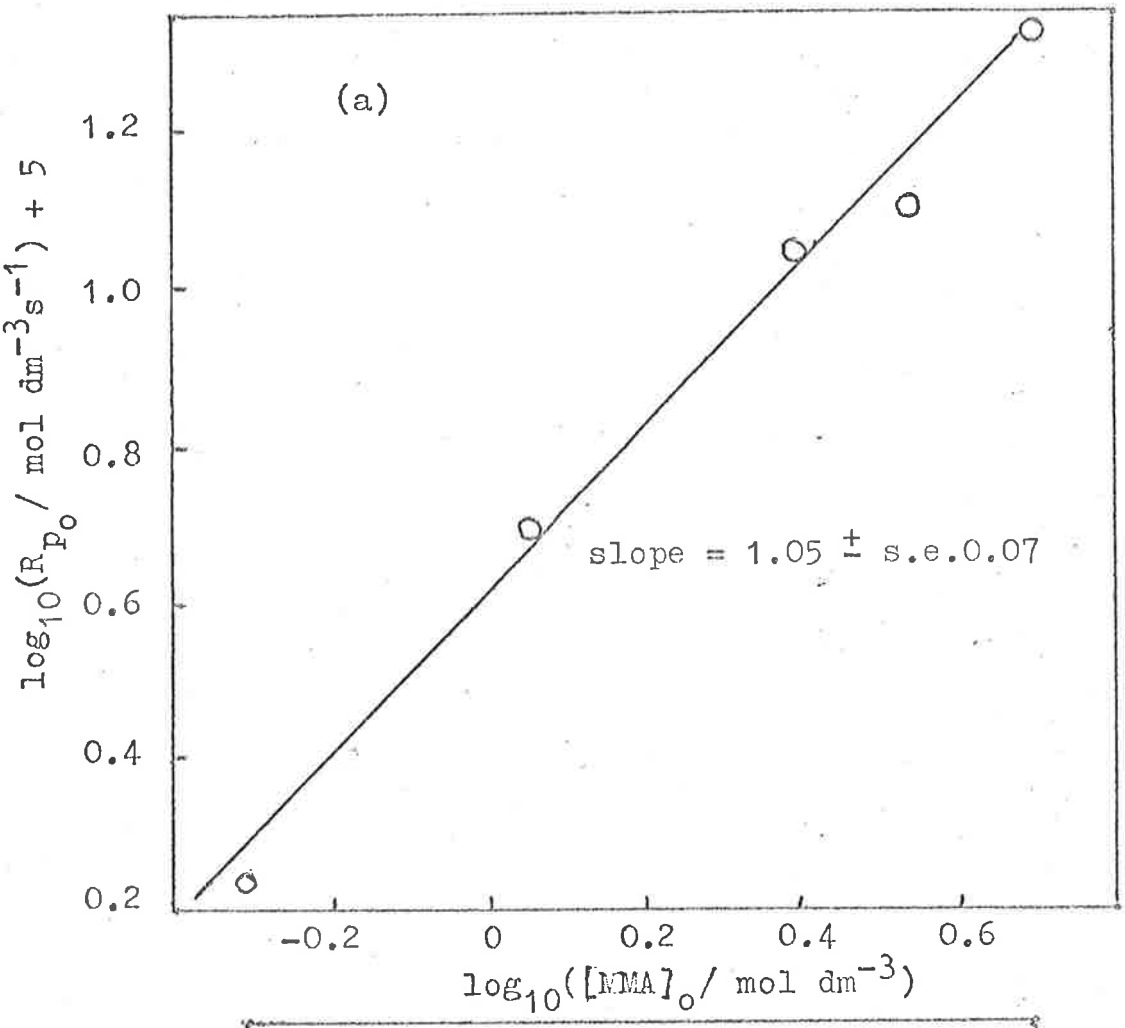
(a)
slope = 1.05 ± s.e.0.07
$\log_{10}(R_{p_o}$ / mol dm^{-3}s^{-1}) + 5
$\log_{10}([MMA]_o$ / mol dm^{-3})
1.2
1.0
0.8
0.6
0.4
0.2
-0.2
0
0.2
0.4
0.6

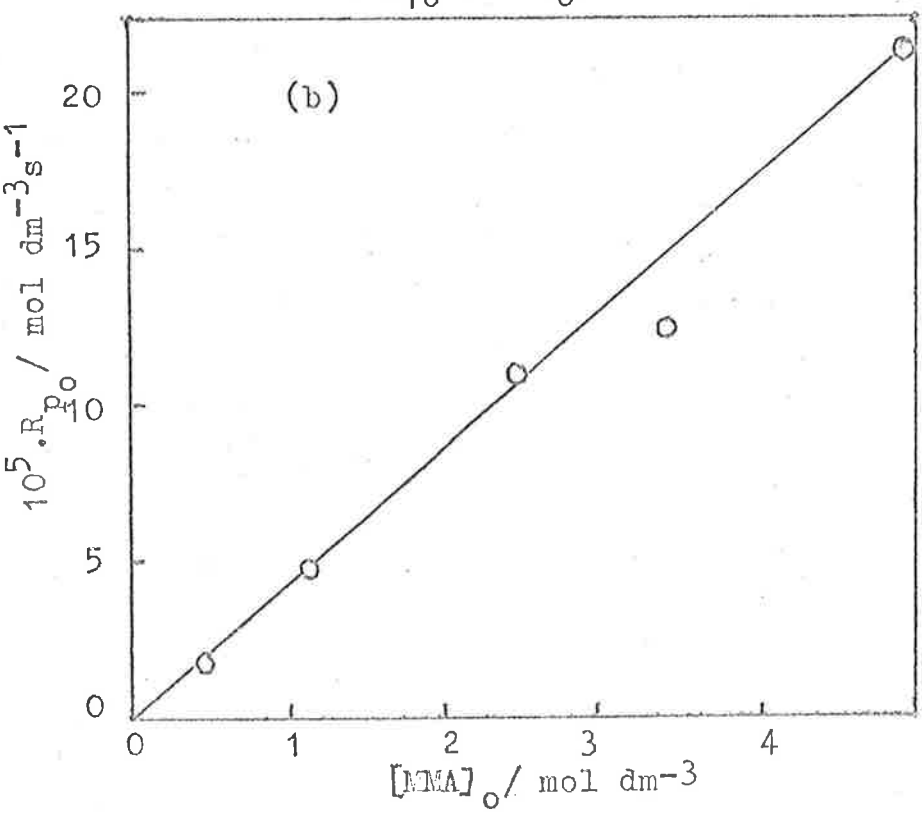
(b)
$10^5 . R_{p_o}$ / mol dm^{-3}s^{-1}
$[MMA]_o$ / mol dm^{-3}
20
15
10
5
0
0
1
2
3
4

and 3.15 it can be seen that the polymerization is *externally* first order in both monomer and dialkylmagnesium concentration.

Just as for n-BuMgBr, the percentage conversion/time curves were linear and although the $\ln([M]_o/[M]_t)$/time curves appeared linear during the initial part of the reaction (< 10% conversion), they were unmistakably non linear when higher conversions were considered, (section 3.3.2).

Low temperature u.v. spectra of polymerizing solutions using $(n\text{-Bu})_2Mg$ as initiator showed identical results to those obtained when n-BuMgBr was used, section 3.3.5.

The similarity between the n-BuMgBr and $(n\text{-Bu})_2Mg$ systems is striking, and will be fully discussed in section 3.6 (c).

The rate of polymerization using $(n\text{-Bu})_2Mg$ appeared to be slightly faster than for n-BuMgBr under identical conditions; e.g. at T = 223K, $[THF] = 1.0_7$ mol dm^{-3}, $[MMA]_o = 0.96$ mol dm^{-3} and $[G_n]_o = 0.03_6$ mol dm^{-3} (where $[G_n]_o$ represents the initial concentration of n-Bu-magnesium bonds in each system), $10^5 R_{p_o}$ /mol.$dm^{-3}s^{-1}$ = 4.36 for $(n\text{-Bu})_2Mg$ and 3.8_6 for n-BuMgBr. Possible reasons for this discrepancy will be discussed in section 3.6 (c).

Gravimetric rate studies were done using $(sec\text{-Bu})_2Mg$ and $(tert\text{-Bu})_2Mg$. The former gave the characteristic colour expected for Grignard reagents when mixed with MMA and the rate of polymerization using $(sec\text{-Bu})_2Mg$ was much faster than for the corresponding sec-BuMgBr, e.g. at $[THF] = 1.0_7$ mol dm^{-3}, $[MMA]_o = 0.96$ mol dm^{-3}, T = 223K, and

Figure 3.15 (a) and (b). Dependence of initial rate of polymerization on the initial concentration of active n-BuMg bonds, $[G_n]_o$. $[MMA]_o$ = 0.50 mol dm^{-3}; [THF] = 2.6 mol dm^{-3}; T = 223K.

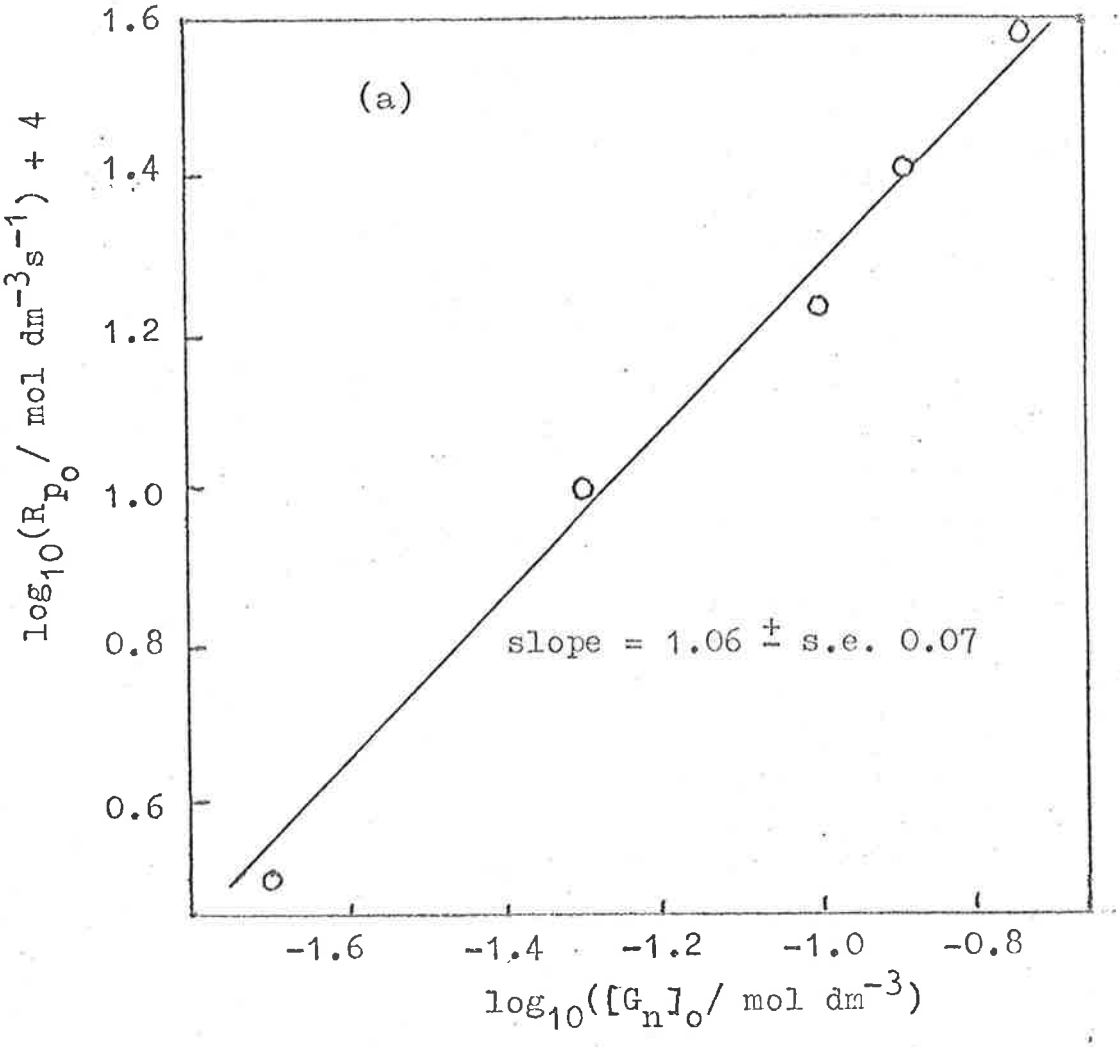
(a)
1.6
1.4
1.2
1.0
0.8
0.6
$\log_{10}(R_{p_o}$ / mol dm^{-3}s^{-1}) + 4
slope = 1.06 ± s.e. 0.07
-1.6
-1.4
-1.2
-1.0
-0.8
$\log_{10}([G_n]_o$/ mol dm^{-3})

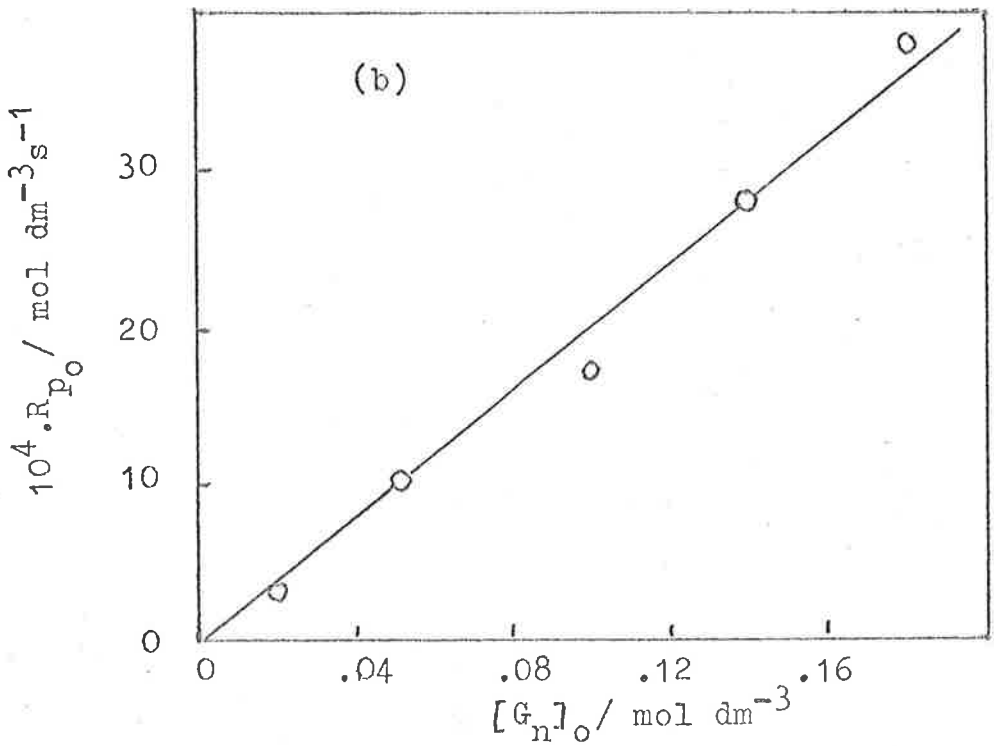
(b)
30
20
10
0
$10^4.R_{p_o}$ / mol dm^{-3}s^{-1}
0
.04
.08
.12
.16
$[G_n]_o$/ mol dm^{-3}

$[G_s]_o$ = 0.02_1 mol dm^{-3} for sec-BuMgBr and $[G_s]_o$ = 0.012 mol dm^{-3} for $(sec\text{-}Bu)_2Mg$; 10^5 R_{p_o} /mol $dm^{-3}s^{-1}$ ≈ 11.0 and 50 for sec-BuMgBr and $(sec\text{-}Bu)_2Mg$ respectively.

However, when $(tert\text{-}Bu)_2Mg$ was used, no colour change was observed when the monomer was added, and the rate of polymerization was very slow, e.g. at [THF] = 2.8_7 mol dm^{-3}, $[MMA]_o$ = 2.76 mol dm^{-3} and $[G_t]_o$ = 0.024 and 0.012 mol dm^{-3} for tert-BuMgBr and $(tert\text{-}Bu)_2Mg$ $10^5R_{p_o}$ /mol dm^{-3} = 76 and 0.5_5 for the Grignard and dialkylmagnesium compounds respectively.

3.6 *Discussion*

The results contained in this chapter have been purely concerned with the kinetics of the polymerization initiated by organomagnesium compounds, and so it would be impossible to propose a mechanism on the basis of these results that would explain those obtained in chapters 4 and 5. Nevertheless, some conclusions can be drawn.

(a) The kinetics of polymerization in THF appear to be simpler than those reported in diethyl ether. In the latter solvent, external second order initiator dependence and first order monomer dependence were observed[55b] whereas in THF external first order initiator and external first order monomer dependence occur.

The deviation from linearity of the internal first order monomer dependence plots ($\ln[M]_o/[M]_t$ versus time) suggests a zero internal monomer dependence since the conversion curves are linear up to 40%.

This deviation from internal first order monomer dependence has been observed by Allen *et al*[54] although in their case, the conversion/time curves were also non-linear at conversions greater than ten percent.

The linear conversion versus time curves suggest that there is no termination during polymerization. There are alternative explanations, such as transfer to monomer with the production of another growth site of identical activity but as will be shown in section 4.4.1 the direct proportionality between the experimental molecular weight and the per cent conversion (at least up to 25%) is in accordance with a living system. Watanabe *et al*[55] observed similar results in diethyl ether and termination free systems have also been proposed for the BuMgCl initiated polymerization of acrylonitrile in toluene at 198K.[64b] Mention has already been made of the similarity observed between these two systems (section 1.4.2), viz. external first order with respect to initiator and linear conversion versus molecular weight dependence as well as the insensitivity of molecular weight to initial monomer concentration. Perhaps this similarity is not surprising when one considers recent reports detailing almost identical mechanisms for the reactions of ketones and nitriles with Grignard reagents.[31e, 41b]

(b) It is unlikely that either initiation or propagation involve the reaction of free ions or loose ion-pairs. This may not be true in the presence of strongly solvating agents such as HMPA which modifies both the initiator and propagating species. The ability of Grignard reagents to polymerize monomers such as styrene[97a] and α-Mestyrene[97b]

in the presence of HMPA but not in its absence supports the above contention. Little more will be said concerning this aspect of the polymerization because the original aim of the work was to investigate the polymerization of MMA by Grignard reagents in solvents of moderate dielectric constant and solvating ability.

Even though charged species and their agglomerates are known to exist in ethereal solutions of Grignard reagents the effect of THF on the rate of polymerization is opposite to that expected for propagation by free ions or various forms of ion-pairs in equilibrium. The absence of any rapid monomer consumption at very low temperature supports this hypothesis. Drawing on comparative studies in the organo/alkali system, low temperatures should favour the more reactive solvent-separated ion pair or free ion species, e.g. ref.98.

The decreasing rate with increasing THF concentration could be explained by the presence of a reactive species at low χ_{THF} and a less reactive one at high χ_{THF} in equilibrium with each other. A similar idea has been suggested involving a rapid pre-exchange in organomagnesium systems.[35]

This idea of a reactive monosolvate and a less reactive disolvate has also been invoked to explain the effect of *catalytic* quantities of THF on the polymerization of styrene by polystyryllithium in benzene.[99] If monomer becomes coordinated with the cation *prior* to its addition to the carbanion, then addition of a second molecule of

ether may hinder propagation. Szwarc[100] uses the following symbolic equation to explain this result where the arrow represents a molecule of ether:

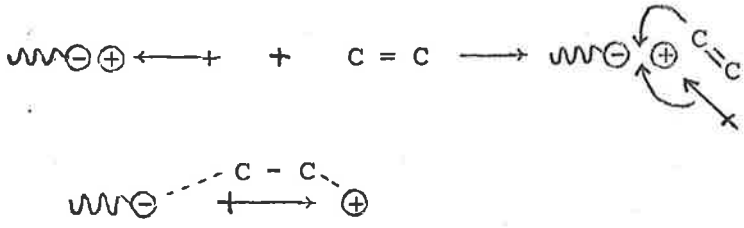

(3.10)

However the dietherate

is assumed to be sterically blocked.

Although this type of mechanism may explain the effect of increasing THF concentration on the rate of polymerization observed in our system where [THF] varied from 0.4_6 to 5 mol dm^{-3} it is only applicable to the polystyryl-Li system when THF is present in catalytic amounts. At higher concentrations, i.e., comparable with our system, ion, ion-pair equilibria will become important in the organo-lithium system.

(c) Some information concerning the initiating species can be obtained, i.e., whether R_2Mg, RMgX or some other associated forms or a mixture of all are the truly active initiating species. It is necessary to examine the published data concerning the Schlenk equilibrium 1.1. As discussed in sections 1.2.1 and 1.2.3, the

Schlenk equilibrium is almost statistically balanced in THF solution at ambient temperature or slightly above, i.e. $K_{1.1} \approx 4$ and is virtually independent of R or X. Using the published data for t-BuMgCl with $K_{1.1} = 4$ and $\Delta H^{o}_{1.1} = 37 kJmol^{-1}$ at 315K, $K_{1.1} = 0.01$ at 223K. Because of the independence of $K_{1.1}$ on R and X it is reasonable to assume that at 223K, for all the Grignard systems studied here, $K_{1.1}$ will be small. This means that in our experiments the predominant species in solution will be the dialkyl-magnesium compound and magnesium bromide, with only a very small amount of RMgX. Comparative studies between the reactivity of dialkyl-magnesium and their corresponding Grignard reagents towards ketones, nitriles and unsaturated esters have shown that the R_2Mg species is far more reactive than RMgX[27,39e,40a,46a, 101] e.g. Ashby has calculated that Me_2Mg is ten times more reactive than MeMgBr towards addition to 2-Methyl-benzophenone.[39e]

Under the conditions chosen for our experiments, the concentration of $R_2Mg >> RMgX$ and it is therefore reasonable to suggest that the initiating species in our system is R_2Mg and not RMgX. In diethyl ether the situation would become more complex because as discussed in section 1.2.3, the Schlenk equilibrium strongly favours RMgX at room temperature and is also dependent on the nature of R and X in this solvent. In diethyl ether association effects are also important. Therefore, when diethyl ether is used, the concentration of RMgX in solution will be appreciable even at low temperatures and

will almost certainly play a significant role in the polymerization. This fact may explain some of the complexities observed by various workers using diethyl ether rather than THF, e.g. the findings by Owens *et al*[52b] (section 1.4.1) that both polymer and cyclic ketone containing at least three monomer units were formed under conditions when $[MMA]_o < [G]_o$ at 273K, could be explained on the basis that in diethyl ether, the small amount of reactive dialkylmagnesium present in the solution may be the cause of these high molecular weight products.

The almost identical results obtained in this work for the n-BuMgBr and $(n\text{-Bu})_2Mg$ systems support the above proposal that the reactive species is R_2Mg. However, some apparent contradictions are obvious: firstly, the relative rates of polymerization initiated by $(n\text{-Bu})_2Mg$ and $(sec\text{-Bu})_2Mg$ are faster than their corresponding Grignard reagents whereas $(tert\text{-Bu})_2Mg$ polymerizes MMA much slower than tert-BuMgBr. Identical rates of polymerization would be expected for both R_2Mg and RMgX solutions if R_2Mg were the predominant reactive species. Also, the polymer microstructure, molecular weight and molecular weight distribution would be expected to be identical for polymerizations with R_2Mg or RMgX.

The polymers prepared using n-BuMgBr or $(n\text{-Bu})_2Mg$ did in fact have identical tacticities and similar molecular weight distributions, however, the tacticity and molecular weight distribution of poly(MMA) prepared using sec-BuMgBr and tert-BuMgBr were completely different

from the polymer prepared using the corresponding dialkylmagnesium compounds.

There are several possible explanations for these apparent discrepancies. Comparison between rates of reactions, especially polymerizations of low initiator efficiency, can be misleading unless specific rate constants can be evaluated. Only when these are known can an increase in rate be correlated to an increased reactivity of the species involved, for example, an increase in polymerization rate may only be due to an increase in the number of active centres brought about by the presence or absence of some reagents as in the polymerization of styrene by n-BuLi in benzene with and without small amounts of ether.

This type of situation may be occurring in our system. It has already been stated that the initiation efficiency is very low in Grignard initiated polymerizations. The presence or absence of $MgBr_2$ may have a pronounced effect on the relative rates of formation of inactive species compared with active species. This effect has been observed in various non-polymerization reactions where the amount of conjugate addition to certain α, β-unsaturated esters decreases with increasing $MgBr_2$ concentration.[102] Complex formation between MMA and $MgBr_2$ may be the cause.

The presence of $MgBr_2$ may also affect the polymerization rate in another way. Exchange reactions are rapid in Grignard systems

(section 1.2.3) and such reactions may influence the overall polymerization rates. A similar effect has been observed in the reaction of ketones and nitriles with Me_2Mg.[31e] In the presence of MgX_2 the initial ketone - Me_2Mg adduct undergoes rapid redistribution according to

$$R_2\underset{Me}{C} - O - Mg - Me + MgX_2 \xrightarrow[\text{rapid}]{k_r} MeMgX + R_2\underset{Me}{C} - OMgX \qquad (3.11)$$

whereas in the absence of MgX_2 a different mechanism is postulated.

$$2R_2\underset{Me}{C} - O - MgMe \longrightarrow MeMg\begin{matrix}\diagup O \diagdown \\ \diagdown O \diagup \\ R\end{matrix}MgMe \xrightarrow{2R_2C=O} 2Mg(OR)_2 \qquad (3.12)$$

Thus our initial proposal that R_2Mg is the reactive species in our system is still justified, but an additional qualification must be included, viz., the presence of $MgBr_2$ not only alters the overall rate of polymerization presumably by influencing the number of active centres formed but also may affect the ultimate mechanism by participating in various complex exchange reactions such as postulated in the ketone system.

(d) The presence of side reactions, even at low temperature, is shown by the low initiation efficiency calculated by comparing the experimental and theoretical molecular weights. The theoretical number average molecular weight ($\bar{M}_{n\ th}$) for a polymer produced in a termination-free system in which the initiation reaction is effectively instantaneous is given by the expression

$$\bar{M}_{nth} = \frac{\alpha \times [M]_o \times (\text{MW monomer})}{\delta \times [In]_o} \qquad (3.13)$$

where α = fractional conversion,

MW (monomer) = molecular weight of the monomer

f = initiation efficiency $\equiv$ $\frac{\text{(concentration of active chains forming high MW polymer)}}{\text{(total amount of initiator)}}$

Thus an *estimate* of f may be obtained from the experimental number average molecular weight ($\bar{M}_{n\text{exp}}$) by invoking the identity relation, $\bar{M}_{n\text{exp}} \equiv \bar{M}_{n\text{th}}$ which will only be valid under the conditions outlined above (see section 6.1 for a more detailed discussion).

The maximum in the Arrhenius plot is partly due to an irreversible termination of the growing chain. There is also a rapid termination step which competes with initiation at high temperatues but is absent below the inversion temperature. The spectral evidence suggests that the species resulting from termination of the initiator and the growing chain are of the same basic type as the species causing the u.v. peak at $T > 253$ K.

This assumption seems reasonable when the following results are considered: the inversion temperature observed from the Arrhenius plots is the same temperature at which the u.v. absorption peak at $\lambda = 296$ nm begins to grow; neither the polymerization nor the appearance of the 296nm peak is reversible when $T > T_i$ and when initiation occurs at $T > T_i$, the polymerization rate is very slow and the 296nm is always present. Here, termination of the initiator only applies to those products formed when $T > T_i$ and not necessarily to those side reactions which occur concommitantly with initiation even at low

temperatures.

A clue to the nature of these high temperature side products is given in the result that their u.v. absorption at λ = 296 nm is not destroyed by oxygen but is by methanol. This same phenomenon has been observed in the polymerization of MMA initiated by $Na_2(\alpha$- Me-styrene$)_4$[82] where a peak at $\lesssim$ 300nm was observed, which grew rapidly at 290K and was destroyed by methanol but not by O_2. The nature of this peak was assigned to an alkoxide, presumably formed by attack of the macro-chain on the monomer carbonyl group, forming the alkoxide I,

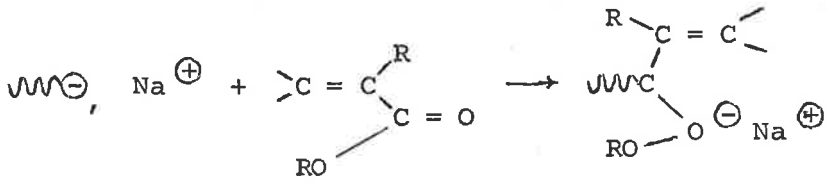

(3.14)

I

This particular mechanism of termination in MMA polymerizations has been postulated before.[56,57] If it occurred in our system an initial product of the type II would be formed which may either rapidly eliminate methoxide to form the ketone III and MeOMgR (path 1) or retain its alkoxide character until termination with a Lewis acid (path 2).

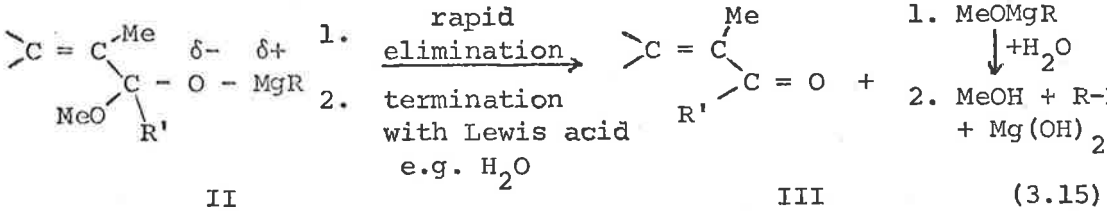

II III (3.15)

where R' is the macro-chain.

Arguments against this particular scheme as being responsible for the spectral behaviour are: the u.v. absorption of I where sodium is the counter-ion and of II with - MgR (or even - MgX) would not be expected to occur at the same wavelength. The effect of cation on the u.v. spectra of anions has not been intensively studied but large red shifts have been reported on changing from Li^+ to Cs^+ ketyls in dioxan.[103] In strongly solvating solvents (e.g. D.M.E. and cyclohexylamine) the reverse effect was observed.[104] The ketone III cannot cause the 296nm peak because of the termination properties of this peak, i.e., destroyed by methanol but not by oxygen. Also carbonyl addition of the type suggested in eqn. (3.15) is thought to be the predominant side reaction competing with initiation at low temperature, section 5.10. If this is true, then any species, such as II or III or their complexes (with e.g. $MgBr_2$) which are formed concommitantly with initiation cannot be responsible for the 296nm peak which appears only at higher temperatures.

Goode *et al*[52a] detected a large proportion of the cyclic trimer, IV in the Ph-MgBr/diethyl ether system at 273K.

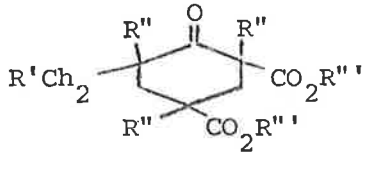

IV

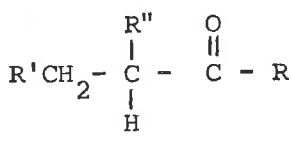

V

However, this cyclic ketone or its precursor is not likely to

be causing the 296nm peak in our system because of the termination properties of this peak and the identical spectra obtained when $[MMA]_o < [G_n^{\cdot}]_o$ and $[MMA]_o >> [G_n^{\cdot}]_o$.

Product V with R' = R was also observed and its proportion increased as the temperature increased from 243K to 293K.[53] It is presumably formed from either 1,4 addition followed by carbonyl addition or vice versa and a precursor to V may be the cause of the 296nm at higher temperatures.

It should be noted that the above argument *does not* imply that termination reactions such at (3.14) and (3.15) do not occur in our system but the argument *does* suggest that such reactions are *not* responsible for the 296nm peak that grows when $T \geq T_i$. The possible products that may be responsible for the 296nm peak will be more fully discussed in section 5.10 but suffice to say here that the substantial increase in methanol produced when a polymerizing solution is allowed to warm to room temperature (prior to hydrolysis) suggests increased carbonyl attack on the monomer at higher temperatures.

If it is assumed that the major side products at 223K are one-fold carbonyl addition products (evidence supporting this assumption is discussed in section 5.10) such as II and/or III where R' = R, then at higher temperatures the precursors of two-fold carbonyl adducts or the precursor of a species such as V *may* be responsible for the 296nm peak formed as the temperature is increased.

CHAPTER 4

POLYMER MICROSTRUCTURE , MOLECULAR WEIGHT AND MOLECULAR WEIGHT DISTRIBUTION

POLYMER MICROSTRUCTURE

4.1 *Introduction*

Polymer chain configuration is very important in determining the physical and mechanical properties of polymers. Hence, the ultimate aim of any mechanistic analysis of the polymerization of any vinyl monomer is to explain the particular chain configuration assumed by the polymer under the influence of the organometallic initiator being used.

Natta and his associates[105] reported the first fully successful preparation of isotactic polypropylene in 1955 and the regular structure of the resulting polymer was thoroughly proved by X-ray analysis.

Since then, Bovey and Tiers[106] developed an n.m.r. technique which permits recognition of both isotactic and syndiotactic linkages in polymeric chains (especially in poly(methyl methacylate)) and to distinguish all three possible sequences of consecutive segments, viz. isotactic, syndiotactic or heterotactic triads,

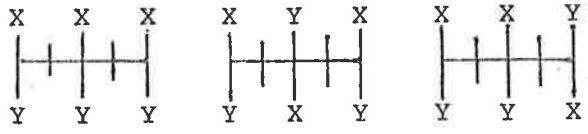

$i \equiv mm$ $\quad s \equiv rr$ $\quad h \equiv mr$

where m and r designate meso and racemic dyads respectively.

In poly(MMA), the methylene protons are equivalent in a racemic dyad (*r*)

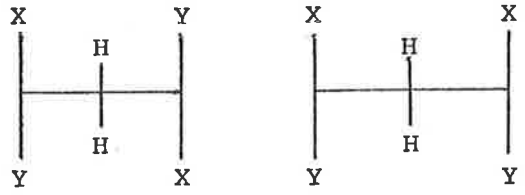

r *m*

and therefore produce only one line in the n.m.r. spectrum. However, in a meso dyad, (*m*), they are not magnetically equivalent even if free rotation around the neighboring C-C bond is allowed. Thus in an isotactic dyad the methylene protons exhibit an AB pattern.

Furthermore, when the above triads are considered, the central α-methyl group, represented as Y (where X ≡ CO_2CH_3) will be in different magnetic environments depending on whether the triad is *i*, *h* or *s*. Hence the presence of each triad is observed by the characteristic chemical shift of the respective protons and peaks at δ = 1.22 ppm, 1.05 ppm and 0.91 ppm represent isotactic, heterotactic and syndiotactic triads respectively. The relative intensities of these peaks give the abundance of the various triads in the investigated polymer. Figure 4.1 shows the 60 MHz n.m.r spectrum of polymers prepared during this research using n-BuMgBr (4.1 (a)) and tert-BuMgBr (4.1 (b)). The former polymer is 55% syndiotactic and the methylene proton region appears as a broad singlet. However, the polymer prepared using tert-BuMgBr was over

Figure 4.1. 60 MHz p.m.r. spectra of poly(MMA) showing the methoxy proton resonance at $\delta \approx 3.5$ ppm, the methylene protons between 1.3 and 2.3 ppm. and the α-methyl protons between 0.9 and 1.2 ppm. depending on whether they are in an isotactic (I), heterotactic (H) or syndiotactic (S) environment.

(a) 'syndiotactic like' polymer prepared using n-BuMgBr at 223K, [THF]= 2.87 mol dm^{-3}, $[MMA]_o$ = 2.76 mol dm^{-3}, $[G_n]_o$ = 0.10 mol dm^{-3}. Proportions of i, h and s triads = 0.14, 0.32 and 0.54 respectively and the methylene peak is a broad singlet.

(b) 'isotactic like' polymer from tert-BuMgBr at 223K, $[MMA]_o$ = 0.94 mol dm^{-3}, $[G_t]_o$ = 0.01 mol dm^{-3}, [THF] = 0.144 mol dm^{-3}. i:h:s = 0.84:0.07:0.09 and methylene region appears as a quartet.

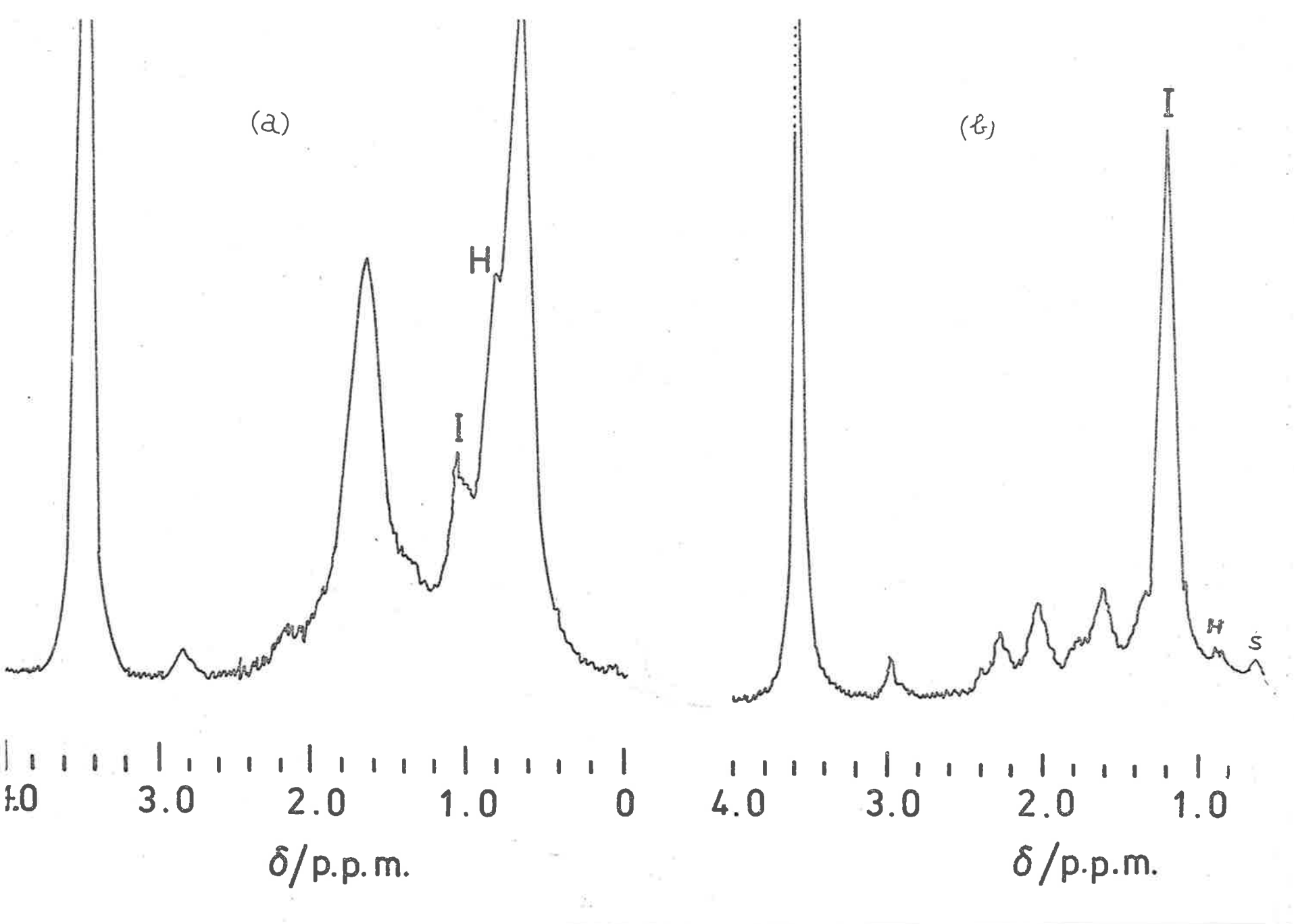
(a)
H
I
4.0
3.0
2.0
1.0
0
δ/p.p.m.
(b)
I
H
S
4.0
3.0
2.0
1.0
δ/p.p.m.

80% isotactic and the methylene region shows a definite quartet, although one peak is partly obscured by the isotactic α-methyl resonance.

Both dyad and triad structure are distinguishable with 60 MH_z n.m.r which is all that we had available. However, with much more sophisticated techniques (C_{13} fourier transform analysis[107]) and better instruments (100MHz and 220MHz) it is possible to distinguish tetrad and pentad sequences.[108]

It is essential to obtain such information before the exact chain configuration can be established and more than one mechanism can be tested. The establishment of the proportion of triads can only be used to test the simplest mechanism, viz, Bernoulli trial statistics, section 4.1.1, and to establish whether the polymer is isotactic, syndiotactic or stereo-block. Nevertheless, even this somewhat limited information is useful and will form the basis of this portion of this chapter.

4.1.1 *Chain configuration statistics.*[108,109]

The abundance of various sequences (triad, tetrad and pentad) is governed by some statistical laws, e.g., Coleman and Fox[110] derived the required functional relations between the abundance of various dyads and triads. Extension of this work to tetrads and pentads has also been reported.[111] Some of these relations are independent of the mechanism of addition and therefore provide checks

for the assignment of the observed lines. Others depend on the stochastic laws which govern the structure of the chain and hence the observed abundance of the various sequences permits the establishment of laws governing a particular mechanism.

Some cases, such as the polymerization of MMA with phenyl-magnesium bromide in toluene at 195K, lead to non stochastic sequences and are better represented by the Coleman-Fox model.[111b]

A detailed review of the configuration statistics related to pentad sequences is beyond the scope of this thesis due to the unavailability of suitable instrumentation but several excellent books have been written on the subject.[108]

We shall be wholly concerned with the information that can be derived from dyad and triad sequences.

Suppose we define the probability that a monomer unit adds to a polymer chain to complete a meso dyad as P_m and to complete a racemic dyad as P_r where P_m and P_r are independent of the previous dyads completed, i.e. the chain structure does not affect the configuration of a dyad being completed.

In this case the chain is built up according to Bernoulli trial statistics and the proportion of isotactic, heterotactic and syndiotactic triads are given by,

$$i = mm = P_m^2 \tag{4.1}$$

$$h = mr + rm = 2 P_m (1-P_m) \tag{4.2}$$

$$s = rr = (1-P_m)^2 = P_r^2 \tag{4.3}$$

and $$i + h + s = 1 \tag{4.4}$$

It is possible to plot the theoretical values of i, h and s determined from eqns. 4.1 to 4.4 for given P_m from 0 to 1 and then try to fit the experimental values of i, h and s determined by spectroscopy. If the experimental points fall on the theoretical curves then Bernoulli trial statistics are followed. This method has been applied in section 4.2.1.

Isotactic polymer forms when $P_m \rightarrow 1$ and syndiotactic if $P_m \rightarrow 0$.

However, if the configuration of the chain end influences the mode of addition, the statistics are non-Bernoullian and the experimental points no longer fall on the theoretical Bernoullian curve, figure 4.3. The simplest non-Bernoullian mechanism is one which follows first order Markov chain statistics in which the configuration of one unit, presumably the chain end, influences the mode of addition. Two parameters are required to characterize this since the probability of a monomer unit completing an r dyad when adding to an m end unit, P_{mr}, is not the same as completing an r dyad on an r end unit, P_{rr}.

Isotactic polymer conforms to first order Markov chain statistics when $P_{mr} \rightarrow 0$ and $P_{rm} \rightarrow 1$. Two other types of polymer can be described by first order Markov chain statistics: heterotactic, when $P_{mr} > 0.5$, $P_{rm} > 0.5$ and stereoblock when P_{mr} and P_{rm} are small but finite (i.e. both less than 0.5).

From triad information Markov models of any order can be fitted

but not tested. First order Markov models may be tested from tetrad information and second order Markov models can only be tested from pentad sequences.

In certain instances, e.g., the polymerization of MMA by PhMgBr in toluene, at 195K,[111b] the sequence distributions fit neither Bernoullian nor finite Markov chain statistics and an alternative mechanism has been proposed by Coleman and Fox.[110] They suggest that in polymerizations initiated by metal alkyls there may be two (or more) states of the propagating chain end, corresponding to chelation by counter-ion (resulting in meso placements) and the interruption of this chelation by solvation (leading to r placements). The intervals between arrival and departure of the solvating species (e.g. THF in our case) are imagined to be longer than that corresponding to an average propagation step, but not necessarily very much longer, since block lengths are often very short.

4.1.2 *Free chain ends*

To account for the stereoregularity of propagation we have to comprehend the interactions through which the stereostructure of the newly formed segment is determined by the geometry of the preceding units. A carbon atom which is tetrahedral as a reactive chain end will normally retain this configuration when a monomer unit adds to it. The addition usually involves insertion into the C-catalyst bond and the new segment emerges with a well defined geometry which is not

altered in the course of the subsequent growth of the polymer.

A planar chain end is only fixed in configuration when the next unit adds to it and the propagation is stereoregular if the geometry of the penultimate unit determined the spatial arrangement around the *last* unit at a time when the latter becomes linked up to a newly added monomer. The planar chain end generally arises in free radical, classical carbonium and carbanion polymerizations and in almost all polymerizations involving these "free" species, Bernoulli statistics characterized by a single parameter, P_m, will prevail.

Under these conditions, the rate constants for isotactic and syndiotactic placement are given by 4.5.

$$\frac{k_{pi}}{k_{ps}} = \frac{P_m}{(1 - P_m)} \tag{4.5}$$

For the free radical polymerization of MMA, the Arrhenius plot of the stereoregularity of poly MMA yields a straight line and differences in the activation parameters are[108]

$$\Delta H_{pi}^{\dagger} - \Delta H_{ps}^{\dagger} = 4 \text{ kJ mol}^{-1} \tag{4.6}$$

$$\Delta S_{pi}^{\dagger} - \Delta S_{ps}^{\dagger} = 4 \text{ kJ mol}^{-1} \tag{4.7}$$

The preference for syndiotactic placement which increases at lower temperatures is due to a small additional energy required for isotactic placement which must outweigh the small favorable entropy.

4.1.3 *Bound chain ends.*

When the chain end is bound, either covalently or in an ion-pair, the situation can become extremely complicated especially when traces of strongly coordinating solvents are present.

The stereospecificity of the anionic polymerization of MMA initiated by Grignard reagents or organo-lithium compounds can present a bewildering picture. Polymer configurations depend on solvent, temperature and the halide and organo groups of the reagent[52c, 55, 109] and changes in any one of these variables can bring about dramatic changes as will be shown in the following section.

Two groups of workers[59,112,113] have studied the polymerization of β-deuterated acrylate esters initiated by PhMgBr, Ph_2Mg and fluorenyl-lithium. Using these monomers they were able to distinguish between cis and trans opening of the double bond because the β-carbon configuration can be determined by n.m.r. spectra of the resulting diisotactic polymer.

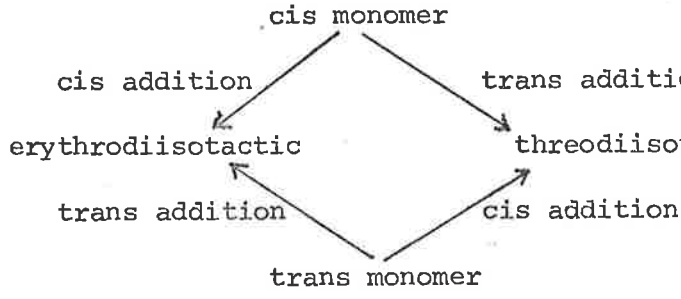

(4.8)

The presence of minute traces of ether in the Grignard reagent was critical. With the cis-monomer, complete absence of ether results in cis addition whereas traces of ether give almost equal proportions

of cis and trans monomer addition. As the ether content increases so does the trans addition. In the complete absence of ether, the system is heterogeneous and is undoubtedly extremely complex.[112,113]

Low temperatures favor cis addition and the proportions of the two mechanisms is determined during the first few minutes of the polymerization.[113]

Some interesting conclusions have been drawn concerning the possible mechanisms operating. Yoshino *et al*[113b] have shown that the concentration of unreacted Ph-Mg bonds increases as the temperature decreases and is determined in the initial stages of the polymerization. The presence of unreacted initiator groups adjacent to the propagating site could influence the rate and mode of addition at the α-carbon atom.

If the initiating species in the Grignard reaction is R_2Mg in equilibrium with RMgX then the proximity of an unreacted R-Mg group to the propagating site is explained. This suggestion is supported by the observation that cis addition increases when Ph_2Mg replaced PhMgBr[113a] and that cis addition is depressed in the presence of excess $MgBr_2$,[59,114] This is in accord with our conclusions in section 3.6 (c).

Unfortunately, the factors controlling the β-carbon symmetry seem to be independent of the α-carbon atom configuration which is our prime interest. However, studies on deuterated isopropylacrylate initiated by PhMgBr have shown that α-carbon isotacticity is established from the beginning of the chain.[114,59]

The polymerization of ethyl cis-β-d1-deuteromethacrylate initiated

Figure 4.2. Stereochemical control theory proposed by Bovey (ref. 115) to account for the observed β-cabon stereochemistry of the diisotactic polymer produced from ethyl-cis-β-deuteromethacrylate initiated by fluorenyl Li in varying THF/toluene mixtures.

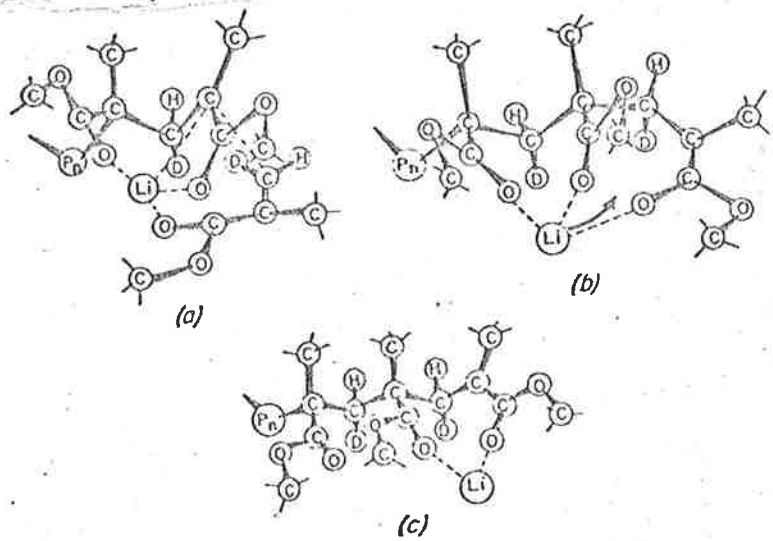

(*a*) An isotactic-like approach of the monomer to the chelated contact ion-pair. (*b*) The new C—C bond has been formed with the methylene D on the same side of the zigzag as the ester function. (*c*) The Li^+ moves up to the new anion, with concurrent rotation of the new penultimate ester group, forming the same chelated structure as in *a*.

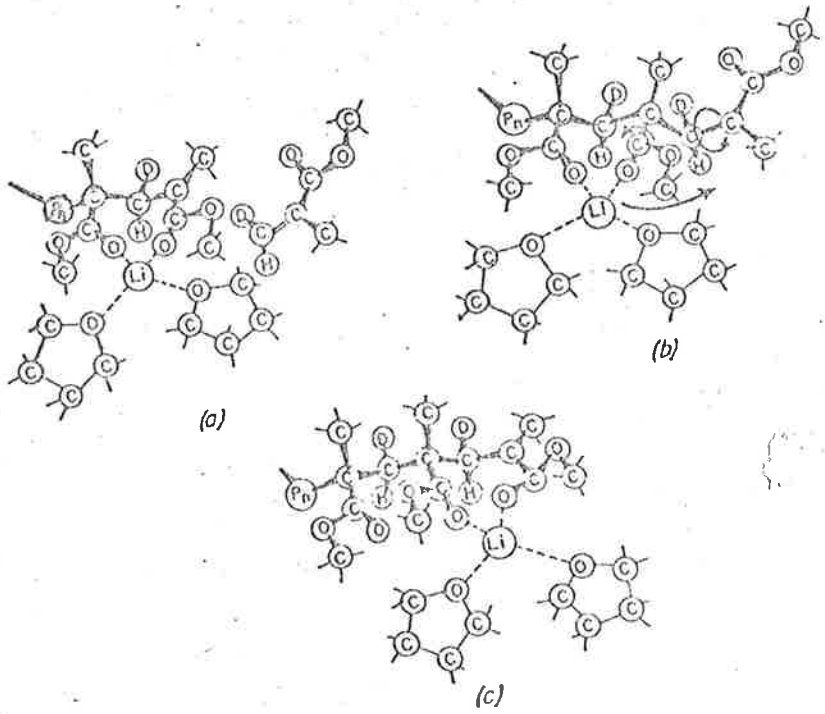

(*a*) A syndiotactic-like approach of the monomer to the peripherally solvated contact ion-pair. There is no coordination of the monomer carbonyl with the counterion, and nonbonded interactions force the approach to be syndiotactic-like. (*b*) The new C—C bond has been formed. (*c*) The Li^+ and its peripheral solvent shell move up to the terminal unit, with concurrent rotation of the ester function. As the new anion resides largely on the carbonyl, there is a simultaneous rotation about the new α,β-bond to reduce charge separation. This results in an *erythro-meso* placement, the methylene D being on the opposite side of the zigzag from the ester groups and the α-carbon now in an incipient isotactic configuration.

by fluorenyl lithium are simpler than the Grignard system and Bovey has detailed an interesting mechanism to account for the stereo-specificity of isotactic polymerization and is reproduced in figure 4.2.[115]

4.2 *Results*

4.2.1 *Grignard reagents.*

n-BuMgBr - The n.m.r spectra of poly MMA prepared using this initiator in toluene/THF solution are singularly uninteresting; only when they are compared with polymers produced by other Grignard reagents does the picture become fascinating, e.g. figure 4.1. However there are some interesting features. All of the polymers are non-Bernoullian, i.e. the proportions of i, h and s triads did not conform to the theoretical proportions predicted assuming Bernoullian trial statistics, figure 4.3. In this test, as outlined in section 4.1.1 the theoretical isotactic, heterotactic and syndiotactic abundance curves were calculated using eqn. 4.1 to 4.4 and plotted against P_m. Each experimentally determined polymer microstructure was tested by placing the syndiotactic abundance on the theoretical curve and then plotting the experimental values of the heterotactic and isotactic abundance at that particular value of P_m.

The different points correspond to polymers prepared at varying THF mole fraction and the results are shown in figure 4.4 and table 4.1. At low THF, there are almost equal proportions of i, h and s

Figure 4.3. The Bernoulli chain configuration test: the solid lines are the theoretical curves predicted from eqns. (4.1) to (4.4) for a polymer that conforms to Bernoulli chain configuration statistics. The experimental values of i, h and s are plotted at the value of P_m calculated (in this case) from $s = (1-P_m)^2$. If the polymer conforms to Bernoulli statistics, the experimental i and h values should fall on the theoretical curves.

○, ◐, ● = s, h and i values respectively, for the polymers in Table 4.1.

□, ◧, ■ = s, h, and i values for poly(MMA) prepared in the presence of HMPA (see text).

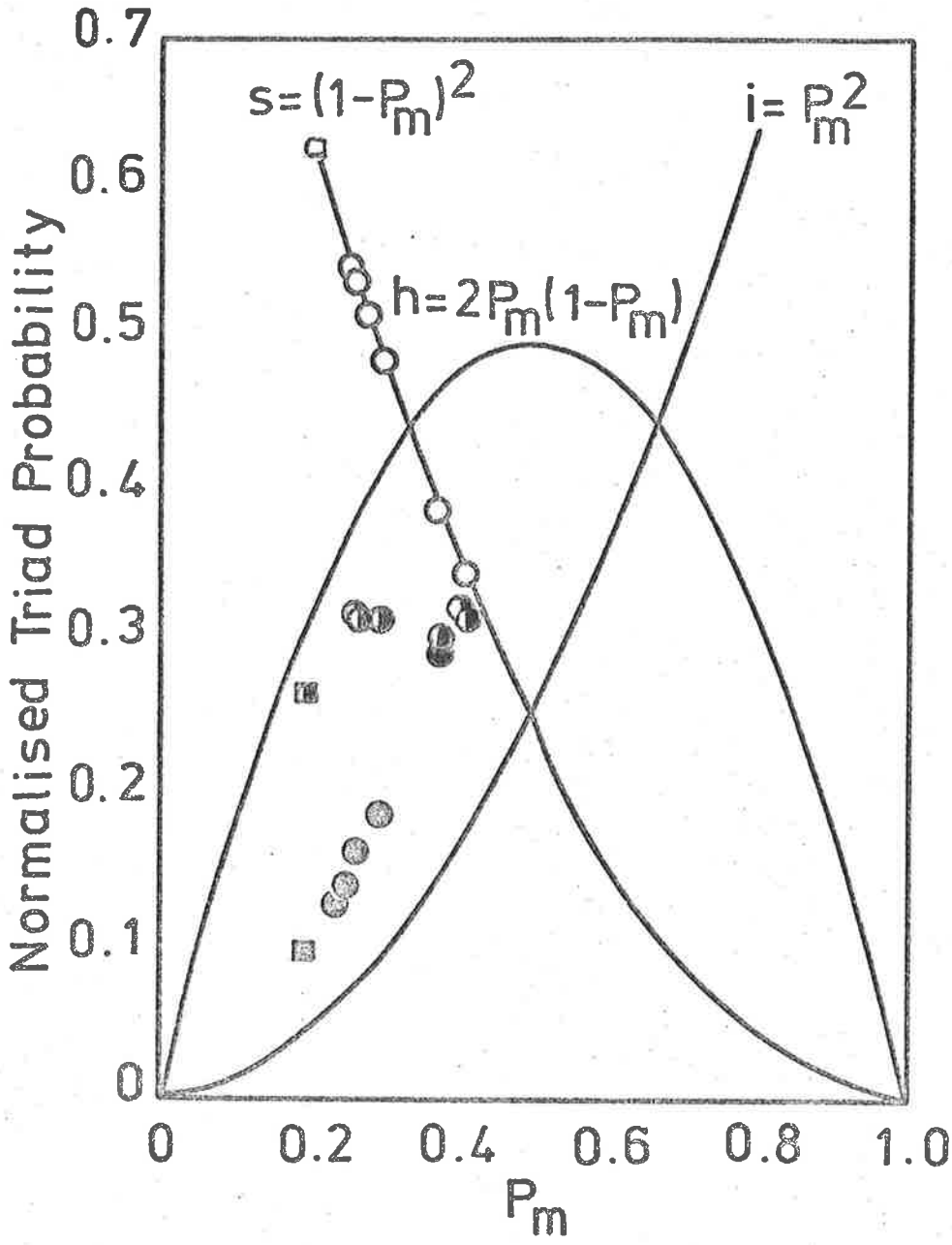
0.7
0.6
0.5
0.4
0.3
0.2
0.1
0
Normalised Triad Probability
s=(1-Pm)2
i= Pm2
h=2Pm(1-Pm)
0
0.2
0.4
0.6
0.8
1.0
Pm

triads but as χ_{THF} increases, the syndiotactic peak increases at the expense of the isotactic peak. Although it is pointless fitting these results to first order Markov statistics because this mechanism cannot be tested, using the relationships

$$P_{mr} = \frac{(mr)}{2(mm) + (mr)} \qquad (4.9)$$

$$P_{mr} = \frac{(mr)}{2(rr) + (mr)} \qquad (4.9a)$$

shows that at low THF the polymers are of the stereoblock type (P_{mr}, P_{rm} < 0.5) and grading into the syndiotactic type (P_{mr} > 0.5, P_{rm} < 0.5) as χ_{THF} increases. The relatively large heterotactic peak implies that the block lengths are very short since the number average sequence length is inversely related to the heterotactic abundance, (ref. 108 b, page 167).

It is interesting to note that when hexamethyl phosphorotriamide was added to the initiator, the resulting polymer was much closer to following Bernoullian chain statistics, figure 4.3, and there was very little change in the tacticity as the temperature changed from 223K (i: h: s = .10: .27: .63) to 211K (i: h: s: = .09: .29: .62), at [THF] = 0.9 mol dm.$^{-3}$ The concentration of THF had little effect when HMPA was present in the system, e.g. at 223K, [THF] = 2.8$_7$mol dm^{-3}, i: h: s = .11: .26: .63 whereas at [THF] = 0.9 mol dm^{-3}, the ratio was .10: .27: .64. This lack of dependence on THF would be expected in view of the extremely strong complexing ability of HMPA.

The effect of temperature on the tacticity of poly (MMA) prepared

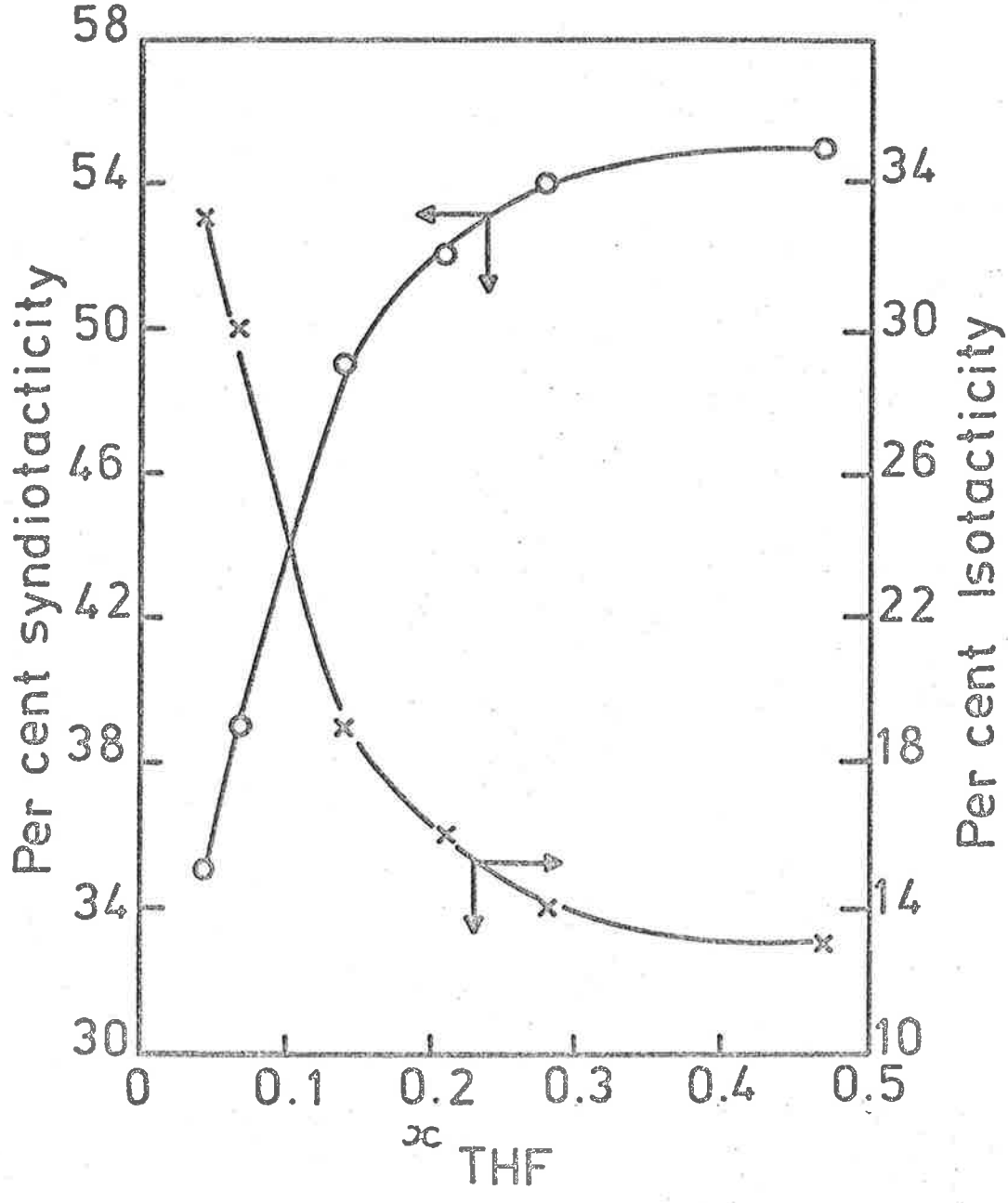

Figure 4.4. Change in isotacticity and syndiotacticity with increasing THF concentration for polymers prepared using n-BuMgBr. (Table 4.1)
T = 223K; $[MMA]_o$ = 2.76 mol dm^{-3}; $[G_n]_o$ = 0.10 mol dm^{-3}.

TABLE 4.1

Effect of THF mole fraction [a] *on stereospecificity of poly (MMA) prepared using n-BuMgBr.* [b]

T = 223K; $[MMA]_o$ = 2.76 mol dm^{-3}; $[Gn]_o$ = 0.10 mol dm^{-3}

x_{THF} [a]	$10^5 R_{p_o}$ mol $dm^{-3} s^{-1}$	*i*	*h*	*s*
0.046	2.92	.33	.32	.35
0.07	2.89	.30	.31	.39
0.14	2.87	.19	.32	.49
0.21	2.47	.16	.32	.52
0.28	2.09	.14	.32	.54
0.47	1.05	.13	.32	.55

(a) The concentration of THF is very nearly ten times the mole fraction.

(b) 60 MH_z spectra of 3% w/w solutions in $CHCl_3$ at 312K.

TABLE 4.2

Effect of temperature on chain structure using n-BuMgBr.

Temp./K	x_{THF} (a)	*i*	*h*	*s*
242	0.12	.20	.32	.48
226	0.12	.20	.32	.48
223	0.07	.30	.31	.39
198	0.07	.25	.29	.46

(a) [THF]/mol dm^{-3} ~ 10 x x_{THF}

using n-BuMgBr is shown in table 4.2.

There appears to be little change in tacticity in going from 242K to 226K, however from 223K to 198K the syndiotacticity slightly increases at the expense of the isotactic peak. The maximum error in the isotactic abundance would be (± 4%) and this trend may well be accounted for by experimental error.

Excess magnesium bromide added to the initiator had no effect on the polymer tacticity, e.g. at [THF] = 1.8 mol dm^{-3}, T = 223K, $[G_n]_o$ = 0.03M, *i*: *h*: *s* = 0.17: 0.32: 0.51 and with a ten fold excess of magnesium bromide the ratio becomes 0.15: 0.33: 0.52. However, the rate of polymerization was reduced. This decrease in rate is consistent with the ideas discussed in section 3.6 (c) where it was suggested that the presence of excess $MgBr_2$ may reduce the amount of conjugate addition.[102]

Figure 4.5 shows a comparison between the tacticity of the methanol-soluble and methanol-insoluble polymer. The relative abundance of triads are .18: .32:.50 for the methanol-insoluble polymer and .30: .33: .37 for the methanol-soluble material.

Sec-BuMgBr - The polymer produced using sec-BuMgBr/THF was much more isotactic than the n-BuMgBr case although the effect of THF was similar, table 4.3. At low χ_{THF} the polymer was "isotactic-like" with smaller heterotactic abundance than observed for the n-BuMgBr case implying longer sequences of isotactic and syndiotactic linkages. However, as χ_{THF} increased the isotactic peak decreased and both the

Figure 4.5. Tacticity of methanol insoluble poly (MMA), figure 4.5 (a) compared with tacticity of methanol soluble poly (MMA).
60 MHz n.m.r. spectra at 312K in chloroform.
T = 223K; $[MMA]_o$ = 1.92 mol dm^{-3};
$[G_n]_o$ = 0.036 mol dm^{-3}; [THF] = 0.99 mol dm^{-3}.

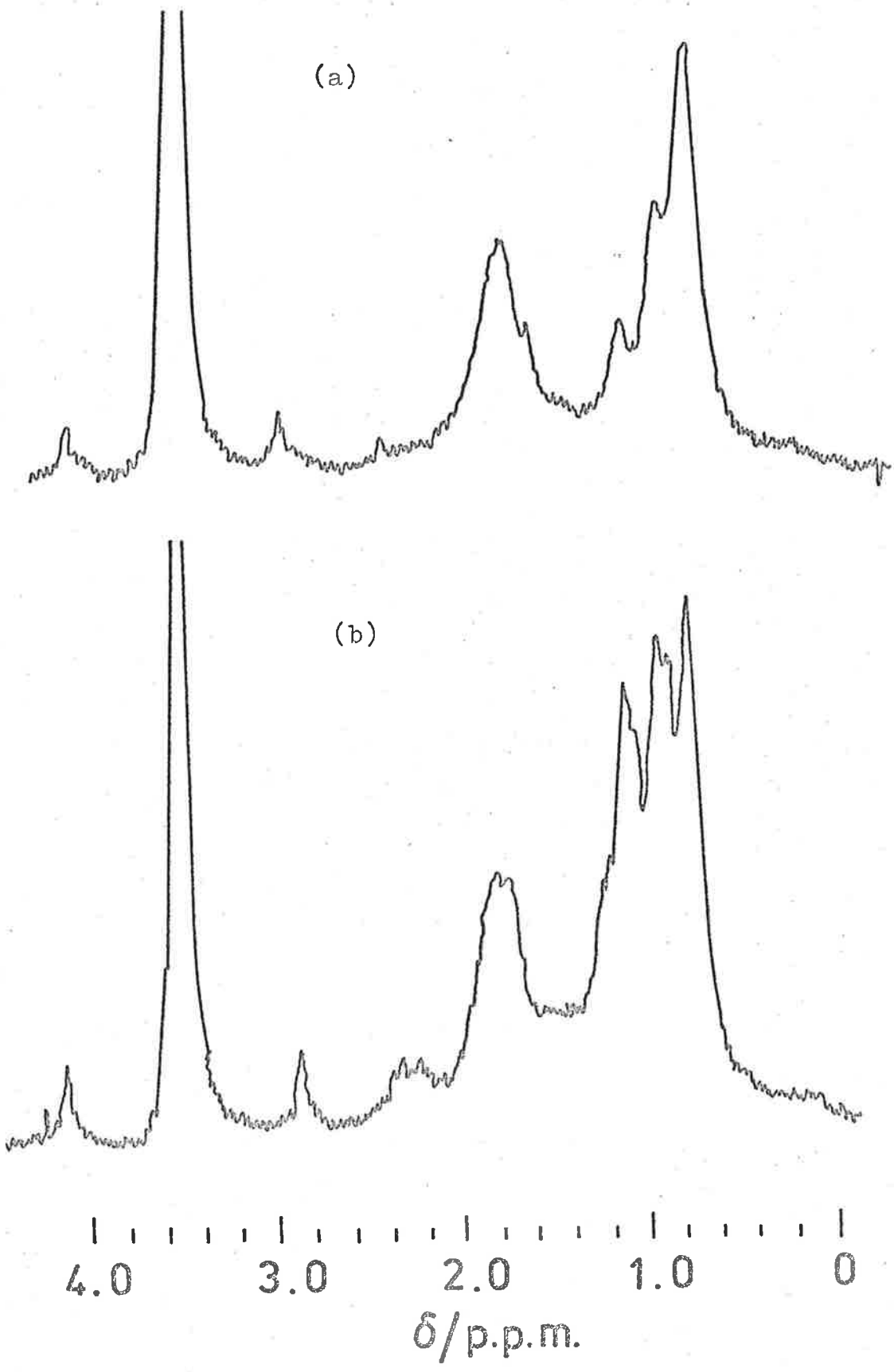
(a)
(b)
4.0
3.0
2.0
1.0
0
δ/p.p.m.

heterotactic and syndiotactic increased to an approximately constant value.

TABLE 4.3

Effect of THF mole fraction [(a)] *on tacticity of polyMMA prepared using Sec-BuMgBr*

$T = 223K$; $[MMA]_o = 0.96$ mol dm^{-3}; $[Gs]_o = 0.009$ mol dm^{-3}

x_{THF} [(a)]	$10^5 R_{p_o}$ /mol $dm^{-3} s^{-1}$	*i*	: *h* :	*s*
0.077	10.12	.67	.17	.16
0.126	10.85	.48	.23	.29
0.358	7.6	.28	.26	.46
0.48	8.5	.33	.25	.42
0.72	5.5	.32	.24	.44

(a) $[THF]$/mol $dm^{-3} \sim 10 \times x_{THF}$

The effect of temperature on the stereospecificity was similar to the n-BuMgBr system, although much more pronounced. Varying the temperature of both initiation and propagation (initiation deemed to be complete within 2 minutes) had little effect between 243K and 223K. However, at 198K, $x_{THF} = 0.14$, $[THF] = 1.44$ mol dm^{-3}, the isotactic portion decreased to only 23% compared with 48% at 223K, figure 4.6. This temperature dependence is non-Arrhenius and although the trend to higher syndiotacticity at low temperatures is observed for free

Figure 4.6. Effect of temperature on the tacticity of poly (MMA) from sec-BuMgBr. 60 MHz p.m.r spectra at 312K in chloroform. $[MMA]_o$ = 2.8 mol dm^{-3}; $[G_s]_o$ = 0.044 mol dm^{-3}; [THF] = 1.44 mol dm^{-3}.
(a) T = 223K; (b) T = 198K

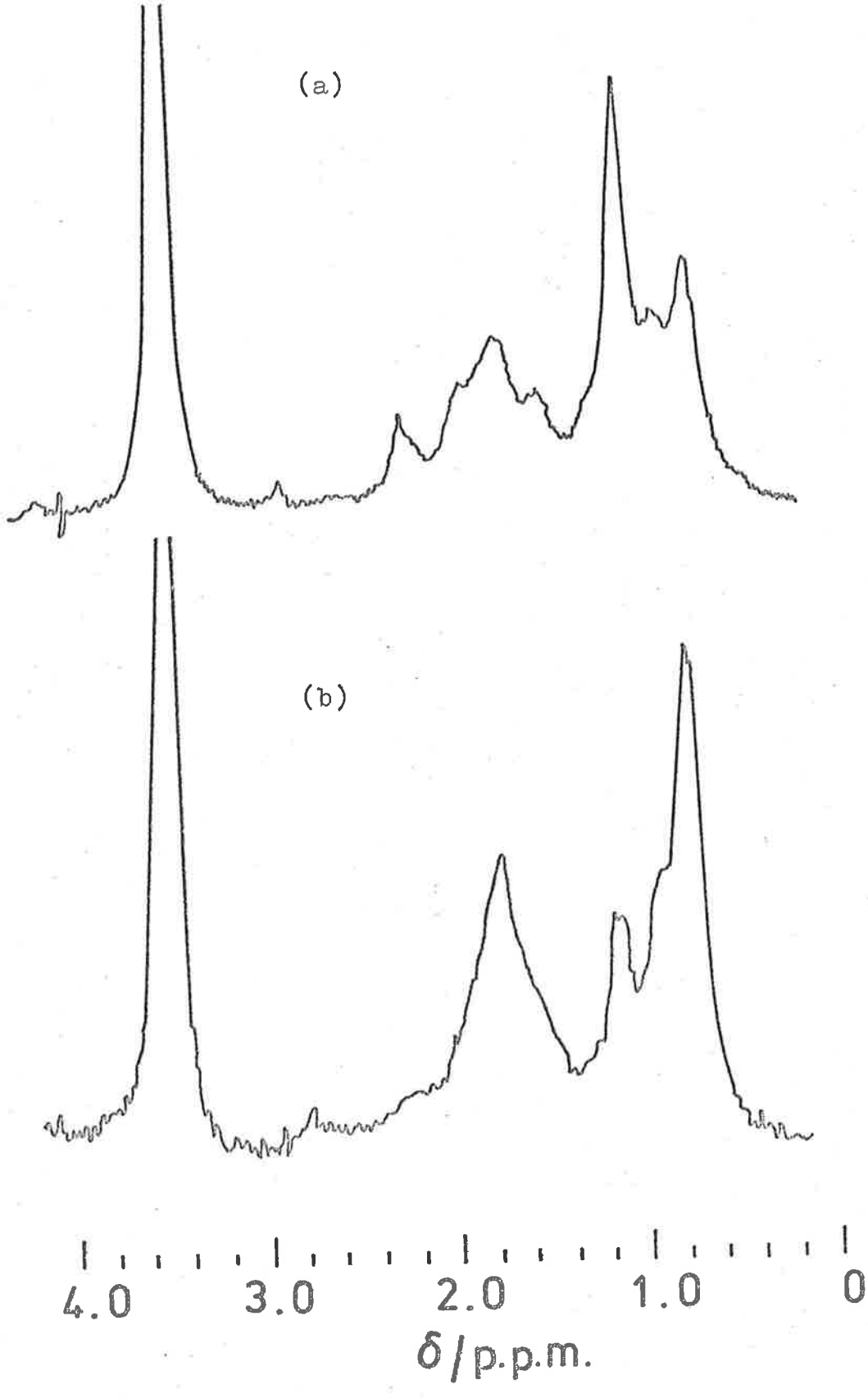
(a)
(b)
4.0
3.0
2.0
1.0
0
δ/p.p.m.

chains, (section 4.1.2) the magnitude of the change observed here is far greater than would be predicted from the relationships in equations 4.6 and 4.7.

The methanol-soluble polymer, unlike the n-BuMgBr case, was less isotactic than the insoluble fraction and was independent of the THF mole fraction e.g., table 4.4

TABLE 4.4

Chain configuration of the methanol insoluble and methanol soluble polymer using sec-BuMgBr.

$[MMA]_o$ = 0.96 mol dm^{-3}; $[G_s]_o$ = 0.009 mol dm^{-3}

Type of polymer	χ_{THF}	Temp. K	*i*	*h*	*s*
insoluble	0.46	223	32	24	44
soluble	0.46	223	15	30	55
insoluble	0.66	223	32	24	44
soluble	0.66	223	15	30	55

In these cases, the quantity of methanol-insoluble material appeared to increase as the THF mole fraction increased, although the amount was considerably less than for the n-BuMgBr system.

Tert-BuMgBr - As shown in figure 4.1 (b), the polymer prepared using this initiator was highly isotactic. This sample was prepared at 223K, χ_{THF} = 0.15, $[MMA]_o$ = 0.94 mol dm^{-3} and $[G_t]_o$ = 0.01 mol dm^{-3}

and the proportions of *i*: *h*: *s* triads was .84: .07: .09. At higher THF mole fractions the syndiotactic peak increased marginally but the heterotactic peak was still almost indistinguishable. This almost complete absence of the *mr* peak means that ther are very long blocks of completely isotactic polymer. Just as for n-BuMgBr and sec-BuMgBr the polymers prepared using tert-BuMgBr did not follow Bernoullian chain configuration statistics. The heterotactic peak should increase faster than the syndiotactic peak for small decreases in the isotactic abundance when Bernoulli chain statistics are observed, but with tert-BuMgBr, when the isotactic triad decreased, the syndiotactic triad increased and the heterotactic triad remained indistinguishable.

The addition of excess magnesium bromide had no effect on the microstructure but did reduce the rate of polymerization as in the n-BuMgBr case.

Reducing the temperature of polymerization from 223K to 198K resulted in a substantial increase in the syndiotactic triad, at the expense of the isotactic triad, figure 4.7.

Iso-BuMgBr - The marked effect that branching at the α-carbon atom of the Grignard reagent has on the stereospecificity of the resulting polymer has been reported for the diethyl-ether/toluene solvent,[55b] and the trend towards isotactic polymer as the α-carbon becomes more branched is similar to our observations. However, the effect of β-carbon branching is completely different.

Figure 4.7. Effect of temperature on the tacticity of poly (MMA) from tert-BuMgBr. 60 MHz p.m.r. spectra at 312K in chloroform. $[MMA]_o$ = 2.5 mol dm^{-3}; $[G_t]_o$ = 0.015 mol dm^{-3} $[THF]$ = 2.6 mol dm^{-3}.

(a) T = 223K (b) T = 198K.

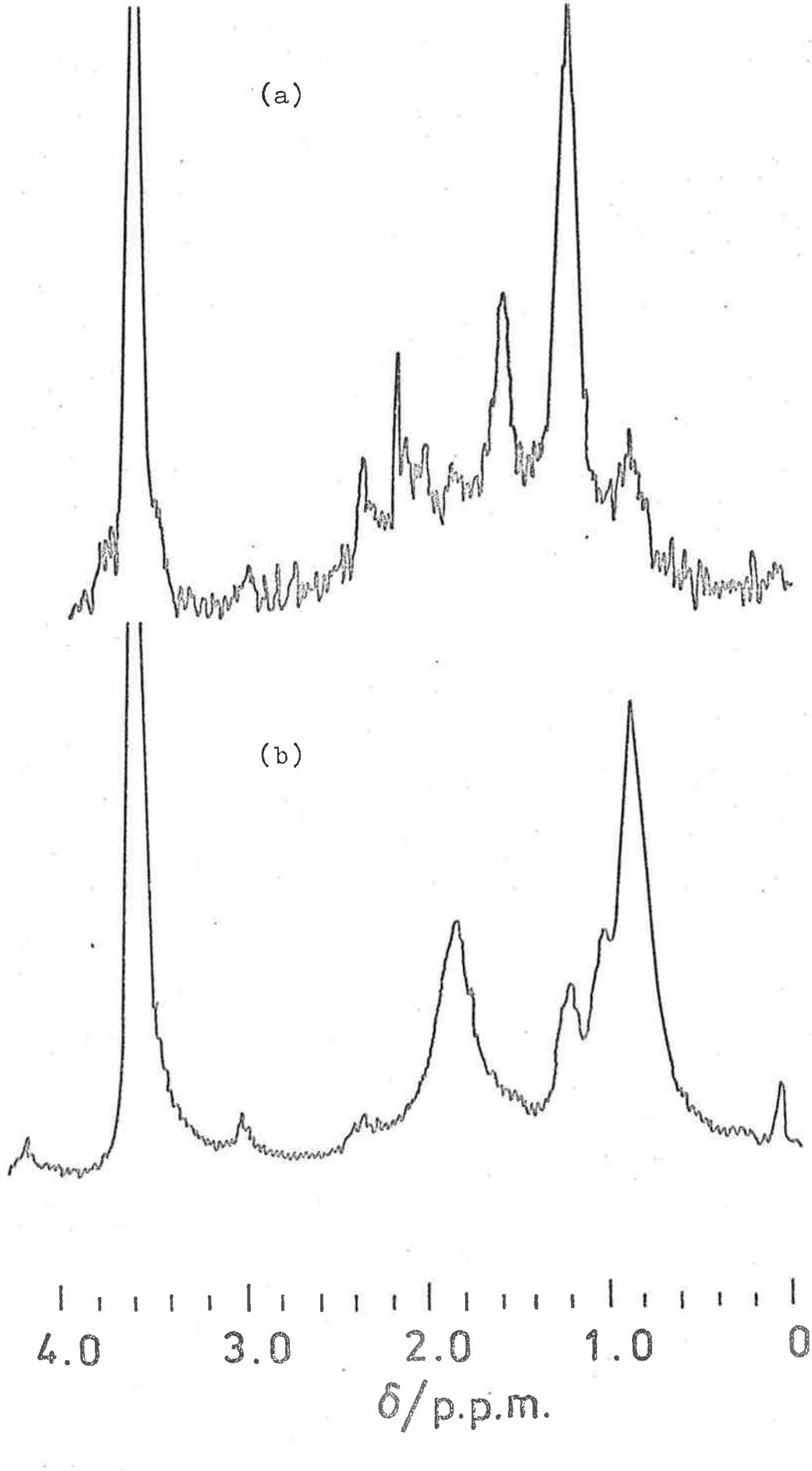
(a)
(b)
4.0
3.0
2.0
1.0
0
δ/p.p.m.

At [THF] = 2.1 mol dm^{-3}, T = 223K, *i*: *h*: *s* = .13: .30: .57 for the iso-BuMgBr initiator which is very similar to the n-BuMgBr case. Watanabe *et al*[55b] found almost 100% isotactic polymer at 223K using iso-BuMgBr in diethyl-ether/toluene mixture, although the mole fraction of ether was not mentioned. Many of their reactions were done under ether free conditions which must be heterogeneous and comparisons cannot be made with too much confidence.

n-BuMgI and tert-BuMgCl - These initiators were used to ascertain the effect of halide on polymer tacticity. With n-BuMgI at 223K, [THF] = 3.5 mol dm^{-3}, *i*: *h*: *s* = .25: .30: .45 compared with .13: .32: .55 for the bromide under identical conditions. The isotactic content has doubled at the expense of the syndiotactic peak.

Using tert-BuMgCl at 223K and [THF] = 4.3 mol dm^{-3} the *i*: *h*: *s* ratio was .20: .26: .54 which represents a drastic reduction in the isotactic nature of the polymer compared with tert-BuMgBr.

When a mixture of tert-BuMgCl = 0.019 mol dm^{-3} and tert-BuMgBr = 0.013 mol dm^{-3} was used the resulting polymer had a stereospecificity of .28: .25: .47, figure 4.8.

4.2.2 *Dialkyl magnesiums*

Table 4.5 shows the proportion of isotactic, heterotactic and syndiotactic triads obtained at 223K using $(n\text{-Bu})_2Mg$, $(sec\text{-Bu})_2Mg$ and $(tert\text{-Bu})_2Mg$ compared with the corresponding Grignard reagents under identical conditions.

Figure 4.8 (a). Poly (MMA) prepared using tert-BuMgBr at 223K. 60 MHz p.m.r. spectra at 312K in chloroform.

(b) poly(MMA) prepared at 223K using a mixture of tert-BuMgBr and tert-BuMgCl.

$[THF] = 4.3$ mol dm^{-3}; $[MMA]_o = 2.5$ mol dm^{-3};

$[G_{t_{Br}}]_o = 0.013$ mol dm^{-3}; $[G_{t_{Cl}}]_o = 0.019$ mol dm^{-3}.

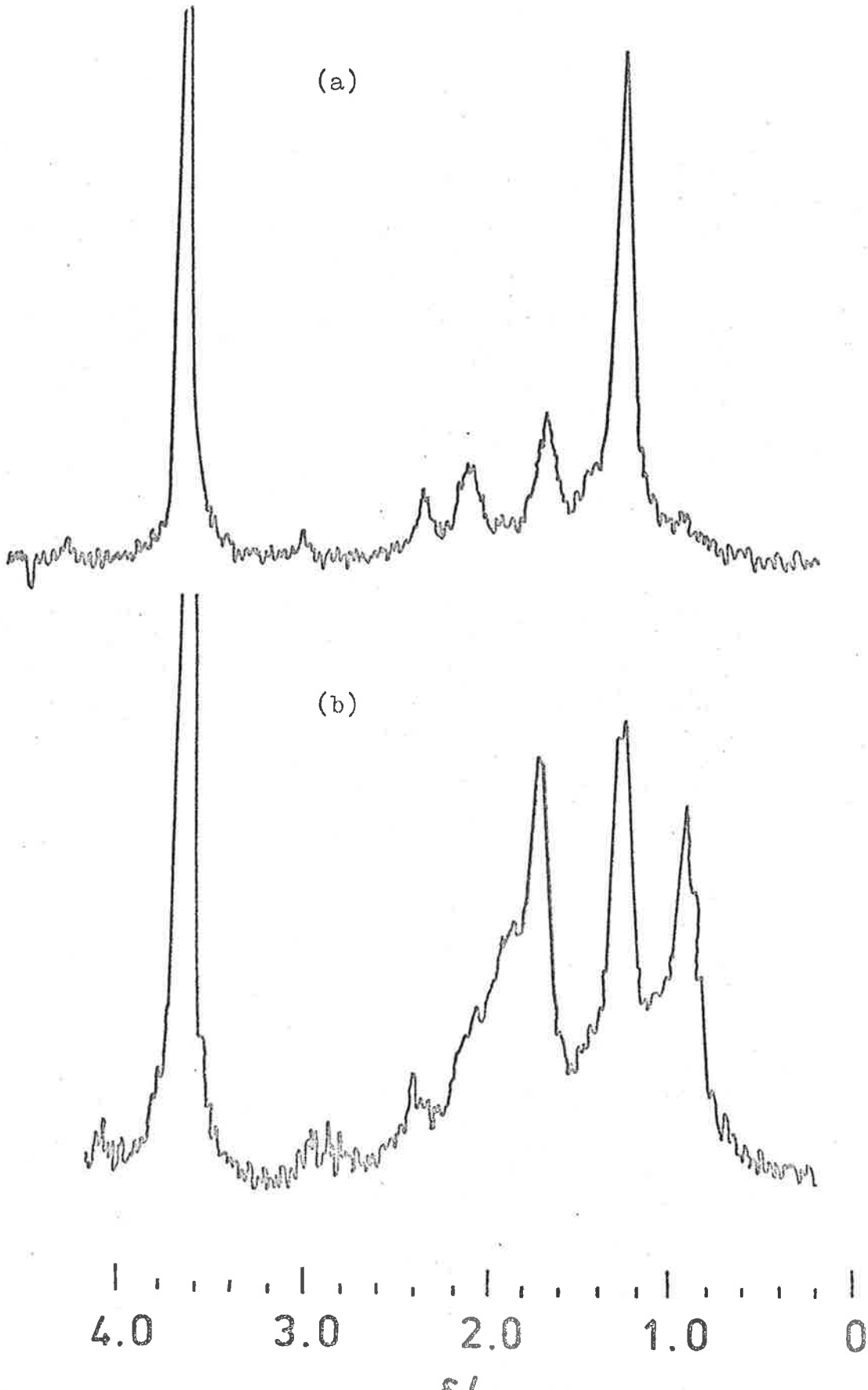
(a)
(b)
4.0
3.0
2.0
1.0
0
δ/ p.p.m.

TABLE 4.5

Stereospecificity of poly(MMA)[a] *using dialkylmagnesium initiators compared with the corresponding Grignard reagents*

T = 223K

Initiator	x_{THF}	*i*	*h*	*s*
n-BuMgBr	0.10	.18	.32	.50
$(n\text{-Bu})_2Mg$	0.10	.19	.31	.50
sec-BuMgBr	0.08	.67	.17	.16
$(sec\text{-Bu})_2Mg$	0.08	.17	.36	.47
tert-BuMgBr	0.28	.84	.06	.10
$(tert\text{-Bu})_2Mg$	0.28	.18	.35	.47

(a) These are the methanol insoluble fractions.

From the identical kinetic results in chapter three it is not surprising that polymers prepared using $(n\text{-Bu})_2Mg$ have very similar micro-structures to those prepared with n-BuMgBr. It is also interesting to note that the polymer prepared using the supernatant liquid when tetraglyme was added to the initiator had identical micro-structures to those prepared using $(n\text{-Bu})_2Mg$ and n-BuMgBr.

The most interesting results in table 4.5 are the comparisons between the polymer tacticities obtained using $(sec\text{-Bu})_2Mg$ and $(tert\text{-Bu})_2Mg$ compared with their corresponding Grignard reagents.

The syndiotactic and heterotactic peaks increase at the expense of the isotactic peak in both the (sec-Bu)$_2$Mg and (tert-Bu)$_2$Mg systems compared with sec-BUMgBr and tert-BuMgBr. The change in tacticity is most dramatic on going from tert-BuMgBr to (tert-Bu)$_2$Mg.

As mentioned before, at the conclusion of this research a 90 MHz n.m.r. spectrometer was acquired. The spectrum of two polymer samples run at ambient temperature are shown in figure 4.9 (a) and 4.9 (b). Figure 4.9 (b) is identical to the polymer sample in figure 4.1 (b) and the methylene quartet is now clearly resolved. The heterotactic peak is virtually non-existent and so determination of the *i*, *h*, *s* triads is very difficult. The polymer did not conform to Bernoulli trial chain configuration statistics and it is doubtful if it conforms to first order Markov statistics. The deviation from first order Markov statistics was not great and may be accounted for by the large experimental error in determining the triad proportions arising because of the very small *mr* and *rr* peaks.

Figure 4.9 (a) is the 90 MHz p.m.r spectrum of a polymer sample prepared using n-BuMgBr at χ_{THF} = 0.046 [THF] = 0.465 mol dm^{-3}, and T = 223K. The greater resolution obtained with this instrument is obvious when the methylene region is inspected, and compared with the methylene region of figure 4.1 (a). Peak assignments were made by comparison with 220 MHz spectra of similar polymers[109] and the assignments were tested using the statistical relationships that must hold irrespective of the mechanism operating, e.g. from the triad

Figure 4.9. 90 MHz p.m.r. spectrum of poly (MMA) in deuterochloroform.
(a) stereoblock polymer from n-BuMgBr
T = 223K; [THF] = 0.46 mol dm^{-3};
$[MMA]_o$ = 2.76 mol dm^{-3}; $[G_n]_o$ = 0.10 mol dm^{-3}.
Tentative tetrad assignments made by comparison with 220 MHz spectra of polymers from ref. 109.
(b) isotactic poly (MMA) from tert-BuMgBr
(see figure 4.1 (b) for 60 MHz spectrum of this polymer).

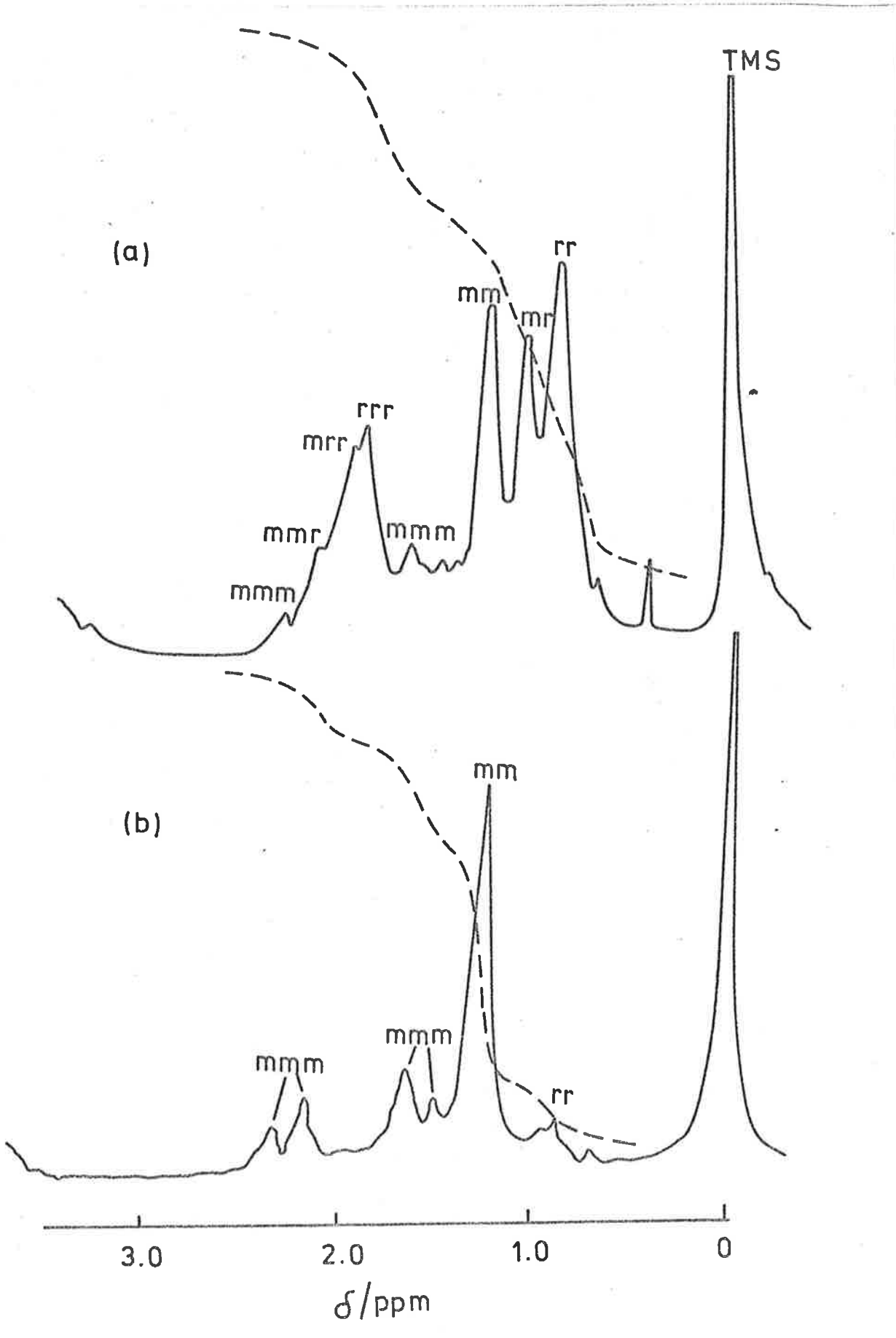
TMS
(a)
rr
mm
mr
rrr
mrr
mmr
mmm
mmm
(b)
mm
mmm
mmm
rr
3.0
2.0
1.0
0
δ/ppm

integrals, mm = .33, mr = .30 and rr = .37.

Using the relationships in eqn. (4.9) and (4.9a)

$$P_{mr} = 0.31, \qquad P_{rm} = 0.29 \text{ and}$$

$$\Sigma_p = P_{mr} + P_{rm} = 0.60$$

For Bernoullian statistics, $\Sigma_{p_r} = 1.0$, so the above polymer is clearly non-Bernoullian and falls in the category of stereoblock with P_{mr} , $P_{rm} < 0.5$. The relatively large mr peak indicates that the block lengths are short.

From the tetrad integrals of the peaks assigned in figure 4.9(a)

$$rrr_{obs} = 0.25 \text{ and } \qquad mrr_{obs} = 0.25$$

One statistical relationship that must hold between triad and tetrad relationships, irrespective of the mechanism is,

$$rr \equiv rrr + \tfrac{1}{2} mrr \tag{4.10}$$

This identity is verified (with in experimental error) when the observed values for rr, rrr and mrr are substituted.

For first order Markov statistics the following relationship must hold,

$$rrr_{obs} = \{P_{mr}(1 - P_m)^2\}/(P_{mr} + P_{rm}) \tag{4.10a}$$

The left hand side is 0.25 and the right hand side 0.26. It appears that this polymer obeys first order Markov chain statistics within experimental error. Of course, to be absolutely certain that the peak assignments are correct, all of the dyad-triad and triad-tetrad

relationships similar to (4.10) should be tested. After the assignments have been confirmed, four of the six relationships similar to 4.10a which must hold for first order Markov chain statistics should be verified, however, as Bovey points out, verifying all the above relationships is very difficult in practice due to overlapping tetrad peaks, etc.[108]

MOLECULAR WEIGHT AND MOLECULAR WEIGHT DISTRIBUTION

4.3 *Introduction*

There are many methods available for the determination of molecular weights (MW) of high polymers.[116] However, unless the polymers are completely monodisperse the MW values obtained are average values and depend upon the particular method employed.

An estimate of the polydispersity can thus be obtained by comparing the molecular weights obtained by different methods. This method of estimating the polydispersity is really only satisfactory if the polymer is known to have a unimodal molecular weight distribution (MWD).

Gel permeation chromatography[117] (g.p.c) is a technique which allows determination of the MWD and the MW of polymers. Unfortunately, at present, the method is not absolute, because quantitative MW measurements must be preceded by accurate calibration with samples precisely characterized in solution.

In gel permeation chromatography a dilute solution of the polymer is pumped through a series of columns packed with a polystyrene gel

crosslinked with divinyl benzene which sorts the macromolecules according to their size in solution. The exact way in which this size sorting occurs is not certain and three mechanisms have evolved:[118] restricted diffusion,[119] steric exclusion[120] and thermodynamic theories.[121]

The restricted diffusion theory[119] assumes that the time required for a molecule to diffuse in and out of a gel pore is significant relative to the time the molecule spends in the vicinity of that pore. Other authors[117,120] suggest that as the solution passes through the column, the smallest molecules enter the gel and are retarded whereas the larger molecules are excluded and pass through the column more quickly. The permeation or diffusion rate of solute into the gel is sufficiently faster than the elution rate, thus allowing diffusion equilibrium to be attained. Separation is then based on the different volumes inside the gel particles which are accessible to solute molecules of different size.

Although each individual theory has merit, probably no single mechanism exists, but rather the true explanation must take account of a combination of these factors.

4.3.1 *Calibration*

As mentioned previously, g.p.c. is not an absolute technique and a detailed knowledge of the necessary calibration curve is necessary for quantitative evaluations of MW and MWD's.[122]

The commonest calibration method is to use well characterized samples of narrow MWD polystyrene and present the data as a plot of peak elution volume V_e versus log $\bar{M}_w$.[123] Here $\bar{M}_w$ is the weight average molecular weight and although its value will be close to $\bar{M}_n$ (the number average MW) it is used in preference to $\bar{M}_n$ because the g.p.c elution curve can be regarded as a direct weight concentration plot.

Table 4.6 and figure 4.10 show the results obtained using various standard polystyrene samples supplied by Water's associates.

The obvious disadvantage of this calibration method is that polystyrene was used as the standard, whereas poly(MMA) is the unknown. Because well characterized standards for most polymers (including poly(MMA)) are not available, most of the recent g.p.c. researchers have attempted to develop a universal calibration curve independent of polymer type.

Grubisic *et al*[124] suggested the use of the hydrodynamic volume, V, for the calibration. According to the Einstein viscosity law

$$[\eta] = K(V/M) \qquad 4.8$$

where $[\eta]$ = viscosity

V = hydrodynamic volume

M = molecular weight

and K = constant

By plotting log $[\eta]\bar{M}_w$ versus V_e for one polymer, Grubisic claims that the plot is universal for other polymers, being independent of

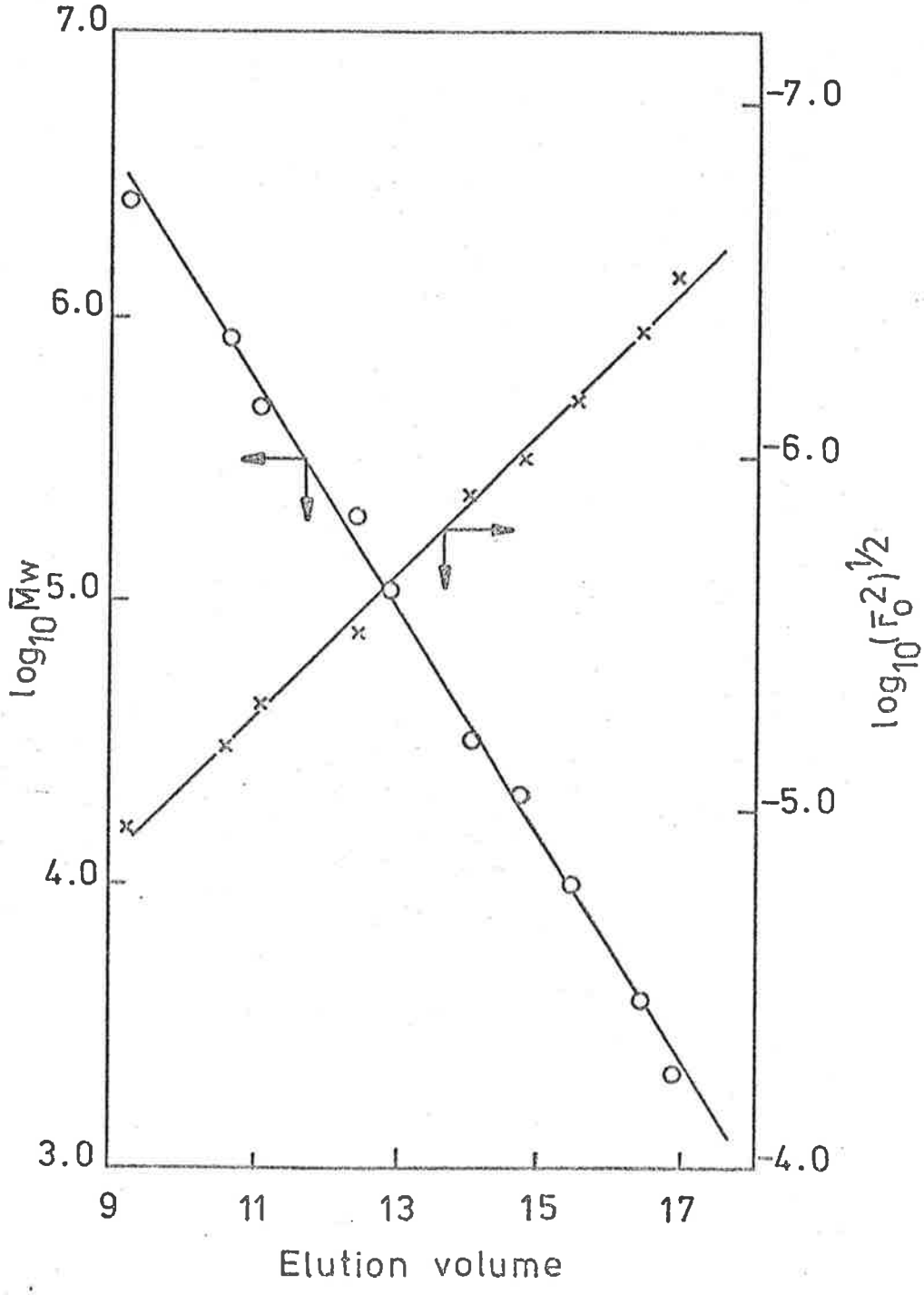

Figure 4.10. Calibration curves for the Waters Associates model 501 ALC/GPC instrument fitted with one linear 10^5 Angstrom column.

$\log_{10}\bar{M}_w = 10.18 - 0.4009(V_e)$

TABLE 4.6

Data for the construction of a calibration curve for g.p.c. analysis. Samples are polystyrene, supplied by Water's Associates

T = 301K; Sample concentration = 0.2% w/v;

Injection time = 2 minutes; flow rate = 1.4 cm^3 $min.^{-1}$

$10^3\bar{M}_w$	$\bar{M}_w/\bar{M}_n$	$\log_{10}\bar{M}_w$	V_e (a)	$10^7(\bar{r}_o^2)^{\frac{1}{2}}$	$\log_{10}(\bar{r}_o^2)^{\frac{1}{2}}$
3.1	1.08	3.332_2	16.89	3.116	-6.506_4
4.0	1.29	3.602_1	16.43	4.307	-6.365_8
10.0	1.04	4.000_0	15.44	6.800	-6.167_5
20.8	1.04	4.318_1	14.78	9.807	-6.008_5
33.0	~ 1.0	4.518_5	14.05	12.353	-5.908_3
111.0	1.00	5.045_3	12.89	22.655	-5.644_7
200.0	1.04	5.301_0	12.44	30.411	-5.517_o
498.0	1.23	5.697	11.16	47.987	-5.318_9
867.0	1.13	5.938_0	10.61	63.316_7	-5.198_5
2610.0	1.31	6.416_6	9.22	109.905	-4.959

(a) V_e = elution volume or strictly speaking; the elution count. The absolution elution volume is obtained by multiplying V_e by the volume of the siphon.

chemical structure and polymer geometry. This method of calibration has been the subject of much recent investigation.[125]

Another method adopted by Dawkins,[126] proposes use of the unperturbed dimensions which may be evaluated from published values of $(\bar{r}_o^2/M)^{\frac{1}{2}}$ where $(\bar{r}_o^2)^{\frac{1}{2}}$ is the root mean square end to end distance.

A plot of log $(\bar{r}_o^2)^{\frac{1}{2}}$ versus V_e is shown in figure 4.10 the value of $(\bar{r}_o^2/M) = 4.49 \times 10^{-17}$ being obtained from the literature.[127]

4.3.2 *Treatment of results*

Apart from the calibration problems, accurate quantitative evaluation of the chromatogram of an 'unknown' is still difficult because of various correction factors. Complicated computer programs have been devised in an attempt to account for these factors.[128]

By far the simplest method of representing the data from the unimodal g.p.c. chromatograms is to plot on normal probability paper, the elution volume versus the cumulative weight percent.

Provided the peaks are Gaussian, the resulting elution volume/cumulative weight plot will be linear and the standard deviation, can be determined from the difference in counts at the 50% and 16% mark. The molecular weight, $\bar{M}_g$, at the 50% mark is the geometric mean and the two averages $\bar{M}_w$ and $\bar{M}_n$ may be obtained from the following relationships

$$\sigma_{mw} = \sigma_g \cdot k \qquad (4.11)$$

$$\bar{M}_w = \bar{M}_g \exp(\sigma^2_{MW}/2) \qquad (4.11a)$$

$$\bar{M}_w / \bar{M}_n = \exp(\sigma^2_{MW}) \qquad (4.11b)$$

where k is the slope of the calibration curve.[129]

Of course this method is inapplicable to systems which are not unimodal.

4.4 *Results*

4.4.1 *Grignard reagents*

n-BuMgBr - The methanol-insoluble polymer was unimodal and ranged in MW from ca. 2×10^4 to 8×10^4 depending on the conditions of the experiment. In some instances, e.g. at low THF, a very small peak appeared at $\bar{M}_g \approx 3 \times 10^6$ figure 4.12. Here $\bar{M}_g$ is the MW calculated at the peak maximum. The peaks were Gaussian as shown by the straight lines obtained when plotting the elution volume versus the cumulative weight, figure 4.11. Although the MWD was broad when compared with samples of polystyrene prepared with n-BuLi, values of $\bar{M}_w/\bar{M}_n$ from 1.18 at low χ_{THF}, to 1.28 at high χ_{THF} were much narrower than expected. Previous workers had obtained values of $\bar{M}_\eta / \bar{M}_n > 20$ using PhMgBr at 273K.

Table 4.7 contains the complete analysis of the g.p.c. chromatograms for polyMMA prepared using different initiator concentrations.

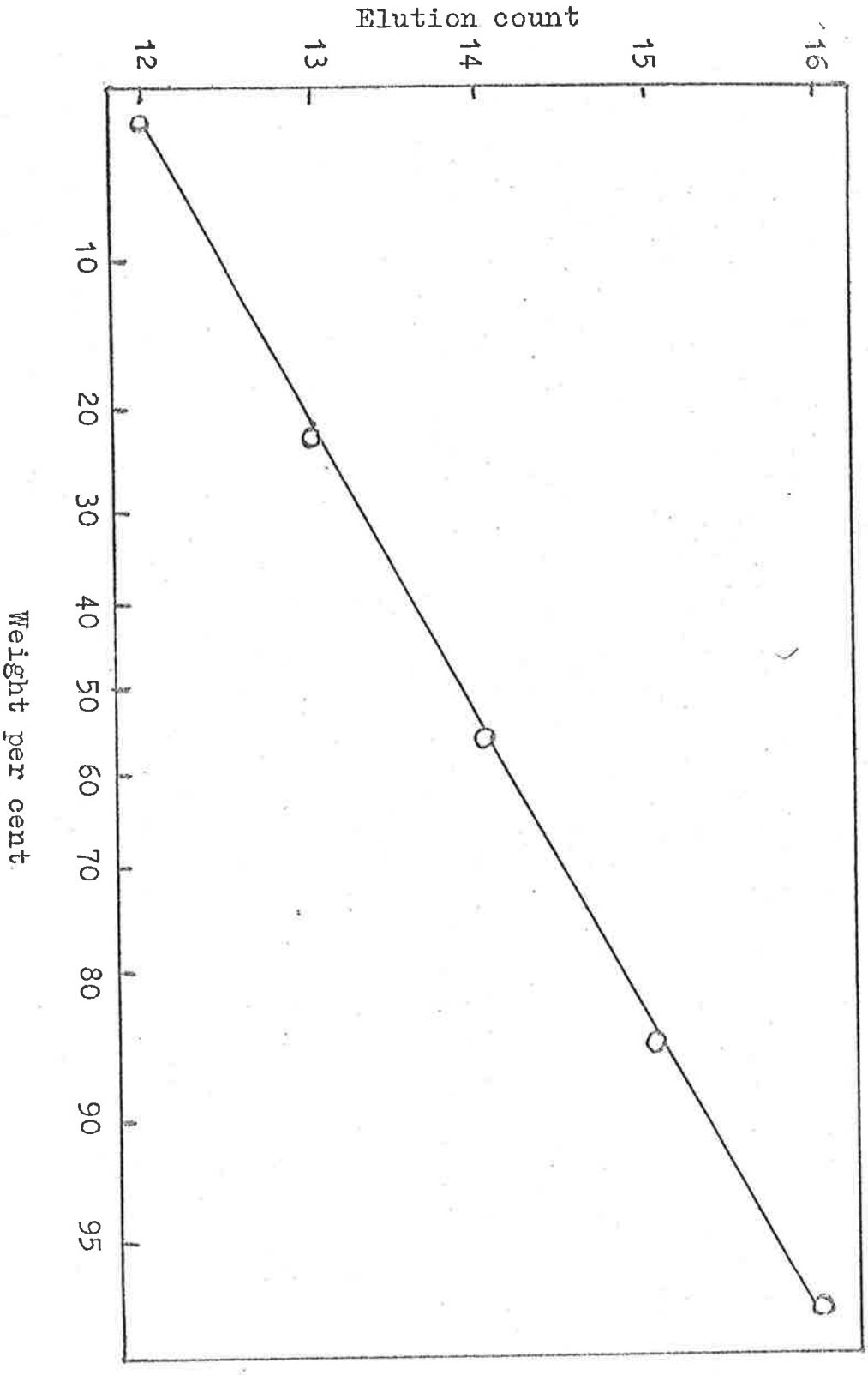

Figure 4.11. Cumulative weight plot for quantitative g.p.c. analysis of the first polymer sample in table 4.7.
σ_c = 1.12; k = 0.4009; σ_{MW} = 0.4490; $\bar{M}_w/\bar{M}_n$ = 1.22; $\bar{M}_n$ = 39000.

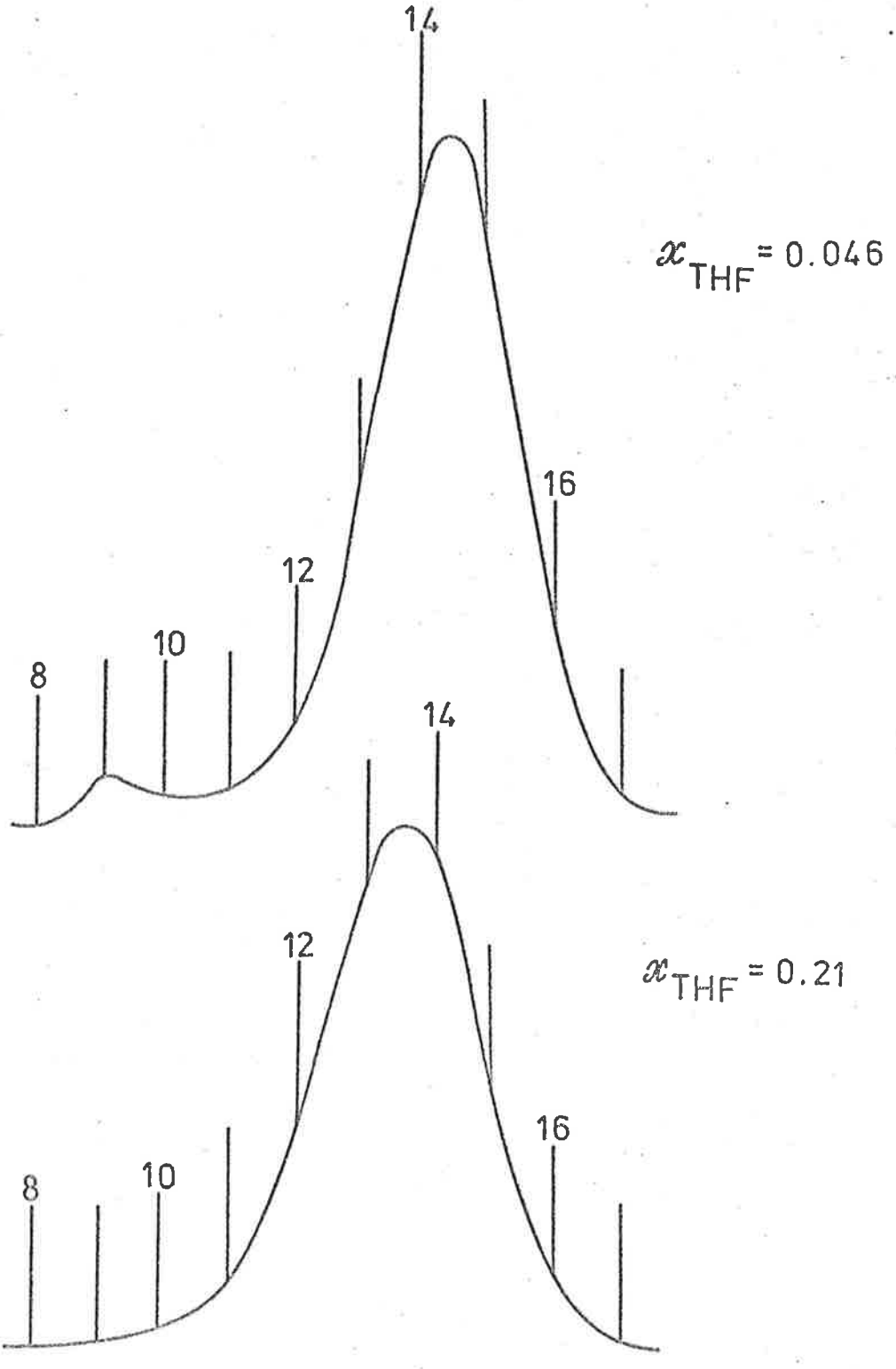

Figure 4.12. Effect of THF concentration on MWD of poly(MMA) from n-BuMgBr. (Methanol insoluble polymer only shown). T = 223K; $[MMA]_o$ = 2.76 mol dm^{-3}; $[G_n]_o$ = 0.10 mol dm^{-3}.

TABLE 4.7

Variation of MW and MWD of poly(MMA) with n-BuMgBr concentration.

Polymerization temp. = 223K; χ_{THF} = 0.28;

[THF] = 2.8$_7$ mol dm^{-3} ; $[MMA]_o$ = 2.76 mol dm^{-3}

$[G_n]_o$ mol dm^{-3}	$\bar{M}_w/\bar{M}_n$	$10^{-4}\bar{M}_n$	%Conversion	$10^{-4}\bar{M}_n$(adj.)[a]
.05	1.22	3.9	6	1.95
.07$_7$	1.21	6.1	14	4.7
0.10	1.21	6.1	16	6.1
0.10	1.22	4.0	9.7	4.0
0.19	1.25	3.5	18	6.6

(a) $\bar{M}_n$ (adj) is the number average MW calculated assuming that $\bar{M}_n \propto \frac{1}{[G_n]_o}$, the values are adjusted to $[G_n]_o$ = 0.10mol dm^{-3}, see text.

The errors in the values of $\bar{M}_w$ and $\bar{M}_n$ are of the order of ± 10% which was due to the fact that only 1 linear column was used for the determinations (section 2.4.5). Using this arrangement, an error of 0.5% in calculating the cumulative weight at 50% will create an error of 10% in the resultant values of $\bar{M}_w$ and $\bar{M}_n$, although the MWD will be almost unaffected. This situation can be easily rectified by using a bank of 2 or more linear columns of the same porosity but the elution time will increase proportionally. Unfortunately, this time factor was critical, since the g.p.c. (like the 100MH$_z$ n.m.r) instrument was

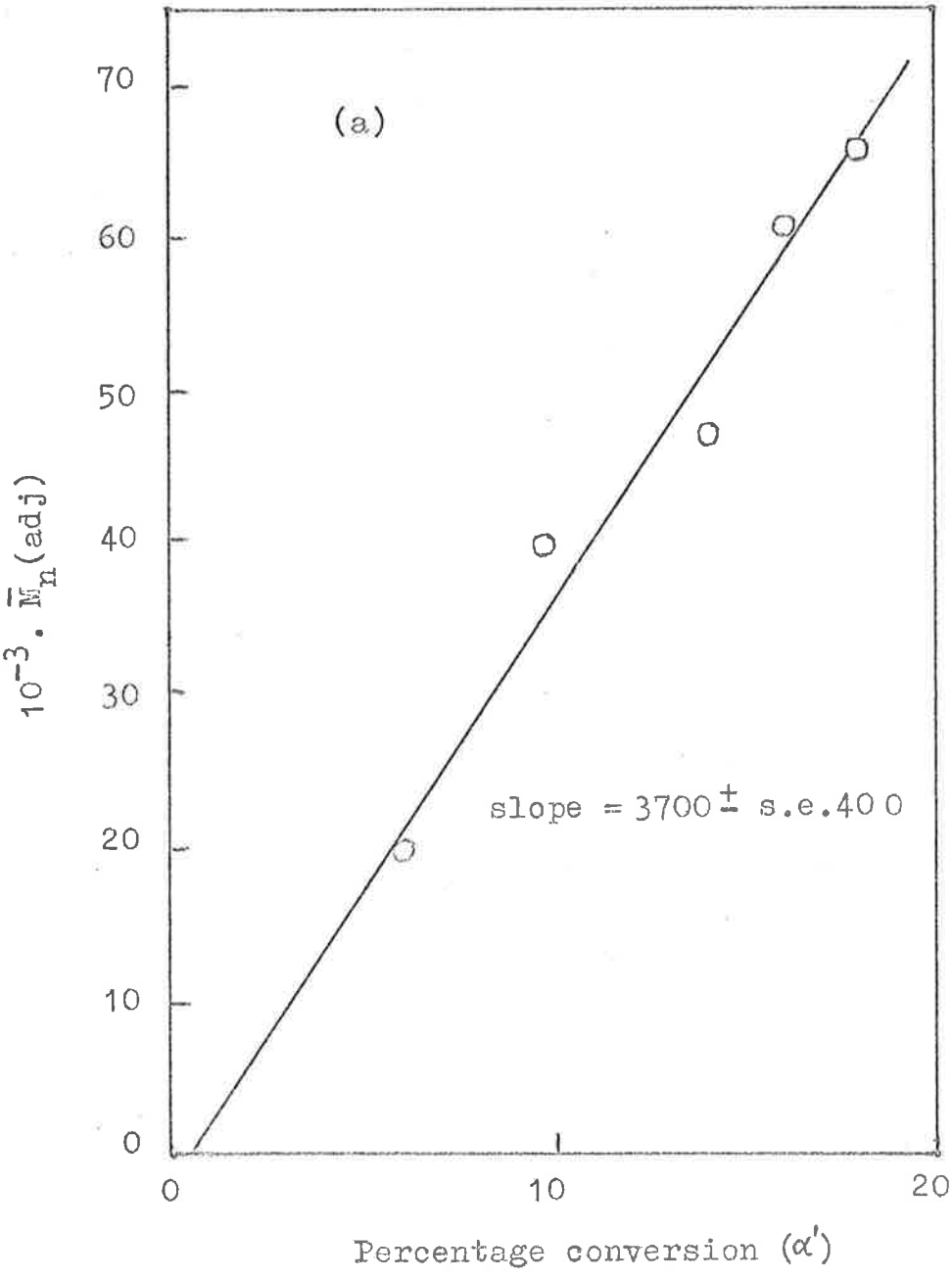

Figure 4.13. Dependence of molecular weight ($\bar{M}_n$(adj)) on percentage conversion, where,

$$\bar{M}_n(adj) = \bar{M}_{nexp} . [G_n]_o \; / \; 0.1 \qquad \text{(see text)}$$

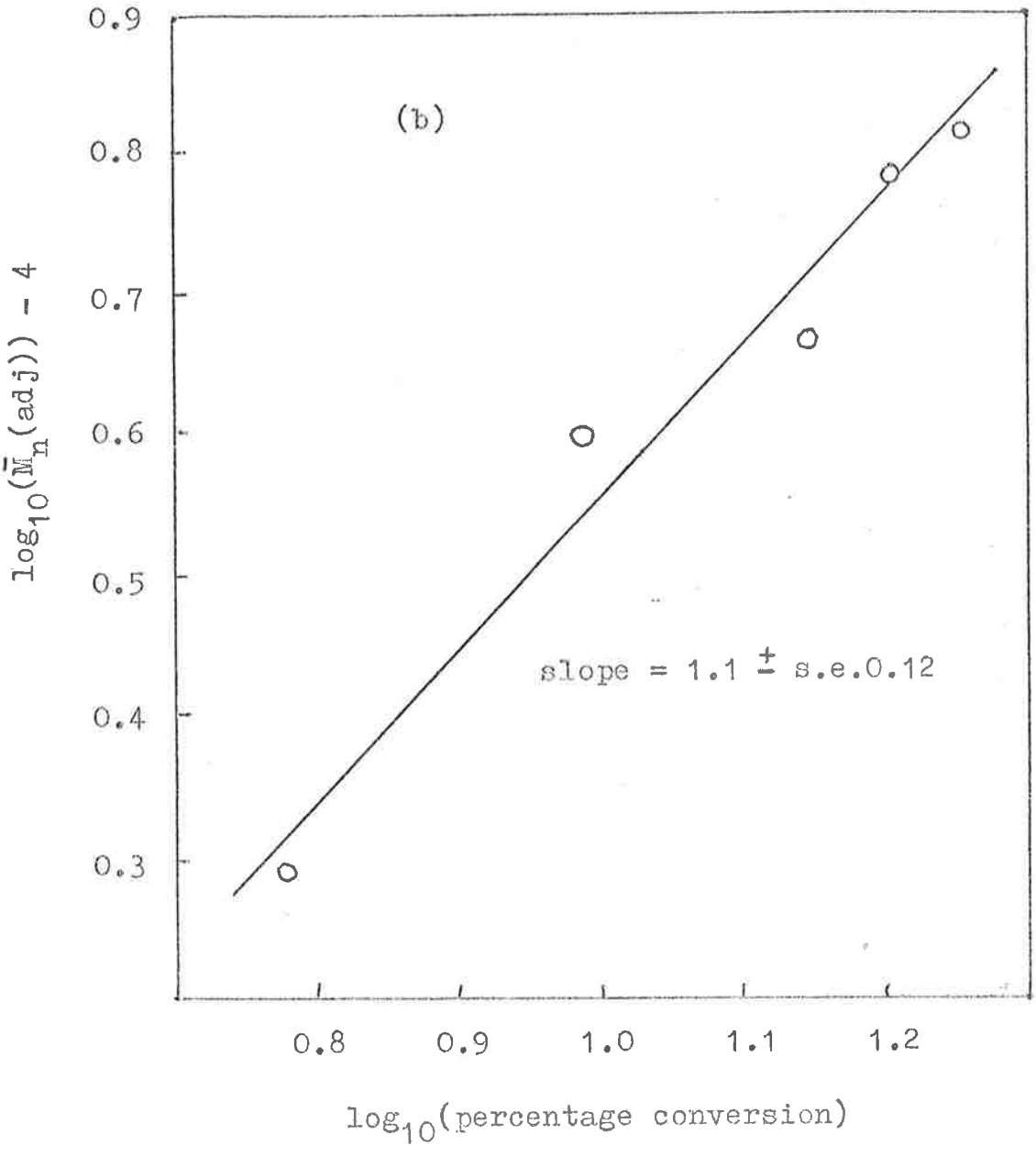

Figure 4.13 (b). Dependence of molecular weight ($\bar{M}_n(adj)$) on percentage conversion, where,

$$\bar{M}_n(adj) = \bar{M}_{nexp} \cdot [G_n]_o \; / \; 0.1$$

only acquired in the closing stages of this research.

The relationship between $\bar{M}_n$ and percentage conversion was determined from the data in Table 4.7 by assuming that $\bar{M}_n$ was inversely proportional to the initial organomagnesium concentration $[G_n]_o$ and adjusting all the values of $\bar{M}_n$ in Table 4.7 to correspond to $[G_n]_o = 0.10$ mol dm^{-3}. The results are shown in figure 4.13. To verify these results the relationship

$$\bar{M}_n \propto \frac{\text{(percentage conversion)}}{[G_n]_o} \qquad (4.12)$$

was tested. Figures 4.14 (a) and 4.14 (b) show the log-log plot and linearity plot respectively which confirms that $\bar{M}_n$ is directly proportional to the percentage conversion and inversely proportional to the initial concentration of organomagnesium species present.

The slopes and lines were calculated using regression analysis and the linear plot through the origin contains the 90% confidence limits calculated using equation (3.8).

The interesting aspect of these investigations was the fact that $\bar{M}_n$ was independent of the initial monomer concentration, e.g. at $\chi_{THF} = 0.10$ and $[G_n]_o = 0.036$ mol dm^{-3}, $\bar{M}_n = 66 \times 10^3$ at $[MMA]_o = 0.96$ mol dm^{-3}; 68×10^3 at $[MMA]_o = 1.92$ mol dm^{-3}, and 61×10^3 at $[MMA]_o = 2.88$ mol dm^{-3} at 8% conversion.

This phenomenon has been noted in the acrylonitrile/n-BuMgCl/toluene system,[64] however, with n-BuMgBr and MMA in diethyl ether at 223K, Watanabe observed a linear dependence between $\bar{M}_n$ at 10% conversion

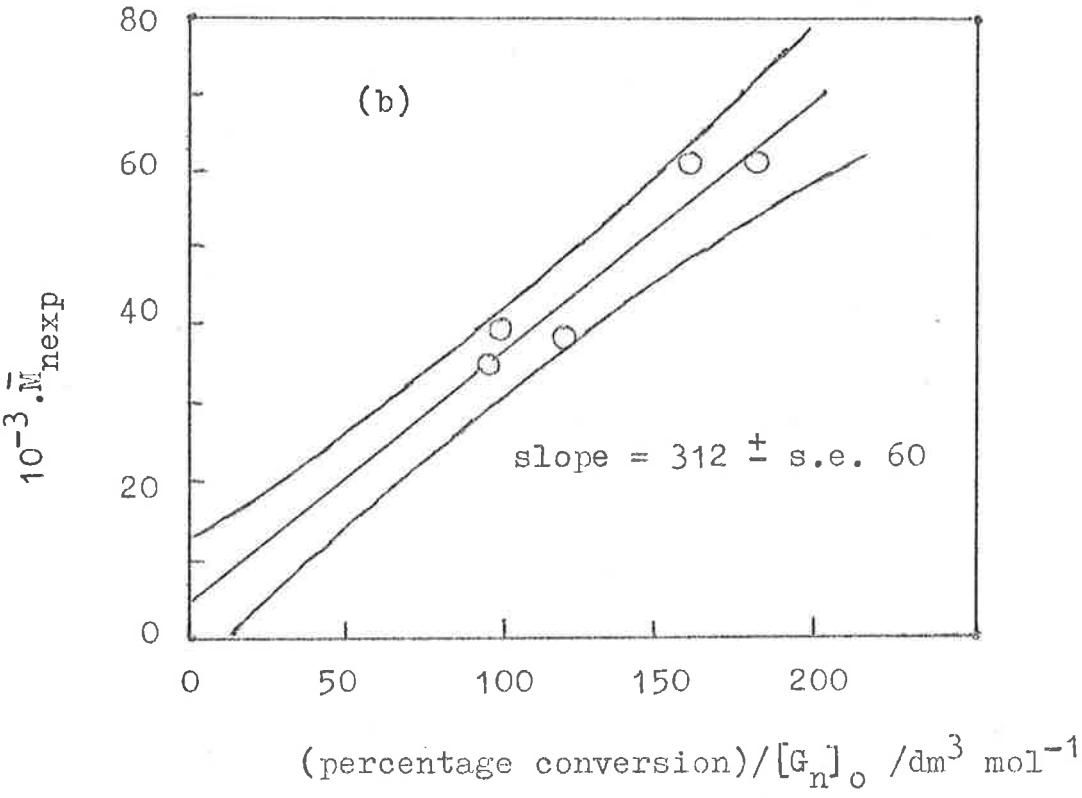

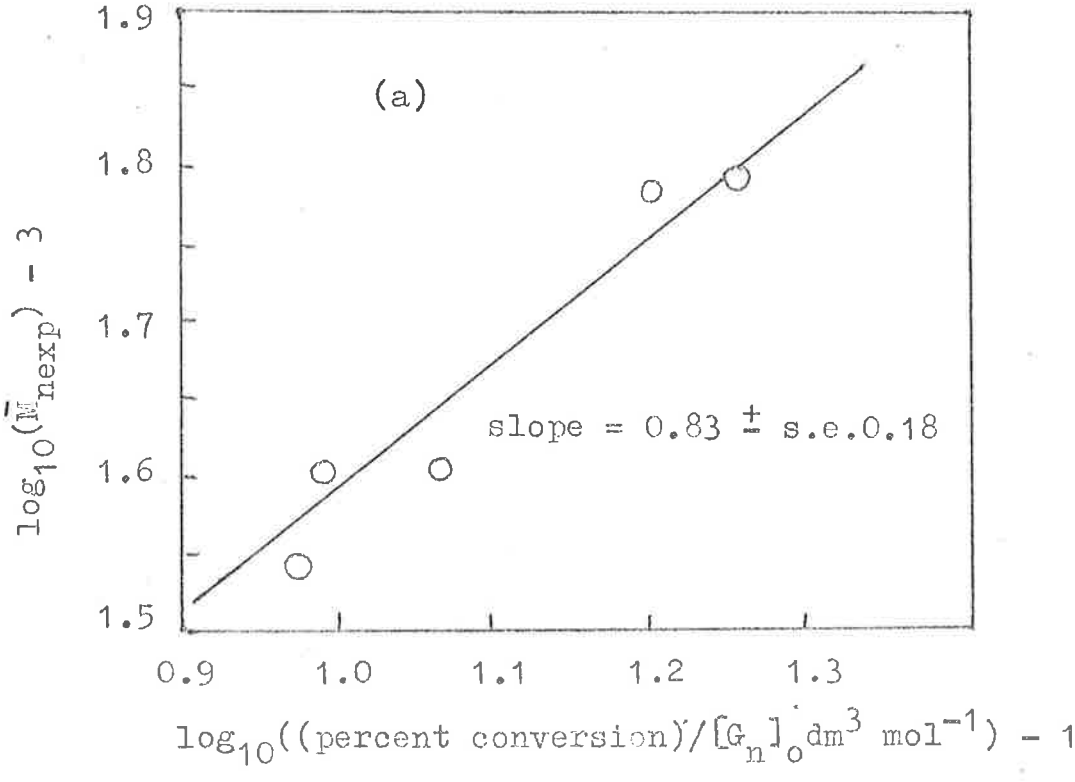

Figure 4.14 (a) and (b). Dependence of molecular weight ($\bar{M}_{nexp}$) on (percentage conversion)/$[G_n]_o$.

and $[MMA]_o$ although the dependence was not first order.

The effect of THF on MWD is shown in figure 4.12. At very low THF mole fraction the distribution is slightly narrower than at higher χ_{THF}. It is very interesting to compare the $\bar{M}_n$ at similar conversion as the mole fraction of THF varies. At $\chi_{THF} = 0.046$, $\bar{M}_n = 27000$ at 15% conversion and at $\chi_{THF} = 0.21$ and 0.28, $\bar{M}_n = 47000$ and 61000 respectively at 16% conversion. Reference to figure 3.7 clearly shows that the rate of polymerization decreases with increasing THF mole fraction whereas the above results show that the molecular weight increases. If it is assumed that the maximum errors in the rates of polymerization are ±5%, which is based on dispensing errors, extrapolation errors, etc, and considering the 10% errors in $\bar{M}_n$ calculation, the increase in $\bar{M}_n$ as χ_{THF} increases can be accounted for by a decrease in the number of active centres formed at higher THF concentrations.

Increasing the polymerization temperature from 223K to 252K had no effect on the MWD.

sec-BuMgBr - The MWD's of poly(MMA) obtained using this initiator were completely different from the n-BuMgBr case. The methanol soluble material, which was only significant at high THF concentration, section 4.2.1, was similar to that produced in the n-BuMgBr case; having a narrow MWD and $\bar{M}_g$ between 4×10^3 and 6×10^3.

The methanol-insoluble polymer ranged from distinctly trimodal

at low χ_{THF}, to bimodal at high χ_{THF}, figure 4.15. It must be remembered that the height of a particular peak does not represent the relative abundance of a particular component, since it is influenced by the abundance of neighbouring species. The elution curve can be regarded as a direct concentration plot and quantitative analysis for amounts of individual components present can only be done if a calibration curve of weight versus peak height is constructed. Nevertheless, comparison of peak heights at the same elution volume for identical sample concentrations can give some idea of the change in abundance of that species under varying conditions.

By comparison with the n-BuMgBr case, figure 4.12 there is a much larger concentration of species at $\bar{M}_g \sim 3 \times 10^6$ and this peak decreases in height as χ_{THF} increases, figure 4.15. There is also a peak at $\bar{M}_g = 93000$ with a shoulder at $\bar{M}_g \approx 9000$ at low THF. As χ_{THF} increases, the 93000 peak decreases whereas the 9000 increases until at $\chi_{THF} = 0.46$ the MWD is as shown in figure 4.15. This type of behaviour where one peak in the MWD grows at the expense of another when certain experimental conditions were changed has been observed in other systems[144] and can possibly be explained by assuming two or more species in equilibrium, the position of the equilibrium being determined by the THF concentration in our case.

Figure 4.15. Effect of the THF concentration on the MWD of poly(MMA) prepared using sec-BuMgBr (methanol insoluble polymer only shown).

$T = 223K$; $[MMA]_o = 0.96$ mol dm^{-3} ;

$[G_s]_o = 0.02_1$ mol dm^{-3}.

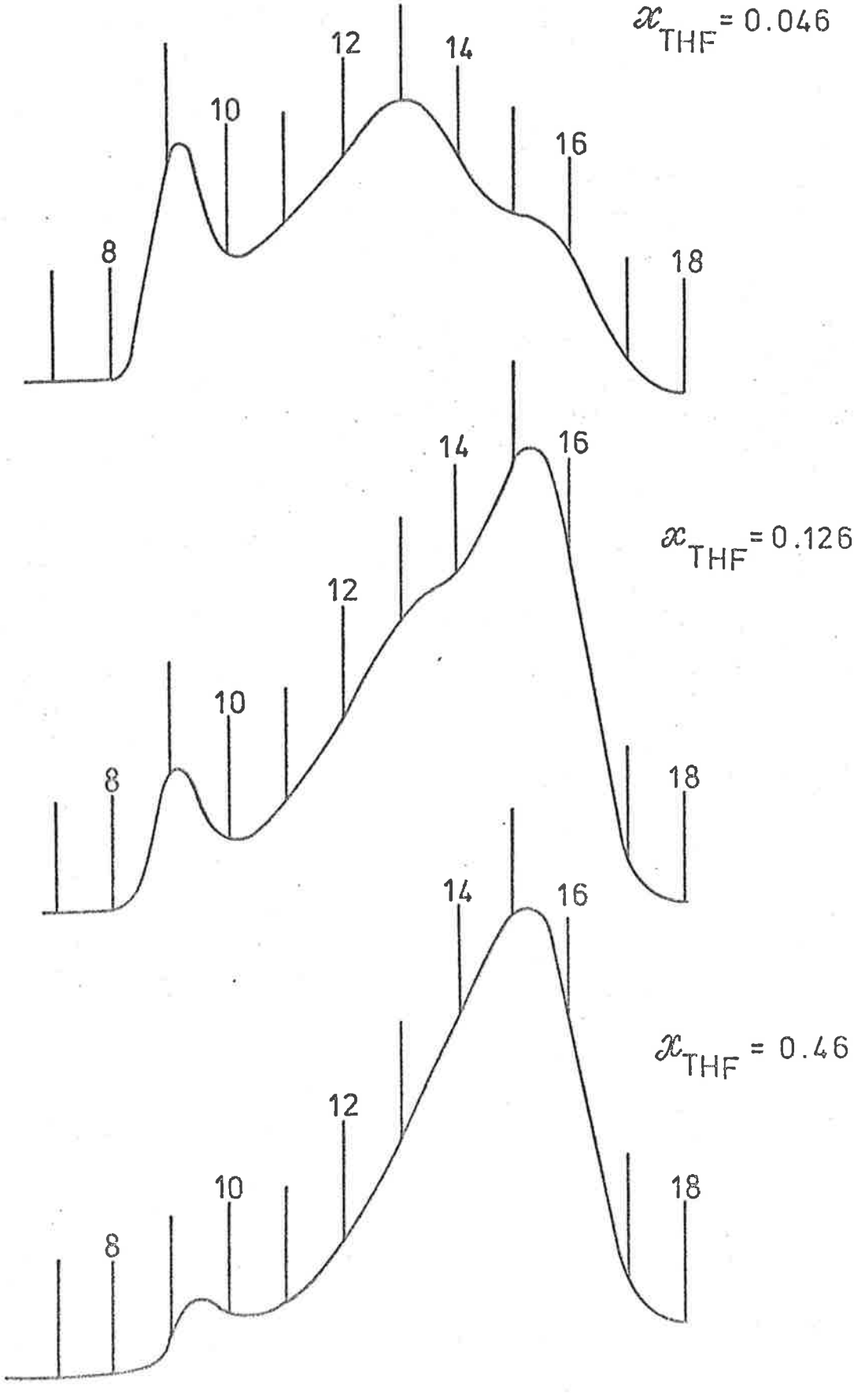
x_{THF} = 0.046
8
10
12
14
16
18
x_{THF} = 0.126
8
10
12
14
16
18
x_{THF} = 0.46
8
10
12
14
16
18

tert-BuMgBr - The polymers obtained using this initiator were of very high molecular weight and were highly isotactic. Figure 4.16 (a) shows the MWD of polymer prepared after 2 minutes at 223K, $\chi_{THF} = 0.26$, with $[MMA]_o$ = 2.76 mol dm^{-3} and $[G_t]_o$ = 0.020 mol dm^{-3}. The cumulative weight plot, figure 4.17, shows that the curve is Gaussian up to V_e = 10 and the value of $\bar{M}_w / \bar{M}_n$ = 1.01 was obtained in this region. The broadening of the peak on the low MW side will increase this ratio but even so, the narrowness of this particular distribution was very surprising when the results of the other Grignard reagents are considered. The value of $\bar{M}_n$ calculated from the cumulative weight plot was 2.8×10^6. Very narrow distributions have previously been recorded for poly(MMA) prepared at 200K using an electron transfer catalyst and adding monomer slowly by distillation.[143]

In our attempts to reduce the molecular weight and the rate of polymerization (section 3.4.2) we could accentuate the observed broadening by allowing the reaction to proceed for longer times, e.g. in figure 4.16 (b) the reaction proceded for 15 minutes and the chromatogram shows a distinct shoulder at V_e = 10 and a new broad peak at V_e = 13.

Unfortunately, towards the end of this research, the gel permeation chromatograph became completely inoperable and some polymer MWD's could not be determined. Among these were the polymer samples prepared at low temperature using n-, sec- and tert-BuMgBr, as well as samples of poly (MMA) prepared using n-BuMgI, tert-BuMgCl amd mixtures of tert-BuMgBr

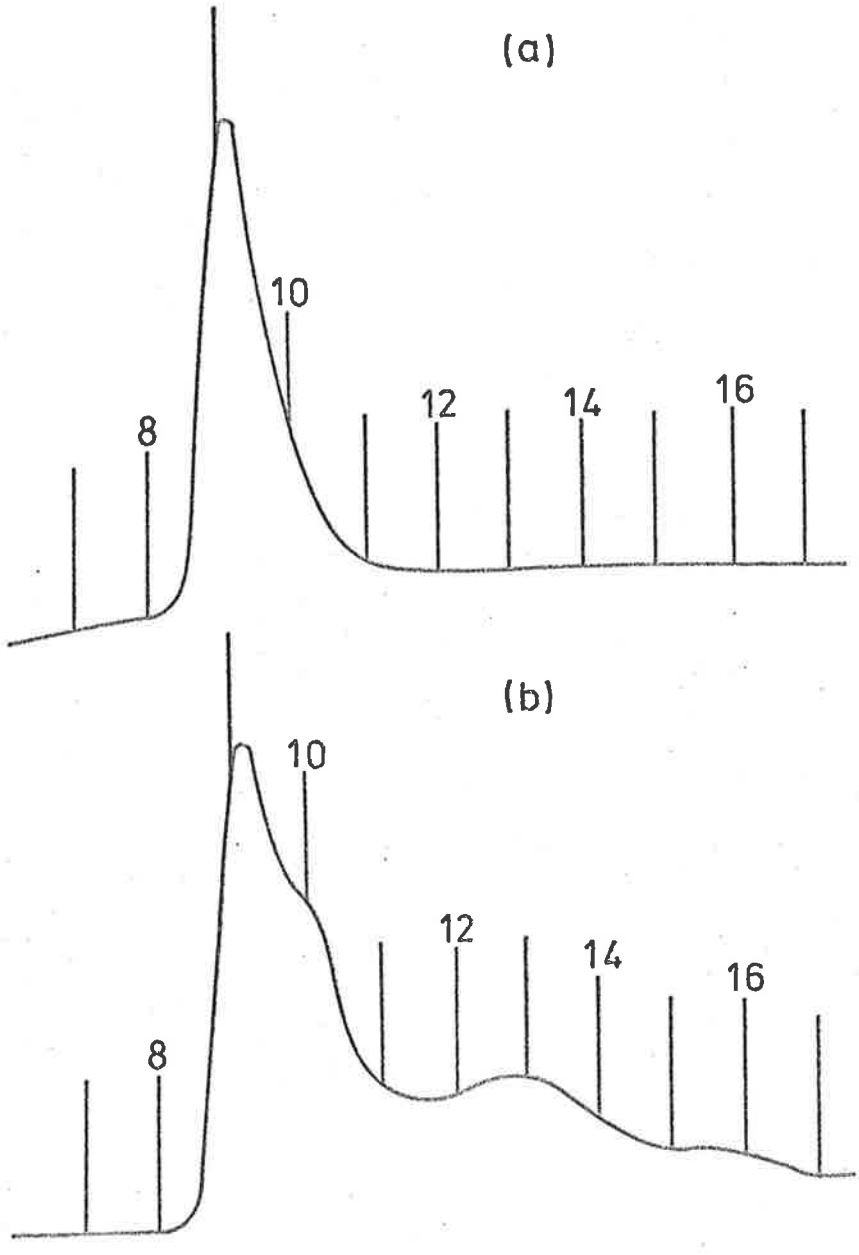

Figure 4.16. MWD of poly(MMA) prepared using tert-BuMgBr. (a) terminated after 2 min; (b) terminated after 15 min. Baseline drift is large because of the much higher sensitivity settings required for these samples compared with those of figs. 4.12 and 4.15. The polymers prepared from tert-BuMgBr were of such high MW that solution concentrations had to be below 0.05% w/v before they could be filtered. Detection of these very low concentrations required higher sensitivity settings with the resultant baseline drift.

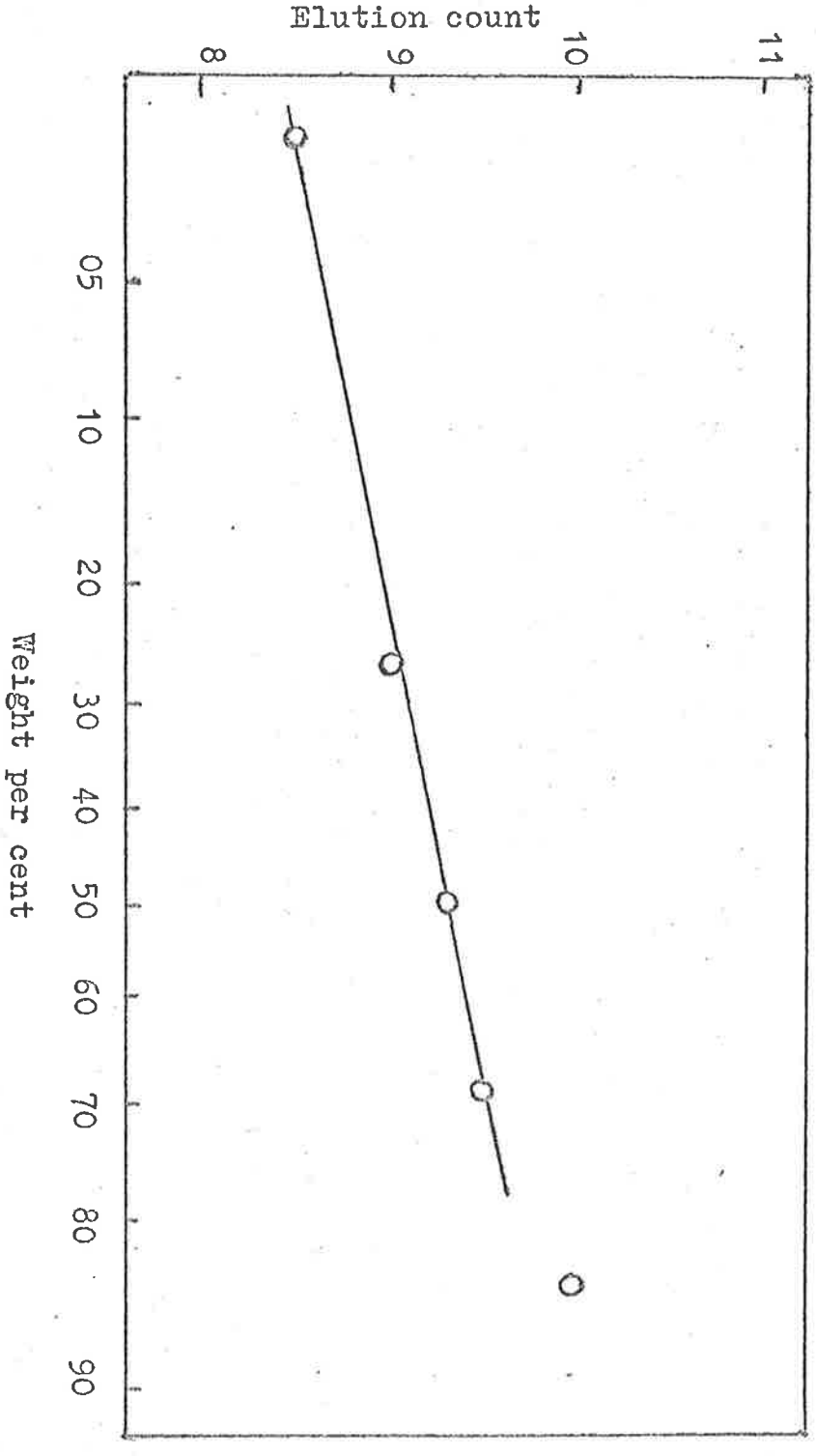

Figure 4.17. Cumulative weight plot for the g.p.c. shown in figure 4.16(a). $\sigma_c = 0.20$; $\sigma_{Mw} = 0.0801$; $\bar{M}_w/\bar{M}_n = 1.01$ for $V_e < 10$; $\bar{M}_n = 2.81 \cdot 10^6$.

and tert-BuMgCl.

The lack of these particular results will not invalidate any of the conclusions drawn from the kinetic results in chapter 3, (section 6.1). However, the discussion in section 6.2 concerning the stereospecificity aspect of the organomagnesium initiated polymerization of MMA will be *slightly* limited due to the lack of knowledge of the polymer MWD at low temperatures. This limitation arises because discussions of polymer tacticities are really only meaningful when the molecular weight distributions are known.

4.4.2 *Dialkyl-magnesiums*

Table 4.8 shows a comparison between the MW and MWD of polymers prepared using dialkylmagnesium initiators and Grignard reagent initiators. All of the polymers prepared using R_2Mg initiators were unimodal and the distributions of $(n\text{-Bu})_2Mg$ and $(tert\text{-Bu})_2Mg$ were broader than MWD's of polymers prepared with their Grignard counterparts.

The similarity between the results obtained for initiation with the supernatant liquid when tetraglyme was added to n-BuMgBr and those obtained for $(n\text{-Bu})_2Mg$ support our contention that tetraglyme precipitates the $MgBr_2$ from the solution leaving $(n\text{-Bu})_2Mg$.

TABLE 4.8

MW and MWD of poly (MMA) prepared using dialkyl-magnesium initiators compared with their corresponding Grignard reagents.

T = 223K

Initiator	χ_{THF} (a)	$\bar{M}_w/\bar{M}_n$	$\bar{M}_n.10^{-4}$	%conversion
$(n\text{-Bu})_2Mg$	0.10	1.32	3.9	17
$(n\text{-Bu})_2Mg$	0.28	1.39	5.4	-
n-BuMgBr	0.10	1.18	6.1	8
n-BuMgBr	0.28	1.21	6.1	16
$(sec\text{-Bu})_2Mg$	0.10	1.28	3.9	17
sec-BuMgBr	0.10	multimodal MWD		
tert-BuMgBr	0.28	1.16	12.5	1
supernatant liquid from tetraglyme	0.28	1.39	-	-

(a) $[THF]/mol\ dm^{-3} \approx 10.\chi_{THF}$

4.5 *Discussion*

Some definite trends are apparent from the results in this chapter.

None of the polymers prepared using Grignard reagents or dialkyl-magnesium compounds as initiators conform to Bernoulli chain configuration statistics with the possible exception of systems to which a small amount of HMPA had been added. The polymerization

is therefore stereospecific, i.e. the configuration of the incoming monomer unit is influenced by at least the configuration of the chain end (first order Markov-model). The observed deviation from Bernoulli (or free chain end) statistics is not surprising in view of the fact that organomagnesium compounds readily form complexes with Lewis bases and from the conclusions reached in section 3.6 (b) that free ions and loose ion-pairs are not involved in initiation or propagation. The most probable mode of addition of monomer to the propagating chain is via coordination, followed by insertion between the essentially covalent macro-chain-magnesium bond.

The polymers prepared using organomagnesium compounds as initiators range from 'syndiotactic-like' through stereo-block to highly isotactic depending on a number of factors. With every initiator used, as the mole fraction of THF increased, the syndiotacticity increased at the expense of the isotacticity. This trend is consistent with the idea that the more solvating agent present in the system, the harder it is for the incoming monomer to coordinate with the counterion, and under these conditions, syndiotactic approach replaces isotactic approach.

Branching at the α-carbon atom of the alkyl group of the Grignard reagent favors isotactic placement, a fact which has been long known, but in our system, β-carbon branching had little effect on the polymer tacticity when compared with polymers prepared using n-alkyl Grignard reagents. The effect of the alkyl group of the initiator on the

resulting polymer tacticity lends support to the conclusion in section 3.6 (c) that the reactive species is R_2Mg and not RMgX. With RMgX, the alkyl group would soon become remote from the chain end, whereas with R_2Mg, the alkyl group can influence the mode of monomer addition. This argument, of course, may be over-simplifying the situation because the presence of MgX_2, which is known to complex with MMA[52c] has been neglected in this argument. Other complexities that should be considered are the possibility of various exchange processes taking place as well as the possible existence of further complexing between the magnesium atom coordinated to the propagating chain end and any unreacted alkyl-magnesium bonds present in the system (section 5.5).

The presence or absence of $MgBr_2$ in the initiator solution does have a pronounced effect on the polymer chain structure. When $MgBr_2$ is absent, i.e., the initiator is R_2Mg, the polymers prepared using $(n\text{-Bu})_2Mg$, $(sec\text{-Bu})_2Mg$ and $(tert\text{-Bu})_2Mg$ all have similar tacticities which are almost identical to the polymer prepared using n-BuMgBr. It appears therefore, that when dialkylmagnesium compounds in the *absence* of $MgBr_2$ are used as initiators for the polymerization of MMA, the resulting polymer tacticity is independent of the alkyl group present in the initiator.

This suggests that the magnesium halide plays a significant role in the propagation step in Grignard reagents which are branched at the α-carbon atom.

The effect of halide is further demonstrated when the chlorides, bromides and iodides are compared. The iodide favours isotactic polymer whereas the chloride favours more syndiotactic polymer. This same effect has been noted by other workers but has not been explained satisfactorily. Goode *et al*[52c] measured the infra red (i.r.) absorption maximum of the carbonyl band of MMA in 1:1 complexes between MMA and various halides and compared these with the value for uncomplexed MMA. They concluded that $MgBr_2$ formed a stronger complex with MMA than $MgCl_2$. This would appear to contradict the intuitive enthalpy and entropy trends. The more electronegative halide (chlorine in this case) would be expected to form a stronger complex with MMA than the bromide not only because of favorable energy considerations, but also because the chloride is smaller than the bromide.

The influence of temperature on the polymer tacticity is difficult to explain. At very low temperatures, i.e. ca 200K, the influence of the alkyl group on the polymer tacticity observed when tert-BuMgBr and sec-BuMgBr are used is reduced. Associated species have been detected in Me_2Mg/THF solutions at 195K by n.m.r.[31] but it is impossible to say what effect the presence of such species, e.g. dimeric propagating chain, will have on the polymer tacticity. One possible argument is that chain end association may well prevent the monomer from complexing with the magnesium coordinated to the macro-chain, thereby forcing the monomer into a syndiotactic rather than isotactic approach at low temperature.

The position of any equilibria in the system will be affected by temperature which also complicates the situation.

When the MWD of polymers prepared using different Grignard initiators are compared, several things become apparent. The n-Butyl, iso-Butyl and tert-Butyl magnesium compounds produce predominantly unimodal methanol insoluble polymer. Polymers with low isotactic content have MW's less than 1×10^5 whereas the highly isotactic polymer from tert-BuMgBr has a MW> 2×10^6. This polymer is formed very rapidly and has a very narrow MWD which becomes distorted towards lower MW's with the appearance of a low MW peak as the polymerization proceeds. This suggests the existence of at least two propagating species leading to isotactic and non-isotactic polymer respectively. The isotactic polymer grows extremely rapidly and is favored by α-carbon branching, iodide in preference to bromide in preference to chloride as well as moderately low temperatures. Along these lines, it may be argued that the n-BuMgBr and tert-BuMgBr are two extremes and the sec-BuMgBr initiator should be intermediate. This does appear to be the case: the isotacticity of poly(MMA) prepared using sec-BuMgBr is moderately high and the MWD multimodal - showing peaks corresponding to both high MW and low MW. Here it should be remarked that it is rather pointless discussing the tacticity of the whole sample of a polymer when its MWD is multimodal, however, a reasonable explanation for the increased isotacticity of the sec-BuMgBr system compared with the

n-BuMgBr case is that it may be due to the larger proportion of very high molecular weight, predominantly isotactic material.

The MWD of polymers prepared using R_2Mg as initiators are also very interesting when compared with their Grignard reagent counterparts. It is not surprising that $(n\text{-Bu})_2Mg$ and n-BuMgBr have very similar MWD's although the former is definitely broader, $\bar{M}_w/\bar{M}_n = 1.32$ compared with 1.22 for n-BuMgBr.

The multimodal MWD observed with sec-BuMgBr becomes unimodal with $(sec\text{-Bu})_2Mg$ (where only the methanol insoluble polymer is being considered) and the very narrow distribution, high MW polymer formed using tert-BuMgBr is reduced in MW from 3×10^6 to 12.5×10^4 with $(tert\text{-Bu})_2Mg$. The MWD of poly(MMA) obtained with $(tert\text{-Bu})_2Mg$ is broader than the MWD obtained using tert-BuMgBr, although the distribution obtained using $(tert\text{-Bu})_2Mg$ is much narrower than the distribution obtained using $(n\text{-Bu})_2Mg$ and $(sec\text{-Bu})_2Mg$.

These results support the hypothesis that the presence or absence of magnesium halide in solution plays a significant role in determining not only the chain configuration, but also the molecular weight distribution.

Possible mechanisms that could account for the above results will be discussed in section 6.2.

CHAPTER 5

MISCELLANEOUS EXPERIMENTS

This chapter, with the somewhat nebulous title of 'miscellaneous experiments', contains an account of all the experiments performed in the hope of obtaining a little more information concerning specific aspects of the polymerization of MMA initiated by organomagnesium compounds.

Most of the experiments have been done using n-BuMgBr as the initiator because this system had been studied most intensively by dilatometry, however, some of the techniques were extended to the sec-BuMgBr and tert-BuMgBr systems where they were applicable.

The experiments which comprise this chapter include a detailed description of the development of an adiabatic reaction calorimeter to enable the heat of polymerization to be determined. We were also able to successfully apply a technique described by Yoshino[113b] to determine the number of active alkyl-magnesium bonds remaining during the polymerization. Unfortunately, for reasons that will be discussed, this method was only applicable to the n-BuMgBr/MMA system.

Finally, we attempted to detect the presence of certain side products, viz. butane and methanol. This work involved vapor phase chromatography (v.p.c) and mass spectrometry (m.s.). No attempt was made to identify the actual addition products which lead to reduced initiator efficiency, because studies of this type have already been exhaustively done[52,53] and the various types of non-polymerization reactions are well documented.

The particular interest in methanol as a side product arose from the possibility of cyclic trimer formation with subsequent elimination of methanol either during polymerization or on termination. This phenomenon has been observed in many MMA polymerizations initiated both by Grignard reagents and various organoalkali initiators.[52a,130]

Butane has been reported as the major side product formed during the reaction between MMA and both Grignard reagents[53] and n-BuLi,[131] however, its production was not accounted for in terms of where the active hydrogen necessary for n-butane formation came from during the polymerization. We attempted, unsuccessfully, to detect the presence of butane by mass spectrometry of the vapor above a polymerizing solution. The solution was terminated with iodine in THF to remove any active R-Mg bonds and then warmed to 278K (boiling point of butane = 272.5K) and a gas sample analysed.

CALORIMETRY

The instantaneous colour change on mixing MMA and n-BuMgBr at 223K suggested some form of complexing and the inability to obtain a u.v. spectrum of this colour without resorting to fast reaction techniques prompted the design of a reaction calorimeter.

5.1 *Apparatus*

The basic design followed that described by Plesch[132] and others[133] but with some modifications. The major difficulty was to

keep the volume of solution as small as possible (ca. 50 cm^3), yet still be able to incorporate a stirrer, temperature probe, heater, monomer and initiator capsules. Figure 5.1 shows the final version. The calorimeter was surrounded by a silvered jacket, J, which could be evacuated via tap T_1. This jacket extended only over that portion of the calorimeter that was immersed in the low temperature thermostat. It was impossible to immerse the whole calorimeter in the bath because the presence of ground glass joints introduced the possibility of leakage at low temperature. These quick fit joints were necessary to allow the cleaning of the calorimeter and easy removal of the temperature probe, P, heater, H, and monomer capsule, M. The probe consisted of a 100Ω platinum wire thermistor and the temperature change was recorded on a Phillips potentiometric pen-recorder (PR 7792) with a sensitivity such that full scale deflection (fsd) could be varied to correspond to a 5, 10, 20 or 50 degree temperature rise.

A heater consisting of a coil of nichrome wire of resistance ca. 30Ω was included to enable determination of the specific heat of the vessel and its contents for each particular experiment. This was done (after the polymerization had been terminated) by supplying a constant direct current (d.c.) of known voltage and amperage for a set period of time and recording the temperature rise from when the current was turned on to when it was turned off. Such a determination is shown in the inset of figure 5.3. The slow temperature decrease after the heater was turned off showed that the calorimeter was not

Figure 5.1. Adiabatic reaction calorimeter with stirrer.

A = outlet to high vacuum and side arms containing initiator and solvent ampoules.

H = heater consisting of a coil of nichrome wire.

J = silvered vacuum jacket.

M = special monomer breakseal.

P = thermistor probe.

S = stirrer bar.

T_1 = tap to evacuate the vacuum jacket when required.

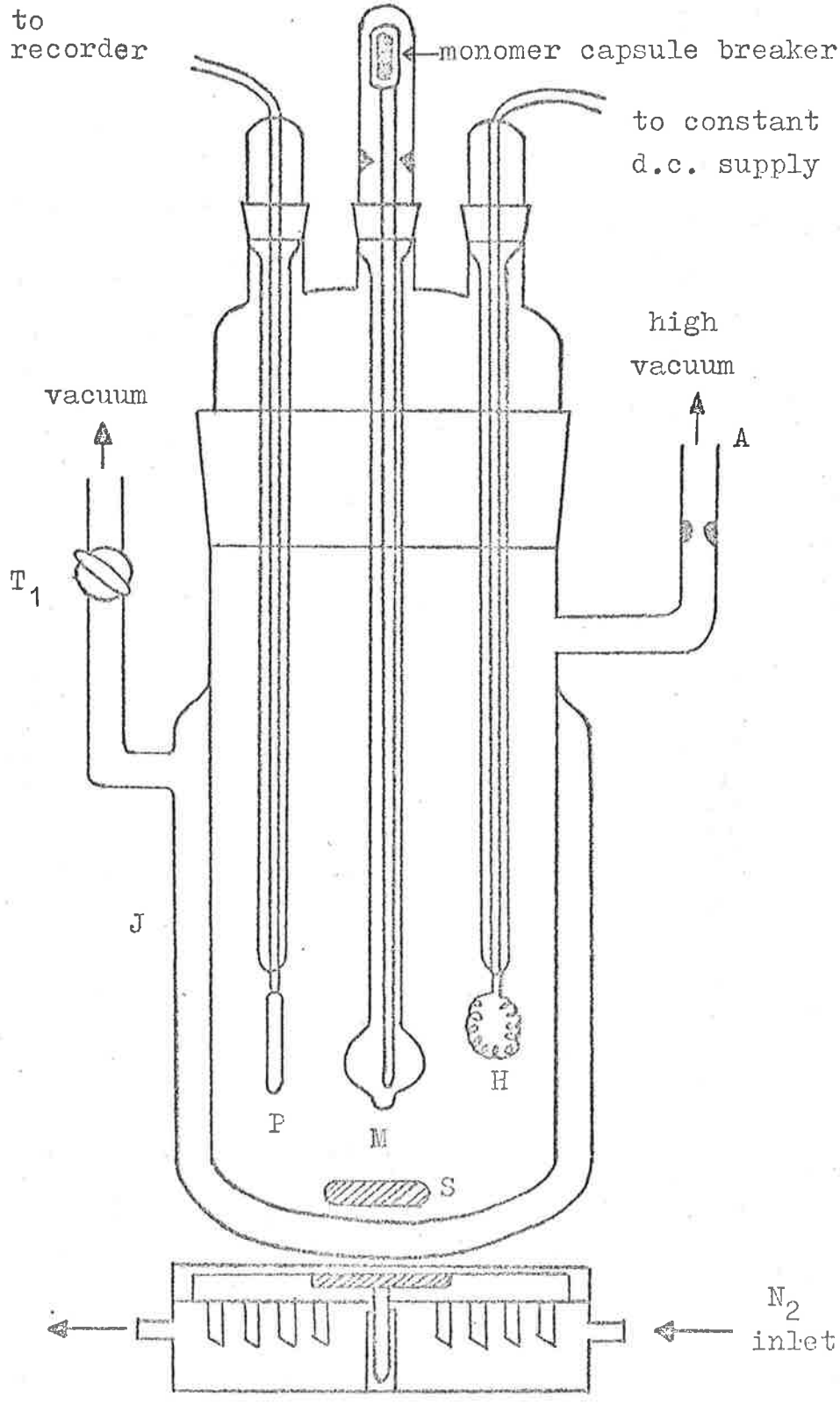
to
recorder
monomer capsule breaker
to constant
d.c. supply
high
vacuum
vacuum
A
T_1
J
P
M
H
S
N_2
inlet

completely adiabatic and the total temperature rise, allowing for these heat losses was calculated by extrapolating the curve to the mid point of the heating period.

The total heat capacity was calculated using the relationship

$$C_p = \frac{v\ i\ t}{\Delta T} \quad \text{joule } K^{-1} \qquad (5.1)$$

where C_p = heat capacity in joule K^{-1}

v = voltage

i = current in ampere

t = time of duration of heating in seconds

ΔT = Total temperature rise allowing for heat loss.

The average heat capacity determined was 79 ± 4 JK^{-1}

Stirring of the solution in the reaction vessel is very important in calorimetry and presented one of our biggest problems. Plesch *et al*[132] used a vertically mounted stirrer with shafts supported by teflon rings but the small size of our apparatus prevented such elaborate methods. We overcame this problem by using an adaption of a water powered magnetic stirrer. A small bar magnet, S, coated with teflon was placed in the calorimeter which was lowered into the thermostat. At the temperatures used in these experiments water could not be used to power the magnetic stirrer and a stream of nitrogen gas was substituted. This method is very simple and also effective.

5.2 *Method*

The specially designed monomer ampoule shown in figure 5.1 was filled prior to assembling the calorimeter. A specially designed breaker was incorporated in the capsule and was prevented from falling through the vessel by the constriction in the ampoule. It was very important to ensure that the bulb of the break-seal was below the level of the initiator solution for the following reasons: due to the pressure difference within the calorimeter and the monomer ampoules, if the latter was shattered with the liquid above the level of the initiator solution, rapid evaporation of the monomer resulted in subsequent cooling of the whole solution, giving an anomalous temperature fall on mixing. Also, this method ensured that the monomer and initiator were in thermal equilibrium and instantaneous, quantitative mixing resulted.

After assembling the calorimeter, the initiator, solvent and terminating break-seals were attached to outlet A, figure 5.1, and the apparatus evacuated to a pressure of 10^{-3} Nm^{-2}. This was then sealed from the line and the initiator and solvent capsules were broken into the calorimeter which was then placed in the low temperature thermostat. The approach to thermal equilibrium was monitored by the temperature probe and when the calorimeter and contents reached the required temperature the outer jacket was evacuated with an Edwards rotary oil pump. During this time the stirrer was started and finally, the monomer capsule was ruptured

with the special breaker. The temperature rise of the solution during polymerization was recorded continuously and the thermostat temperature periodically.

The solution was terminated with methanol (0.1 cm^3) and the heat rise again recorded. When the temperature of the terminated solution had returned to its initial temperature the heat capacity was determined as outlined in the previous section.

The polymer was collected and treated as in section 2.4.3.

5.3 *Treatment of results*

The reaction between MMA and Grignard reagents to form high MW polymer is very inefficient (section 3.6 (d)) and the simplest representation of the reaction is the following:

$$In + M \longrightarrow \text{side products} \qquad (5.2a)$$

$$In + M \longrightarrow M^* \qquad (5.2b)$$

$$M_n^* + M \longrightarrow M_{n+1}^* \qquad (5.2c)$$

where In = initiator molecule,

M_n^* = propagating chain of degree of polymerization n

$n = 1,2 \ldots n$

and M = monomer molecule.

The side reactions are single step processes and if the polymerization chain length is long, i.e. $n >> 1$, then even though the initiation efficiency is low, the heat evolved during reaction in which monomer is

in excess will be mainly due to reaction (5.2c). Reaction (5.2a) will contribute only a small amount of the total heat of reaction.

Under these conditions, the heat of polymerization, ΔH_p is given by the expression

$$\Delta H_p = \frac{C_p \cdot \Delta T}{1000 \times Y} \quad k\ J\ mol^{-1} \qquad (5.3)$$

where C_p = heat capacity as defined in 5.1

ΔT = *total* temperature rise

and Y = yield of polymer

≡ mol. monomer consumed

As mentioned in 5.1, the calorimeter was not completely adiabatic, which was probably due to the fact that the whole vessel could not be completely immersed in the thermostat. To allow for this heat loss the following method was adopted:

The rate of thermal heat transfer $\frac{dq-}{dt}$ from a vessel is given by the expression[145]

$$\frac{dq-}{dt} = \frac{kA}{V} (T - T_o) \qquad (5.4)$$

where $q-$ = heat lost to surroundings

k = thermal conductivity of vessel

$\frac{A}{V}$ = area per unit volume

and $(T - T_0)$ = temperature difference between system and surroundings.

Now the apparent heat of reaction, dq, is

$$dq = dq_+ - dq_- \qquad (5.5)$$

where dq_+ = true heat of reaction

dq_- = heat lost to surroundings.

Thus

$$\frac{dq}{dt} = \frac{dq_+}{dt} - \frac{kA}{V}(T - T_0) \qquad (5.4a)$$

After the reaction has been terminated and the heat of termination has ceased, $\frac{dq_+}{dt} = 0$ and the rate of change of heat $\frac{dq}{dt}$ is actually the rate of heat loss to the surroundings.

i.e., $$\frac{dq}{dt} = \frac{-kA}{V}(T - T_0) = \frac{dq_-}{dt} \qquad (5.6)$$

But $$\frac{dq}{dt} = C_p \frac{dT}{dt} \qquad (5.7)$$

and so combining (5.6) and (5.7) and rearranging

$$\frac{dT}{(T - T_o)} = -\frac{kA}{VC_p}\, dt \qquad (5.8)$$

which on integration between the limits $T = T_o$ and T, and $t = 0$ and t, gives the expression

$$\ln (T - T_o) = -\frac{kA}{VC_p}\, t \qquad (5.9)$$

Hence a plot of $\ln (T - T_o)$ versus t should be a straight line, figure 5.2 with the slope $-kA/VC_p$. This allows the value

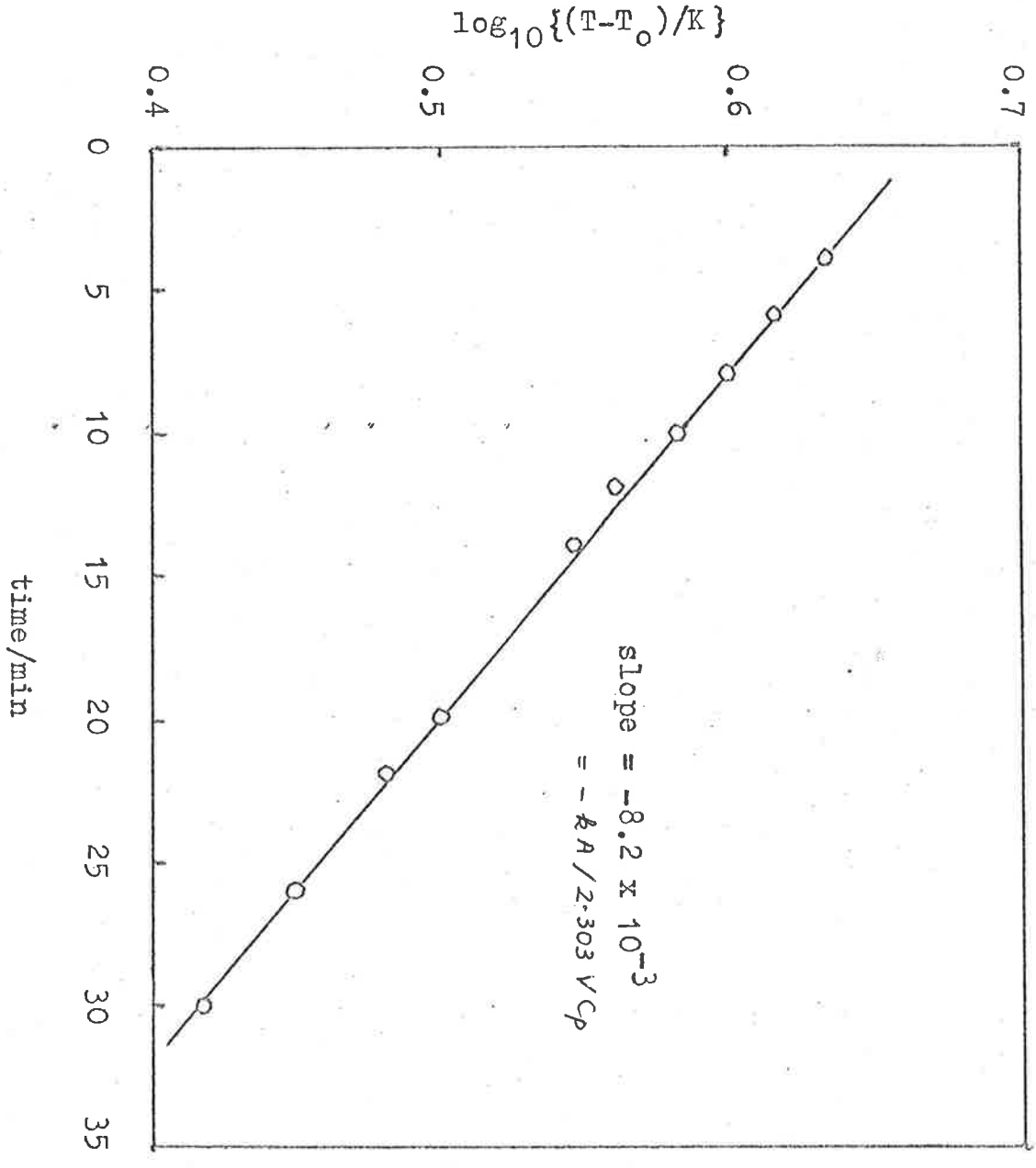

Figure 5.2. Estimation of the rate of heat loss from the calorimeter to the surroundings. T_o = 228K.

of kA/V to be calculated, and the rate of heat lost to the surroundings at any particular temperature to be calculated from (5.3).

In this way, an estimate of the heat lost from the calorimeter could be obtained and *corrected* temperature versus time curves were constructed.

5.4 *Results*

n-BuMgBr - Figure 5.3 shows the corrected temperature rise versus time curve for the n-BuMgBr system. Here $\chi_{THF} = 0.10$ [THF] = 0.99 mol dm^{-3}, $[MMA]_o$ = 0.96 mol dm^{-3}, $[G_n]_o$ = 0.36_6mol dm^{-3} and T_o, the initial temperature, 228K. The temperature curve was 'corrected' for heat loss using the method outlined in section 5.3. The rate of heat loss, dq/dt at every two minute interval was calculated using equation (5.6) and the previously determined value of kA/V. $\frac{dq}{dt}$ was multiplied by 2 to allow for an average heat loss for the minute either side and then this quantity was added to the total heat loss calculated for each preceding 2 minute interval. The corresponding temperature change was obtained by dividing the heat loss by C_p, e.g., from the recorder trace, $(T = T_o) = 0.5$K at t = 2 minutes and 0.86K at t = 4 minutes.

The correction calculations were as follows:

$$\frac{dq}{dt} = 1.48\ (T - T_o) \text{ joule min}^{-1}$$

$$= .740 \text{ joule min}^{-1}$$

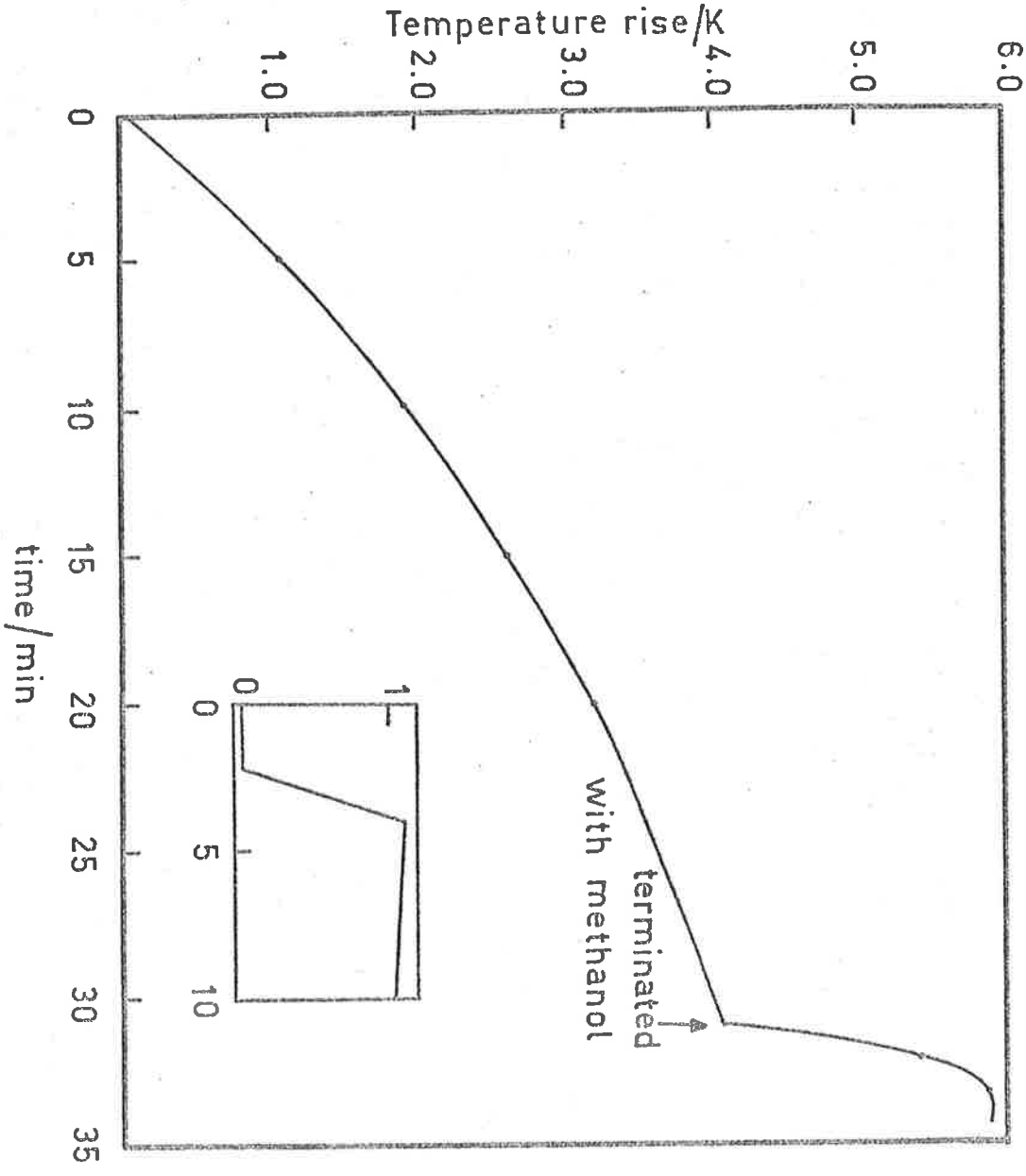

Figure 5.3. Corrected temperature rise versus time curve for n-BuMgBr. T_o = 228K. Inset is the determination of the heat capacity of the calorimeter and its contents after termination.
$[MMA]_o$ = 0.96 mol dm^{-3}; $[G_n]_o$ = 0.036 mol dm^{-3}
[THF] = 0.99 mol dm^{-3}.

The heat loss to the surroundings between 1 and 3 minutes is assumed to be twice $|dq^-/dt|$ at 2 minutes, i.e. 1.480 joule.

$\therefore$ Temperature decrease = 0.019K $\simeq$ 0.020K

Corrected temperature

at t = 2 minutes = 0.52K

At t = 4 minutes $\frac{dq^-}{dt}$ = 1.27 joule min^{-1}

$\therefore$ Temperature decrease at 4 minutes = 0.032K

Total temperature decrease after 4 minutes = 0.05_2K

$\therefore$ Corrected temperature at t = 4 minutes = 0.91K

In this way, an estimate of the total heat of reaction could be obtained.

From figure 5.3, ΔT (total corrected) = 4.1K and the yield of polymer was 0.628 gm (13.5% conversion).

Using eqn. 5.2, ΔH_p = 52 ± 5 kJ mol^{-1}. This value agrees favorably with the values of 54.5 and 58 kJ mol^{-1}, determined by other workers,[137] especially considering the various assumptions made and the experimental difficulties.

The interesting feature of figure 5.3 is that it only becomes linear after ca 22 minutes whereas the percentage conversion curves are linear from 10 minutes or before, figure 3.1. The linearity after 22 minutes of the temperature versus time curves, although not particularly evident from figure 5.3 was checked by continuing the polymerization over extended periods, e.g. 90 minutes.

sec-BuMgBr - Figure 5.4 shows the heat evolved for the sec-BuMgBr system. At χ_{THF} = 0.10, [THF] = 0.99 mol dm^{-3}, $[MMA]_o$ = 0.96 mol dm^{-3} and $[G_s]_o$ = 0.02 mol dm^{-3} the heat evolved is much greater than for the n-BuMgBr system. This is consistent with the faster rates. The corrected curve becomes linear after 8 minutes and the heat of polymerization was calculated to be 50 ±5 kjoules mol^{-1}.

tert-BuMgBr - At χ_{THF} = 0.15, [THF] = 1.44 mol dm^{-3}, $[MMA]_o$ = 0.94 mol dm^{-3} and $[G_t]_o$ = 0.01 mol dm^{-3} the corrected temperature/time curve, I, is shown in figure 5.5. There are two distinct regions - a rapid rise of 0.5K within the first 30 seconds and then a slower rise grading into a linear slope after ca 10 minutes. The errors in this system are large because, as described in chapter 3, the solution became so viscous that stirring was impossible. Accurate gravimetric yields were impossible because the high molecular weight polymer could not be freeze dried effectively. Curve II is a similar run, terminated after 2 minutes to check whether the rapid initial rise was due to complexing or polymerization. After terminating with methanol, the polymer separated was again of too high molecular weight to dissolve in benzene after stirring for 1 week. The peculiar shape of curve I is probably due to the sudden increase in viscosity, which stops the stirrer, preventing efficient heat transfer through the solution.

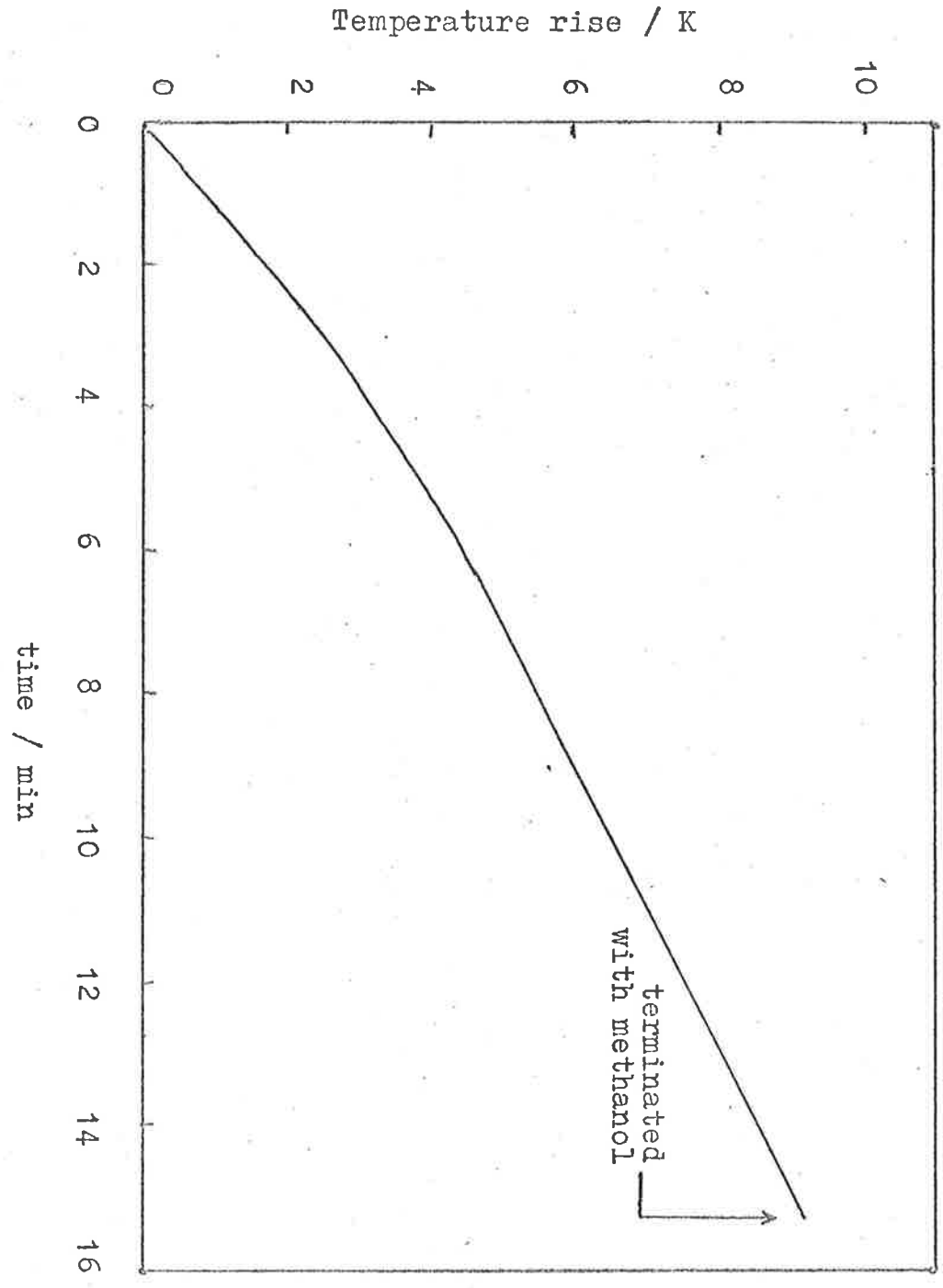

Figure 5.4. Corrected temperature rise versus time curve for sec- BuMgBr. T_o = 228K; [THF]= 0.99 mol dm^{-3}; $[MMA]_o$ = 0.96 mol dm^{-3}; $[G_S]_o$ = 0.02 mol dm^{-3};

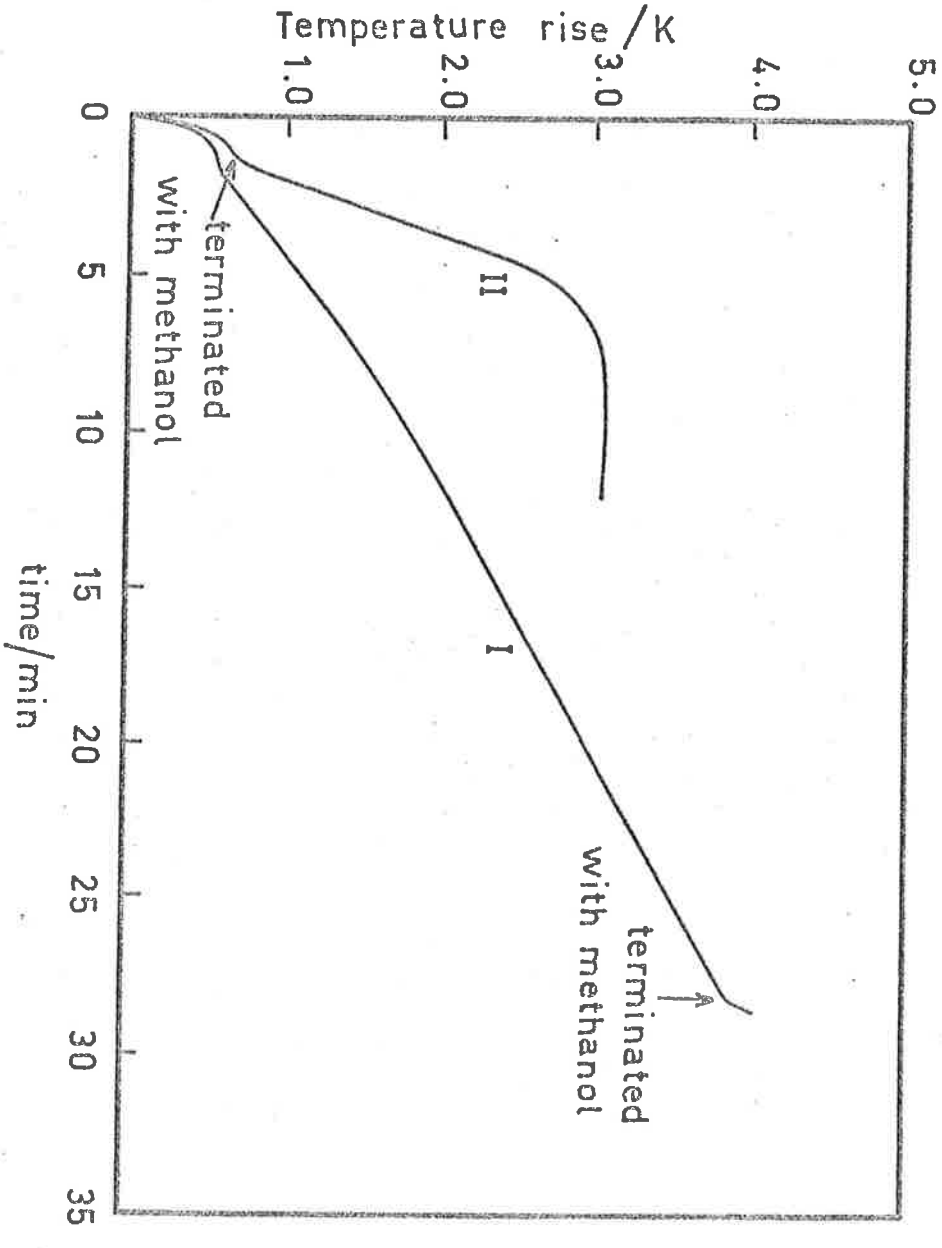

Figure 5.5. Corrected temperature rise versus time curve for tert-BuMgBr. T_o = 228K; [THF] = 1.44 mol dm^{-3}.
Curve I - solution terminated at 28 min.
Curve II - solution terminated at 2 min.
$[NMA]_o$ = 0.94 mol dm^{-3}; $[G_t]_o$ = 0.01 mol dm^{-3}.

DETERMINATION OF REMAINING ACTIVE ALKYL-MAGNESIUM BONDS

5.5 *Introduction*

As mentioned in section 4.1.3, Yoshino *et al*[113b] have found that in the low temperature polymerization of iso-propyl α-cis-β-d_2-acrylate with Ph-MgBr in toluene, there is a detectable amount of unreacted Ph-Mg bonds that remain throughout the duration of the polymerization. The proportion increased as the temperature decreased and was independent of the initial monomer and initiator concentrations.

The presence of these unreacted alkyl-magnesium bonds may influence the resulting polymer chain configuration.

With this in mind we attempted to apply Yoshino's method to our system.

5.6 *Method*

The number of active alkyl-magnesium bonds present in the system was determined by reacting the polymerizing solution with a solution of iodine (I_2) in THF and analysing the resultant solution using vapor phase chromatography for the appropriate alkyl iodide.

Excess iodine was removed with aqueous sodium thiosulphate and the organic layer analysed using vapor phase chromatography (v.p.c.).

The apparatus is shown in figure 5.6. Ampoules containing initiator, solvent and cumene were attached to a flask joined to a

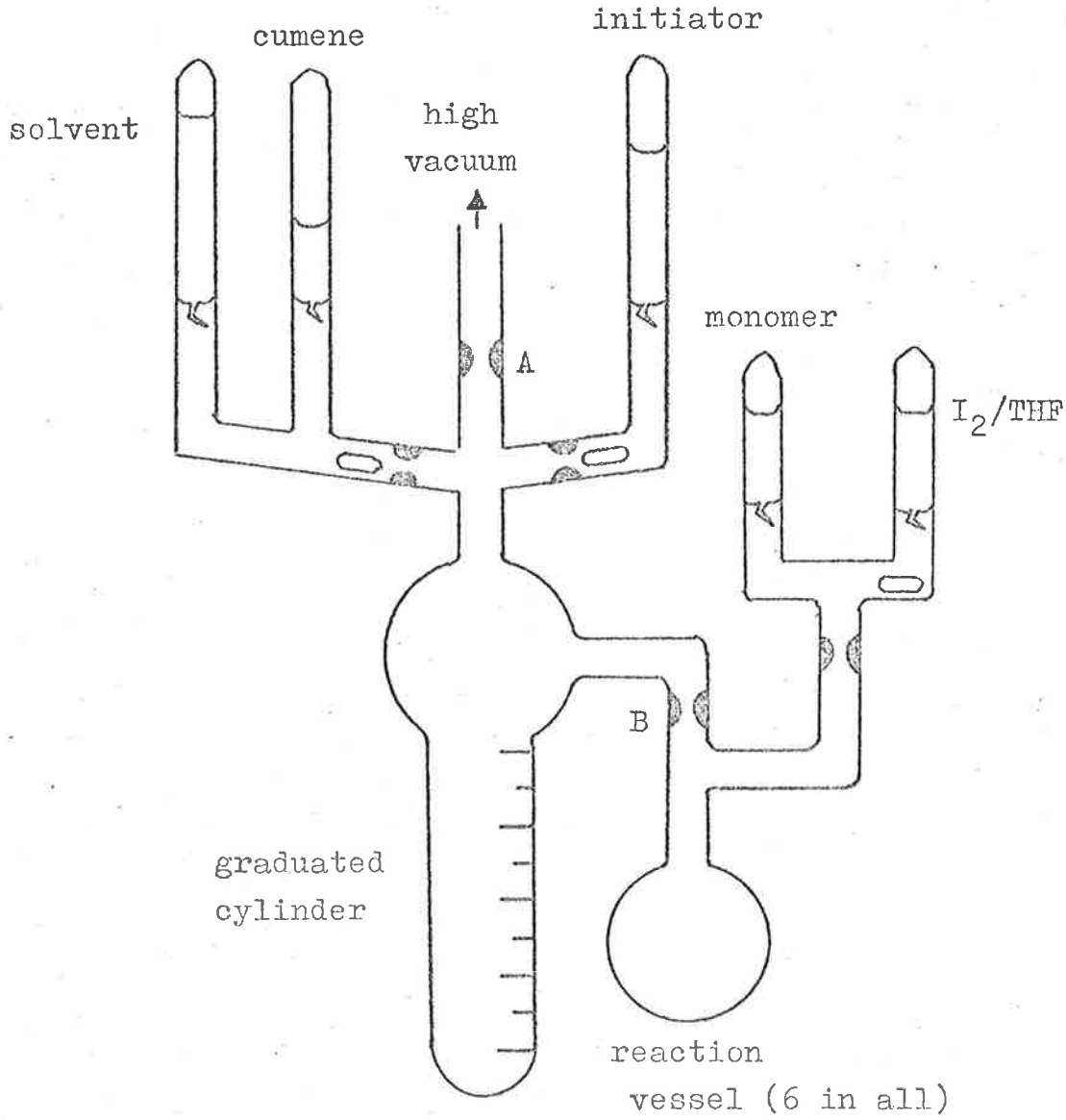

Figure 5.6. Apparatus for determining the concentration of remaining active n- BuMg bonds during the polymerization.

graduated measuring cylinder. Separate reaction vessels (6 in all) were sealed onto the flask and each vessel had individual ampoules of monomer and I_2/THF (concentration 100gm dm^{-3}) attached.

The cumene was needed as an internal standard for quantitative v.p.c. analysis.

After evacuating and baking the apparatus to a pressure of $10^{-3}Nm^{-2}$ it was sealed from the line at constriction A, the initiator, solvent and cumene breakseals were ruptured and the mixture thoroughly shaken. Equal volumes of this solution were poured into each reaction vessel which was sealed off at B. These were then placed in the thermostat at the required temperature. The monomer, which had been precooled, was added and the polymerization terminated at time intervals varying between 0.5 and 50 minutes. The solutions were then warmed to room temperature and the excess iodine reduced with aqueous sodium thiosulphate (concentration 200 gm dm^{-3}). The organic layer was then inspected by v.p.c. and the area under the peak corresponding to n-BuI was compared to that of cumene. Areas were calculated by cutting out and weighing and results were expressed as a percentage of the total concentration of active alkyl-magnesium bonds determined by this method.

When determining the total concentration of active alkyl-magnesium bonds at the temperature of polymerization, the monomer solution was only broken in after the I_2/THF solution had been added.

V.p.c's were measured on a Perkin Elmer F-111 gas chromatograph

with dual ionization flame detectors. Nitrogen was used as the carrier gas and a 2 m column packed with 15% Apiezon L supported on Chromosorb P (80-100 mesh).

The oven temperature was 363K and injection temperature 383K with a 7×10^{-4} cm^3 sample volume.

5.7 *Results*

Unfortunately, this method was only applicable for n-BuMgBr and not for either sec-BuMgBr or tert-BuMgBr. The sec-BuMgBr was unsuitable because the retention time of sec-BuI was very similar to toluene and the much larger toluene peak obscured the smaller sec-BuI peak.

Tert-BuMgBr is unsuitable because the tert-BuI formed is unstable in water, forming tert-Butanol which would become distributed between the two phases. Also, the much smaller concentrations of tert-BuMgBr used, and the extremely viscous nature of the polymerizing solution after very short times makes this method unsuitable.

Figure 5.7 shows the results obtained for n-BuMgBr at 229K and varying monomer and initiator concentrations. The proportion of active n-BuMg bonds falls very rapidly (50% being consumed within 0.5 minutes) and after 10 - 12 minutes becomes almost constant at 16%$\pm$ 2% for up to 50 minutes. The curve appears to be independent of initial monomer concentration which is consistent with the results obtained using Ph-MgBr/isopropyl acrylate,[113b]

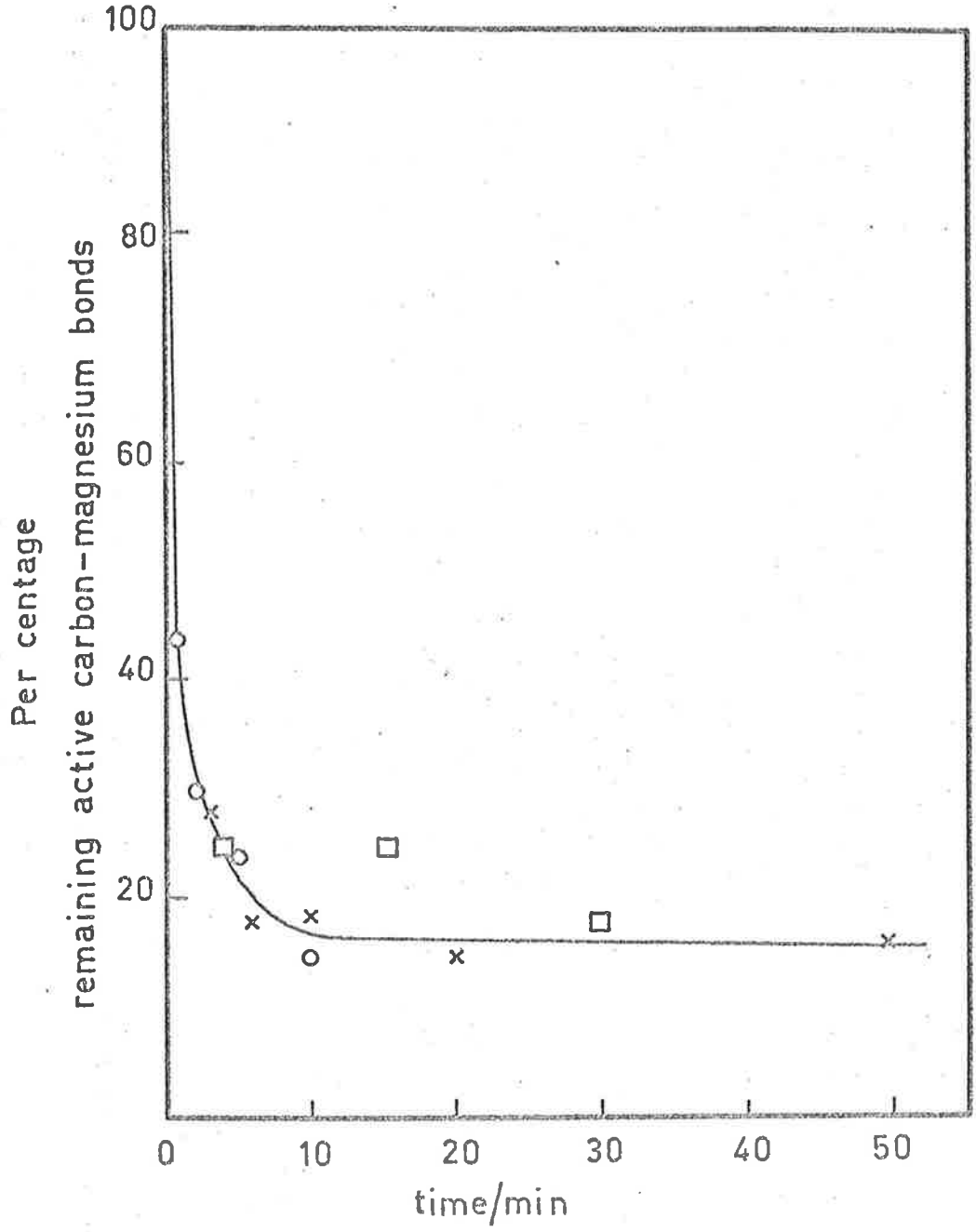

Figure 5.7. Percentage remaining active n- BuMg bonds versus time. T = 229K. (o) and (□), $[MMA]_o$ = 3.14 mol dm^{-3}; $[G_n]_o$ = 0.044 mol dm^{-3}; [THF] = 1.2 mol dm^{-3}.
(x), MMA_o = 1 mol dm^{-3}; $[G_n]_o$ = 0.036 mol dm^{-3};

although the percentages of remaining active bonds are different.

DETECTION OF SIDE PRODUCTS

5.8 *Vapor Phase Chromatography (v.p.c.)*

Polymerizations of acrylate esters initiated by organometallic compounds are inefficient. This is mainly due to susceptibility of the carbonyl group of the monomer to nucleophilic attack. Initiation efficiencies (f) for MMA polymerization by organolithium compounds have been reported in the range 0.18[134] to 0.65[135] dependent on the initiator, solvent and temperature. When Grignard reagents are used as initiators, values of f below .01 for initiation of macro-chains have been reported for the polymerization of acrylonitrile and MMA.[64] The reactions leading to low f values are thought to include butane formation, carbonyl addition and cyclic trimer formation. Any reactions involving carbonyl (1,2) addition should lead to formation of methanol either during the polymerization or more likely, on termination with an active hydrogen atom.

The purpose of this section was not to identify the various addition products but to identify methanol and/or butane. The apparatus was identical to that used for the kinetic experiments, figure 2.4, except that the dilatometer was replaced by a receiving vessel (volume ca. 10 cm^3).

After the polymerization was initiated, half of the solution

was poured into the side arm which was sealed from the main vessel. This portion of the solution was allowed to warm to room temperature while the remainder was maintained at 223K. The solutions were terminated by breaking open the reaction vessels in a glove box filled with nitrogen saturated with water vapour. This 'wet nitrogen' was obtained by bubbling nitrogen through hot water and then into the glove box. The solutions were left in the glove box for ca. 2 hours. This particular method of termination was used because when water is added in bulk, any methanol in the solution will become distributed between the aqueous and non-aqueous phases. Other workers have used acetic acid as terminating agent.[53] Samples were analysed by v.p.c using the same instrument and column as described in section 5.6. The optimum oven temperature was 333K with an injection temperature of 473K.

A control sample of initiator solution (n-BuMgBr in THF) was terminated in the same way as described above and the resulting vapor phase chromatogram is reproduced in figure 5.8 (a). The two largest peaks, C and B, are toluene and THF respectively. The only other peak, A, of any significant height occurs at a retention time, T_R = 43 sec. The sensitivity range of the instrument was such that peaks could be recorded at 20 x 10^4 (lowest sensitivity) to 5 x 1 (highest sensitivity) and the figures at the top of each peak are the sensitivities at which they were recorded. The very low retention time of peak A suggested that it was n-Butane.

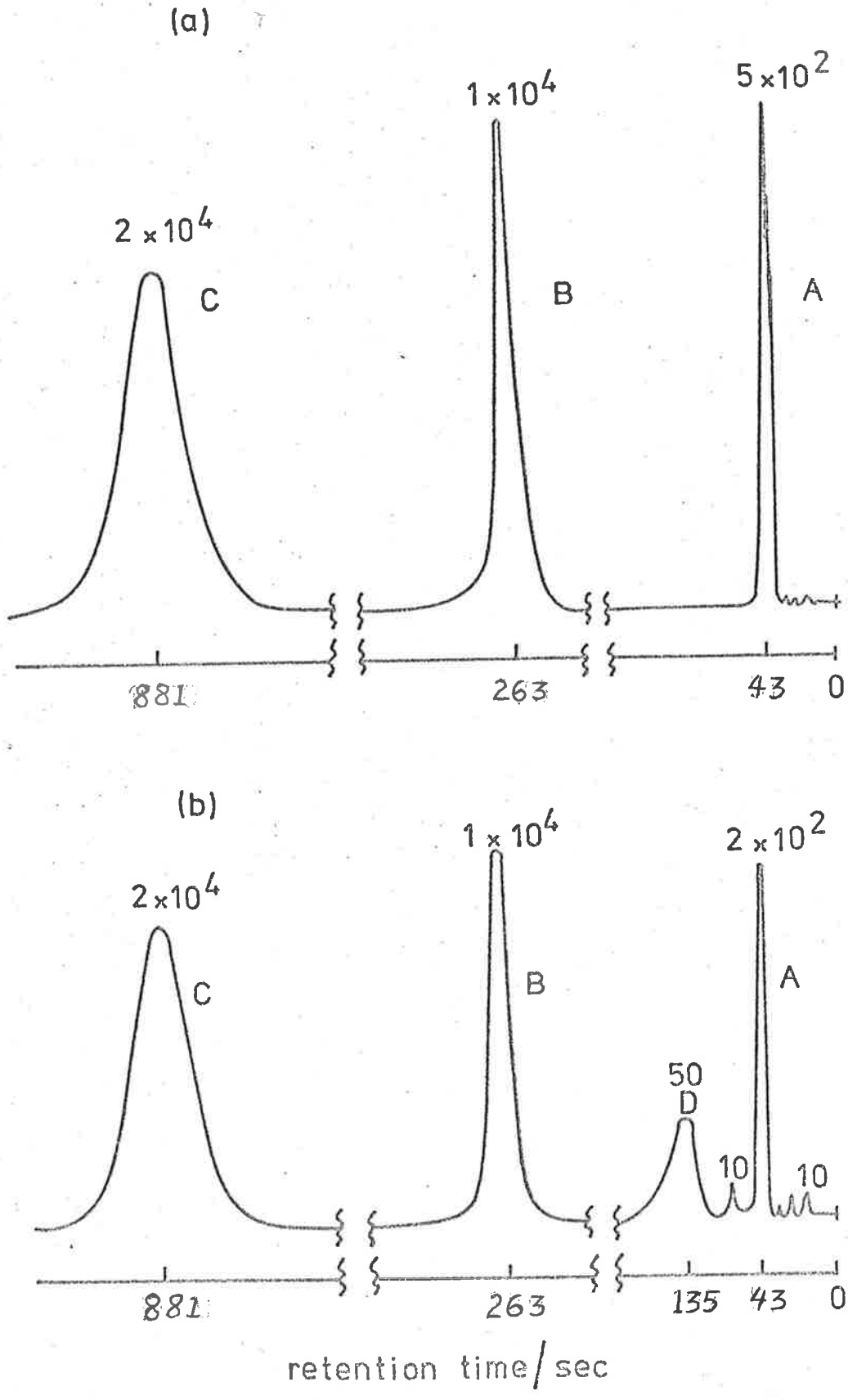

Figure 5.8. Vapor phase chromatogram of (a) hydrolysed solution of n-BuMgBr, (b) hydrolysed solution of polymerizing mixture maintained at T = 223K.

Figure 5.8 (b) shows the v.p.c. of the terminated polymerizing solution held at 223K and it can be seen that peak A has decreased in height and there is a new peak (D) at T_R = 135 sec. This peak was very asymmetric and has tentatively been assigned to methanol. This assignment was made from results obtained by "spiking" the terminated solution with added methanol and observing the changes in the chromatogram. During these "spiking" experiments some interesting observations were made. When methanol ($5 \times 10^{-4} cm^3$) was added to the solution (ca. 1 cm^3) the size of peak D was doubled. However, when larger amount of methanol were added, although the size of D increased, the retention time decreased until at excess methanol, T_R = 93 sec. This phenomenon was checked by adding small amounts of methanol (5×10^{-4}, 5×10^{-3} cm^3 etc.) to benzene (1 cm^3). Once again, the retention time shifted towards shorter times as the concentration of methanol increased. Ethanol showed a similar behaviour. The reason for this shift is uncertain but it may be due to a change in partition coefficient at different concentrations, or more likely the apparent shift in retention time is a property of the stationary phase of the column used. Such behaviour is more than just a nuisance for it can lead to incorrect conclusions, e.g. when T_R of pure methanol was compared with T_R of trace amounts, completely different conclusions were drawn. Initially the v.p.c. results suggested that no methanol was formed because there was no significant peak at T_R = 93 secs, however, when the solution was "spiked" with very small amounts, the

retention time of peak D corresponded exactly to that of methanol.

An *estimate* of the quantity of peak D present in the system was made in the following way: the areas of peaks D and C were calculated using a planimeter. For methanol, the relative sensitivity (i.e. weight per cent response for a flame ionization detector, FID) is 0.23, whereas for toluene it is 1.07.[136] The peak areas were divided by these FID response values and the weight per cent ratio of methanol:toluene was obtained. The theoretical weight per cent ratio of methanol:toluene expected if all the R-Mg bonds present could react with MMA to form methanol was calculated, and this value was compared with the experimental value.

The above calculation indicated that ca.47% of the total number of n-Bu-Mg bonds in the system had been consumed by methanol formation.

Although this value was reproducable to within $\pm$ 1% for consecutive injections, the actual error may be much larger due to the inaccuracies incurred when estimating the area under an asymmetric peak. The method used here was to draw tangents to the points of inflection and calculate the area using a planimeter. The methanol peak was less asymmetric when 15% carbowax 20 M columns on chromosorb P were used, but these columns were unsuitable for analysing reaction mixtures because the retention time of THF was reduced to such an extent that it interfered with the methanol peak.

A similar calculation on peak A (n-Butane) of the hydrolysed reaction using the FID response factor 1.09 for n-Butane showed that 8%

of initiator formed n-Butane. This value is extremely unreliable since n-Butane boils at ca. 273K and would be expected to escape from solution as it warmed to room temperature. This hypothesis was confirmed by results obtained on hydrolysed samples of the initiator solution, fig. 5.8 (a). Analysis of the chromatogram of the hydrolysed initiator solution showed that the total butane in solution was only ca. 50% of the theoretical yield expected on complete hydrolysis of a 0.45 mol dm^{-3} n-BuMgBr solution.

The chromatogram of the sample stored at room temperature was similar to figure 5.8 (b). However, the methanol percentage had increased to ca.96% of the total active R-Mg bonds and the butane peak had decreased to 3.5%. It is very significant that the amount of methanol has doubled compared with solutions stored at 223K prior to hydrolysis and implies that a significant proportion of R-Mg bonds are 'dormant' at 223K, but become active at higher temperatures, section 5.10.

5.9 *Mass spectrometry and infra-red spectroscopy*

Little additional information was obtained using either of these techniques. Identification of butane in the vapour above the polymerizing solution was hampered by the presence of MMA, toluene and THF.

Mass spectra of the polymerizing solution showed the presence of some oligomeric material with peaks at $^{m}/e \leq 258$. This may correspond

to a fragment of the type

$$CH_3CH_2CH_2CH_2[CH_2C(Me)CO_2CH_3]_n^{+}H$$

I

where n = 1 or 2.

Peaks at 158, 127, 99 and 59 correspond to I when n = 1 and the fragments $R'\text{-}CO^{+}$, R'^{+} and $^{+}CO_2CH_3$ respectively, where $R' = CH_3CH_2CH_2CH_2CH_2C(Me)H$.

These were not the only observable peaks and the above assignment is not the only possible one, e.g. 1,4 conjugate addition followed by 1,2 (carbonyl) addition to give a ketone of the type II

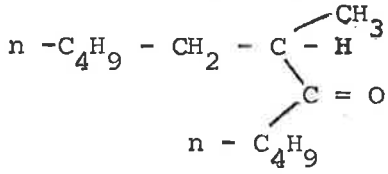

II

would be expected to show peaks at $^{m}/_{e}$ = 184, 127, 99 and 85 corresponding to the parent ion, $R'\text{-}C\text{-}O^{+}$, R'^{+} and $R\text{-}C\text{-}O^{+}$ where $R = n\text{-}C_4H_9$ and $R' = CH_3(CH_2)_4C(Me)H$. All of these peaks were observed.

Infra-red spectra of the low molecular weight polymer was tried in an attempt to reproduce similar experiments by Goode *et al*[52a] where the i.r. spectra of poly MMA prepared at 273K using PhMgBr/toluene showed a strong carbonyl absorption at 1730 cm^{-1} (corresponding to the monomer carbonyl) and a weaker band at 1712 cm^{-1} which was attributed

to the carbonyl in the cyclized end groups, III

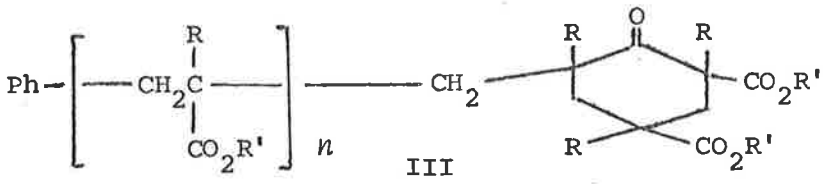

III

Spectra were obtained by grinding a small portion of the polymer with KBr and then pressing into a thin transparent disc. Even under conditions of maximum resolution of the Perkin-Elmer 457 Grating infra-red spectrometer only one carbonyl band at 1730 cm^{-1} could be detected. This does not necessarily mean that species such as III do not exist in our system because the MW of our polymers was ca.5000 (compared to ≤500 for Goode's samples) which would make identification of 1 carbonyl group in 50, very difficult. C^{13} Fourier transform n.m.r. would be much more suitable for this kind of end group detection problem.

5.10 *Discussion*

Some of the results in this chapter are difficult to interpret, e.g., the distinctly non-linear heat output versus time curve for the n-BuMgBr system compared with the linear conversion versus time curves in figure 3.3. The temperature/time curve for sec-BuMgBr appears to be more consistent with the kinetic results, the curve becoming linear after ca. 8 minutes. The non-linearity between t = 0 and 8 minutes may be due to rapid heat evolution resulting from rapid complexing

and initiation reactions. The tert-BuMgBr case seems to fit into this general scheme although difficulties in this case arise due to the lack of supporting dilametric evidence (section 3.4.2).

The calculated heat of polymerization, ΔH_p, in section 5.4 agrees well with the values reported by other workers. This value of ΔH_p did not include the heat liberated when the solution was terminated with methanol. This heat of termination will be due to the reaction of all the active organometallic species present in the system. These organometallic species that liberate heat on reaction with methanol will include; the active propagating chains and dormant propagating species, the residual n-Butyl-Mg bonds remaining throughout the polymerization and any species such as MeOMgX (X = R, Br etc.) resulting from carbonyl attack of initiator on monomer and possibly chain end cyclization. Although, only a very small percentage of initiator is consumed in forming high and low MW poly (MMA), the heat of formation of low molecular weight (i.e. one fold adducts) oligomeric side products will be small compared with heat of formation of high MW polymer. This explains why, although a large percentage of initiator forms side products, the total heat evolved is predominantly associated with polymer formation.

Various complexing reactions between monomer and R_2Mg, RMgX and/or MgX_2 could account for some of the initial heat evolution, e.g. if all the initial active butyl-magnesium bonds complexed with MMA with a heat

of complexing, $\Delta H_c \approx 50.\text{kJ mol}^{-1}$, the temperature rise would be approximately one degree. This value of ΔH_c is an estimate based on the probable strength of complexing between MMA and triethyl-aluminium.[138]

The apparent anomaly in the calorimetric results is the n-BuMgBr system in which the heat output versus time curve only becomes linear at much longer times than was observed for the corresponding percentage conversion versus time curves to become linear. No satisfactory explanation can be given for the unexpectedly long elapsed time for the heat evolution/time plot for the n-BuMgBr system to become linear.

This initial non-linear heat evolution will not affect the dilatometric conversion curves because the total temperature rise (at least from 10 to 20 minutes) is so small that the polymerization rate will not be affected in the dilatometric experiment which is close to isothermal.

The proportion of remaining active n-Butyl-Mg bonds during polymerization is also difficult to explain. The explanation is complicated all the more since comparative studies could not be done using the secondary or tertiary Grignard systems for reasons discussed previously (section 5.7). No precise answer can therefore be given to this question concerning the origin of the remaining active n-Bu-Mg bonds but some of the various possibilities that may explain the results will be discussed.

As proposed previously, section 3.6 (c) the reactive species in the Grignard solution is R_2Mg and not RMgX. However, the remaining active R-Mg bonds are unlikely to be due to the unreactive RMgX because as soon as R_2Mg is consumed in initiating macro-chains and side product formation, the Schlenk equilibrium will be forced towards more R_2Mg. Of course, this argument assumes that the Schlenk equilibrium is labile, an assumption which is supported by n.m.r. studies on exchange rates between R_2Mg, RMgX and MgX_2.[31] Even redistribution reactions such as eqn. (3.11) between MgX_2 and MMA : R_2Mg carbonyl adducts to form RMgX could not account for the remaining active R-Mg bonds because the RMgX formed would rapidly disproportionate to R_2Mg and MgX_2.

The proportions of initiator consumed in methanol formation even at low temperatures is very large and must result from either inter or intra-molecular substitution on the monomer carbonyl. As stated in section 5.8, the percentage initiator consumed in methanol formation was calculated assuming *all* the R-Mg bonds present in solution could react with MMA via carbonyl addition - however, if R_2Mg is the active species only half of the R-Mg bonds may be available, e.g.

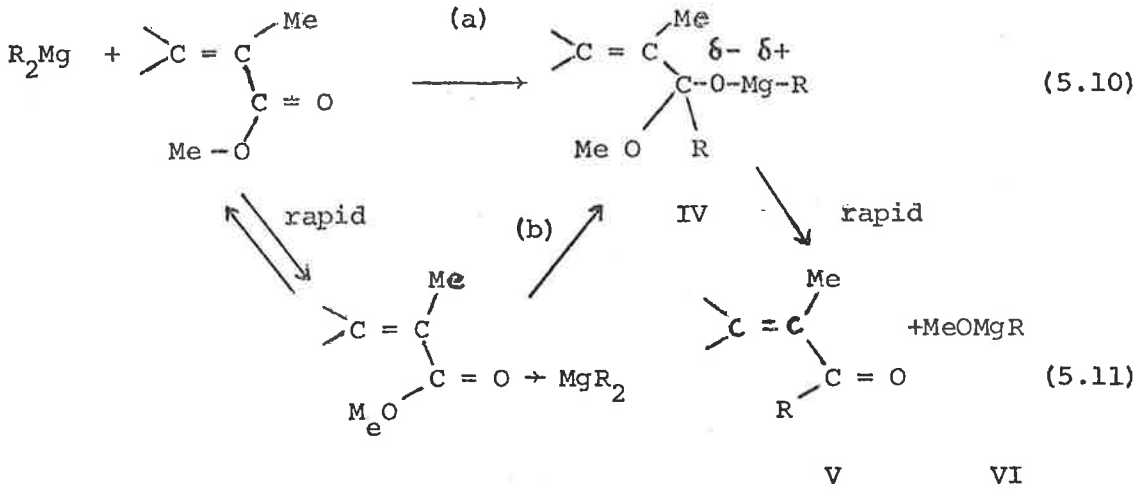

where either direct bimolecular reaction (path (a))or rearrangement of a 1:1, MMA :R_2Mg complex (path (b)), to the carbonyl adduct IV may occur. If species IV does not participate in any redistribution equilibria (at least at 223K) or if it reacts rapidly via (5.11) to form the ketone V, then the 47% of n-Bu-Mg bonds consumed in methanol formation at low temperature actually represents 94% of the initiator that is consumed in side reactions. With the errors involved in calculating the methanol present,(section 5.8), this value could easily be reduced to 80%, leaving 16% of a species different from IV or VI to account for the remaining active R-Mg bonds. This is where the difficulty arises: the R-Mg bond of any species such as IV and/or VI (eqn. 5.11) would be expected to react with I_2 and thus produce a much larger amount of n-BuI than the 16% actually observed. This of course assumes that (5.10 and 5.11) is the predominant reaction forming side products. Double carbonyl addition and/or carbonyl

addition followed by conjugate addition is possible provided that either (a) or (b) of eqn. (5.10) is the rate determining step (to preserve first order dependence on $[G_n]_o$). As mentioned above, species IV may react rapidly to form the ketone V and MeOMgR.

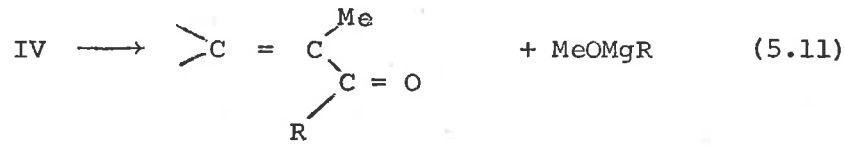

(5.11)

V VI

Ketone V may then be susceptible to further carbonyl or conjugate attack from any active R-Mg bonds remaining in the system, e.g. species VI. However, the formation of large quantities of these two fold adducts at low temperature is inconsistent with the hypothesis that the much larger amount of methanol produced when a polymerizing solution at 223K is allowed to warm to room temperature must result from activation of the remaining R-Mg bonds in species such as IV and/or VI. Since it has already been stated that species such as Iv and VI should react with iodine, but apparently do not, the implication is that the R-Mg bonds associated with these side products are in some way deactivated at low temperatures. Dimerization via double methoxy bridges may account for the unreactivity of the RMg groups at low temperatures. Such dimeric structures involving -OR bridges are known to occur in THF (section 1.2.1, ref. 20).

At higher temperatures, these R-Mg bonds must become reactive either in their monomeric form for compounds such as VI, or, they may take part in redistribution reactions with $MgBr_2$ to form RMgX and R'OMgX where R' = Me in VI and $CH_2C(Me)CO(OMe)R$ in IV, e.g.

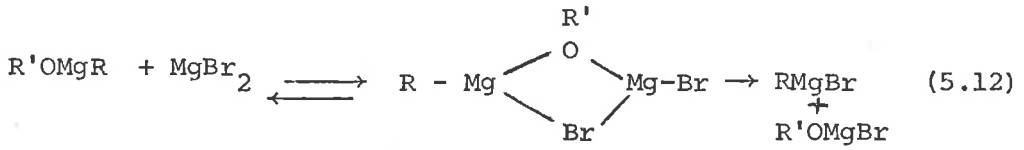

(5.12)

In either case, at higher temperatures, the macro-chain becomes deactivated and extra carbonyl additions occur resulting in greatly increased methanol formation. There is also a possibility of conjugate rather than carbonyl addition to species such as IV and V to form mixed 1,2 and 1,4 addition products.

The above discussion still does not answer the question as to the nature of the species giving rise to the 16% remaining active R-Mg bonds, since we have assumed that species such as IV and/or V and VI constitute the major side products. One possibility is the deactivation of the propagating species at an early stage of the polymerization via a reaction such as the much quoted cyclic trimer formation,

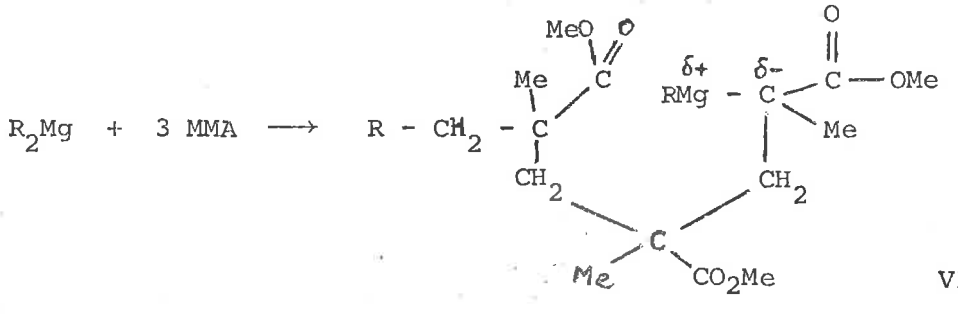

(5.12a)

VII

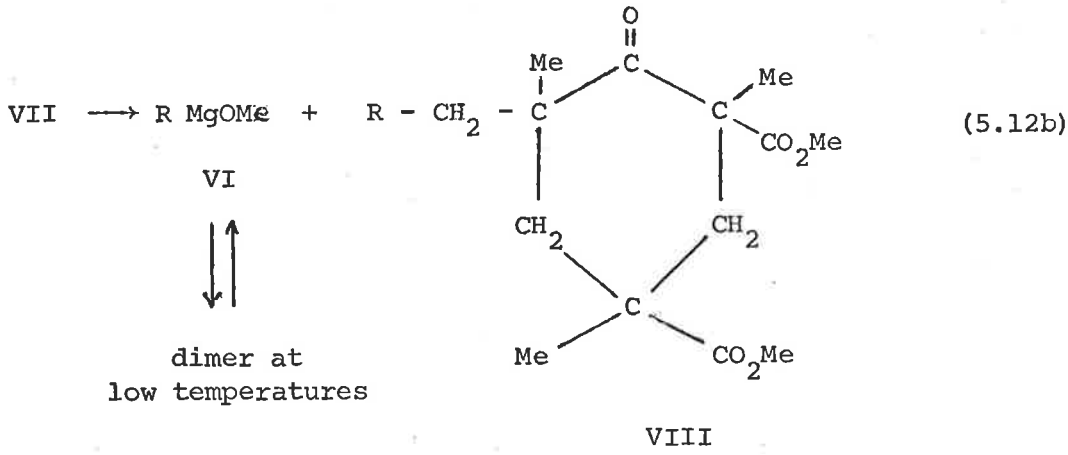

(5.12b)

Reaction (5.12b) is unlikely to be the major path leading to methanol formation because at the concentrations of initiator used (i.e. 0.1 mol dm^{-3}) ca. 0.3 gms. of VIII would be expected to be formed in the methanol soluble material. This amount of methanol soluble material was never observed and g.p.c. analysis of the actual methanol soluble material obtained, indicated a molecular weight $\bar{M}_n \gtrsim 5000$. Reaction (5.12a) may contribute the 16% remaining active n-Bu-Mg bonds because the R-Mg bond of species such as VII would be expected to react with iodine at low temperatures.

The above arguments have been speculative, there is no proof that the hypothesis proposed is correct, however, it is extremely difficult to think of other complete schemes which can account for the observed results.

Finally, the u.v. spectra of the polymerizing and non-polymerizing solutions (section 3.3.5 and 3.6(d)) impose some restrictions on the

properties of the methanol forming side products. The predominant low temperature side products such as IV, V, VI, VII or VIII or their associates (which are possibly formed at low temperature), cannot be responsible for the ultra violet absorption peak at λ = 296 nm observed as the temperature of a polymerizing or non-polymerizing system is raised from 223 to ambient. The similarity between IV and the proposed methoxide formed by attack of the growing chain on the monomer carbonyl supports the statements made in section 3.6(d) that this species is *not* responsible for the observed spectral results. The u.v. peak appearing at T> 253K most probably arises from reactions of the R-Mg groups which are unreactive at low temperature but become activated as the temperature rises above 253K. The 296 nm peak may arise from precursors of double addition products to the macro-chain as suggested in section 3.6 (d) or may be due to other side products which are formed at higher temperatures. In fact, in view of the extremely small concentration of active chains(even though they are no doubt terminated by some form of carbonyl addition) the u.v. peak observed may result from one of the subsequent addition reactions of the original side products as the temperature is raised. This would explain the similarity between the u.v. spectra of the polymerizing and non-polymerizing solutions.

CHAPTER 6

POSSIBLE MECHANISMS

6.1 *The Kinetic Aspect*

The distinction between this section and the following one is rather arbitrary since the factors influencing the reactivity, also influence the stereospecificity. Nevertheless, there are some aspects of the kinetic results of chapter 3 that can be discussed independently of the stereospecificity results in chapter 4.

Polymerizations initiated by anionic reagents are generally categorized as propagating by an anionic or anionic-coordination mechanism. The latter description, although convenient, is inaccurate in that no anions, either free or paired, appear to be involved in the reaction. Anionic-coordination mechanisms are generally postulated for reactions of the covalent alkyl compounds of Group IA, IIA and IIIA metals where the incomplete coordination shell of the metal in the monomeric form of the compound provides an open invitation to an electron pair from the filled π or n orbitals of the monomer.

The propagation step in these systems and also of the ionic pair type may involve a two stage process involving some formof monomer complexing followed by incorporation into the chain.

$$R - Me + M \overset{a}{\rightarrow} R - Me \leftarrow M \overset{b}{\rightarrow} RM - Me \qquad (6.1)$$

$$\text{or } R, Me + M \overset{a}{\rightarrow} R, \quad Me \leftarrow M \overset{b}{\rightarrow} RM, Me \qquad (6.2)$$

where R - Me and R, Me are the covalent carbon-metal bond and tight ion-pair respectively.

Of course, in neither case is it essential that the mechanism involves two steps; a one step reaction via a four centre transition state is quite possible. However, if two step reactions such as eqns. (6.1) and (6.2) are involved, assessment of the relative parts played by each of the stages (a) and (b) is difficult. Monomer complexing during anionic chain propagation has *not* been directly proved in a single case and schemes such as (6.1) and (6.2) have been postulated either on the basis of kinetic results or on the results obtained with model systems, e.g. ref 139.

In a more recent review of 'some of the problems of anionic polymerization theory', Erusalimskii discusses the propagation reaction of an ionic pair M_n^- , Me^+ with monomer, in terms of the following scheme:[140]

$$M_n, Me \xrightarrow[(a)]{+M} M_n, Me \leftarrow M \xrightarrow[(b)]{} M_n - Me \xrightarrow[(c)]{} M_{n+1}, Me \qquad (6.3)$$

$$\text{with } \succ C = C \prec$$

The results of their studies using acrylonitrile initiated by organomagnesium[64] and organolithium compounds[141] in hydrocarbon media at low temperatures showed that both systems were in many ways similar but differed in one respect. The dependence of molecular weight on monomer concentration was "near-linear" for BuLi but was independent of monomer concentration for the organomagnesium initiators, (see section 1.4.2.) The dependence of molecular weight on monomer concentration observed using n-BuLi was attributed to (6.3a) being rate determining although the same results would be observed if propagation was a one step reaction. The independence of MW on monomer concentra-

tion observed in the organomagnesium initiated system was attributed to either (6.3b) or (6.3c) being rate determining.

A similar mechanism was proposed for the organomagnesium initiated polymerization in the presence of catalytic amounts of DMF where the rates were much faster, but the MW was still independent of monomer concentration.

Since, in this research, the most detailed kinetic experiments were done using the n-BuMgBr/MMA/toluene/THF system at 223K, the purpose of this section is to discuss possible mechanisms consistent with the observed facts reported in the preceding chapters. The propagating species will be denoted as M_n^* (where n is the degree of polymerization) and the initiator as I_n. The possible structure of M_n^* will be the topic of discussion in the following section.

The most pertinent facts required for outlining a general mechanism for the polymerization are the following: (a) the polymerization is extremely inefficient. Here, the initiation efficiency, f, is defined as the (concentration of active chains forming high MW polymer)/(total amount of initiator) i.e.

$$f = \frac{[C]}{[I_n]_o} \qquad (6.4)$$

where $[I_n]_o \equiv [G_n]_o$ in this system.

Even when the low MW polymer ($4000 < MW < 6000$) is included, f is still below 5%. A rough estimate of f may be made by comparing the experi-

mental MW ($\bar{M}_{exp}$) with the theoretical MW($\bar{M}_{th}$) calculated for an anionic polymerization without transfer or termination with instantaneous initiation and initiator efficiency, f,

$$\bar{M}_{th} = \frac{\alpha \times [M]_o \times (\text{MW monomer})}{f\ [I_n]_o} \qquad (6.5)$$

where α = fractional conversion

and (MW monomer) = molecular weight of the monomer, (c.f., section 3.6 (d))

(b) The conversion versus time curves are linear, up until at least 40% conversion, but the $\ln([M]_o/[M]_t)$ versus time plots, although linear at low conversions, show a distinct *upward* deviation from linearity at high conversion. This means that the polymerization has an internal order of zero with respect to monomer concentration. The external orders with respect to monomer and total active R-Mg bonds are unity.

(c) The molecular weight of the polymer is directly proportional to the fractional conversion, α, and inversely proportional to $[I_n]_o$ where $[I_n]_o \equiv [G_n]_o = [RMgX]_o + 2[R_2Mg]_o$. This suggests that the polymerization is termination free, at least up to $\alpha = .25$ where deviation from linearity was observed. The fact that the conversion/time curves were linear beyond 25% suggest some type of slow monomer transfer mechanism regenerating an active centre of identical reactivity to the original propagating species.

(d) The initiator species are monomeric in THF. At 298K or slightly above, the proportions of R_2Mg, MgX_2 and RMgX are such that $K_{1.1} \approx 4$. However, as the temperature decreases, $K_{1.1}$ decreases and the proportion of R_2Mg and MgX_2 increases. Evidence to hand suggests that R_2Mg is much more reactive than RMgX which leads to the conclusion that R_2Mg is the reactive species in THF at low temperatures. Exchange studies between R_2Mg and $*MgBr_2$ and n.m.r. studies show that the equilibrium is labile in most cases - rates of exchange in the tert-BuMgCl are relatively slow, relaxation times being approximately 4 seconds at room temperature.[31] In the tert-BuMgBr and sec-BuMgBr systems rates of exchange may be in the minute range, at 223K, a factor which may be significant in determining the stereospecificity of the resulting polymer. Even in these systems, the actual part played by RMgX in initiation will be small not only because RMgX is less reactive than R_2Mg but also because the concentration of RMgX at 223K, will very low, e.g., for tert-BuMgCl, $K_{1.1} = 10^{-2}$ at 223Kusing Ashby's data, whereas for n-BuMgBr, $K_{1.1} \approx 1$ at 223 using the approximate data of Holm.[40a]

(e) The approximate inverse dependence of the polymerization rate on THF/coven suggests that both initiation and propagation reactions do not involve ion-pair equilibria as encountered in certain organo-alkali systems, where increasing concentrations of solvating solvents such as THF, accelerate polymerization rates by increasing the concentrations of the more reactive loose ion-pairs and free ions. The effect of solvent on the rates and mechanisms of the

less reactive organometallic compounds (i.e.essentially covalent) of Group IIA and IIIA will be discussed later.

(f) The instantaneous formation of a green colour when monomer and initiator are mixed at 223K suggests some form of complexing, probably of the Wittig-at type, between the monomer carbonyl and the magnesium of the organomagnesium compound. The observed colour probably arises from the charge-transfer band of the Wittig-at complex. The particular species giving rise to the colour observed in our system is not the same as the species which produces a similar colour in the MMA polymerization initiated by Na_2 (α-Mestyrene)$_4$ at 198K.[82] In the sodium system, polymerization is extremely rapid under conditions when the colour is present, which is completely different from the observations in the organomagnesium systems. Direct evidence for complexing between RMgX, MgX_2 and R_2Mg and various substrates has been obtained[39,40,45,47,142] and mechanisms have been proposed involving rearrangement of cyclic four membered and six membered transition rates formed from substrate: Grignard complexes. In our system, it is extremely difficult to determine whether complex formation is a termination step or whether it is associated with side product formation, propagating chain formation or both. It has already been noted that some workers consider that reaction proceeds via the complex in certain instances and by direct bimolecular reaction in others.[40] The evidence accumulated during this work suggests that complex formation *may* be the precursor

to initiation. The increase in intensity of the colour at low χ_{THF} accompanied by increasing rate and decreasing MW (i.e. δ increases) supports this contention. Also the shorter lifetime of the colour with sec-BuMgBr and complete absence with tert-BuMgBr are consistent with the faster rates of polymerization observed using these initiators. However, this is not enough evidence to state positively whether or not the complex is the active species.

It is interesting to compare the likely relative strengths of the complexes formed between MMA and RMgX, MgX_2 and R_2Mg. Consideration of likely group electronegativities predicts that the relative equilibrium constants for the reaction, MMA + B $\overset{K}{\rightleftharpoons}$ MMA : B should decrease in the order $MgBr_2$ > RMgX > R_2Mg. This does appear to be the case in the MeMgBr/ 2 - Me-benzophenone system[39e] in diethyl ether at 298K where the respective values of K were 4; 1.35 and ~0 ('insignificant'). These values of K will no doubt vary for different systems and should substantially increase at lower temperatures. The identical colour changes observed when R_2Mg was used instead of the Grignard system also support the hypothesis that initiation may result from complex formation between R_2Mg and MMA.

With the above results in mind, the following schemes have been proposed to account primarily for the kinetic results of chapter 3.

SCHEME 1

$$I_n + M \underset{\text{rapid}}{\overset{K_1}{\rightleftharpoons}} (I_n . M) \xrightarrow[k_1 \text{ (slow)}]{+M} M^* \qquad (6.6)$$

$$(I_n . M) \xrightarrow[k_3 \text{ (slow)}]{} \text{methanol forming side products} \qquad (6.7)$$

$$M_n^* + M \underset{\text{rapid}}{\overset{K_2}{\rightleftharpoons}} (M_n^* . M) \xrightarrow[\text{slow}]{k_2} M_{n+1} \qquad (6.8)$$

where n = degree of polymerization

The specific rates of reactions (6.6) →(6.8) with rate constants k_1, k_2, and k_3 are:

$$R_1 = k_1 [I_n.M] [M] = k_1 K_1 [I_n]_o [M]_o^2 \qquad (6.9)$$

$$R_2 = k_2 [M_n.^*M] \qquad (6.10)$$

$$R_3 = k_3 K_1 [I_n]_o [M]_o \qquad (6.11)$$

Now the initiator efficiency, δ, is given by eqn. 6.4

$$\delta = [C]/[I_n]_o \qquad (6.4)$$

$$\equiv R_1/(R_1 + R_3) \qquad (6.12)$$

i.e. $$\delta = R_1/(R_1 + R_3) = k_1[M]_o/(k_1[M]_o + k_3) \qquad (6.13)$$

We know from the results of section 5.8 that R_3, the rate of side product formation is much larger than R_1, the rate of formation of

active chains, i.e. $R_3 >> R_1$. We also know that initiation and side product formation are rapid and complete at low monomer consumption and that after initiation, the active polymerizing chains propagate without termination. Under these conditions the efficiency of initiation, f, is defined as

$$f = \frac{[C]}{[I_n]_o} \approx \frac{R_1}{R_3} = \frac{k_1[M]_o}{k_3} \qquad (6.14)$$

where $[C]$ = *total* concentration of active chains

$\equiv [M_n^*] + [M_n^*.M]$ and is independent of time after steps 1 and 3 are complete.

The rate of propagation, R_p, is conventionally defined as the rate of disappearance of monomer,

$$R_p = \frac{-d[M]}{dt} = R_2 = k_2[M_n^*.M] \qquad (6.15)$$

which is valid, since after the initial period, initiation and side product formation are now complete.

In general, assuming that k_2 is small and does not perturb the equilibrium of the first step of (6.8) significantly

$$\frac{[M_n^*.M]}{[M_n^*]} \equiv K_2[M] \qquad (6.16)$$

and $[M_n^*.M] + [M_n^*] \equiv [C]$ (6.17)

Two limiting cases arise; firstly, when

$K_2[M] \longrightarrow \infty$, $[M_n^*.M] \rightarrow [C]$

and $R_p = k_2 [C]$ (6.18)

$\lim_{K_2[M]\to\infty}$

$$= \frac{k_2 k_1}{k_3} [M]_o [I_n]_o \quad (6.18a)$$

from (6.14) above.

This scheme corresponds to the observed kinetic relationships from chapter 3, that the reaction is internally zero order with respect to monomer concentration, and that the external orders with respect to monomer and initiator are unity.

In the other limit, i.e., $K_2[M] \to 0$, $[M^*] \to [C]$ and

$$[M_n^* M] = K_2 [M] [M^*]$$

Under these conditions,

$$R_p = k_2 K_2 [M] [C] \quad (6.19)$$

$\lim_{K_2[M]\to 0}$

$$= \frac{k_1 k_2 K_2}{k_3} [M]_o [I_n]_o [M] \quad (6.19a)$$

This introduces an extra monomer dependence and predicts an internal first order dependence with respect to monomer which is contrary to the observed kinetics. It appears therefore, that scheme I is consistent with the observed kinetics only under the conditions $K_2[M] \to \infty$.

Scheme I strongly favors the previous suggestion that initiation

occursvia complex formation and *not* via a direct reaction between monomer and initiator. In the absence of complex formation, initiation would require a termolecular reaction in order to fit the observed kinetics.

$$I_n + M \xrightarrow[k_1'']{+M} M^* \qquad (6.19)$$

$$I_n + M \xrightarrow[k_3'']{} \text{methanol forming side products} \qquad (6.20)$$

The bimolecular reaction 6.6 is more likely than the termolecular reaction 6.19.

An alternative mechanism involving complexing of monomer and initiator is the following.

SCHEME II

$$I_n + M \underset{\text{rapid}}{\overset{K_1}{\rightleftharpoons}} (I_n.M) \xrightarrow[\text{slow}]{k_1'} M^* \qquad (6.21)$$

$$(I_n.M) \xrightarrow[\text{slow}]{k_3'} \text{methanol forming side products} \qquad (6.22)$$

$$M_n^* + M \underset{\text{rapid}}{\overset{K_2}{\rightleftharpoons}} (M_n^*.M) \xrightarrow[\text{slow}]{k_2} M_{n+1}^* \qquad (6.8)$$

The same calculations as in Scheme I, eqns. 6.9 to 6.14 gives

$$\delta = \frac{[C]}{[I_n]_o} \approx \frac{R_1}{R_3} = \frac{k_1'}{k_3'} \qquad (6.23)$$

$$R_p \simeq R_2 = k_2[M_n^* M] \qquad (6.16)$$

The same two limiting cases arise,

Firstly when $K_2[M] \rightarrow \infty$;

$$\lim_{K_2[M] \rightarrow \infty} R_p = \frac{k_1' k_2}{k_3'} [I_n]_o \qquad (6.24)$$

which is inconsistent with the observed kinetics.

The other limiting case is when $K_2 [M] \rightarrow 0$;

Under these conditions,

$$R_p = K_2 k_2 [M^*] [M] \qquad (6.25)$$

$$\lim_{K_2[M] \rightarrow 0} = \frac{k_1' k_2 K_2}{k_3'} [I_n]_o [M] \qquad (6.26)$$

Although eqn. (6.26) is consistent with the observed external orders of reaction with respect to monomer and initiator, eqn. (6.25) predicts internal first order monomer dependence which is not observed.

Similarly, other permutations of kinetic possibilities within the frame work of general mechanisms of this type, fail to fit all the kinetic observations.

It would appear that the only mechanism that fits all the kinetic results is that outlined in SCHEME I with the assumptions $R_1 << R_3$ and $\lim K_2 [M] \rightarrow \infty$.

Under these conditions:

$$\delta = \frac{k_1 [M]_o}{k_3} \tag{6.14}$$

$$R_p = k_2 [C] \tag{6.18}$$

$$R_p = \frac{k_1 k_2}{k_3} [I_n]_o [M]_o \tag{6.18a}$$

The independence of MW on monomer concentration can be explained when (6.14) is considered in conjunction with eqn. (6.5). The theoretical number average molecular weight expression for our system becomes,

$$\bar{M}_{nth} = \frac{k_3 \alpha . 100.15}{k_1 [I_n]_o} \tag{6.27}$$

In chapter 4, section 4.4.1, the following expression was verified,

$$\bar{M}_{nexp} = \frac{A \text{ (percentage conversion)}}{[G_n]_o} \tag{4.12}$$

where A = constant

and $[G_n]_o$ has been defined previously, eqn. (2.6)

Comparison between (4.12) and (6.27) shows that the value of A, the slope of figure 4.14 (b), should be given by

$$A = \frac{k_3 . 100.15}{k_1 . 100} \tag{6.28}$$

where the value of 100 arises from the conversion of percentage conversion to fractional conversion.

From fig. 4.14(b); $A = 312 \pm$ S.E. 60 mol dm^{-3}

Hence, $$\frac{k_1}{k_3} = 3{\cdot}2(\pm\ 0.5) \times 10^{-3}\ \text{dm}^{+3}\ \text{mol}^{-1} \qquad (6.29)$$

at [THF] $= 2.8_7$ mol dm^{-3} and T = 223K

This value is similar to that obtained in the acrylonitrile/organomagnesium system in toluene at 198K.[64b]

Using the data in Table 3.1, a value of k_2, the rate constant of propagation (6.18) was obtained using the above value of k_1/k_3. This gave an average value for k_2, the first order propagation rate constant, at [THF] $= 2.8_7$ mol dm^{-3} and T = 223K of

$$k_2 = 0.09\ (\pm\ .01_6)\ \text{s}^{-1} \qquad (6.30)$$

Although the value cited is statistically reliable, there are reasons to believe that systematic errors may greatly exceed the random deviation cited.

The basic premise in the calculations, (i.e. (6.29)) is that *all* of the propagating species formed via k_1 in reaction (6.6) form the high MW polymer. If not, then the value of k_1/k_3 above will be reduced to a value k_1'/k_3 where $k_1' < k_1$ and represents the rate constant of the reaction leading to active centres which propagate to high MW. The presence of low MW polymer in the n-BuMgBr *and* $(n\text{-Bu})_2\text{Mg}$ systems suggests that the value of k_2 obtained in (6.30) may indeed be too large. This will apply if the methanol soluble

polymer is formed via (6.6). For this reason the actual reliability of the value of k_2 may be more likely within an order of magnitude rather than the random deviation cited. Comparatively little information concerning methanol soluble polymer has been obtained. The fact that it is formed in both n-BuMgBr and $(n\text{-Bu})_2Mg$ systems suggests it is not a peculiarity of the Grignard system. The amount formed decreases in the series n-BuMgBr> sec-BuMg > tert-BuMgBr. In the tert-BuMgBr system, only trace amounts were observed and in the sec-BuMgBr system, the quantity increased as the THF concentration increased.

The completely different tacticities between the two fractions (methanol insoluble and methanol soluble), e.g. figure 4.5 suggest that a different mechanism may be operating. The methanol soluble polymer had a relatively high degree of polymerization ($40 < \overline{DP} < 60$) and showed a reasonably narrow distribution about this $\overline{DP}$ value. It is unlikely that the methanol soluble polymer is caused by cyclization of the last three monomer units of the polymer chain (as in Goode's work[52a]) because there is no reason why cyclization should occur predominantly at this size.

A more plausible explanation would be that there are two independent reactive centres (i.e. propagating chains of differing reactivity and stereospecificity). It must be emphasized that they are independent centres - not in equilibrium. It has been well

established that propagating centres in equilibrium with each other lead to a *broadening* of the MWD and not a bimodal distribution.[146]

Hitherto, the discussion has been solely concerned with the n-BuMgBr and $(n\text{-Bu})_2Mg$ systems. SCHEME I, subject to the conditions outlined, appears to be consistent with the experimental facts. The similarity between the kinetic results obtained using sec-BuMgBr with those for n-BuMgBr would suggest that a mechanism similar to SCHEME I is operating in this system. The multimodal MWD of the polymer (figure 4.15) clearly indicates the presence of more than one form of propagating species and it is pointless to discuss the dependence of MW on initiator concentration. The complete lack of kinetic evidence in the tert-BuMgBr case makes the proposal of a mechanism impossible although the MW did appear to be independent of the monomer concentration, even though the rate of polymerization could be controlled by decreasing the monomer concentration.

Table 6.1 shows a comparison between the percentage rates of polymerization of the different initiators used throughout this work at two different THF concentrations. The numbers in brackets are the values of $R_p\%$ expected at $[I_n]_o$ = 0.10 mol dm^{-3} assuming first order dependence in all systems studied. Notice that $R_p\%$ is independent of $[M]_o$ if the external order is unity with respect to monomer. The values of $\bar{M}_n$ and the percentage conversion are also listed. The only multimodal MWD's observed were for the sec-BuMgBr system.

Comparison between the percentage rates of polymerization, $R_p\%$, of the different initiators used throughout this work.

$[THF] = 2.8_7$ mol dm^{-3}; T = 223K.

Initiator	$[I_n]_o$/mol dm^{-3} (a)	$[M]_o$/mol dm^{-3}	$R_p\% \times 10^3/s^{-1}$ (b)	$\bar{M}_n \times 10^{-3}$	% conversion	$10^{-3} \times 1/\bar{\nu}$ (c)	$1/\bar{\nu} \times \frac{0.1 R_p\%}{[I_n]_o}$
n-BuMgBr	0.10	2.76	3	61	16	1.38	414
n-Bu_2Mg	max 0.10	2.76	~ 4	54			
sec-BuMgBr	0.02	0.96	8 (40)	low MW peak 7	16	.088	3.5
tert-BuMgBr	0.02_4	2.76	33 (132)	2800	4	6	792
tert-Bu_2Mg	0.012	2.76	0.2(1.6)	125	1	0.54	0.87
iso-BuMgBr	0.10	2.76	11.6	21	14	.054	0.63
		$[THF] = 0.9_9$ mol dm^{-3} ; T = 223K					
n-BuMgBr	0.036	0.96	3.86 (115)	66	8	.31	3.6
n-Bu_2Mg	0.036	0.96	4.36 (13)	39	17	$.08_6$	1.1
sec-BuMgBr	0.02_1	0.96	11.5 (57)	multimodal	20		
sec -Bu_2Mg	0.01_2	0.9_6	55 (440)	82	40	.026	11

(a) $[I_n]_o = [RMgX]_o + 2[R_2Mg]_o$

(b) $R_p\% = R_p.100/[M]_o$; number in brackets are the percentage rates of polymerization at $[I_n]_o = 0.10$ mol dm^{-3} calculated according to $0.1\ R_p\%/[\text{Init.}]$

(c) $1/\bar{\nu} \simeq A/[M]_o = \bar{M}_{n\ ex}.\ [I_n]_o/\{(\text{percent. conversion})\ [M]_o\}$ from eqns. 4.12 and 6.14.

The decreasing rates of polymerization in the Grignard systems were; tert-BuMgBr > sec-BuMgBr > iso-BuMgBr > n-BuMgBr. These are similar to those reported by Watanabe except for the tert-BuMgBr case which, in their case, was found to be the least reactive reagent in diethyl-ether/toluene.[55b] The order of decreasing rates for the dialkyl magnesiums was: $(sec\text{-}Bu)_2Mg > (n\text{-}Bu)_2Mg > (tert\text{-}Bu)_2Mg$. When these relative rates are inserted in the Grignard system the following decreasing order results:

$$(sec\text{-}Bu)_2Mg \gtrsim tert\text{-}BuMgBr > sec\text{-}BuMgBr > iso\text{-}BuMgBr > (n\text{-}Bu)_2Mg \gtrsim n\text{-}BuMgBr > tert\text{-}BuMgBr \quad (6.31)$$

The assignment of relative *reactivities* (as opposed to *relative rates*) to a series of initiators can be quite difficult, especially when efficiencies of initiation are very low. Comparison of relative rates of polymerization for similar initial catalyst concentrationsis not enough because, if the efficiencies of initiation are different, then the observed rate of polymerization will not reflect the true reactivity of the system e.g. if the rate of polymerization for initiator A is twice that for initiator B, but the efficiency of initiator A is twice that for B, then the reactivities of A and B are the same. Here, the reactivities being compared are the reactivity of active chains towards reaction with monomer. Initiators with low f values imply high reactivity to form side products although not necessarily a high reactivity towards propagation.

Waack and Doran[147] estimated the relative rates of *initiation* of styrene in THF by a series of organo-Li compounds by comparing the reciprocal of the molecular weights of the polymer formed at complete conversion. This method is obviously inapplicable in our system since side products are formed. Reference to table 6.1 shows that while tert-BuMgBr is the least efficient initiator, the active centres formed are the most reactive. Also, the very low rate of polymerization observed when $(\text{tert-Bu})_2$ Mg is used does not necessarily mean that this initiator is the least reactive towards propagation. The very low f value must be considered. A rather crude method which has been adopted in this work to allow for varying initiation efficiencies when placing the initiators in order of decreasing reactivity towards monomer is the following. From eqn. (4.12), the value of A may be obtained using the experimentally determined values of $\bar{M}_{n\text{exp}}$.

$$\bar{M}_{n\text{exp}} = A \frac{(\text{percentage conversion})}{[I_n]_o} \qquad (4.12)$$

From scheme I, $1/f \sim A/[M]_o$, using eqn. (6.28) and (6.14). When the values of R_{p_o} % in table 6.1 (converted to $[I_n]_o = 0.1$ mol dm^{-3}) are multiplied by $1/f$, the values obtained are the theoretical polymerization rates at 100% initiator efficiency. From the values of $1/f$ and $\{0.1 \times R_p\%\}/[I_n]_o$ in table 6.1, the following conclusions can be drawn:

the initiator efficiencies decrease in the order,

$$(\text{sec-Bu})_2 > \text{iso-BuMgBr} > \text{sec-BuMgBr} > (\text{n-Bu})_2\text{Mg} > \text{n-BuMgBr} > (\text{tert-Bu})_2\text{Mg} > \text{tert-BuMgBr} \quad (6.32)$$

where the position of $(\text{sec-Bu})_2$ Mg is rather doubtful because of the inherent errors in extrapolating values of $^1/_{\phi}$ from one THF concentration to another. The value of $^1/_{\phi}$ will undoubtedly increase on going from low χ_{THF} to high χ_{THF} but the exact magnitude is uncertain. The increase in $^1/_{\phi}$ from χ_{THF} = 0.1 to 0.28 is unlikely to be sufficient to reverse the order of $(\text{sec-Bu})_2\text{Mg}$ and sec-BuMgBr especially since the falue of $^1/_{\phi}$ calculated for sec-BuMgBr at χ_{THF} = 0.28 is the minimum value, since the low MW peak was used.

The interesting facts from eqn. (6.32) are that the initiation efficiencies of the dialkyl-magnesium compounds are larger than those for their corresponding Grignard counterparts. This is in accord with the suggestion in section 3.6(c), that the presence of $MgBr_2$ in the system reduces the proportion of conjugate addition, which is usually associated with initiation of propagating chains.

The rate of polymerization observed using dialkyl-magnesiums is thus greater than the rate observed using an identical initial concentration of R-Mg bonds in the form of $R_2Mg + MgBr_2$.

However, the last column of table 6.1 shows that the reactivities of propagating species formed depends strongly on the initiator used. The propagating species decreases in reactivity throughout the

following series of initiators used.

$$\text{tert-BuMgBr} >> \text{sec-BuMgBr} > (\text{tert-Bu})_2\text{Mg} \geq \text{iso-BuMgBr} \geq \text{n-BuMgBr} > (\text{n-Bu})_2\text{Mg} \qquad (6.33)$$

Here it is impossible to predict with any confidence the likely position of $(\text{sec-Bu})_2\text{Mg}$ because such a prediction would require the extrapolation of both $^1/_{\bar{n}}$ *and* R_p % from $\chi_{THF} = 0.1$ to $\chi_{THF} = 0.28$.

The method is crude because of, the large errors in $\bar{M}_n$, the necessity of having unimodal MWD polymer and the assumption that all of the initiators obey SCHEME I and the necessity of having to extrapolate some results from one THF concentration to another.

In spite of these limitations, the following interesting conclusions may be drawn:
that tert-BuMgBr is the least efficient Grignard reagent used but the propagating species formed from it are the most reactive, and the most stereospecific species of any of the organomagnesium compounds used.

The discussion of relative reactivities of organometallic initiators is in general, more difficult than their estimation. This is true, even in systems where ion-pairs are known to exist, because effects other than the simple correlation between anion reactivity must be considered, e.g. initiation of dienes by 1,1-diphenylhexyl-Li (DPHL) is faster than by the butyl-lithiums despite the fact that the DPHL ion should be less reactive than an alkyl anion.[148] The

reason is because DPHL is unassociated whereas the n-alkyl lithiums are associated. The rate of initiation is strongly dependent on the equilibria governing the various forms of the reagent present in solution.

In the essentially covalent organomagnesium systems, there are still so many unknown factors (effects of exchange rates for example) that could affect the reactivity that a meaningful discussion of (6.31), (6.32) and/or (6.33) cannot be confidently attempted.

The role of the solvent in the addition reactions of organometallic compounds is usually neglected in the proposed mechanisms for the sake of simplicity. Recently, however, the importance of solvent in the alkylation of ketones by Grignard reagents has been discussed and the following detailed scheme was discussed.[96,149]

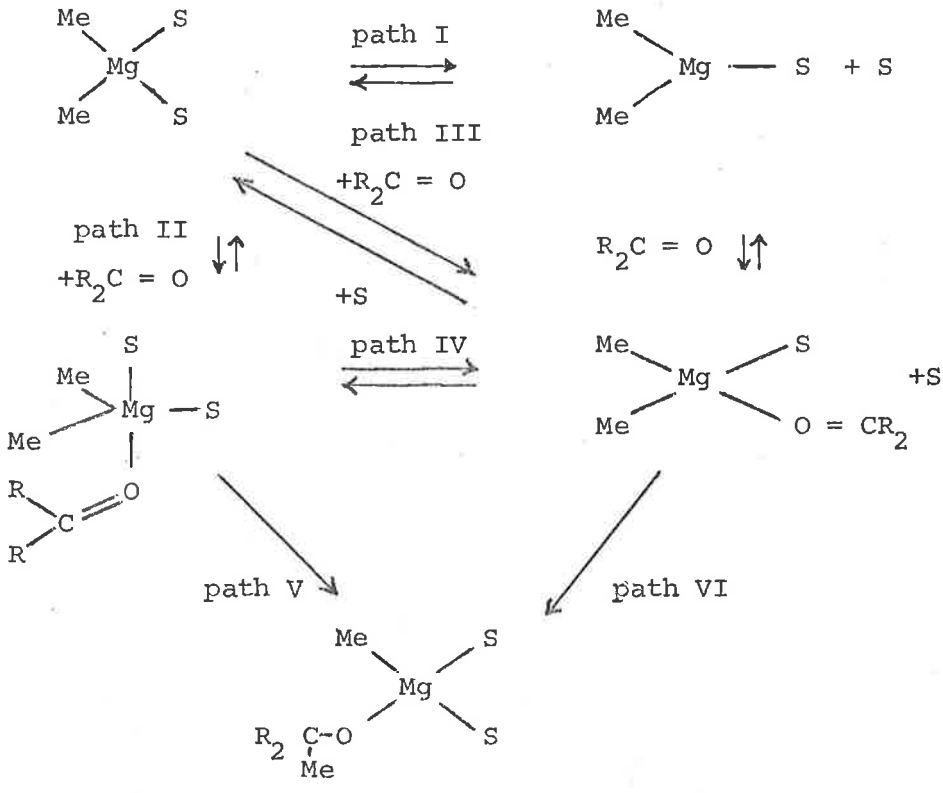

(6.34)

Path II followed by path V has been proposed by one group to explain the acceleration or retardation observed when certain bidentate ligands were added to a diethyl ether solution of $(CH_3)_2Mg$ and it was suggested that only steric bulk properties of the ligand affects the reaction via the penta-coordinate transition state. This conclusion has been argued by Ashby *et al* [149] who prefer the idea that the relative magnitude of the solvent effects on the *complex formation* and *product formation* steps determines the acceleration or retardation of the reaction and that the observed results can also be explained assuming solvent dissociation prior to complexing. The decreasing rate with increasing THF concentration observed in our system suggests that a reaction path which requires dissociation (I) or displacement (III) prior to formation of the complex will be retarded as the donor contrentration increases.

The participation of at least one ether ligand in the transition state involving organomagnesium compounds has been indicated by asymmetric induction involving the reaction between $(CH_3)_2Mg$ and benzaldehyde in the presence of an optically active ether.

6.2 *The stereospecificity aspect*

This aspect of organometallic initiated polymerizations is perhaps the most interesting and certainly the most difficult to explain. No general and uncontestable stereo-regulation theory

has evolved to explain the tacticity of poly (MMA) prepared using different organometallic initiators. The organomagnesium initiators appear to be the stumbling block even though they have been the subject of some very intensive stereochemical control studies. One of the reasons for the difficulty in proposing a stereochemical control theory for polymerizations initiated by organomagnesium compounds is the lack of knowledge concerning not only the structure of the propagating species but also the various exchange and complexing reactions that may occur.

The mechanism proposed by Bovey *et al*[115] (figure 4.2) appears to be consistent with the results observed in the fluorenyl-Li (Fl-Li) initiated polymerization of ethyl cis-β -deuteromethacrylate in toluene and/or THF (section 4.1.3). As mentioned in section 4.1.3, it is not possible to establish whether an acrylate ester double bond is opening cis or trans. However, this can be done with cis and trans-β-deuteroacrylate esters where cis or trans opening will determine the configuration at the β-carbon atoms which is superimposed on the α-carbon stereochemistry .

Cis addition to a cis monomer results in erythro-diisotactic polymer whereas trans addition gives the threo-diisotactic polymer.

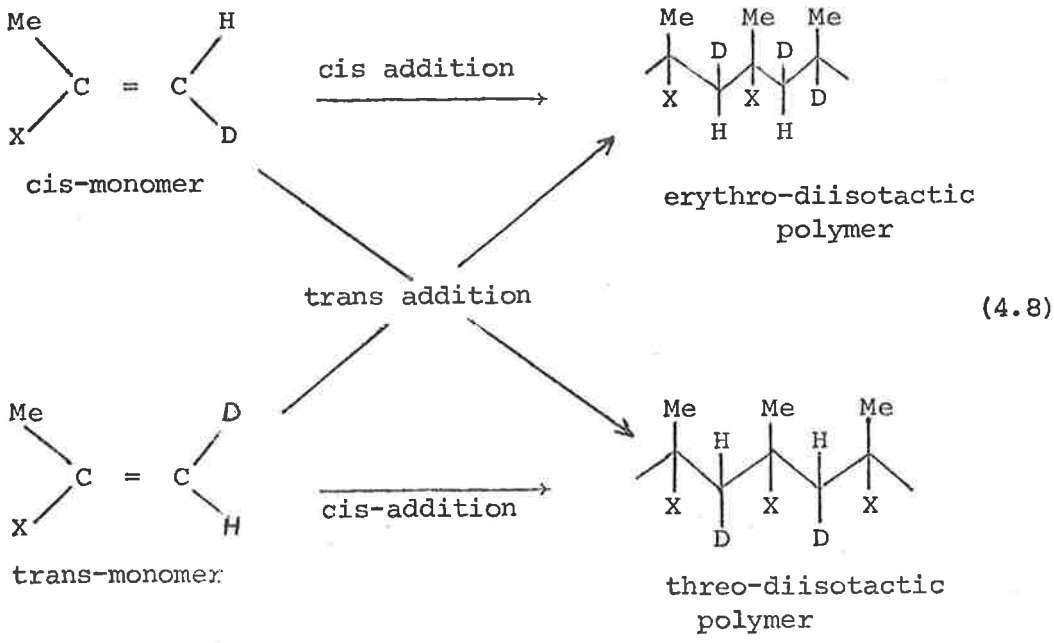

Bovey's mechanism for Fl-Li correctly predicts an increase in erythro-diisotactic polymer (cis-addition) at high ether concentration and threo-polymer (trans-addition) at low ether concentration. Notice that the β-carbon configurations produced in the mixed ether/hydrocarbon solvents and predicted by Bovey with fluorenyl-Li initiator, are *not* consistent with the simple conclusion that both contact ion-pairs and solvated ion-pairs are present (their concentrations depending on the ether concentration), these species interchanging in a Coleman-Fox type mechanism. Were this the case, then from eqn. (4.8) trans addition to the cis monomer should result in threo-diisotactic polymer irrespective of the concentration of ether. This is not the case - in excess ether, the meso protons are erythro and not threo. To account for the apparent

cis addition from trans opening of the double bond, and a third species propagating by *m* placement but with ultimate cis addition was postulated.

When PhMgBr is used as catalyst witn iso-propyl-cis-α-β-dideutero-acrylate, the presence of small amounts of THF give rise to equal proportions of erythro- and threo-diisotactic polymer, but in the presence of excess ether, trans addition (threo-polymer) predominates,[112,113] which is opposite to the fluorenyl-Li case.

Bovey's mechanism assumes a planar chain end so that the tetrahedral configuration is not fixed until the next unit is added. The counter-ion is assumed to hold the chain end in an incipient isotactic configuration and to direct the incoming monomer into an isotactic approach. In the Grignard system, the chain end is unlikely to be planar. Yoshino and Iwanaga[114] have established that polyacrylate chain ends act stereospecifically with terminating agents such as water. This suggests that the chain end is already in a tetrahedral configuration which it conserves in reaction with all types of reagent.

Under the conditions of our experiments, where there was a significant excess of THF under all conditions, the predominant mode of opening of the monomer double bond would be expected to be trans, from comparison with the above results. This prediction could only be proved using a β- deuterated form of MMA.

All of the information obtained in our research concerned the

configuration around the α-carbon atom and unfortunately, the factors determining α- and β- C-atom symmetry appear to operate independently.

The most interesting features of the Grignard initiated polymerization of MMA in THF/toluene mixtures were the following:

(a) None of the polymers obeyed Bernoulli chain configuration statistics and in this sense, all of the propagating centres are stereospecific.

(b) Preliminary measurements of polymer tacticity using 90MHz p.m.r spectroscopy suggest that the poly(MMA) formed from n-BuMgBr at low THF concentrations obeys first order Markov chain statistics. It is uncertain at this stage, whether the highly isotactic polymer prepared using tert-BuMgBr obeys these statistics or not. The almost complete absence of an *mr* triad (figures 4.1 (b) and 4.9(b)) suggests a possible Coleman-Fox 'two-site' model with one site propagating in an isotactic configuration and the other, syndiotactic.

(c) Polymer tacticity is very dependent on the structure of the alkyl group in the Grignard reagent. Branching at the α-carbon atom of the Grignard reagent increases the isotacticity whereas branching at the β- carbon atom of the initiator produces polymers with similar tacticities to those prepared using Grignard reagents with straight chain alkyl groups. The effect of α-carbon branching appears to be only observed

when MgX_2 is present. When MgX_2 is present, the isotacticity decreases in the order; iodide> bromide > chloride. In the absence of MgX_2, the polymers are still non-Bernuollian, but are 'syndiotactic like', even when $(tert\text{-}Bu)_2Mg$ is used. The presence of excess MgX_2 has no effect on polymer tacticity, however, when $MgCl_2$ is added (in the form of t-BuMgCl) to tert-BuMgBr the resultant polymer microstructure is a mixture between that observed for tert-BuMgCl and tert-BuMgBr separately.

(d) Increasing the temperature from 223K to 242K has no effect on the tacticity, however, when the temperature is decreased from 223K to 200K, the effect of α-carbon branching in the Grignard initiator is removed.

(e) The changes in the MW and MWD of polymers appear to be related to changes in the polymer tacticities. As mentioned in section 4.5, the sec-BuMgBr appears to be intermediate between two extremes, viz., the highly isotactic polymer obtained using tert-BuMgBr has a very narrow MWD, is of very highMW and forms very rapidly whereas the 'syndiotactic like' polymer from n-BuMgBr and iso-BuMgBr has a much lower MW, broader MWD and is formed much more slowly. At low THF concentrations the MWD of polymers prepared using sec-BuMgBr are distinctly trimodal. At higher THF mole fractions the MWD becomes bimodal

although the low MW peak is very asymmetric. The general appearance of these MWD's suggest that there are *at least* two different propagating species present in the sec-BuMgBr system - one forming very high MW polymer and the other moderately high MW polymer. The suggestion has already been made in section 4.5 that the very high molecular weight polymer in the sec-BuMgBr system may be similar to the highly isotactic, very high MW polymer that is formed very rapidly in the tert-BuMgBr system. This infers that the lower MW polymer (i.e. $10 < \bar{10}^{3}.\bar{M}_{n} < 100$) is similar to that produced in the n-BuMgBr system.

The explanation of these particular results is very difficult at this stage and it is futile to attempt to postulate any one stereochemical control theory that will account for all the observed results. The difficulty of course arises because of the lack of knowledge of the exact structure of the propagating chain end that produces highly isotactic polymer in the tert-BuMgBr system. Such information will be very difficult to obtain because of the very low concentration of propagation species ($\lesssim 1.6 \times 10^{-4}$ mol dm^{-3}) and the high proportion of non-propagating side products that must be formed in view of the very low δ values for the tert-BuMgBr system. There is also the possibility of complex formation between various side products (in the form of

alkoxides) and the propagating chain end. The theory that the species MeOMgX formed from the reaction (6.35)

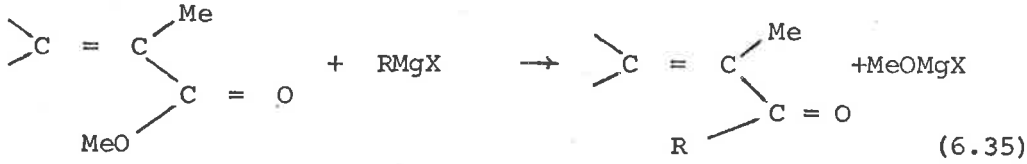

(6.35)

complexes with the propagating chain end has been proposed by Erusalimskii to account for the dependence of polymer tacticity on the initiator R group.[140] He proposed that different R groups produced different amounts of MeOMgX and hence "different relative contents of contra-ion complexes".

The presence of alkoxides such as MeOMgX or MeOMgR may have a pronounced effect on the polymer chain configuration, but Erusalimskii's proposal that the effect is due solely to differing amounts of MeOMgX produced seems grossly over-simplified, especially for our system. The extremely low initiator efficiencies (table 6.1) observed for all systems and the suggestion in section 5.10 (eqn. 5.11) that eqn. (6.35) (with X = R) is the major reaction leading to side products would imply that a significantly larger proportion of MeOMgR than propagating chains would be formed in each system studied. Complexing between MeOMgR and the chain end may explain the effect of the alkyl group on polymer tacticity observed in different Grignard systems, e.g.

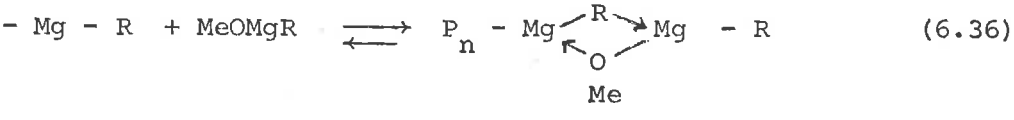

(6.36)

However,, (6.36) does not explain the apparent lack of alkyl group influence on polymer tacticity in the absence of MgX_2 or the effect of different halide groups in any particular Grignard reagent. Even if MeOMgR in (6.36) is replaced by MeOMgX, the bridging group should still be the methoxy group. If this is the case, the proximity of the halide to the chain end would be rather too remote to be expected to cause such a drastic change in polymer tacticity as observed in the tert-BuMgX system when X changes from Br to Cl, section 4.2.1.

A particularly tempting hypothesis to explain the tacticity and MWD results is that there are at least two different propagating species in solution possibly in equilibrium with each other: one species (P_i) propagating very rapidly to high MW, narrow MWD and highly isotactic polymer and the other (P_s) propagating to low MW, relatively broad MWD and 'syndiotactic like' polymer.

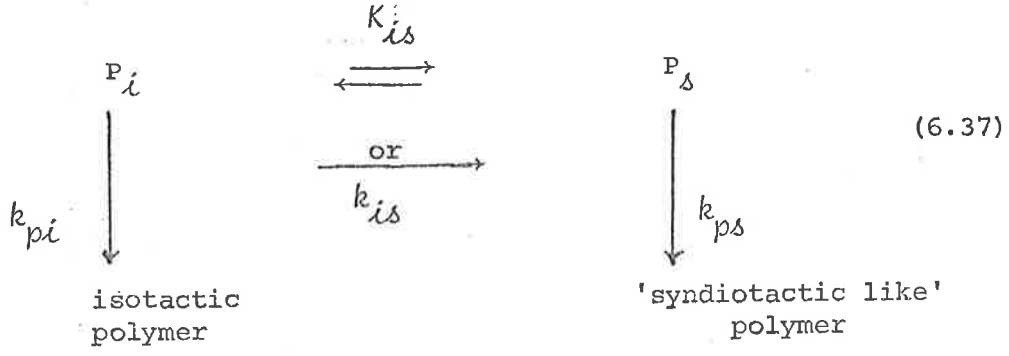

(6.37)

where $k_{pi} > k_{ps}$ and P_i and P_s are related by the equilibrium constant K_{is} or P_i is converted into P_s with a rate constant k_{is}.

If P_i and P_s are in equilibrium, then in order to obtain very narrow MWD isotactic polymer, this equilibrium must be frozen, otherwise a broadening of the MWD towards lower MW's will occur, e.g. see ref. 146. Broadening will also occur if P_i is slowly converted to P_s in a reaction with rate constant k_{is}, and in this case a bimodal distribution should be observed.

Evidence in support of this type of scheme is the intermediate nature exhibited by sec-BuMgBr compared with tert-BuMgBr and n-BuMgBr and the fact that in the tert-BuMgBr system the MWD changes form unimodal at short reaction times (i.e. $\leq$ 2 minutes) to multimodal at longer times (e.g. 10 minutes), figure 4.16.

This hypothesis embodied in eqn. 6.37 predicts that; in the n-BuMgBr, iso-BuMgBr and tert-BuMgCl systems, P_s predominates; in tert-BuMgBr and possibly n-BuMgI(at low χ_{THF}), P_i predominates and in the sec-BuMgBr system both P_i and P_s exist in such proportions as to account for the observed MWD. In the dialkyl magnesium system, either P_s predominates, or (6.37) does not occur, the propagating species in the R_2Mg system having a structure slightly different to P_s to account for the broader MWD of n-Bu_2Mg compared with n-BuMgBr but not different enough to alter the tacticity significantly in the n-BuMg case.

The fact that the reactivities towards propagation of the propagating species formed from the dialkyl magnesium initiators are

intrinsically less reactive than the active species formed from their Grignard counterparts (eqn. (6.33)) suggests a different structure for P_s in the n-BuMgBr system compared with P_s in the n-Bu_2Mg system. The reader should not confuse this statement with the statement in section 3.6(c) that R_2Mg is more reactive than RMgX. In our particular system we have shown that the species R_2Mg is less reactive towards propagation than R_2Mg + MgX_2 (from table 6.1) which is completely different from the reactivity of R_2Mg compared with the species RMgX. For the sake of brevity we have consistently denoted the Grignard system which occurs at low temperatures in THF (viz. R_2Mg + MgX_2) as the RMgX *system* to distinguish it from the dialkyl-magnesium compound in the absence of MgX_2.

The increased syndiotacticity and reduced isotacticity observed when the temperature was reduced from 223K to 200K in the sec-BuMgBr and tert-BuMgBr systems would be consistent with a negative value of ΔH_{is}, however, this does not explain the apparent independence of tacticity and MWD on temperature in the sec-BuMgBr system when the temperature was raised from 223K to 243K. If $\Delta H_{is} < 0$, raising the temperature from 223K to 243K should increase the concentration of P_i significantly at least in the sec-BuMgBr system. This effect was not observed. Of course if only k_{is} is involved then the observed effects on polymer tacticity in the tert-BuMgBr and sec-BuMgBr at low temperatures could be accounted for by aggregation of the chain end

thereby forcing the monomer into syndiotactic approach.

So far nothing has been said concerning the structures of P_i, P_s or P_s' (where P_s' is the structure of the propagating species in the absence of MgX_2).

From the above discussion both the halide and the alkyl group must be closely associated with the propagating chain end in P_i and a possible representation for P_i would be the chain end complexed with MgX_2, similar to eqn. (6.36).

$$P_n - Mg - R + MgX_2 \longrightarrow P_n - Mg\begin{matrix} R \\ X \end{matrix}Mg - X \qquad (6.38)$$

$$I \equiv P_i$$

Structure I is very similar to the intermediate proposed by Ashby to account for the exchange reactions observed in Grignard reagents and the redistribution reaction between R'OMgR and MgX_2 in the reaction of ketones and Grignard reagents, (sections 1.2.3 and 1.3.1).

This immediately suggests that (6.37) can be rewritten in the form

$$P_nMgR + MgX_2 \underset{\text{or}}{\overset{}{\rightleftharpoons}} P_n - Mg\begin{matrix} R \\ X \end{matrix}Mg - X \underset{\text{or}}{\overset{K_{is}}{\rightleftharpoons}} P_n - Mg - X + RMgX \qquad (6.37a)$$

$$\overset{k_{is}}{\longrightarrow}$$

$I \equiv P_i$ $\quad$ P_s

k_{pi} $\quad$ k_{ps}

isotactic polymer $\quad$ syndiotactic polymer

where the species P_i is an active intermediate in the exchange reaction between P_nMgR and MgX_2. Unfortunately, this scheme has several apparent inconsistencies, e.g. the stability of I would be expected to decrease as R becomes branded at the α- C-atom and X changes from chloride to iodide. This implies that when R ≡ n-Bu and X ≡ Br, the polymer should be more isotactic than when R ≡ tert-Bu and X ≡ Br. This is the opposite to what is actually observed. Of course, the relative rates of k_{is} and k_{pi} must be considered in each instance. If $k_{is} > k_{pi}$ when R ≡ n-Bu, but $k_{is} < k_{pi}$ when R≡ tert-Bu, then the polymer should be more isotactic when tert-BuMgBr was used. When X is changed from bromine to chlorine in the tert-BuMgX case, the stability of I with X = Cl would be expected to be greater than when X = Br. However, to explain the observed tacticity, $k_{is} > k_{pi}$ when X = Cl but $k_{is} < k_{pi}$ when X = Br. The difficulty in justifying the above inequalities as well as the greatly enhanced reactivity of P_i compared with P_s, make this mechanism difficult to accept.

Just to reiterate the problem: the greatest difficulty in proposing a stereochemical control theory for our system is the fact that the polymer tacticity is independent of R in the absence of MgX_2, but greatly dependent on R *and* X in the presence of MgX_2.

There is another possible explanation of these results which again assumes two propagating species (P_i' and P_s), possibly inter-converted via (6.37a), but in this case, the isotactic centre is no

longer the mixed bridge intermediate. The isotactic propagating species may be P_nMgR in the presence of MgX_2 which either complexes with monomer to facilitate isotactic propagation, or exchanges with P_n - MgR via (6.37a) to the syndiotactic centre, P_s,

$$K_{is} = k_{is}/k_{-is}$$

$$P_n - MgR + MgX_2 \rightleftharpoons P_n - MgX + RMgX \quad \text{(or } \xrightarrow{k_{is}}\text{)} \qquad (6.37b)$$

P_i', k'_{pi}, $+MMA.MgX_2$ → isotactic polymer

P_s, k_{ps}, $+MMA\ (\text{or } MMA.MgX_2)$ → 'syndiotactic like' polymer

where P'_i is the new isotactic centre consisting of P_nMgR in the presence of MgX_2, which complexes with monomer before addition to the propagating chain.

Now the criterion for isotactic or 'syndiotactic like' polymer is the relative rate of k_{is} compared with k'_{pi}. If the rate of exchange is very rapid, then 'syndiotactic like' polymer should predominate and since the exchange reaction (6.37a) presumably proceeds via the mixed bridge intermediate or transition state I,

$P_n - Mg\begin{matrix}\nearrow R \searrow \\ \nwarrow X \swarrow\end{matrix}Mg - X$, then the factors influencing the stability of I should influence the polymer tacticity.

When exchange is rapid, as is the case when R = straight chain or branched at β-C- atom, then syndiotactic polymer predominates provided that $k_{is} > k'_{pi}$. Changing X from iodide to chloride should favour exchange also because of the increased stability of I. As R becomes branched at the α-C-atom, the exchange rate becomes much slower (e.g. 4 secs. at 315K for $(tert\text{-}Bu)_2Mg$, $MgCl_2$ system) and if $k_{is} < k'_{pi}$, isotactic polymer results. When Cl replaces Br in the tert-BuMgX system, the exchange rate (although still slow at 223K) should be faster than the bromide and if Goode's observations are correct, the $MMA.MgX_2$ complex will be weaker when X = Cl than Br.

Also the kinetics of polymerization with respect to monomer and initiator are not altered when eqn. (6.37b) is included in SCHEME I. An extra dependence of rate on MgX_2 arises if the propagating species is assumed to propagate via a $MMA.MgX_2$ complex rather than uncomplexed monomer. However, the overall order with respect to monomer is unaltered if $K_c[M] >> 1$ where K_c is defined by (6.39).

$$MMA + MgX_2 \overset{K_c}{\rightleftharpoons} MMA.MgX_2 \qquad (6.39)$$

The higher reactivity of P'_i compared with P_s is also easier to explain using the mechanism in eqn. (6.37b) rather than (6.37a). The complexed monomer (eqn. (6.39) where complexing is presumably via a Wittig-at carbonyl complex), would be expected to be more susceptible to vinyl addition than uncomplexed monomer.

Prediction of the effect of temperature on polymer tacticity is very difficult from eqn. (6.37b). If $\Delta H_{is} < 0$, a reduction in temperature should result in an increase in $[P_s]$ and hence an increase in 'syndiotactic like' polymer. However, this does not explain the apparent independence of polymer tacticity on temperature in the range 223K to 253K. The position of other equilibria, such as eqn. (6.39) may compensate the effect of increasing temperature on K_{is}.

In the absence of MgX_2, either P_n-MgR adds monomer to form a 'syndiotactic like' polymer with the resulting tacticity independent of R, which seems rather unlikely because of the proximity of R to the chain end, OR P_n-MgR slowly adds monomer to form a 'double headed' propagating species, P'_s

$$P_n - Mg - R + MMA \longrightarrow \underset{P'_s}{P_n - Mg - P_n} \qquad (6.40)$$

If this is the case in the absence of MgX_2, the influence of the R group on polymer tacticity is removed and the MWD would be predicted to be unimodal but broader than the corresponding Grignard reagents because of the presence of a second propagating chain attached to the magnesium. The monomer order will be preserved if

$$[P_nMg - P_n] = [P_nMgR]_o \qquad (6.41)$$

6.3 *Conclusion*

The polymerization of MMA initiated by organomagnesium compounds in THF/toluene solution is undoubtedly a complex system and the various mechanisms operating can only be resolved by studying not only the kinetics of the polymerization but also the polymer chain configuration and molecular weight distribution.

Throughout this work, we have attempted to investigate as many different aspects of the polymerization as possible in order to gain an overall picture, rather than a minutely detailed account of one specific aspect of any one particular system. This approach has definitely been rewarding since we can now predict with a fair degree of confidence, the effect of alkyl group, halide group and temperature as well as varying THF/toluene mixtures on the resulting polymer tacticity and molecular weight distribution.

Detailed kinetic studies on the n-BuMgBr initiated polymerization of MMA have lead to the proposal of an apparently unique kinetic scheme which is consistent with all of the observed kinetic results of this system. This scheme is similar to the one proposed for the organomagnesium initiated polymerization of acrylonitrile in toluene at 198K but it is certainly the most detailed mechanism yet proposed to account for the observed facts in the polymerization of MMA initiated by organomagnesium compounds.

Perhaps the most disappointing aspect of this research was the

complete lack of detailed kinetic results for the tert-BuMgBr system which produced the most stereoregular polymer of all the initiators used. The difficulties in obtaining rate measurements using conventional techniques for the tert-BuMgBr system have already been discussed and development of a stop-flow reactor may permit meaningful results to be obtained.

Although most of the factors influencing polymer tacticity have been established during this and other work, the mechanism proposed in the previous section to account for the observed chain configuration is only tentative because of lack of fundamental knowledge concerning the exact structure of the propagating chain end.

The ultimate stereoregulation control theory for organomagnesium compounds will have to explain not only the effect of alkyl, halide, temperature and solvent, but also the mode of opening (cis or trans) of the monomer double bond.

More detailed n.m.r studies on the polymers prepared with the different organomagnesium compounds should be carried out. The use of a proton magnetic resonance at $90MH_z$ and carbon 13 magnetic resonance (with Fourier transform techniques) should enable tetrad and pentad sequences to be distinquished, which will allow first and second order Markov models to be tested. ^{13}C studies on the methanol soluble polymer should be able to confirm whether or not this low MW polymer contains cyclicysed end groups and detailed low temperature n.m.r investigations

on THF/toluene solutions of R_2Mg and $R_2Mg + MgX_2$ in the presence of *slightly* excess monomer may provide valuable information on the nature of the propagating species.

It is obvious that there are still a great many unanswered questions about the polymerization of MMA initiated by organomagnesium compounds, and there is scope for a lot more useful further work to be done. However, the assignment of priorities for this future research must be given careful consideration to ensure that the results obtained justify the great amount of effort required to obtain them. It would be pointless duplicating our research on say, the propyl Grignard reagents unless some major differences were apparent.

REFERENCES

1. a Wakefield, B.J., *Organometal. Chem.Rev.*, 1, 131 (1966)

   b Coates, G.E., and Wade, K., *Organometallic Compounds*, Vol.1, Third Edition, Methuen (London) (1967)

2. Ashby, E.C., *Quart. Rev.*, 21, 259 (1967)

3. Ashby, E.C., *Bull. Soc. Chim, de France*, 2133 (1972)

4. Kharasch, M.S., and Reinmuth, O., *Grignard reactions of Non-Metallic Substances*, Prentice Hall, N.Y., (1954)

5. Ashby, E.C., *Organometallic Chem. Rev., B*, 6 (1), 73 (1970)

6. Blomberg, C., *Organometallic Chem. Re., B*, 8 (2), 341 (1971)

7. Crosse, B.C., *Organometallic Chem., Specialist Periodical Report, The Chemical Society*, 1, 17 (1972)

8. Grignard, V., *Compt. rend.*, 130, 1322 (1900)

9. Jolibois, P., *ibid.*, 155, 353 (1912)

10. Schlenk, W. and Schlenk, W. jun., *Ber.*, 62, B, 920 (1929)

11. Ashby, E.C. and Becker, W., *J.Amer.Chem.Soc.*, 85, 118 (1963)

12. Ashby, E.C. and Smith, W.B., *ibid.*, 86, 4363 (1964)

13. Mosher, H.S. and Ashby, E.C., *ibid.*, 86, 1782 (1964)

14. Smith, M.B. and Becker, W.E., *Tetrahedron Lett.*, 43, 3843 (1965)

15. Smith, M.B. and Becker, W.E., *Tetrahedron*, 22, 3027 (1966)

16. Ashby, E.C. and Walker, F., *J. Organometal. Chem.*, 7, 17 (1967)

17. Walker, F. and Ashby, E.C., *J. Amer. Chem. Soc.*, 91, 3845 (1969)

18. Ashby, E.C. Yu,S. and Beach, R., *J. Amer.Chem.Soc.* 92, 433 (1970)

19. Ashby, E.C. and Nackashi, J. *J. Organometal.Chem.*, 24, C, 17 (1970)

20. a. Coates, G.E., Heslop, J.A., Redwood, M.E. and Ridley,D., *J. Chem. Soc.*, A,1118 (1968)

b. Coates, G.E. and Ridley, D., *Chem. Commun.*, 560 (1966)

c. Moseley, P.T. and Shearer, H.M.M., *ibid.*, 279 (1968)

21 Evans, W.V. and Pearson, R., *J. Amer.Chem.Soc.*, 64, 2865 (1942)

22. Zeil, W.,Z. *Elektrochem.*, 56, 789 (1952)

23. Dessy, R.E. and Handler, G.S., *J.Amer.Chem.Soc.*, 80, 5824 (1958)

24. a. Evans, W.V. and others, *ibid.*, 56; b. 654 (1934); c. 58, 720 (1936); d. 61, 878 (1939); e. 62, 534 (1940).

25. Stucky, G.D. and Rundle, R.E., *J. Amer.Chem.Soc.*, 86, 4825 (1964)

26. Stucky, G.D. and Rundle, R.E., *J. Amer.Chem.Soc.*, 85, 1002 (1963)

27. Holm, T., *Acta Chem. Scand.* 20, No. 4, 1139 (1966)

28. Wanklyn, J.A., *Annalen* , 140, 353 (1866)

29. Coates, G.E. and Ridley, D., *J. Chem. Soc., A, Inorg., Phys., Theoret.* p. 56 (1967)

30. Coates, G.E. and Heslop, J.A., *H. Chem.Soc., A. Inorg. Phys., Theoret.*, pg. 26 (1966); b. *idem, ibid,* p. 514 (1968)

31. Parris, G.E. and Ashby, E.C., *J. Amer.Chem. Soc.*,93,5, 1206 (1971)

32. Evans, D.F. and Khan, M.S., *Chem. Commun.* 67 (1966)

33. Evans, D.F. and Khan, M.S., *J. Chem. Soc., A, Inorg. Phys. Theoret.*, 1643 (1967)

34. Whitesides, G.M., Kaplan, F. and Roberts, J.D., *J. Amer. Chem. Soc.*, 85, 2167 (1963)

35. House, H.O., Latham, R.A. and Whitesides, G.M., *J. Org. Chem.*, 32, 2481 (1967)

36. Hughes, E.D. and Volger, H.C., *J. Chem. Soc.*, 2359 (1961)

37. a. Teventjew, A., *Z. anorg. Chem.*, 156, 73 (1926)

b. Slough, W. and Ubbelhode, A.R., *J. Chem. Soc.*, 108 (1955)

38. a. Swain, C.G. and Boyles, H.B., *J. Amer.Chem.Soc.*, 73, 870 (1951)

b. Anteunis, M., *J. Org., Chem.*, 26, 4214 (1961)

39. a. Meisenheimer, J. and Casper, J., *Chem. Ber.*, 54B, 1655 (1921)

b. Smith, S.G. and Su, G., *J. Amer. Chem.Soc.*, 86, 2750 (1969)
idem, ibid, 88, 3995 (1966)

c. Ashby, E.C., Laemmle, J. and Neumann, H.M., *ibid.*, 93, 4601, (1971)

d. *idem. ibid.*, 93, 5120 (1971)

e. *idem, ibid.*, 94, 5421 (1972)

40. a. Holm, T., *Acta Chem. Scand.*, 20, (10), 2821 (1966)

b. *idem, ibid.*, 19 No. 8, 1819 (1965)

c. *idem. ibid.*, 23, 579, (1969)

41. a. Ashby, E.C., Neumann, H.M., Walker, F.W., Laemmle, J. and Chao, L.-C., *J. Amer. Chem. Soc.*, 95, 2597 (1973)

b. Ashby, E.C., Chao, L. -C., and Neumann, H.M. *ibid.*, 95, 4896 (1973)

42. Allén, P.E.M., Casey, B.A. and Dankiw, W.I., *J. Macromal Sci. Chem.* A4, 1091 (1970)

43. Gilman, H. and Kirby, R.H., *J. Amer. Chem. Soc.*, 63, 2046 (1941)

44. Sullivan, W.I., Swamer, F.W., Humphett, W.J. and Hauser, C.R., *J. Org. Chem.*, 26, 2306 (1961)

45. Lutz, R.E. and Revely, W.G., *J. Amer. Chem. Soc.*, 63, 3180 (1941)

46. a. House, H.O., Traficante, D.D. and Evans, R.A., *J. Org. Chem.*, 28, 348 (1963)

b. House, H.O. and Thompson, H.W., *ibid.*, 360.

47. Jacobsen, S., Jart, A., Larsen, T.K., Anderson, I.G.K., and Munch-Petersen, J., *Acta Chem.Scand.*, 17, 2423 (1963)

48. Eicher, J., *The Chemistry of the Carbonyl Group*, (edited by S. Patai), Interscience, London, p.621 (1966)

49. a. Ashby, E.C., Walker, F.W. and Neumann, H.M., *Chem. Commun.*, 330, (1970)

b. Rudolph, S.E. and Smith, S.C., *ibid.*, 1428

50. a. Beaman, R.G., *J. Amer. Chem. Soc.*, 70, 3115 (1948)

b. Landler, I., *Rec. Trav. Chim.*, 68, 992 (1949)

51. Erusalimskii, B.L., Krasnosel'skaya, I.G. and Kulerskaya, I.V., *Russian Chemical Reviews*, 37 (11), 874 (1968)

52. a. Goode, W.E., Owens, F.H. and Myers, W.L., *J. Polymer Sci.*, 47, 75 (1960)

b. Owens, F.H., Myers, W.L. and Zimmerman, F.E., *J. Org. Chem.*, 26, 2288 (1961)

c. Goode, W.E., Owens, F.H., Fellmann, R.P., Synder, W.H. and Moore, J.E. *J. Polymer Sci.*, 46, 317 (1960)

53. Yasirda, Y., Kawabata, N. and Tsuruta, T., *J. Macromol. Sci-Chem.*, A1 (4), 669 (1967), & *J. Polymer Sci. A 1*, 6(5), 1209 (1968)

54. a. Allen, P.E.M. and Moody, A.G., *Makromol.Chem*, 81, 234 (1965)

b. *idem, ibid.* 83, 220 (1965)

55. a. Watanabe, H., *J. Chem.Soc. Japan*, 82, 362 (1961)

b. Nishioka, A. Watanabe, H., Abe, K., and Sono, I., *J. Polymer Sci.*, 48, 241 (1960)

c. Watanabe, H., *J. Chem. Soc.Japan, Ind.Chem. Sect.*, 65, 1104 (1962)

d. Watanabe, H. and Nishioka, A., *ibid.*, 65, 976 (1962)

56. Rempp, P., Volkov, V.I., Parro, Zh, and Sandron, SH. *Polymer Sci. U.S.S.R.*, 3, 398 (1962)

57. Higgison, W.C.E. and Wooding, N.S., *J.Chem. Soc.*, 760 (1952)

58. a. Scheurch, C., Fowells, W., Yamada, A., Bovey, F., Hood, F. and Anderson, E. *J.Amer.Chem.Soc.*, 86, 4481 (1964)

b. *idem* , *ibid.*, 89, 1396 (1967)

59. a. Yoshino, T. and Juno, K., *ibid.*, 87, 4404 (1965)

b. Yoshino, T. and Kominyama, J. *ibid.*, 88, 176 (1966)

c. Yoshino, T., Kominyama, J. And Iwanaga, H., *ibid.*, 89, 6925 (1967)

d. Yoshino, T., Komiyama, J. and Kenjo, H., *J.Polymer Sci.*, B4, 991 (1966)

60. Graham, R.K., Dunkelburger, D.L. and Goode, W.E., *J. Amer. Chem. Soc.*, 82, 400 (1960)

61. Dawans, F. and Smets, Gr., *Makromol. Chem.*, 59, 163 (1963)

62. Kulevskaya, I.V., Erusalimskii, B.L. and Mazurek, V.V., *Vysokomol. Soed.*, 8, 876 (1966)

63. Eurasalimskii, B.L., *Plaste and Kantschuk*, 11, 15 (1968)

64. a. Erusalimskii, B.L., Kulevskaya, I.V. and Mazurek, V.V. *International Sympsoium on Macromolecular Chem.*, Prague, 1965, Preprint 126.

b. idem, *J. Polymer Sci.*, C16, 1355 (1967)

65. a. Secre, A., Ciampelli, F. and Dall'Astra, G., *J. Polymer Sci.*, 4B, 633 (1966)

b. Kotake, Y., Yoshikara, T., Sato, H., Yamada, N. and Joh, H., *ibid.*, 5B, 163 (1967)

c. Suzuki, T., Koshiro, S. and Takagami, Y., *Polymer* , 14 (11) 549 (1973)

66. a. Natta, G., Mazzanti, G., Longi, P., Dall'Astra, G. and Bernardini, F., *J. Polymer Sci.*, 51, 487 (1961)

b. idem, *Makromol. Chem.*, 37, 160 (1960)

c. Geuskens, G., Lubikulu, J. and David, C., *Polymer* 7, 63 (1966)

d. Matzuzaki, K. and Sugimoto, T., *J. Polymer Sci.*, 5,A2, 1320 (1967)

67. a. Guyot, A. and Pham Quang Tho, *Compt. rend.*, 256, 165 (1963)

b. *ibid.*, 266, 1139 (1968)

c. *J. Polymer Sci.*, 1, C4, 299 (1964)

68. a. Furukawa, I., Saegusa, T. and Fujij, H., *Makromol. Chem.*, 44-46, 398 (1960)

b. Sobue, H. and Kubota, H., *J. Polymer Sci.* 1C, 147 (1963)

68. c. Vogl, O., *ibid.*, 2A, 4607 (1964)

69. Tsuruta, T, Fujio, R. and Furukawa, J., *Makromol Chem.*, 80, 172 (1964)

70. a. Wang Fo-sung, Dolgoplosk, B.A. and Erusalimskii, B.L., *Vysokomol. Soed.*, 2, 541 (1960)

b. idem., *J. Polymer Sci.*, 53, 27 (1961)

71. a. Cray, R., *J. Polymer Sci.*, 44, 264 (1960)

b. Inasaki, K., Fukutani, H., Tsuchida, Y. and Nakano, S., *ibid.*, A1, 2371 (1963)

72. Szwarc, M., *Carbanions, Living Polymers and Electron Transfer Processes*, Interscience, New York, p. 648 (1968)

73. There are many papers describing this preparation and only some of them will be listed here.

a. Cope, A.C., *J. Amer. Chem. Soc.*, 57, 2238 (1935),

b. Wotiz, J.H., Hollingsworth, C.A. and Dessy, R.E., *ibid.*, 78, 1221 (1956)

74. Coates, G.E. and Wade, K. *Organometallic Compounds*, vol 1, Third Edition, Methuen, London, p. 98 (1967)

75. Ashby, E.C. and Arnott, R.C., *J. Organomet. Chem.*, 14, 1 (1968)

76. Vogel, A.I., *Quantitative Inorganic Analysis*, (2nd edition) Longmans, London (1960) p. 259

77. Jones, R., *J. Organomet. Chem.* 18, (1), 15 (1969)

78. Gorog, S., Szepesi, G., *Analyst London* , 95, 727 (1970)

79. a. Barniko, W.K.R. and Schultz, G.V., *Z. physik. Chem.*, (Frankfurt), 47, 89 (1965)

b. Hostalka, H., Figini, R.V. and Schultz, G.V., *ibid*, 45, 286 (1965)

c. Bohm, L.L., Chmelir, M., Loohr, G., Schmitt, B.J. and Schultz, G.V. *Fortschritte; Hockpolymeren - Forsch* 9,1 (1972)

d. Bhattacharyya, D.N., Lee, C.L. Smid, J. and Szwarc, M., *Polymer*, 5, 54 (1964); *J. Phys. Chem.* 69, 612 (1965)

80. East, G.C., Margerison, D. and Pulat, E., *J. Faraday Soc.*, 62, 1296 (1966)

81. Naim, M.A., *Ph. D. Thesis* , Adelaide (1966)

82. Allen, P.E.M., Chaplin, R.P. and Jordan, D.O., *European Polymer J.*, 2, 271 (1972)

83. a. Wiles, D.M. and Bywater, S., *Polymer* 3, 175 (1962)

b. idem., *J. Phys.Chem.*, 68, 1983 (1964)

c. idem., *Trans-Faraday Soc.*, 61, 150 (1965)

84. a. Kawabata, N. and Tsuruta, T., *Makromol. Chem.*, 86, 231 (1965)

b. idem., *ibid.*, 98, 262 (1966)

85. Glusker, D.L., Lysloff, I. and Stiles, E., *J. Polymer Sci.* 49, 315 (1961)

86. a. Roig, A., Figueruelo, J.E. and Llano, E., *ibid.*, B, 3, 171 (1965)

86. b. idem., *ibid.*, C, 16, 4141 (1968)

87. Matheson, M.S., Aver, E.E., Bevilacqua, E.G. and Hart, E.J. *J. Amer. Chem. Soc.*, 71, 497 (1949)

88. Moody, A.G., *Ph. D. Thesis*, Birmingham (1963)

89. Chaplin, R.P., *Ph. D. Thesis*, Adelaide, (1970)

90. Brooks, C.J., Betteley, I.G. and Loxston, S.M., *Mathematics and Statistics for Chemists*, Wiley, New York, (1966) p. 354

91. Wiles, D.M. and Bywater, S., *J. Polymer Sci.*, C, 2, 1175 (1964)

92. Busfield, W.K. and Methuen, J.M., *Polymer*, 14, 137 (1973)

93. a. Kulevskaya, I.V. and Erusalimski, B.L., *Vysokomol, Soedin*, 876 (1966), b.*ibid.*, A9, 107 (1967)

94. Levresse, B., Franta, E. and Rempp, P., *Die Makromol. Chem.*, 142, 111 (1971)

95. Ebel, H.F. and Wagner, B.D., *Chem. Ber.*, 104, 320 (1971)

96. House, H.O. and Oliver, J.E., *J. Org. Chem.*, 33 (3) 929 (1968)

97. a. Tomoi, M. and Kakiuchi, H., *Kogyo Kagaku Zasshi* [*J. Chem. Soc. Soc. Japan, Ind. Chem. Sect.*] 73, 2367 (1970)

b. idem., *Polymer J.*, 5 (2), 195 (1973)

98. Hogen-Esch, T.E. and Smid, J., *J. Amer. Chem. Soc.*, 88, 307 (1966), *b*, 87, 669 (1965)

99. Worsfold, D.J. and Bywater, S., *Can. J. Chem.*, 38, 1891 (1960)

100. Szwarc., M., *Carbanions, Living Polymers and Electron Transfer Processes*, Interscience, New York, Ch. 8, p. 509 (1968)

101. a. Billet, J. and Smith, S.G., *J. Amer. Chem. Soc.*, 90, 4108 (1968)

b. *Tetrehedron Lett.*, 4467 (1969)

c. House, H.O. and Traficante, D.D., *J. Org. Chem.*, 28, 355 (1963)

d. Holm, T., *Acta Chem. Scand.*, 21, 2753 (1967)

e. idem, *Tetrahedron Lett.*, 3329 (1966)

102. Jabobsen, S., Bitsch, and Munch-Petersen, J., *Acta Chem. Scand.*, 17 (1), 825 (1963)

103. Carter, H.V., McClelland, B.J., and Warhurst, E., *Trans. Faraday. Soc.*, 56, 455 (1960)

104. Streitweisser Jr, A. and Brauman, J.I., *J. Amer. Chem. Soc.*, 85, 2633 (1963)

105. a. Natta, G., *J. Polymer Sci.*, 16, 143 (1955)

b. Natta, G., Pino, P. Corradini, P., Danusso, F., Mantica, E., Mazzanti, G. and Moraglio, G., *J. Amer. Chem. Soc.*, 77, 1708 (1955).

106. a. Bovey, T.A. and Tiers, G.V.D., *J. Polymer Sci.*, 44, 173 (1960)

b. Bovey, F.A., *Advan. Polymer Sci.*, e, 149 (1963)

c. idem., *Pure. Appl. Chem.*, 12, 525 (1966)

107. Peat, I.R. and Reynolds, W.F., *Tetrahedron Lett.*, 14, 1359 (1972)

108. a. Bovey, F.A. *Polymer Conformation and Configuration*, Academic, New York (1969)

b. *High resolution NMR of Macromolecular*, Academic, New York (1971)

109. Goodman, M., *Topics in Stereochemistry*, 2, 73 (1967)

110. Coleman, B.D. and Fox, T.G., *J. Chem. Phys.*, 38, 1065 (1963) *J. Polymer Sci.*, A, 1, 3183 (1963)

111. a. Frisch, H.L., Mallows, C.L. and Bovey, F.A., *J. Chem. Phys.* 45, 1565 (1966)

b. *Macromol.*, 1, 533 (1968)

112. Schuerch, C., Fowells, W., Yamada, A., Bovey, F.A. and Hood, F.P., *J. Amer. Chem. Soc.*, 86, 4481 (1964)

113. Yoshino, T. and Komiyama, J. a. *J. Amer. Chem. Soc.*, 88, 176 (1966) b. *J. Polymer Sci.*, B, 4, 991 (1966)

114. Yoshino, T. and Iwanaga, H., *J. Amer. Chem. Soc.* 90, 2434 (1968)

115. Fowells, W., Schverch, C., Bovey, F.A., and Hood, F.P., *J. Amer. Chem. Soc.*, 89, 1396 (1967)

116. Billmeyer, Jr, F.W., *Textbook of Polymer Sci.* Interscience, New York. Ch. 3, P. 53 (1962)

117. Moore, J.C., *J. Polymer Sci.*, A, 2, 835 (1964)

118. a. Altgelt, K.H. *Advances in Chromatography*, edited by Giddings, J.C. and Keller, R.A., Dekker, New York. 7 (1968)

b. Determan, H., *Gel Chromatography*, Springer-Verlag, New York (1968)

c. Pecsok, R.L. and Saunders, D., *Separation Sci.*, 1 (5), 613 (1966)

119. Ackers, G.K., *Biochemistry*, 3 (5), 723 (1964)

120. Laurent, T.C. and Killander, J., *J. Chromatography*, 14, 317 (1964)

121. De Vries, A.J., Le Page, M., Beau, R. and Guillemin, C.L. *Anal. Chem.*, 39, 935 (1967)

122. a. Osterhoudt, H.W. and Ray, L.N. Jr., *J. Polymer Sci.*, A (2) 5, 569 (1967)

b. Prusinowski, L.R., *Polym. Lett.* 5, 1153 (1967)

123. Maley, L.E., *J. Polymer Sci.*, C, 8, 253 (1965)

124. Grubisic, Z., Rempp, P. and Benoit, H. *J. Polymer Sci.*, B, 5, 753 (1967)

125. a. Weiss, A.L. and Cohn-Ginsberg, E., *Polym. Lett.* 7, 379 (1969)

b. Coll, H. and Gilding, D.K., *J. Polymer Sci.*, A (2), 8, 89 (1970)

126. a. Dawkins, J.V., *J. Macromol. Sci., Phys.*, B. 2 (4), 623 (1968)

b. Dawkins, J.V., Denger, R. and Maddock, J.W., *Polymer*, 10, 154 (1969)

127. *Polymer Handbook*, Interscience, New York, p. IV. 48 (1966)

128. a. Tung, L.H., *J. Appl. Polymer Sci.*, 10, 375 (1966)

b. Smith, W.N., *ibid.*, 11, 639 (1967)

c. Hess, M. and Kratz, R.F., *J. Polymer Sci.*, A (2), 4, 731 (1966)

d. Duerksen, J.H. and Hamielec, *J. Polymer Sci.*, C, 21, 83 (1968)

129. Herdan, G., *Small Particle Statistics*, Butterworths, p. 95 (1960)

130. Glusker, D.L., Lysloff, I. and Stiles, E., *J. Polymer Sci.*, 49, 315 (1961)

131. Kawabata, N. and Tsurata, T., *Makromol. Chem.*, 86, 231 (1965)

132. Biddulph, R. and Plesch, P.H., *Chem. and Ind.* 1482 (1959)

133. Bawn, C.E.H., Fitzsimmons, C., Ledwith, A., Penfold, J., Sherrington, D.C. and Weightman, J.A., *Polymer*, 12, 119 (1971)

134. Glusker, D.L., Galluccio, R.A., and Evans, R.A., *J. Amer. Chem. Soc.*, 86, 187 (1964)

135. Wiles, D.M. and Bywater, S., *Polymer*, 3, 175 (1962)

136. Dietz, W.A. *J. Gas Chromatography*, 68, 5 (1967)

137. a. Bywater, S., *Trans. Faraday Soc.*, 51, 1267 (1955)

b. Ivin, K.J., *ibid.*, 1273

c. Ekegren, S., Ohrn, O., Granath, K. and Kinell, P.O., *Acta Chem. Scand.* 4, 126, (1950)

138. Allen, P.E.M. and Casey, B.A., *European Polymer, J.*, 6, 793 (1970

139. a. Oliver, J.P., Smart, J.B. and Emerson, M.T., *J. Amer. Chem. Soc.* 88, 4101 (1966)

b. Glaze, W.H. and Jones, P.C. *Chem. Commun.*, 1434 (1969)

140. Erusalimskii, B.L., *Vysokomol. Soedin.*, A 13 (6) 1293 (1971)

141. *ibid.*, B 12, 327 (1970)

142. Rudolph, S.E., Charbonneau, L.F. and Smith, S.G., *J. Amer. Chem. Soc.*, 95, 7083 (1973)

143. Roig, A., Figueruelo, J.E. and Llano, E., *International Macromolecular Symposium, Prague, Preprint*, 548 (1965)

144. Dankiw, W., *Ph. D. results*, Adelaide (1974)

145. Kondratev, B.H., *Kinetics of Chemical Gas Reactions*, ch.10 537 (1958) (Russ.)

146. a. Szwarc, M. and Hermans, J., *J. Polymer Sci.*, B2, 815 (1964)

b. Figini, R.V., *Makromol. Chem.*, 43, 1 (1961)

147. Waack, R. and Doran, M.A. *J. Organic Chem.*, 32, 3395 (1967)

148. a. Tsuruta, T. and O'Driscoll, K.F. (Editors), *Structure and Mechanisms in Vinyl Polymerization*, Dekker, New York, Smid, J. p. 345 (1969)

b. Szwarc, M., *Carbanions, Living Polymers and Electron Transfer Processes*, Interscience, New York, ch. 8 p. 476 (1968)

149. Ashby, E.C., Yu, S.H. and Roling, P.V., *J. Org. Chem.*, 37, 1918 (1972).

APPENDIX

Papers published by candidate but not related to this research.

Journal of Organometallic Chemistry
Elsevier Sequoia S.A., Lausanne
Printed in The Netherlands

REACTIONS AND COMPLEX FORMATION BETWEEN TRIETHYLALUMINIUM AND METHYL METHACRYLATE

P. E. M. ALLEN, B. O. BATEUP AND B. A. CASEY*

Department of Physical and Inorganic Chemistry, University of Adelaide, Box 498D, G.P.O., Adelaide, South Australia 5001 (Australia)

(Received December 15th, 1970)

SUMMARY

The reaction of triethylaluminium and methyl methacrylate (MMA) was followed at room temperature in sealed NMR tubes. Hydrolysed reaction products were also analysed. Ethylation of MMA occurs only when MMA/Al < 1.0. At higher ratios a strong, unreactive 1/1 complex prevails. Evidence presented suggests that a second 1/2 complex is responsible for the reactions at lower ratios. The normal reaction is carbonyl addition: twofold carbonyl adducts of the type: CH_2=CMeC-Et_2OAl<, forming rapidly. Subsequent changes appear to involve only slow exchange or association of these ethylaluminium alkoxides. Reduction of the carbonyl group occurs to a minor and irreproducible extent. There is no evidence for 1/4 attack on MMA.

INTRODUCTION

In common with other alkyl compounds of the more electropositive metals of Groups I–III, triethylaluminium initiates polymerization of acrylate esters[1,2]. However there are essential differences, in that it does so only by photoinitiation[1] and the mechanism is a free radical one[2]. Nucleophilic attack on acrylate esters does occur[2,3] but only the products of stoichiometric addition reactions are formed: anionic polymerization chains do not develop. In conjunction with our characterization of the kinetics and mechanism of the polymerization we investigated the mechanism of the stoichiometric addition reactions and report our findings below.

EXPERIMENTAL

Triethylaluminium (Ethyl Corporation) was drawn into a high-vacuum line under dried, oxygen-free nitrogen (which had been bubbled through an Et_3Al solution). The line was evacuated, receiving vessels flamed at ca. 10^{-3} Nm^{-2} to desorb water from the walls and the reagent distilled (at $\leqslant 371°K$). The first 70% was collected and dispensed under high-vacuum into baked glass break-seal capsules. Tests showed

* Central Research Laboratories, I.C.I.A.N.Z., Ascot Vale, Victoria.

a hydride content $<1\%$ (by analysis of gases evolved on hydrolysis) and no ethoxide detectable by NMR. Methyl methacrylate ("Tensol cement No. 3"-ICI) was de-inhibited by alkaline washes, washed till alkali free, dried and fractionally distilled. After further drying with calcium hydride the reagent was distilled (from CaH_2) on a high-vacuum line into baked, break-seal capsules. Solvents were similarly treated. Reference samples for gas-chromatography and mass-spectrometry were procured as follows: 2-methylpentenal by the oxidation of 2-hexanol with lead tetraacetate[4]; 2-methyl-2-propen-1-ol from Fluka; 3-ethyl-2-methyl-1-penten-2-ol by reaction of ethyllithium and MMA, and methyl 2-methylpentanoate by methylation of "α-methyl-valeric acid" (K&K Laboratories).

Reactions were carried out in sealed vessels or NMR tubes, filled on a high-vacuum line in a tap-free system. Break-seal capsules were sealed to the reaction tube. After baking-out under high-vacuum, the seals were broken and the reagents run in. Once it was certain that pressure was not rising, the tube was sealed off and removed from the line.

NMR spectra were run at 60 MHz on a Varian HA-60-IL at ambient temperature using benzene as an internal lock. The amount of benzene in each tube was standardized within a series because of solvent shifts on the MMA spectrum. Reagent ratios within a tube were estimated from the ratio of the integrated OCH_3 or α-CH_3 regions of MMA to one-third of the integrated organometallic CH_3 region. Shifts are reported as δ values relative to tetramethylsilane at $\delta = 0.00$ ppm.

Hydrolysed reaction products were analysed on a Perkin–Elmer 800 Gas Chromatograph using 5-foot columns packed with 5% Ucon Oil LB550X on Chromosorb W at 80° and a Perkin–Elmer–Hitachi RMU6-D mass spectrometer. Products were isolated, where possible, using an Aerograph A 700 Preparative Gas Chromatograph using a 10-foot 20% LB550X column at 120°.

RESULTS AND DISCUSSION

(a). *Dependence of mechanism on stoichiometry*

The salient feature of the reactions between triethylaluminium and methyl methacrylate (MMA) is the sharp change in mechanism that occurs at the stoichiometry MMA/Al = 1.0. We have reported on some aspects of this change of mechanism in previous papers[1–3].

When MMA/Al > 1.0, a yellow 1/1 complex (I) is formed. Under ambient illumination (or near-UV) this complex is responsible for a photoinitiated polymerization of MMA, which has been shown to be a free radical mechanism[2]. In the dark (or when illuminated by a red photographic safe-light) the complex is quite stable. On hydrolysis, MMA is regenerated and the volume of ethane evolved is equivalent to the number of Et–Al groups originally present. With the exception of occasional traces attributable to local triethylaluminium excesses during mixing, no products of nucleophilic attack on MMA were found, either in the dark or as concomitants of the photopolymerization.

The stoichiometry and strength of the complex (I) are demonstrated by Fig. 1 which shows the change of the internal chemical shift of the 60 MHz proton magnetic resonances of the Et–Al group as MMA/Al increases. NMR spectra of the vinyl region showed only a slight change (downfield) in the chemical shift of the vinyl protons of

MMA on the formation of the complex. The absence of strong changes suggests that it is essentially a carbonyl complex of the Wittig "-ate" type.

When MMA/Al < 1 several addition products could be isolated and up to 20% of the Et–Al groups were not recovered as ethane when reaction mixtures were hydrolysed after 5–10 min in the dark. The yellow colour faded as the reaction proceeded. At ratios close to MMA/Al = 0.5 a sudden intensification of the colour to red was sometimes observed some minutes after mixing. The red "flash" was accompanied by sudden evolution of heat, acceleration of the reaction and the mixtures rapidly became colourless. When MMA/Al ≤ 0.5 the reaction was much faster than in the 0.5–1.0 range.

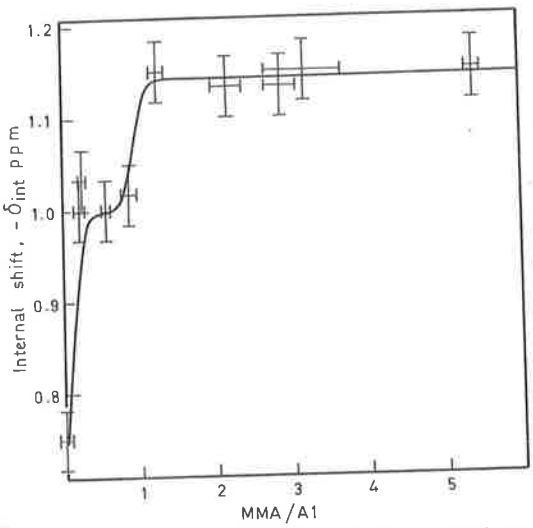

Fig. 1. Internal chemical shift of the aluminium ethyl protons: $\delta_{int} = \delta(CH_3) - \delta(CH_2)$ ppm as a function of MMA/Al ratio. The two points where MMA/Al < 0.5 refer to products, but all other points were taken when the MMA vinyl resonances were still present and the ethyl resonances retained the structure of EtAl.

Similar changes in mechanism at 1/1 stoichiometry have been observed in the reactions of trialkylaluminiums with the ketones[5,6], though in these cases the change is less drastic and alkylation of the carbonyl compound does proceed, though at a reduced rate, when $R_2CO/Al > 1$.

Fig. 1 appears to show the presence of a second complex (II): an aluminium-rich complex, presumably with the stoichiometry MMA/Al = 0.5, though this is by no means well defined. However this is a reacting system. When MMA/Al < 0.5 the reaction is fast and the points obtained in this range are those of a product not a complex. The methyl and methylene resonances have been transformed and the vinyl resonances of MMA extinguished [see (*c*)]. In the range 0.5 < MMA/Al < 1.0, it was possible to measure the internal chemical shift while the methyl and methylene still showed the characteristic triplet-quartet pattern of Et_3Al and the MMA vinyls persisted (Fig. 2). Fig. 1 shows a slight deviation from what might be expected if the shifts over this range were governed by equilibrium between triethylaluminium and

complex (I) only. The deviation could also be due to participation of a product in the ethyl exchange equilibria (note the small, but developing product vinyl peak in Fig. 2) and so is not in itself very convincing evidence for the existence of complex (II). The hypothesis is however supported by the shifts observed in the methoxyl resonances, which suggest that MMA is complexed in a different manner when $1.0 > MMA/Al > 0.5$ than when $MMA/Al > 1.0$. When $MMA/Al > 1.0$, only one methoxy resonance is observed and this in the same position of that in free, uncomplexed MMA. This is true even when MMA is only slightly in excess and the bulk of it must be in complex (I): *e.g.* at $MMA/Al = 1.3$ the methoxyl resonance was at 3.42 ppm, still within experimental error of that of free MMA (note: the methoxyl and vinyl resonances are subject to a benzene solvent shift[7,8] and values quoted are for equivalent benzene concentration). Clearly the chemical shift in complex (I) is very similar to

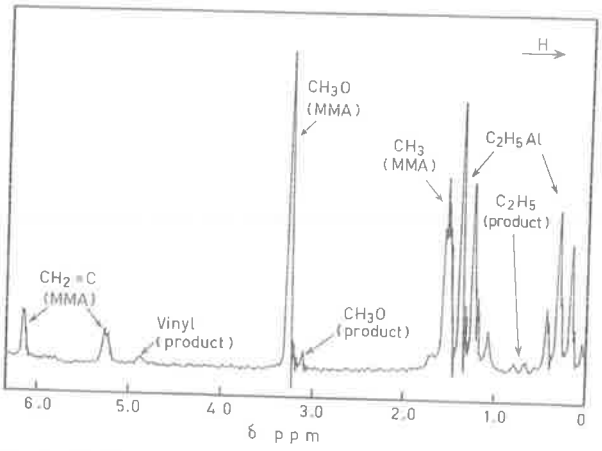

Fig. 2. 60 MHz NMR spectrum of a mixture of triethylaluminium and MMA ($MMA/Al = 0.9$) some 20 min after mixing, showing the MMA vinyl peaks still intact and the triplet-quartet pattern of EtAl. A product vinyl peak is appearing at 4.85 ppm and a product methoxyl peak at ca. 3.08 ppm.

that in pure MMA. Between $1.0 > MMA/Al > 0.5$ the methoxyl resonance shifts upfield; *e.g.* to 3.25 ppm at $MMA/Al = 0.9$ (Fig. 2), which strongly suggests that a complex other than (I) is present. The precise structural reasons for the upfield shift and why it occurs with excess Et_3Al are uncertain. A complex where a second Et_3Al is coordinated to the methoxyl oxygen of MMA is structurally plausible but should lead to a downfield shift (*cf.* the 0.39 ppm downfield shift of ethyl resonances of diethyl ether in the complex $Et_2O \cdot AlEt_3$[9]). The upfield shift is most probably due to the loss of the anisotropic deshielding effect of the π-electrons on the carbonyl. Such a loss cannot be due to ethylation of this group (Fig. 2 shows that at this stage of reaction 90% of ethyl groups were still attached to aluminium), but it could be due to participation of the π-system in coordination to a second Et_3Al. If this were the case complex (I) (where the methoxyls are shielded to the same extent as in free MMA) and complex (II) might be written as:

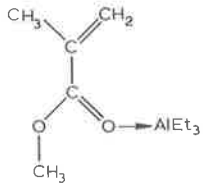

(I)

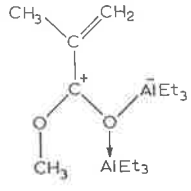

(II)

Complex (II) must be the precursor of the nucleophilic addition products. The absence of such reactions when MMA is in excess is due to the strength of the unreactive complex (I) which at these ratios ties up all available Et_3Al.

(*b*). *Analysis of hydrolysed reaction mixtures* ($MMA/Al < 1.0$)

The reaction mixtures were hydrolysed with water and the oil and water phases separated. The aqueous phase was tested for methanol. Its presence was confirmed by the iodoform test showing that methoxyaluminium species were present in the unhydrolysed reaction products.

The non-aqueous phase on gas chromatographic analysis showed five regular products and one present on a single occasion only. The peaks were isolated on a preparative column. The products are listed in order of retention volume:

(*III*). $CH_3CH_2CH_2CH(CH_3)CHO$. This could not be isolated because it overlapped the unreacted MMA peaks. It was observed as a trace on the analytical chromatograph in only one reaction mixture. Its identification rests on an identical retention volume to a test sample of 2-methyl pentanal. The reduction of esters to aldehydes by trialkylaluminiums has been reported[10]. It would seem probable that this aldehyde arose from the addition of a second molecule of reagent to the product of an initial reduction, though there is no conclusive evidence that the order of these two reactions was not reversed.

(*IV*). *An unidentified trace.* Always present.

(*V*). $CH_2{=}C(CH_3)CH_2OH$. The retention volume, mass spectrum and 60 MHz NMR spectrum were identical with a known sample of 2-methyl-2-propen-1-ol.

(*VI*). $CH_2{=}C(CH_3)CH(C_2H_5)OH$. The mass spectrum: parent peak at $m/e =$ 100, base peak at 71 (parent ion less C_2H_5), and prominent peaks at 85 (parent ion less CH_3) and 41 ($C_3H_5^+$), suggested 2-methyl-1-penten-3-ol. The NMR spectra, before and after the exchange of the hydroxyl with D_2O, were consistent with this assignment. These two alcohols (peaks V and VI) were always minor products. Peak V is the result of two reduction attacks on the carbonyl group and peak VI of successive reduction and alkylation.

(*VII*). $C_2H_5CH_2CH(CH_3)COC_2H_5$. Assignment based on its mass spectrum: $m/e = 128$ (parent peak), 71 (base peak-parent ion less C_3H_5O), 86 [McLafferty rearrangement: $CH_3CH{=}C(C_2H_5)OH^+$], 57 (parent less C_5H_{11}), 43 ($C_3H_7^+$), 99 (parent less C_2H_5). The McLafferty rearrangement is characteristic of a carbonyl compound. The mass spectrum suggests that it is 4-methyl-3-heptanone. It was a minor product, sometimes only present as a trace.

(*VIII*). $CH_2{=}C(CH_3)C(C_2H_5)_2OH$. The major product, is an isomer of peak VII showing the mass-spectrum peaks at 128 (parent), 99 (in this case the base peak),

43, 57 and 71. The McLafferty peak is absent, but a peak at 87 (parent less C_3H_5) is third in order of intensity. The assigned structure was confirmed by its NMR spectra, before and after exchange of the hydroxyl with D_2O.

The mass spectrum of the non-aqueous phase of the hydrolysed reaction products showed no peaks above $m/e = 128$ which precludes the presence of linear and cyclic oligomers which are known to accompany anionic polymerization of MMA initiated by Grignard reagents, butyllithium, (diphenylamino)diethylaluminium and (butylthio)diethylaluminium (see ref. 3). The precursor of these oligomers: $C_2H_5CH_2$-$C(CH_3)COOCH_3$, the hydrolysed product of a 1/4 adduct, is also absent. A test sample of methyl 2-methylpentanoate had a retention time different from any gas chromatographic peak found in our reaction mixtures and its mass spectrum showed a parent peak at $m/e = 130$, and a base peak at 88 (McLafferty rearrangement). Both were absent in the reaction products.

(*c*). *NMR spectra of reacting mixtures.*

When $0.5 <$ MMA/Al < 1.0, the MMA vinyl resonances eventually disappeared and were replaced by an unresolved broad peak at δ 4.85 ppm, which is just beginning to develop in Fig. 2. At the same time the ethyl region of the spectrum became complex due to the superimposition of the back-to-front methyl–methylene pattern of $C-C_2H_5$ resonances on the $Al-C_2H_5$. The methoxyl peak split, the new peak (just visible in Fig. 2) appearing 0.17 ppm upfield at $\delta \simeq 3.08$ ppm. When MMA/Al < 0.5 these changes had already occurred before the spectrum could be run (Fig. 3).

The 4.85 ppm peak is very similar in shape and position to the vinyl resonance of the major hydrolysed product (VIII): CH_2=$CMeCEt_2OH$ and it is clearly a precursor having a very similar structure in the vinyl region. We believe it is the double carbonyl adduct: CH_2=$CMeCEt_2OAl$<. At reagent where carbonyl addition is rapid no further change occurred in the vinyl region of the spectrum over a period of months (Fig. 3). In these cases the integrated resonances of the vinyl region remained in a ratio of 2/3 of the methoxyl integral, showing that no significant ethylation of the vinyl group had occurred.

In two experiments, both in the range $0.5 <$ MMA/Al < 1.0, where the ethylation is slower, long term changes did occur in the vinyl regions in the form of a new peak: a sharp singlet at 5.27 ppm. In these cases some saturation of the vinyl group had occurred, the vinyl/methoxyl integral ratios having declined to 1/2. There is no additional evidence to assist in the assignment of this peak, though a 1/4 adduct of 2-methylpropenal [a feasible, but unidentified reduction product and possible precursor of 2-methyl-1-pentanal, product (III), see (*b*)] is a possibility.

The methoxyl resonance always showed a long time effect (Fig. 3). The 3.08 ppm, which appears rapidly when MMA/Al < 0.5 and slowly at higher ratios, also split over a period of days and was superseded by a developing peak at 3.18 ppm. Both these peaks must refer to $Al-OCH_3$ groups. The analysis of hydrolysed reaction products showed no evidence of intermediates such as CH_2=$CMeCEt(OMe)OAlEt_2$. The 3.08 ppm resonance was contemporaneous with the resonance in the vinyl region attributed to a doubly ethylated carbonyl group, at which stage the methoxyl group must have transferred to aluminium.

The methoxyl resonance of ethylaluminium methoxides moves upfield with increasing methoxide content. In a series of tubes prepared by the partial titration of

triethylaluminium with methanol the δ values for $Et_{3-x}AlOMe_x$ were: 3.34 ppm at $x=0.34$, 3.27 ppm at $x=0.94$, and 3.17 ppm at $x=1.11$.

When $x<1$ most methoxyl oxygens would be coordinated to a second Al atom, as in the cyclic trimer known to be the predominant species when $x=1$. When $x>1$, there is an aluminium deficiency and the coordination of all alkoxy groups cannot be maintained. The upfield shift may be due to the decrease in the overall extent of coordination of methoxyls.

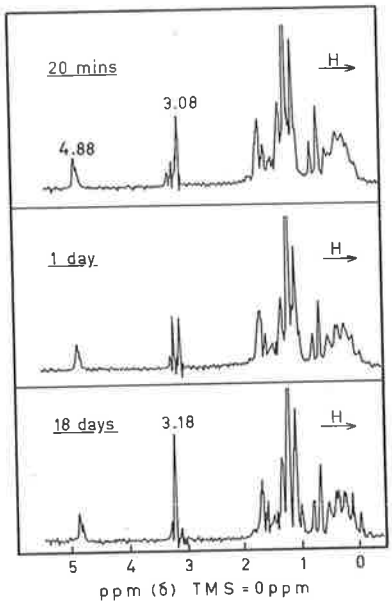

Fig. 3. Long term changes in the NMR spectrum of a mixture of Et_3Al and MMA (MMA/Al = 0.29) showing the splitting and progressive extinction of the 3.08 ppm methoxyl peak.

The time dependence of the MeO resonance of Et_2AlOMe showed a striking resemblance to that in the reacting mixtures. The original line at 3.18 ppm decreased and was replaced by one at 3.27 ppm. After 2 days the new peak was 9 times the intensity of the original, but the original did not disappear entirely, remaining as an unresolved shoulder on the upfield side of the 3.27 ppm peak 8 months later. The splitting of the MeO resonance has been reported previously[11] and attributed to a slow association equilibria analogous to those observed in dimethylaluminium phenoxide (several hours at room temperature[11]) and aluminium triisoproxide (weeks[12]). It was suggested that the dimer $\rightleftarrows$ trimer equilibrium is the one observed.

The conditions in our reacting mixtures were not entirely analogous since we were observing species of the overall empirical formula: $Et_{3-2x}Al(OMe)_x(OCEt_2\text{-}CMe{=}CH_2)_x$ where $x<1$ ($=0.29$ in Fig. 3). Assuming the 3.08 ppm resonance arises from the immediate product of an intramolecular reaction of complex (II), it can be attributed to either (IX), (X) or rapid exchange between (IX) and (X):

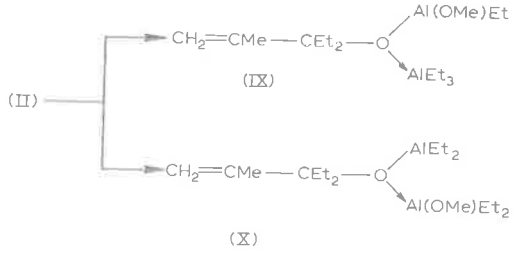

The downfield shift suggest that the 3.18 ppm peak arises from a methoxyl group in which the oxygen is coordinated to another Al atom. The closely similar behaviour of the dialkyl aluminium alkoxides is strong evidence that here too a slow association is involved. However a slow exchange would also explain the observations. It is known that alkoxide groups retard the exchange of alkyls, and the larger the group the slower the exchange. With R_2AlO-i-Bu the half life for exchange of R (= Me or Et) is as long as 2 h at 313°K [13].

CONCLUSIONS

The 1/1 complex between Et_3Al and MMA (I) is very stable and unreactive in absence of light and excess Et_3Al. When Et_3Al is in excess carbonyl addition proceeds readily. The NMR shifts when $0.5 < MMM/Al < 1.0$ lead us to postulate that another complex (II) is present and this is the precursor of carbonyl addition. NMR evidence for such a complex is quite strong, but the rapid reaction occurring under these conditions makes it unlikely that its presence can be proved conclusively. In which case, the possibility that the addition reaction arises from the attack of uncomplexed triethylaluminium on (I) cannot be entirely excluded.

The NMR evidence suggests that carbonyl addition is normally the exclusive reaction. The exceptions were two cases where reduction of the carbonyl occurred. Only in the cases where reduction occurred did the NMR spectra show saturation of the vinyl group. Two cases of ethylation of the vinyl group were observed in hydrolysed reaction products. Product (III) arises from the alkylation of the product of an initial reduction and product (VII) most probably from the alkylation of an initial carbonyl adduct. There is no reason for supposing that 1/4 attack on MMA occurs. In the case of the normal reaction the first ethylation of the carbonyl group is quickly followed by double ethylation. There is no evidence that significant concentrations of the intermediate: CH_2=CMeCEt(OMe)O·$AlEt_2$ develop.

ACKNOWLEDGEMENT

All work described in this paper is supported by the Australian Research Grants Commitee, to whom we express our gratitude.

REFERENCES

1 P. E. M. ALLEN AND B. A. CASEY, *Eur. Polym. J.*, 2 (1966) 9.
2 P. E. M. ALLEN AND B. A. CASEY, *Eur. Polym. J.*, 6 (1970) 793.

3 P. E. M. ALLEN, B. A. CASEY AND W. DANKIW, *J. Macromol. Sci., Chem. A*, 4 (1970) 1091.
4 R. E. PARTCH, *Tetrahedron Lett.*, (1967) 3071.
5 T. MOLE AND R. SURTEES, *Aust. J. Chem.*, 17 (1964) 961.
6 E. C. ASHBY, J. LAEMMLE AND H. M. NEUMANN, *J. Amer. Chem. Soc.*, 90 (1968) 5179.
7 J. RONAYNE AND D. H. WILLIAMS, *J. Chem. Soc. C*, (1967) 2642.
8 B. O. BATEUP, Honours Thesis, University of Adelaide, 1970.
9 Y. TAKASHI, *Bull. Chem. Soc. Jap.*, 40 (1967) 612.
10 S. PASYNKIEWICZ, L. KOZERSKI AND B. GRABOWSKI, *J. Organometal. Chem.*, 8 (1967) 233.
11 E. A. JEFFERY AND T. MOLE, *Aust. J. Chem.*, 21 (1968) 2683.
12 V. J. SHINER, D. WHITTAKER AND V. P. FERNANDEZ, *J. Amer. Chem. Soc.*, 85 (1963) 2318.
13 T. MOLE, *Aust. J. Chem.*, 19 (1966) 381.

European Polymer Journal, 1972, Vol. 8, pp. 329–338. Pergamon Press. Printed in England.

POLYMERIZATION OF METHYL METHACRYLATE BY ORGANOMETALLIC COMPOUNDS—VI

KINETICS AND MECHANISM OF POLYMERIZATION INITIATED PHOTOCHEMICALLY BY TRIETHYL ALUMINIUM—MONOMER COMPLEXES

P. E. M. ALLEN, B. O. BATEUP and B. A. CASEY*

Department of Physical and Inorganic Chemistry, University of Adelaide, Box 498D, G.P.O., Adelaide, South Australia 5001

(*Received* 1 *September* 1971)

Abstract—The initial rate of polymerization is

$$v_{p0} = kI_0^{\frac{1}{2}}[Al_2Et_6]_0^{\frac{1}{2}}[MMA]_0$$

where I_0 is the incident illumination and $[Al_2Et_6]_0$ is the total molar concentration of trialkyl aluminium dispensed, estimated as dimer. Direct photolysis of the 1:1 MMA:$AlEt_3$ Wittig-"ate" complex is not responsible for polymerization. Initiation is thought to occur by the bimolecular reaction of a photo-excited state of this complex with a molecule of the complex in its ground state to form a species which then decays to radicals. Abnormally long induction and decay periods suggest a slow step prior to the formation of free radicals which then initiate a radical chain polymerization. Ethyl aluminium alkoxides that form rapidly when MMA/Al $\leqslant$ 0·5 did not polymerize excess MMA in bulk at 248 K in the dark or under ambient illumination.

PREVIOUS papers[1,2] showed that the polymerization of methyl methacrylate (MMA) promoted by aluminium triethyl (Et_6Al_2) occurs by a photo-initiated, free radical mechanism. When monomer is in excess, i.e. MMA/Al > 1 where Al represents all alkyl aluminium compounds assayed as monomeric species, a strong 1:1 complex having a Wittig-"ate" structure (I) predominates and the free radicals are formed by

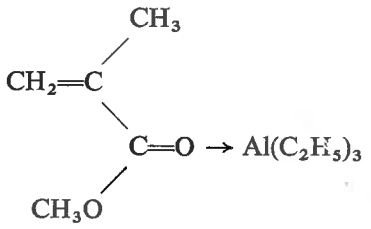

(I)

a photo-excited state (I)*. The absorption maximum of (I) occurs in the near ultraviolet and irradiation with visible or near u.v. light initiates the polymerization. However, when Al/MMA > 1, rapid stoichiometric reactions occur in the dark with the possible formation of a 1:2 complex when Al/MMA > 2.[3]

Preliminary kinetic investigations[2] on the polymerization indicated half-order dependence on light intensity and first order on both monomer and triethyl aluminium. In this paper we report more detailed kinetic investigations which show that the order with respect to triethyl aluminium is one-half.

* Central Research Laboratories, I.C.I.A.N.Z., Ascot Vale, Victoria, Australia.

In conjunction with these experiments, we investigated the possible initiation of polymerization of excess MMA by the stoichiometric products formed when MMA/Al < 1. Under these conditions, the products are ethyl aluminium alkoxides with the overall empirical formula:[3]

$$Et_{3-2x}Al(OMe)_x(OCEt_2CMe{:}CH_2)_x$$

(II)

where $x < 1$. Various workers[4] have reported aluminium tertiary alkoxides to be effective catalysts for the polymerization of MMA.

1. EXPERIMENTAL

General purification and manipulation procedures have been described previously.[1] Toluene was used as diluent for all experiments unless otherwise stated. Kinetic and spectroscopic measurements were made using previously described[2] procedures.

Light from an Hanovia 220/A mercury arc with stabilized power supply was filtered using a Zeiss M 365 nm monochromatic filter. Dilatometer bulbs were constructed from 1 cm square boro-silicate tubing. The light intensity was varied by inserting in the light path silica discs coated with a thin layer of nichrome. These neutral density filters were calibrated on a Unicam SP700 spectrophotometer which had been previously calibrated with a potassium chromate solution. A clear silica disc was used as reference. The uniformity of the metal coating was found to be very good. Five filters with transmissions between 17 and 100 per cent were used.

Molecular weights of polymers were determined by means of intrinsic viscosity measurements in chloroform at 298 K using the relationship (5)

$$[\eta] = 4{\cdot}4 \times 10^{-5}\,\bar{M}_v^{0{\cdot}80}.$$

Attempts to obtain accurate number average molecular weights using a Mechrolab automatic membrane osmometer failed. Reasons for this will be discussed.

The unsaturated alkoxy-ethyl-aluminium compounds (II) were prepared in the absence of diluent by mixing previously prepared samples of Et_6Al_2 and MMA at reduced temperature. After the initial vigorous reaction had ceased, excess monomer was added; the dilatometer was filled as before and then transferred to the darkened thermostat. The exact MMA/Al ratio was determined using 60 MHz NMR at 302 K with benzene as internal reference.

2. RESULTS

(a) *Intensity exponent.* The dependence of rate (v_p) on the intensity of the absorbed light (I_{abs}) at constant monomer and trialkyl concentrations was determined at 262·5 and 256·2 K. Figure 1a and 1b at 262·5 K, show that the intensity exponent is 0·5 which is also the case at 256·2 K.

It should be noted that these and all subsequent runs were performed at concentrations of trialkyl that ensured complete absorption of incident light (I_0). This was necessary because the absorption maximum of the yellow 1:1 complex (I) shifted to shorter wavelengths during the course of a polymerization.[2] Possible errors introduced by the "skin-effect" under these conditions were minimized by keeping the initiator concentration, conversion and polymerization rate low.

(b) *Order with respect to monomer.* The internal order of reaction was unity with respect to MMA. Plots of log ($[MMA]_0/[MMA]$) against time were linear after an initial induction period (Fig. 2). Ratios of MMA/Al > 20 were used. The external order with respect to monomer can reasonably be assumed to be unity. Confirmation, of this would require a large decrease in the [monomer]/[alkyl] ratio with the possibility of a change in initiation mechanism (cf. very long decay period at high alkyl concentration, Fig. 5).

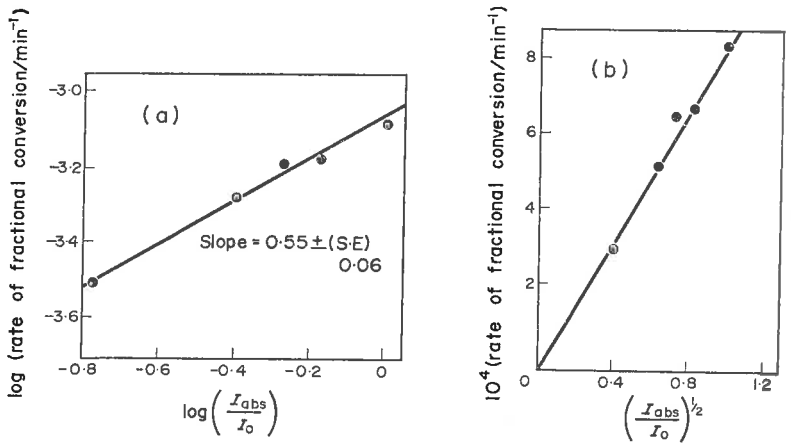

FIG. 1(a) and 1(b). Dependence of fractional rate of polymerization on light intensity at 262·5 K in toluene. $[MMA]_0 = 3{\cdot}08$ M, $[Al_2Et_6]_0 = 0{\cdot}115$ M.

(c) *Order with respect to Et_6Al_2.* At constant I_0, $[MMA]_0$ and solvent concentration, the external order of reaction with respect to triethyl aluminium was found to be one-half. Six different alkyl concentrations were used and a least squares analysis on the resulting log $(v_p/[MMA])_0$ against log $[Al_2Et_6]_0$ gave a slop of $0{\cdot}49 \pm$ (S.E.) $0{\cdot}03$. The possibility of a first order alkyl dependence was eliminated by considering the standard error (S.E.) of the intercept of the $v_p/[MMA]_0$ against $[Al_2Et_6]_0^n$ plot with $n = 0{\cdot}5$ and $1{\cdot}0$ respectively (Table 1). The intercept when $n = 0{\cdot}5$ lies within the standard error of the origin.

It appears therefore that, under conditions of total absorption of incident illumination (I_0), the external orders of reaction are defined by the initial rate equation

$$-[d[MMA]/dt]_0 = k_{obs}\, I_0^{\frac{1}{2}}\, [Al_2Et_6]_0^{\frac{1}{2}}\, [MMA]_0 \qquad (1)$$

where the subscript refers to the time after a brief induction period.

The yellow colour of the complex decayed only slowly during the course of a kinetic run and its internal order could not be estimated.

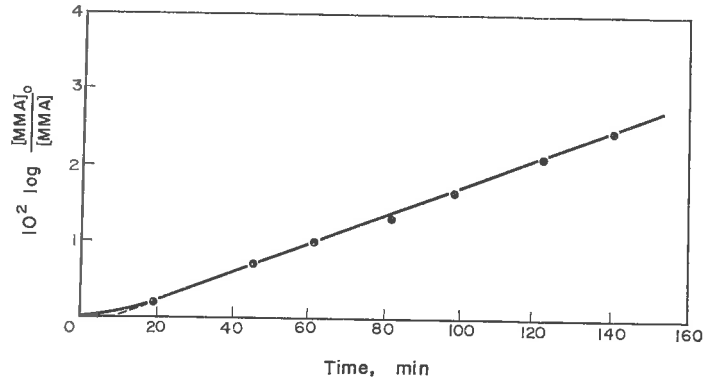

FIG. 2. Internal first order of reaction with respect to monomer in toluene at 262·5 K. $[MMA]_0 = 4{\cdot}73$ M, $[Al_2Et_6]_0 = 0{\cdot}046$ M.

TABLE 1. LEAST SQUARES ANALYSIS ON DATA FOR THE DEPENDENCE OF RATE ON TRIALKYL ALUMINIUM CONCENTRATION AT 262·5 K IN TOLUENE $[MMA]_0 = 4{\cdot}97$ M

Plot	Regression equation $Y = A + BX$
$(v_p/[MMA]_0$ vs. $[Al_2Et_6]_0$	$Y = 2{\cdot}59 + 1{\cdot}335X$ S.E. of $A = 0{\cdot}03$ S.E. of $B = 0{\cdot}68$
$(v_p/[MMA]_0$ vs. $[Al_2Et_6]_0^{\frac{1}{4}}$	$Y = 0{\cdot}048 + 11{\cdot}90X$ S.E. of $A = 0{\cdot}055$ S.E. of $B = 0{\cdot}92$
$\log(v_p/[MMA])_0$ vs. $\log [Al_2Et_6]_0$	$Y = 0{\cdot}244 + 0{\cdot}49X$ S.E. of $A = 0{\cdot}004$ S.E. of $B = 0{\cdot}03$

(d) *Arrhenius parameters.* An Arrhenius equation was obeyed between 281 K and 238 K (Fig. 3) with an overall activation energy (E_0) of $16 \pm$ (S.E.) 2 kJ mol^{-1}. The pre-exponential factor could not be calculated since the absolute value of I_0 was not determined.

(e) *Non-stationary state observations.* Experiments conducted at 262·5 K, 253 K and 242 K with $[MMA]_0 = 4{\cdot}97$ M, $[Al_2Et_6]_0 = 0{\cdot}05$ M with toluene as diluent indicated induction periods of *ca.* 10, 20 and 30 min respectively before a stationary state was achieved (Fig. 4). When the conversion curve became linear, it was assumed that stationary state conditions were established. Contributions to the induction periods from reactive impurities in the reactants were eliminated by purging each dilatometer

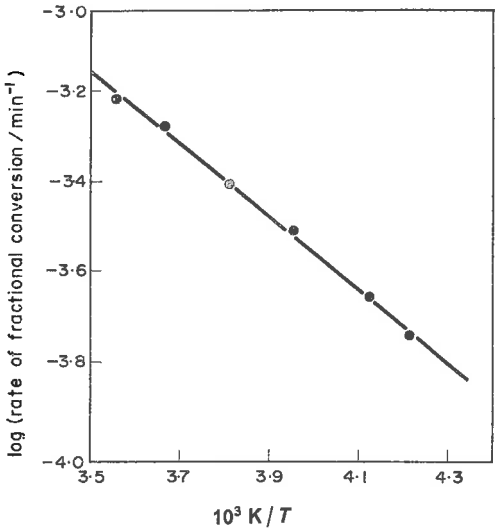

FIG. 3. Dependence of fractional rate of polymerization on temperature. $[MMA]_0 = 4{\cdot}97$ M, $[Al_2Et_6]_0 = 0{\cdot}05$ M. Toluene as solvent.

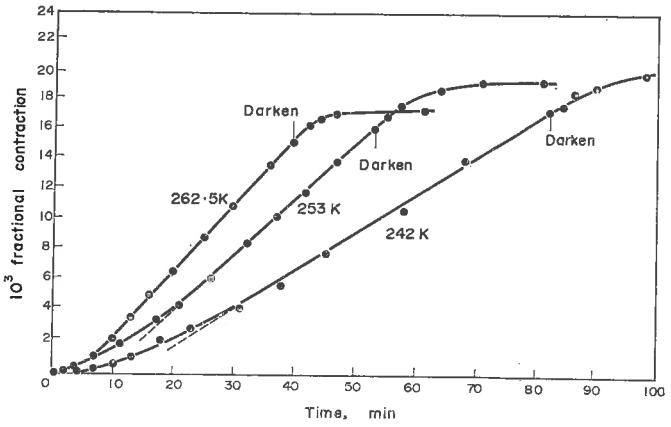

FIG. 4. Fractional contraction versus time curves showing induction and decay periods at 262·5 K, 253 K and 242 K, respectively. $[MMA]_0 = 4{\cdot}97$ M, $[Al_2Et_6]_0 = 0{\cdot}05$ M.

with the polymerizing mixture before making one set of determinations. No side products were detectable after hydrolysis of the polymerizing mixture.[6] Figure 5 shows the fractional decay of polymerization when illumination had ceased compared to the theoretical decay for a simple free radical polymerization. The theoretical curves were calculated from the data in reference.[7]

(f) *Molecular weights.* The molecular weights of polymers prepared at 258 K in toluene were low. At $[MMA]_0 = 3{\cdot}5$ M, $[Al_2Et_6]_0 = 0{\cdot}36$ M, $\bar{M}_v$ increased slowly with conversion, being approximately 10^4 (below 20 per cent conversion) and approxi-

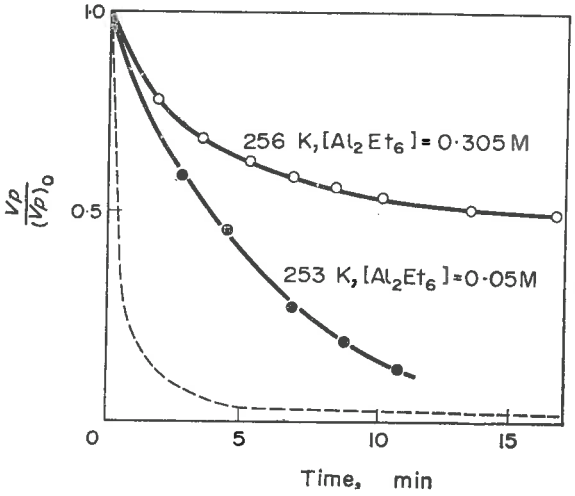

FIG. 5. Decay of polymerization at 256 K and 253 K after illumination ceases. v_p, v_{p0} are the non-stationary and stationary state rates respectively. Solid surves were experimentally determined whereas the broken line is the limiting theoretical decay curve predicted for a radical polymerization at 256 K using the termination coefficients of Hughes and North.[7] NOTE—very slow decay at 256 K where $[Al_2Et_6]_0 = 0{\cdot}305$ M; $[MMA]_0 = 3{\cdot}86$ M compared to that at 253 K where $[Al_2Et_6]_0 = 0{\cdot}05$ M, $[MMA]_0 = 4{\cdot}97$ M.

mately 2×10^4 (between 50 and 80 per cent conversion). Beyond this $\bar{M}_v$ decreased again. A crude fractionation showed the molecular weight distribution was broad. For polymers prepared at 262·5 K and with $[MMA]_0 = 4{\cdot}97$ M and $[Al_2Et_6]_0$ between 0·025 and 0·05 M, measurements on an automatic membrane osmometer in toluene at 298 K indicated values of $\bar{M}_n$ between 2×10^4 and 3×10^4. Accurate values of $\bar{M}_n$ could not be determined presumably due to membrane seepage of low molecular weight materials. The formation of low molecular weight polymer even at greatly increased MMA/Al ratios can be attributed to the high activity of organo-aluminium compounds as chain transfer agents in radical polymerization.[8] It has been shown[9] that the chain transfer constant for the 1:1 $Al(i\text{-}Bu)_3$/MMA complex was 0·6 at 273 K.

(g) *Activity of* (II) *as an initiator.* An initial solution with MMA/Al = 0·52 was prepared. As reported previously[3] at 0·5 < MMA/Al < 1·0 the reaction was slow and after 10 min the solution was still a greenish-yellow similar to that observed in the 1:1 Wittig-"ate" complex but more intense. A 50-fold excess of MMA was then added but no polymerization was evident even after 30 hr at 248 K.

When MMA/Al = 0·30 the reaction was very rapid and the solution turned colourless within seconds of mixing at reduced temperature. When excess MMA was added the characteristic green colour of the 1:1 complex appeared instantaneously. Again no polymerization was observed at 248 K. However, at 298 K under ambient illumination, slow polymerization did occur. The green colour observed in this experiment probably resulted from 1:1 complex formation between MMA and the free triethyl aluminium in excess of the MMA/Al = 0·5 stoichiometry of the 1:2 complex in the system. This would account for the observed slow polymerization at room temperature under ambient illumination. It seems that the 1:2 complex and its products (II) are not active initiators of methyl methacrylate at low temperature.

3. DISCUSSION

The kinetic results contra-indicate initiation by direct photolysis of (I).

Firstly, the slow decay of the concentration of the complex under conditions of total absorption suggests a process of low quantum efficiency implying that the photo-excited state involved is efficiently quenched [see reaction (8)].

Secondly, with a direct photolytic mechanism of initiation under conditions of total absorption, the initial rate of polymerization would be independent of $[Al_2Et_6]_0$.

Thirdly, the observed induction periods [2(e)] are not consistent with a simple free radical mechanism. Comparison with data in reference[7] at 253 K would require the induction period to be much less than one minute for a simple free radical mechanism. If it is assumed that the propagation and termination processes in our system are the same as those for a simple photo-initiated polymerization of MMA, then the unusually long induction (and decay) period cannot be correlated to the lifetime of a propagating MMA radical. The build-up period must therefore be due to a slow step prior to the formation of propagating radicals.

The observed rate law [Eqn. (1)] under conditions of total absorption requires that free radicals are formed in a bimolecular reaction of a photo-excited state, (I)*, with a molecule of (I). Provided this reaction is slow, the relatively long induction periods can be explained but, if the quenching of (I)* is efficient, a long decay period (Fig. 4)

would not be expected. This suggests that the build up *and* decay of polymerization is determined by the rate of decomposition of an intermediate species (I)*(I) formed by the bimolecular, reversible reaction between (I)* and (I):

$$(I)^* + (I) \underset{k_{-1}}{\overset{k_1}{\rightleftharpoons}} (I)^*(I) \xrightarrow{k_d} \text{radicals} \qquad (2)$$

$$(I)^*(I) \xrightarrow{k_2} 2(I)$$

where k_1, k_{-1}, k_2 and k_d are the rate constants for the respective reactions. The rate of destruction of (I)*(I) and hence the rate of formation of radicals is determined by the term $(k_d + k_{-1} + k_2)$. When illumination commences, a stationary state concentration of the excited state (I)* of the 1:1 complex (I) is rapidly achieved since all quenching processes are presumably efficient. This is valid since the high extinction coefficient,[2] coupled with the slowness of decay of the absorption maximum [2(c)] during polymerization, suggests that quenching of (I)* to the ground state is more rapid than the formation of radicals.

The species (I)*(I) decays (via k_d) to free radicals and providing k_d is small the induction period will be long. When illumination ceases, (I)* is rapidly removed by efficient quenching reactions but if k_2, k_{-1} and k_d are small the concentration of (I)*(I) will decay more slowly.

The evidence that decay is not dependent on the lifetime of the polymerizing species is strengthened by the fact that in this system decay followed an approximate first order law when illumination ceased (Fig. 6). For a simple photo-initiated polymerization

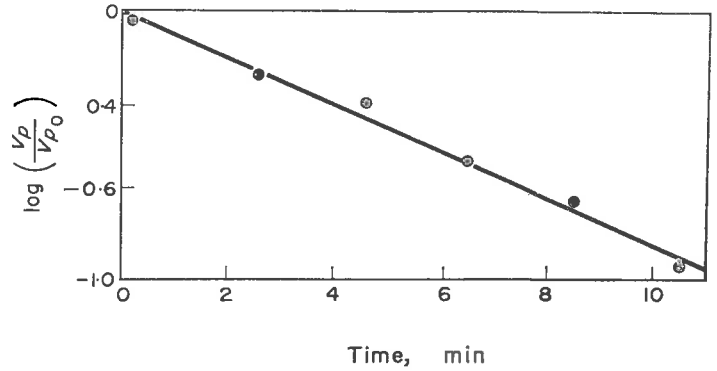

FIG. 6. Approximate first order decay of polymerization at 253 K when illumination ceases. $[MMA]_0 = 4{\cdot}97$ M; $[Al_2Et_6]_0 = 0{\cdot}05$ M.

involving direct photolysis, termination occurs by the normal bimolecular reaction between macroradicals according to the following equation

$$(v_p)^{-1} - (v_p)_0^{-1} = (2k_{tc} + 2k_{td})t/k_p[M]. \qquad (3)$$

In none of our experiments was the above expression followed.

At high triethyl aluminium concentrations, e.g. $[Al_2Et_6]_0 = 0{\cdot}30$ M, $[MMA]_0 = 3{\cdot}86$ M (Fig. 3), abnormal decays were observed not following either first or second order decay laws. A further abnormality is that the duration of the decay period, after

illumination ceases, is much longer than the induction period. With the mechanisms discussed the decay period cannot exceed the induction period. In a previous paper[2] these abnormally long decay periods were attributed to a slow inter-system crossing from (I)* to another excited state (I)**, so that the decay period is lengthened either by the slow reaction of (I)** and (I) to form radicals, or the slow reconversion of (I)** to (I)*. However, the dependence of the effect on triethyl aluminium concentration suggests that the process must have a higher order in $[Al_2Et_6]$ and it seems more likely that another complex is formed by the interaction of (I)* and (I) which is only slowly reconverted to (I)* or converted to (I)*(I) or radicals.

The activation energy (E_i) for the initiation reaction shown in Eqn. (2) is given by

$$E_i = \Delta H_{(I)*(I)} + E_d \tag{4}$$

where $\Delta H_{(I)*(I)}$ is the enthalpy of formation of (I)*(I) and E_d is the activation energy associated with k_d. Since $\Delta H_{(I)*(I)}$ is negative, E_i will be small if $|\Delta H_{(I)*(I)}| \approx |E_d|$. This would explain the seemingly low value obtained for the overall activation energy E_0 [2(d)].

4. KINETIC ANALYSIS

The above results have led to the following kinetic scheme based on a free radical mechanism for the polymerization

$$Al_2Et_6 \rightleftarrows 2AlEt_3 \qquad \text{fast} \tag{5}$$

complexing $$AlEt_3 + MMA \xrightarrow{K} AlEt_3 \,.\, MMA\ (I) \qquad K \text{ large} \tag{6}$$

excitation $$(I) \xrightarrow{h\nu} (I)^* \qquad I_{abs} = I \qquad \text{(complete absorption)} \tag{7}$$

quenching
$$\left.\begin{aligned} &(I)^* \xrightarrow{k_f} (I) + h\nu' \\ &(I)^* + Q \xrightarrow{k_q} (I) + Q^* \end{aligned}\right\} k_q' = k_f + k_q[Q] \tag{8}$$

$Q \equiv$ all quenching molecules

initiation $$(I)^* + (I) \underset{k_{-1}}{\overset{k_1}{\rightleftarrows}} (I)^*(I) \xrightarrow{k_d} \text{radicals} \tag{2}$$

deactivation $$(I)^*(I) \xrightarrow{k_2} 2(I)$$

propagation $$R\cdot_n + M \xrightarrow{k_p} R\cdot_{n+1} \tag{9}$$

termination $$R\cdot_n + R\cdot_m \xrightarrow{k_t} \text{polymer.} \tag{10}$$

Assuming a stationary state concentration of (I)*, (I)*(I) and radicals, the following relationship can be derived

$$[(I)^*] = \frac{I_0 + k_{-1}\,[(I)^*(I)]}{k'_q + k_1[(I)]} \tag{11}$$

$$[(I)^*(I)] = \frac{k_1[(I)^*]\,[(I)]}{(k_{-1} + k_d + k_2)} \tag{12}$$

$$\sum [R\cdot_n] = \left(\frac{v_i}{2k_t}\right)^{\frac{1}{2}} \tag{13}$$

where v_i, the rate of initiation is given by

$$v_i = k_d\,[(I)^*(I)]. \tag{14}$$

The rate of polymerization, v_p, is

$$v_p = k_p[M]\left(\frac{v_i}{2k_t}\right)^{\frac{1}{2}}. \tag{15}$$

Substitution of (11) into (12) and assuming $k_{-1}[(I)^*(I)] \ll I_0$ and $k_1[(I)] \ll k_q$ Eqn. (15) becomes

$$v_p = k_{obs}\, I_0^{\frac{1}{2}}\,[Al_2Et_6]^{\frac{1}{2}}\,[MMA] \tag{16}$$

where if K is large and MMA/Al >1 then $[(I)] = 2[Al_2Et_6]$.

5. CONCLUSIONS

(a) The initiation mechanism in this system does not involve the direct photolysis of the 1:1 Wittig-"ate" complex.

(b) There is no evidence to suggest that propagation and termination processes are different from those in a simple free radical polymerization.

(c) The unusually long induction and decay periods suggest a slow step prior to the formation of free radicals.

(d) The low activation energy (E_0) can be explained by the formation of a complex species as suggested in Eqn. (2).

Acknowledgement—All work described in this paper is supported by the Australian Research Grants Committee, to whom we express our gratitude. The step k_2 of reaction (2) was added at the suggestion of a referee, who is probably correct in preferring it to k_{-n} as a route for the spontaneous removal of (I)*(I).

REFERENCES

(1) P. E. M. Allen and B. A. Casey, *Europ. Polym. J.* **2**, 9 (1966).
(2) P. E. M. Allen and B. A. Casey, *Europ. Polym. J.* **6**, 793 (1970).
(3) P. E. M. Allen, B. O. Bateup and B. A. Casey, *J. Organomet. Chem.* **29**, 185 (1971).
(4) K. S. Minsker, A. I. Graevskii and G. A. Razuvaev, *Izv. Akad. Nauk SSSR* 1483 (1963).
(5) D. L. Glusker, B. Yoncoskie and E. Stiles, *J. Polym. Sci.* **49**, 297 (1961).
(6) P. E. M. Allen, B. A. Casey and W. A. Dankiw, *J. Macromol. Sci.-Chem.* **A4**, 1091 (1970).
(7) J. Hughes and A. M. North, *Trans. Faraday Soc.* **60**, 960 (1964).
(8) T. Huff and E. Perry, *J. Am. chem. Soc.* **82**, 4277 (1960).
(9) E. B. Milovskaya, L. V. Zamoyskaya and S. I. Vinogradova, *Europ. Polym. J.* **6**, 1589 (1970).

Résumé—La vitesse initiale de polymérisation est

$$v_{po} = k\, I_0^{1/2}\,(Al_2Et_6)_0^{1/2}\,(MMA)_0$$

où I_0 est le flux lumineux incident et $(Al_2Et_6)_0$ la concentration molaire totale du trialkyl aluminium supposé sous forme de dimère. La photolyse directe du mélange 1:1 MMA:$AlEt_3$, complexe Wittig "ate" n'est pas responsable de la polymérisation. On pense que l'amorçage se fait selon une réaction bimoléculaire entre un état photo excité de ce complexe et une molécule de ce complexe fondamentale en formant une espèce qui ensuite se transforme en radicaux. Les périodes d'induction anormalement longues et de décroissances des radicaux font penser qu'il existe une étape lente avant la formation des radicaux libres qui ensuite amorcent une polymérisation radicalaire en chaîne. Les alkoxides diéthyl aluminium qui se forment rapidement quand MMA:Al $\leqslant$0,5, ne polymérisaient pas l'excès de MMA en masse à 248°K dans le noir ou à la lumière ambiante.

Sommario—La velocità iniziale di polimerizzazione è

$$v_{p0} = kI_0{}^{1/2}\,[Al_2Et_6]_0{}^{1/2}\,[MMA]_0$$

in cui I_0 rappresenta l'illuminazione incidente e $[Al_2Et_6]$ la concentrazione molare totale di alluminio trialchilico somministrato, calcolato come dimero. La fotolisi diretta del complesso Wittingato 1:1 MMA:$AlEt_3$ non causa la polimerizzazione. Si pensa che l'iniziazione abbia luoga mediante reazione bimolecolare di tale complesso in stato fotoeccitato, con una molecola del complesso in stato normale, con formazione di una specie che si traforma decadendo in radicali. Un'induzione anormalmente lunga e l'esistenza di periodi di decadimento lasciano supporre che vi sia una fase lenta prima della formazione di radicali liberi i quali poi danno inizio ad una polimerizzazione a catena radicalica. Etil alluminio alcossidi che si formano rapidamente quando MMA/Al$\leqslant$0,5, non polimerizzano l'eccesso di MMA a 248 K, nell'oscurità oppure con illuminazione ambientale.

Zusammenfassung—Die Anfangsgeschwindigkeit der Polymerisation ist

$$v_{p0} = k\,I_0{}^{1/2}\,[Al_2Et_6]_0{}^{1/2}\,[MMA]_0$$

wobei I_0 die einfallende Bestrahlung und $[Al_2Et_6]_0$ die gesamte molare Konzentration des eingesetzten Trialkylaluminiums, als Dimer abgeschätzt, bedeuten. Eine direkte Photolyse des 1:1 MMA:$AlEt_3$ Wittig-"at" Komplexes ist für die Polymerisation nicht verantwortlich. Es wird angenommen, daß der Kettenstart erfolgt durch die bimolekulare Reaktion eines licht-angeregten Zustandes dieses Komplexes mit einem Molekül desselben Komplexes in seinem Grundzustand, unter Bildung einer Spezies, die weiter in Radikale zerfällt. Die anormal lange Induktions- und Zerfallsperiode weist auf einen langsamen Schritt hin, der der Bildung von freien Radikalen vorausgeht, die dann eine Radikalkettenpolymerisation starten. Äthylaluminiumalkoxide, die sich rasch bilden, wenn MMA/Al $\leqslant$ 0,5 ist, führten nicht zur Polymerisation von überschüssigem MMA in Substanz bei 248 K im Dunkeln oder bei Bestrahlung bei Raumtemperatur.

European Polymer Journal, 1973, Vol. 9, pp. 1283–1288. Pergamon Press. Printed in England.

THE INFLUENCE OF SOLUTE–SOLVENT INTERACTIONS ON THE KINETICS AND STEREOSPECIFICITY OF POLYMERIZATION—THE RELEVANCE OF AROMATIC SOLVENT SHIFTS OBSERVED ON THE NMR SPECTRUM OF METHYL METHACRYLATE

P. E. M. ALLEN and B. O. BATEUP

Department of Physical and Inorganic Chemistry, The University of Adelaide, Box 498, G.P.O., Adelaide, South Australia 5001, Australia

(*Received* 28 *April* 1973)

Abstract—The effect of certain aromatic compounds on the PMR spectrum of methyl methacrylate (MMA) was investigated. The magnitude of observed aromatic-induced shifts decreased in the order

benzene ⩾ styrene > chlorobenzene ≈ bromobenzene.

Assuming that the interaction arises from a stoichiometric 1:1 complex, equilibrium parameters for the MMA–benzene interaction have been estimated. $\Delta H \pm$ S.E. $(\Delta H) = -(8 \pm 4)$ kJ mol^{-1}. These effects are likely to have a small influence on the kinetics of copolymerization with aromatic monomers and polymerization in aromatic solvent. The stereochemistry of the solute–solvent interactions suggests that MMA takes a *cis*-conformation in solution, which is relevant to the mechanism of stereoregular polymerizations of this monomer.

SOLVENT shifts in the NMR spectrum of the monomer can be an inordinate nuisance during use of this technique to study the interactions of monomer with initiator (e.g.[1]). However, the interactions responsible for the observed spectroscopic shift, if sufficiently strong, could exert a solvent effect on the kinetics of polymerization.

There is considerable literature on the effects of halogenated aromatic solvents on the radical polymerization of MMA; conflicting views have arisen as to the exact way the solvent influences the rate. Some authors[2,3] have attributed the effects to solvent participation in the initiation step, but the general conception now is that the main contributions are in the propagation and termination steps with only a minor solvent effect on initiation. Henrici-Olivé and Olivé[4] postulated that the macroradical formed charge-transfer complexes with monomer and solvent where only the complex with monomer could lead to propagation. Bamford and Brumby[5] and later Burnett *et al.*[6] have taken into account the effects of solution viscosity on the termination step. They found that k_t varied inversely as the viscosity of the medium, as would be expected for a diffusion controlled termination step.[7] Bamford and Brumby[5] suggested that the variation of k_p in halogenated aromatic solvents could arise from either interaction of monomer with solvent or any other additive (e.g. complex formation between MMA and $ZnCl_2$[8]) or interaction of radicals with solvent by means of π or σ complexing between the aromatic solvent and the trigonal ultimate C-atom of the macro-radical.

This paper is concerned with effect of solvent on monomer under non-polymerization conditions, as observed by PMR techniques.

EXPERIMENTAL

A Varian HA-IL 60 MHz NMR spectrometer fitted with a variable temperature unit controlling to ±1°C was used for all runs, with cyclohexane (A-R spectroscopic grade) as an internal reference. Benzene and MMA were purified as previously described.[1] Styrene, chlorobenzene and bromobenzene were dried over CaH_2 and distilled prior to use. Spectra were run in unscaled NMR tubes and chemical shifts with respect to the internal lock were obtained to within ±0·002 ppm using a frequency counter. ΔH for the benzene–MMA interaction was estimated using a method described by Hanna and Ashbaugh[9] for obtaining the association constants for 1:1 molecular complexes between a donor (D) and an acceptor (A) in dilute solution. When [A] ≫ [D] the equilibrium constant, K, for the association

$$A + D \rightleftarrows^{K_{AD}} AD \tag{1}$$

can be determined from the expression

$$\Delta/[A]_0 = -\Delta K_{AD} + \Delta_0 K_{AD}, \tag{2}$$

where $[A]_0$ is the initial concentration of the acceptor (MMA),

$$\Delta = \delta_D - \delta_D^0,$$

where δ_D, δ_D^0 are the observed chemical shifts of the donor resonance (benzene) in solution and in the absence of acceptor, respectively, and

$$\Delta_0 = \delta_{AD} - \delta_D^0,$$

where δ_{AD} is the chemical shift of the donor resonance in the pure complex.

Solutions were prepared volumetrically with a constant donor concentration of 0·15 M and an acceptor concentration between 2·0 and 5·0 M. At each concentration, Δ was obtained at different temperatures by measuring the chemical shift of the benzene resonance from the cyclohexane internal lock.

RESULTS

(a) *Effect of aromatic solvents on PMR spectrum of MMA*

The effects of benzene, styrene, brombenzene and chlorobenzene on the PMR

TABLE 1. EFFECTS OF AROMATIC SOLVENTS ON PMR SPECTRUM OF MMA AT 302 K

Solvent	Concentration (vol. % solvent)	Chemical shift of vinyl peaks (ppm)		Separation of vinyls (ppm)	Methoxyl protons (ppm)	α Methyl protons (ppm)
Benzene*	33·3	5·957	5·340	0·617	3·498	1·773
	50·0	5·990	5·307	0·683	3·465	1·773
	66·6	6·023	5·273	0·750	3·431	1·790
Styrene*	30	6·000	5·455	0·545	3·633	1·850
	43	6·031	5·381	0·650	3·557	1·849
	60	6·043	5·343	0·700	3·527	1·843
Bromobenzene†	33·3	6·950	6·350	0·600	4·533	2·783
	50·0	6·966	6·366	0·600	4·533	2·783
	66·6	7·066	6·383	0·683	4·583	2·866
Chlorobenzene†	33·3	6·945	6·334	0·611	4·516	2·783
	50·0	6·966	6·350	0·616	4·516	2·783
	66·6	7·033	6·366	0·667	4·550	2·833

* Chemical shifts quoted relative to TMS = 0 ppm.
† Chemical shifts quoted relative to lock offset to 8·116 ppm.

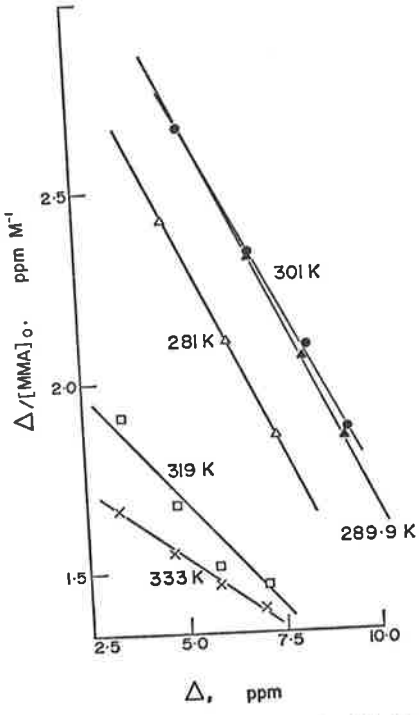

FIG. 1. Plot of $\Delta/[MMA]_0$ ppm M^{-1} against chemical shift (Δ ppm) for benzene–MMA interaction at various temperatures. Cyclohexane used as internal reference. [benzene] = 0·15 M; $[MMA]_0$ varying between 2 and 5 M.

spectrum of MMA at 302 K are shown in Table 1. In benzene and styrene the downfield vinyl proton of MMA is shielded and the chemical shift increases as the concentration of the solvent increases, whereas the high field vinyl, methoxyl and to a lesser extent the α-methyl MMA resonances are all deshielded—the chemical shifts decreasing with increasing aromatic compound concentration. Chlorobenzene and bromobenzene also shield the downfield vinyl resonance of MMA but, unlike benzene and styrene, they have a very small shielding effect on the remaining MMA protons. This suggests that the interaction between these solvents and MMA is weaker than that of benzene or styrene.

(b) *Strength of interaction between benzene and MMA*

Figure 1 shows plots of $\Delta/[A]_0$ vs Δ at various temperatures; values of association constants obtained from the slope of these graphs [Eqn. (2)] are listed in Table 2. The van't Hoff plot of K_{AD} is shown in Fig. 2 and the enthalpy of association, $\Delta H^\circ_{AD} = -8(\pm \text{SE4})$ kJ mol^{-1}, was calculated. This value is dependent on the assumptions, embodied in Eqns. (1) and (2), that the solvent shifts observed are due to the formation of 1:1 solute–solvent interactions.

(c) *Conformation of MMA in benzene*

The aromatic solvent induced solvent effect (ASIS) has been used to predict the

TABLE 2. ASSOCIATION CONSTANTS FOR THE BENZENE–MMA INTERACTION ASSUMING A 1:1 COMPLEX

Temp. (K)	K_{AD}* (M^{-1})
281	0·21
289·9	0·20
301	0·19
319	0·13
333	0·12

* Values of K_{AD} averaged from two successive determinations.

conformation of rigid steroidal ketones in solution[10] and α,β-unsaturated compounds.[11]

Timmons[12] has proposed reference planes for non-rigid α,β-unsaturated carbonyl compounds which have been used for predicting the preferred conformation of these compounds in aromatic solvents. The shielding of one methylene proton and the deshielding of the other in styrene and benzene suggest that in these solvents, MMA takes the *s-cis* form in the monomer–solvent complex and the simplest model is that in which the benzene ring lies in a plane parallel to that of the *s-cis* conformer of the monomer (see Fig. 3).

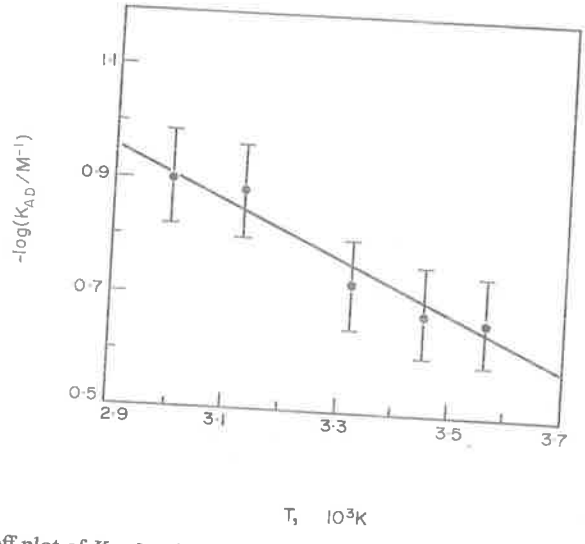

FIG. 2. Van't Hoff plot of K_{AD} M^{-1} for benzene–MMA interaction assuming a 1:1 complex.

DISCUSSION

The interpretation of solvent shifts observed in NMR spectra in terms of the formation of weak stoichiometric 1:1 solvent–solute complexes is conjectural,[13] though, in the present case, the hypothesis does provide a simple explanation of the stereo-

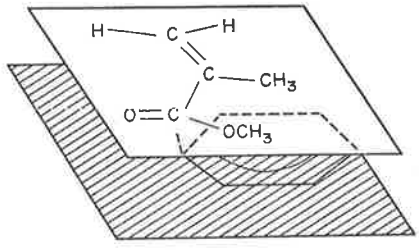

FIG. 3. Simplest model for the benzene–MMA interaction assuming a 1:1 complex.

chemistry of the solute–solvent interaction. Whether this assumption is correct or not, there is a significant solute–solvent interaction, which should be taken into account when considering the reactions of the solute. There is no evidence of a specific interaction of this type between aromatic solvents and the base unit of polymethyl methacrylate, so we would expect the monomer–solvent interaction to make a contribution of some 8 kJ mol^{-1} to the enthalpy of polymerization of a dilute solution of this monomer in benzene. A similar, though smaller, effect on the energy of activation of the propagation reaction can be expected. It must be emphasized that the magnitude is small. It is too small to explain the strong kinetic solvent effects observed on radical polymerization in aromatic solvents. These effects are strongest in the halogenated aromatics where the monomer–solvent interaction is weakest. The predominant cause of these effects seems to be the dependence of k_t on solvent-viscosity.[6]

The weak interaction between methyl methacrylate and styrene will contribute a slight alternating tendency to the composition distribution of the copolymers if the complex pair adds as a unit.

If the *cis*-conformation of MMA in the complex is evidence that this conformer predominates in aromatic solutions, it is an important consideration which must be taken into account when postulating mechanisms for the stereospecific polymerization of this monomer. The mechanisms discussed all refer to anionic polymerizations initiated by organo-metallic reagents. In most models, it is assumed that the aspect of presentation of the monomer to the growing chain or the rotation of end units whose final configuration is still undetermined are restricted by steric clashes between side groups on the monomer and the growing chain or by interaction between the monomer side group and the counter-ion.[14,15] The detailed structures of such models will be very dependent on whether a *cis* or *trans* conformation of the monomer is assumed.

Acknowledgement—The observations on which this paper is based were made during an investigation supported by the Australian Research Grants Committee. B.O.B. is supported by a Commonwealth Postgraduate Award. We gratefully acknowledge this assistance.

REFERENCES

(1) P. E. M. Allen, B. O. Bateup and B. A. Casey, *J. organometal. Chem.* **29,** 185 (1971).
(2) G. M. Burnett, W. S. Dailey and J. M. Pearson, *Trans. Faraday Soc.* **61,** 1216 (1965).
(3) G. M. Burnett, D. B. Anderson and A. C. Gowan, *J. Polym. Sci.* **1A,** 1465 (1963).
(4) G. Henrici-Olivé and S. Olivé, *Makromolek. Chem.* **96,** 221 (1966).
(5) C. H. Bamford and S. Brumby, *Makromolek. Chem.* **105,** 122 (1967).
(6) G. M. Burnett, G. G. Cameron and M. M. Zafar, *Europ. Polym. J.* **6,** 823 (1970).
(7) S. W. Benson and A. M. North, *J. Am. chem. Soc.* **81,** 1339 (1959).
(8) C. H. Bamford, S. Brumby and R. P. Wayne, *Nature, Lond.* **209,** 292 (1966).

(9) M. W. Hanna and A. L. Ashbaugh, *J. phys. Chem.* **68,** 811 (1964).
(10) N. S. Bhacca and D. H. Williams, *Tetrahedron Lett.* **42,** 3127 (1964).
(11) J. Ronayne and D. H. Williams, *J. chem. Soc.* **C,** 2642 (1967).
(12) C. J. Timmons, *Chem. Commun.* 576 (1965).
(13) J. Ronayne and D. H. Williams, *Ann. Rep. NMR Spect.* **2,** 83 (1969).
(14) F. A. Bovey, *Polymer Conformation and Configuration*, pp. 65–67. Academic Press, New York (1969).
(15) M. Goodman, *Topics in Stereochemistry*, **2,** 73 (1967).

Résumé—On a étudié l'effet de certains composés aromatiques sur le spectre RMN du méthacrylate de méthyle (MMA). L'amplitude des déplacements observés dus aux composés aromatique diminue dans l'order: benzène ⩾ styrène > chlorobenzène ≈ bromobenzène. En supposant que l'interaction provient d'un complexe stoechiométrique 1:1, on a déterminé les paramètres d'équilibre de l'interaction MMA–benzène: $\Delta H \pm SE$ ($\Delta H = -(8 \pm 4)$ kJ mol^{-1}. Ces effets ont probablement une petite influence sur la cinétique de copolymérisation avec des monomères aromatiques et sur la polymérisation dans un solvant aromatique. La stéréochimie des interactions fait supposer que le MMA a une conformation *cis* ce qui concorde avec le mécanisme des polymérisations stéréorégulières de ce monomère.

Sommario—Si è indagato sugli effetti che certi composti aromatici hanno sullo spettro del metilmetacrilato (MMA). L'ampiezza dello spostamento osservato con composti aromatici diminuisce nel seguente ordine

benzene ⩾ stirene > clorobenzene ≈ bromobenzene.

Supponendo che l'interazione nasca da un complesso stechiometrico 1:1, si è fatta una stima dei parametri di equilibrio per l'interazione MMA–benzene. $\Delta H \pm$ S.E.$(\Delta H) = -(8 \pm 4)$ kJ mol^{-1}. È probabile che questi effetti abbiano una piccola influenza sulla cinetica di copolimerizzazione con monomeri aromatici e di polimerizzazione in solventi aromatici. Secondo la stereochimica delle interazioni soluto–solvente, il MMA assume in soluzione una conformazione *cis*, ciò che è pertinente al meccanismo di polimerizzazione stereoregolare di questo monomero.

Zusammenfassung—Untersucht wurde der Effekt, den gewisse aromatische Verbindungen auf das NMR-Spektrum von Methylmethacrylat (MMA) ausüben. Die Größe der beobachtenten, durch die Aromaten induzierten chemischen Verschiebung nimmt in der Reihenfolge Benzol ⩾ Styrol > Chlorbenzol ≈ Brombenzol ab. Unter der Annahme, daß diese Wechselwirkung aus einem stöchiometrischen 1:1-Komplex resultiert wurden die Gleichgewichtsparameter für MMA–Benzol abgeschätzt zu $\Delta H \pm$ S.E. $(\Delta H) = -(8 \pm 4)$ kJ mole^{-1}. Diese Effekte haben vermutlich einen kleinen Einfluß auf die Kinetik der Copolymerisation mit aromatischen Monomeren und die Homopolymerisation in aromatischen Lösungsmitteln. Die Stereochemie der Gelöstes-Lösungsmittel-Wechselwirkungen legt nahe, daß MMA in Lösung in der *cis*-Konformation vorliegt, die für den Mechanismus der stereoregulierten Polymerisation dieses Monomeren von Bedeutung ist.